# Transdermal delivery of selected statins formulated in apricot kernel oil emulsions

**SM Maree**

orcid.org/ 0000-0002-2073-3477

Dissertation submitted in fulfilment of the requirements for the degree *Master of Science in Pharmaceutics* at the North West University

Supervisor: Prof M Gerber

Co-supervisor: Prof. J du Plessis

Co-supervisor: Prof. L du Plessis

Examination: May 2019

Student number: 22819509

# ACKNOWLEDGEMENTS

To our Heavenly Father, thank You for providing me with the health and strength I needed to complete this dessertation.

Johan Maree and Susan Maree my perfect parents, thank you for all your love, support and encouragement.

My two siblings, Alecia Verster and Louwrie Maree, thank you for the example that you set for me to follow, and for being strong when I am at my weakest.

Suzanne Marais, thank you for the motivation and encouragement, you have always been there for me. Thank you for being my best friend.

Professor Minja Gerber, my supervisor, thank you for your dedication and willingness to help, and for always shining the brightest when times seem dark.

Professor Jeanetta du Plessis, my co-supervisor, thank you for your advice and insight.

Professor Lissinda du Plessis, and Dr. Wihan Pheiffer, thank you for assistance during cytotoxicity studies.

Professor Jan du Preez, thank you for your assistance regarding HPLC analysis.

Professor Faans Steyn, thank you for all the help and assistance with the statistical analysis.

NRF (National Research Foundation) and the North-West University, my highest appreciation for the financial support you have provided during my post-graduate studies.

*If you always do what you've always done, you'll always be where you've always been*

# ABSTRACT

Statins are the leading active pharmaceutical ingredient (API) in the oral treatment of elevated cholesterol levels in the bloodstream. Oral administered statins claim to have gastro-intestinal side-effects, which could affect life quality and low bioavailability due to hepatic clearance. The goal was to formulate statins within nano-emulsions and nano-emulgels, to avoid first-pass clearance, produce an increased bioavailability and improve patient compliance.

A single high performance liquid chromatographic (HPLC) method was developed and validated to produce accurate and reproducible analytical results of the statins (atorvastatin, fluvastatin, pitavastatin and pravastatin).

Since these statins are incompliant to the ideal physiochemical characteristics for effective transdermal delivery of APIs, nano-emulsions and nano-emulgels containing apricot kernel oil (a natural penetration enhancer) and surfactants were used as transport systems. Subsequently, characterisation techniques were performed on the different formulas (nano-emulsions and nano-emulgels) to ensure these formulas complied with the required parameters. Cytotoxicity studies were performed on the pre-malignant human immortalised keratinocytes (HaCaT) to determine whether HaCaT cell lines were adversely affected by the statins and/or other compounds in the formulas.

The Franz diffusion cell method was utilised to conduct membrane release studies to determine if the statins were released from formulas. Finally, skin diffusion studies and tape stripping were performed to evaluate the transdermal and/or topical delivery of the statins, respectively. Statistical analyses were performed to analyse the variances between the means of the data obtained from membrane release studies, as well as skin studies (transdermal and topical).

Membrane release studies concluded that the nano-emulsion containing fluvastatin (**NE1F**) had the highest median flux amongst the nano-emulsions, while the nano-emulgel containing pravastatin (**NEGPr**) prevailed amongst the nano-emulgels and of all nano-formulas (nano-emulsions and nano-emulgels). Skin diffusion studies revealed that the nano-emulgels had higher median amount of statins per area that diffused through the skin when compared to their respective nano-emulsions, as the nano-emulgel containing fluvastatin (**NEGF**) dominated all tested nano-formulas. Tape stripping data indicated that the median statin concentrations of the nano-emulsions were generally higher in the skin layers than the nano-emulgels.

Average receptor concentrations after transdermal delivery of the statins (obtained in this study) were compared to the research found on the plasma concentrations after oral administration; it was observed that nano-formulas had higher receptor concentrations, except for **NEGF**, **NE1F** and nano-emulsion containing pitavastatin (**NE1Pi**).

Keywords: nano-emulsion, nano-emulgel, plasma concentrations, statins, transdermal delivery, cytotoxicity

# OPSOMMING

Statiene is die vernaamste aktiewe farmaseutiese bestanddeel (AFB) vir die orale behandeling van verhoogde cholesterolvlakke in die bloedplasma. Statiene wat oraal toegedien word, het sogenaamde gastro-intestinale newe-effekte wat lewenskwaliteit en lae biobeskikbaarheid weens hepatiese deurgangseffek affekteer. Die doel was om statiene in onderskeidelike nano-emulsies en nano-emuljelle te formuleer om eerste-deurgangseffek te vermy, 'n verhoogde biobeskikbaarheid te lewer en pasiëntmeewerkendheid te bevorder.

'n Enkele hoëdrukvloeistofchromatografiese (HDVC) metode is ontwikkel en gevalideer om akkurate en herhaalbare analitiese resultate van die statiene (atorvastatien, fluvastatien, pitavastatien en pravastatien) te produseer.

Aangesien hierdie statiene nie aan die ideale fisieschemiese kenmerke van effektiewe transdermale aflewering van AFB's voldoen nie, is nano-emulsie- en nano-emuljelformules gebruik as transportsisteem wat appelkoospitolie ('n natuurlike penetrasie-bevorderaar) en oppervlakaktiewe middels bevat. Gevolglik is karakteriseringstegnieke op die formules (nano-emulsie- en nano-emuljelle) uitgevoer om te verseker dat die stabiliteit van die formules binne die spesifieke parameters val. Sitotoksisiteit-studies is uitgevoer op premaligne menslike keratonisietselle (HaCaT) om te bepaal of die HaCaT-sellyne benadeel word deur statiene en/of ander samestellings in die formules.

Die Franz-selmetode is gebruik om membraanvrystellingstudies uit te voer om te bepaal of die statiene uit die formules vrygestel het. Laastens is veldiffusie- en kleefbandstropingstudies uitgevoer om die transdermale aflewering van die statiene te evalueer. Statistiese analises is uitgevoer om die variansies te analiseer tussen die gemiddeldes vanaf die data (membraanvrystelling- en veldiffusiestudies).

Membraanvrystellingstudies het aangedui dat die nano-emulsie wat fluvastatien (**NE1F**) bevat, die hoogste mediaan vloedwaarde onder die nano-emulsies gehad het; gevolglik het pravastatien (**NEGPr**) onder die nano-formules (nano-emuljel-, asook nano-emulsieformules) oorheers. Veldiffusiestudies het getoon dat nano-emuljelformules met hoër mediaan hoeveelhede per area deur die vel gediffundeer het in vergelyking met die betrokke nano-emulsies, omdat die fluvastatienbevattende nano-emuljel (**NEGF**) dominant was in al die getoetsde formules. Kleefbandstroping het getoon dat die mediaan statienkonsentrasies van die nano-emulsies oor die algemeen hoër was as die nano-emuljelformules in die onderskeie lae van die vel.

Gemiddelde reseptorkonsentrasies na transdermale aflewering van die statiene (verkry in die studie) in vergelyking met vorige navorsing wat gedoen is, het gevind dat die plasmakonsentrasies na orale toediening aangedui het dat die nano-formules hoër reseptorkonsentrasies gehad het, met **NEGF**, **NE1F** en die pitavastatien-bevattende nano-emulsie (**NE1Pi)** as uitsonderings.

**Sleutelwoorde:** nano-emulsie, nano-emuljel, plasmakonsentrasies, statiene, transdermale aflewering, sitotoksisiteit

# TABLE OF CONTENTS


| | | |
|---|---|---|
| **ACKNOWLEDGEMENTS** | | i |
| **ABSTRACT** | | ii |
| **OPSOMMING** | | iv |
| **LIST OF FIGURES** | | xxi |
| **LIST OF TABLES** | | xxx |
| **LIST OF EQUATIONS** | | xxxvi |
| **ABBREVIATIONS** | | xxxviii |

## CHAPTER 1: INTRODUCTION, RESEARCH PROBLEM AND AIMS

| | | |
|---|---|---|
| **1.1** | Introduction | 1 |
| **1.2** | Research problem | 4 |
| **1.3** | Aims | 4 |
| References | | 5 |

## CHAPTER 2: FORMULATION AND TRANSDERMAL DELIVERY OF NANO-EMULSIONS COMPARED TO SEMI-SOLID (NANO-EMULGEL) FORMULATIONS CONTAINING STATINS AND APRICOT KERNEL OIL

| | | |
|---|---|---|
| **2.1** | Introduction | 9 |
| **2.2** | Defining cholesterol | 11 |
| **2.2.1** | High density lipoprotein | 12 |
| **2.2.2** | Low density lipoprotein | 12 |
| **2.2.3** | Very low-density lipoprotein | 12 |
| **2.3** | Hyperlipidaemia | 13 |
| **2.3.1** | Pathophysiology of hyperlipidaemia | 13 |
| **2.3.1.1** | Primary hyperlipidaemia | 13 |

| | | |
|---|---|---|
| **2.3.1.2** | Secondary hyperlipidaemia | 13 |
| **2.3.2** | Diagnoses of primary hyperlipidaemia | 13 |
| **2.3.3** | Medical treatment of primary hyperlipidaemia | 14 |
| **2.4** | Statins | 14 |
| **2.4.1** | Administration of statins | 18 |
| **2.4.2** | Impediments of oral treatment with statins | 18 |
| **2.4.3** | Alternative route of administration of statins | 19 |
| **2.5** | Transdermal route | 19 |
| **2.6** | The human skin | 19 |
| **2.6.1** | Viable epidermis (stratum granulosum, stratum spinosum and stratum basale) | 21 |
| **2.6.2** | Non-viable epidermis | 21 |
| **2.6.3** | Dermis | 22 |
| **2.6.4** | Hypodermis | 22 |
| **2.7** | Transport of APIs through the skin | 22 |
| **2.7.1** | Follicular route | 23 |
| **2.7.2** | Transcellular route | 23 |
| **2.7.3** | Intercellular route | 24 |
| **2.8** | Physiochemical characteristics | 24 |
| **2.8.1** | Log P and log D | 24 |
| **2.8.2** | Molecular weight | 25 |
| **2.8.3** | Melting point | 25 |
| **2.8.4** | Aqueous solubility | 25 |
| **2.8.5** | Diffusion coefficient | 26 |
| **2.8.6** | pH, pKa and ionisation | 26 |
| **2.8.7** | Requirements for specific statins | 27 |
| **2.9** | Transport agents | 28 |

| | | |
|---|---|---|
| **2.10** | Nano-emulsions | 28 |
| **2.11** | Emulsification | 29 |
| **2.11.1** | High energy emulsification | 30 |
| **2.12** | Penetration enhancers | 30 |
| **2.12.1** | Natural penetration enhancers | 30 |
| **2.12.1.1** | Apricot kernel oil as a natural penetration enhancer | 31 |
| **2.13** | Surfactants | 31 |
| **2.14** | Semi-solid formulations | 33 |
| **2.14.1** | Nano-emulgel | 33 |
| **2.14.2** | Gelling agents | 34 |
| **2.14.3** | Carbopol® Ultrez 20 | 34 |
| **2.15** | Conclusion | 35 |
| References | | 36 |

**CHAPTER 3: A NOVEL HPLC METHOD DEVELOPED AND VALIDATED FOR THE DETECTION AND QUANTIFICATION OF ATORVASTATIN, FLUVASTATIN, PITAVASTATIN AND PRAVASTATIN IN TRANSDERMAL DELIVERY STUDIES**

| | | |
|---|---|---|
| Abstract | | 47 |
| **1** | Introduction | 47 |
| **2** | Investigations, results and discussion | 48 |
| **3** | Experimental | 50 |
| | Acknowledgements | 50 |
| References | | 51 |
| Disclaimer | | 51 |
| Tables | 1 | 53 |
| Figures | 1 | 54 |
| | 2 | 55 |

**CHAPTER 4: ARTICLE FOR THE PUBLICATION IN THE INTERNATIONAL JOURNAL OF PHARMACEUTICS**


| | | |
|---|---|---|
| Abstract | | 58 |
| Graphical Abstract | | 59 |
| **1** | Introduction | 60 |
| **2** | Materials and Methods | 62 |
| **2.1** | Materials | 62 |
| **2.2** | Methods | 62 |
| **2.2.1** | Formulation of statin nano-emulsions and nano-emulgels | 62 |
| **2.2.2** | Analysis of statins | 63 |
| **2.2.3** | Standard preparation | 64 |
| **2.2.4** | Physicochemical properties | 64 |
| **2.2.4.1** | Aqueous solubility | 64 |
| **2.2.4.2** | Octanol-buffer distribution coefficient (log D) | 64 |
| **2.3** | Characterisation of optimal statin nano-emulsions and nano-emulgels | 65 |
| **2.3.1** | Visual inspection | 65 |
| **2.3.2** | pH | 65 |
| **2.3.3** | Zeta-potential | 66 |
| **2.3.4** | Droplet size and distribution | 66 |
| **2.3.5** | Viscosity | 66 |
| **2.4** | Diffusion studies | 66 |
| **2.4.1** | Membrane release studies | 66 |
| **2.4.2** | Skin preparation | 67 |
| **2.4.3** | Skin diffusion studies | 67 |
| **2.4.4** | Tape stripping | 68 |
| **2.5** | Data analysis | 68 |

| | | |
|---|---|---|
| **2.6** | Statistical analysis | 69 |
| **3** | Results and Discussion | 69 |
| **3.1** | Formulation of nano-emulsions and nano-emulgels | 69 |
| **3.2** | Analysis of statins | 69 |
| **3.3** | Physicochemical properties | 69 |
| **3.3.1** | Aqueous solubility | 69 |
| **3.3.2** | Log D | 70 |
| **3.3.3** | Characterisation of NEGs and NE1s | 70 |
| **3.4** | Membrane release studies | 71 |
| **3.5** | Diffusion experiments | 71 |
| **3.5.1** | Skin diffusion studies | 72 |
| **3.6** | Tape stripping | 73 |
| **3.6.1** | Stratum corneum-epidermis | 73 |
| **3.6.2** | Epidermis-dermis | 73 |
| **3.7** | Statistical analysis | 74 |
| **3.7.1** | Membrane release studies | 74 |
| **3.7.2** | Skin diffusion studies | 74 |
| **3.7.3** | Statin diffusion through the skin | 75 |
| **3.7.4** | Tape stripping | 75 |
| **4** | Conclusion | 76 |
| Acknowledgements | | 78 |
| Conflict of Interest | | 78 |
| References | | 79 |
| Tables | | 82 |
| Figures | | 86 |

## CHAPTER 5:CONCLUSION AND FUTURE PROSPECTS

Conclusion 89

References 93

**APPENDIX A: VALIDATION OF AN HIGH PERFORMANCE LIQUID CHROMATOGRAPHIC (HPLC) ASSAY FOR ATORVASTATIN, FLUVASTATIN, PITAVASTATIN AND PRAVASTATIN**


| | | |
|---|---|---|
| **A.1** | Purpose of validation | 94 |
| **A.2** | Chromatographic conditions | 94 |
| **A.3** | Guidelines to the method validation | 95 |
| **A.3.1** | Linearity | 98 |
| **A.3.1.1** | Linearity method | 99 |
| **A.3.2** | Accuracy | 104 |
| **A.3.3** | Precision | 108 |
| **A.3.3.1** | Repeatability (intra-day precision) | 109 |
| **A.3.3.2** | Intermediate precision (inter-day precision) | 112 |
| **A.3.3** | Robustness | 115 |
| **A.3.4** | System stability | 120 |
| **A.3.5** | System repeatability | 124 |
| **A.3.6** | Specificity | 127 |
| **A.3.7** | Limit of detection | 130 |
| **A.3.8** | Limit of quantitation | 131 |
| **A.3.9** | Conclusion | 134 |
| References | | 135 |

## APPENDIX B: FORMULATION AND STABILITY DETERMINATION OF AN OPTIMISED O/W NANO-EMULSION CONTAINING SELECTED STATINS


| | | |
|---|---|---|
| **B.1** | Introduction | 137 |
| **B.1.1** | The oil phase | 138 |
| **B.1.2** | Water phase | 138 |
| **B.1.3** | Surfactants | 139 |
| **B.2** | Method to determine the solubility of API in apricot kernel oil | 140 |
| **B.2.1** | Preparation of samples | 140 |
| **B.2.2** | Standard | 140 |
| **B.2.3** | Placebo | 140 |
| **B.3** | Goal of formulation | 140 |
| **B.4** | Formula and formulation method used to prepare the nano-emulsions | 141 |
| **B.5** | Methods used during the characterisation of the nano-emulsions | 143 |
| **B.5.1** | Visual inspection | 143 |
| **B.5.2** | pH | 144 |
| **B.5.3** | Surface potential (zeta-potential) | 145 |
| **B.5.4** | Droplet size and distribution | 148 |
| **B.5.5** | Viscosity | 150 |
| **B.5.6** | Transmission electron microscopy (TEM) | 152 |
| **B.5.7** | Entrapment efficacy | 154 |
| **B.6** | Conclusion | 156 |
| **B.7** | Optimised o/w nano-emulsion method and formula with and without statins | 157 |
| **B.8** | Methods used during the characterisation of the optimised o/w nano-emulsions | 158 |
| **B.8.1** | Visual inspection | 158 |
| **B.8.2** | pH | 159 |
| **B.8.3** | Surface potential (zeta-potential) | 159 |

| | | |
|---|---|---|
| **B.8.4** | Droplet size and distribution | 162 |
| **B.8.5** | Viscosity | 164 |
| **B.8.6** | Transmission electron microscopy | 164 |
| **B.9** | Conclusion | 166 |
| References | | 168 |

**APPENDIX C: FORMULATING AND CHARACTERISATION OF A NANO-EMULGEL COMPARED TO AN OPTIMISED O/W NANO-EMULSION BOTH CONTAINING STATINS IN COMBINATION WITH APRICOT KERNEL OIL**

| | | |
|---|---|---|
| **C.1** | Introduction | 174 |
| **C.2** | Purpose of the formulation | 176 |
| **C.2.1** | Formula and formulation method of the nano-emulgel | 176 |
| **C.3** | Methods used during characterisation of a formulation | 178 |
| **C.3.1** | Visual inspection | 178 |
| **C.3.2** | pH | 179 |
| **C.3.3** | Surface potential (zeta-potential) | 180 |
| **C.3.4** | Droplet size and distribution | 182 |
| **C.3.5** | Viscosity | 184 |
| **C.3.6** | Light microscopy | 185 |
| **C.3.7** | Conclusion | 187 |
| References | | 188

**APPENDIX D: DIFFUSION STUDIES OF O/W NANO-EMULSIONS AND NANO-EMULGELS CONTAINING STATINS AND APRICOT KERNEL OIL**


| | | |
|---|---|---|
| **D.1** | Introduction | 192 |
| **D.2** | Methods | 193 |
| **D.2.1** | HPLC analysis of statin samples | 193 |
| **D.2.2** | Solubility of statins | 193 |
| **D.2.2.1** | Solubility in PBS (pH 7.4) | 193 |
| **D.2.2.2** | Solubility in *n*-octanol | 194 |
| **D.2.3** | Octanol buffer distribution coefficient (log D) of statins | 194 |
| **D.2.4** | Franz cell method | 195 |
| **D.2.4.1** | Donor phase preparation | 196 |
| **D.2.4.2** | Preparation of PBS (pH 7.4) as receptor phase of the Franz cells | 196 |
| **D.2.4.3** | Membrane release studies | 197 |
| **D.2.4.4** | *In vitro* skin diffusion studies | 199 |
| **D.2.4.4.1** | Skin collection and ethical aspects | 199 |
| **D.2.4.4.2** | Preparation of skin for *in vitro* diffusion studies | 200 |
| **D.2.4.4.3** | *In vitro* skin diffusion studies | 200 |
| **D.2.4.4.4** | Tape stripping | 200 |
| **D.2.5** | Data analysis | 201 |
| **D.2.6** | Statistical data analysis | 201 |
| **D.3** | Results and discussions | 202 |
| **D.3.1** | Solubility | 202 |
| **D.3.2** | Octanol buffer distribution coefficient of statins | 203 |
| **D.3.3** | Membrane release studies | 203 |
| **D.3.4** | *In vitro* skin diffusion studies | 213 |
| **D.3.5** | Tape stripping | 219 |

| | | |
|---|---|---|
| **D.3.6** | Statistical analysis | 230 |
| **D.3.6.1** | Statistical analysis of membrane release studies | 230 |
| **D.3.6.2** | Statistical analysis of the *in vitro* skin diffusion studies | 231 |
| **D.3.6.2.1** | Statistical analysis of the statin that diffused through the skin from the NE1s and NEGs | 230 |
| **D.3.6.2.2** | Statistical analysis of the statins present in the skin layers (SCE and ED) | 232 |
| **D.4** | Conclusion | 235 |
| References | | 239 |


## APPENDIX E: CYTOTOXICITY STUDIES OF O/W NANO-EMULSIONS


| | | |
|---|---|---|
| **E.1** | Introduction | 243 |
| **E.2** | Preparation for cell toxicity studies | 245 |
| **E.2.1** | Materials | 245 |
| **E.2.2** | Cell line selection | 245 |
| **E.2.3** | Seeding of cells | 246 |
| **E.2.4** | Haemocytometer and cell counting | 246 |
| **E.2.5** | Preparation of treatments | 248 |
| **E.2.6** | Concentration of treatments to be dosed on separate 96-well plates | 248 |
| **E.3** | *In vitro* toxicity testing | 251 |
| **E.3.1** | Methylthiazol tetrazolium (MTT) | 251 |
| **E.3.1.1** | MTT-assay | 251 |
| **E.3.1.2** | MTT-assay results and discussion on treated HaCaT cells | 252 |
| **E.3.1.2.1** | Cell viability of the statin solutions during MTT-assay on treated HaCaT cells | 252 |
| **E.3.1.2.2** | Cell viability of the NE1s and PNE1 during MTT-assay on treated HaCaT cells | 255 |
| **E.3.1.2.3** | Cell viability of the excipients during MTT-assay on treated HaCaT cells | 257 |
| **E.3.1.2.4** | $IC_{50}$ values during the MTT-assay | 259 |

| | | |
|---|---|---|
| **E.3.2** | Neutral red (NR) | 260 |
| **E.3.2.1** | NR-assay | 261 |
| **E.3.2.2** | NR-assay results and discussion on treated HaCaT cells | 261 |
| **E.3.2.2.1** | Cell viability of the statin solutions during NR-assay on treated HaCaT cells | 261 |
| **E.3.2.2.2** | Cell viability of the NE1s and PNE1 during NR-assay on treated HaCaT cells | 263 |
| **E.3.2.2.3** | Cell viability of the excipients during NR-assay on treated HaCaT cells | 265 |
| **E.3.2.2.4** | $IC_{50}$ values during the NR-assay | 268 |
| **E.4** | Conclusion | 269 |
| References | | 270 |

## APPENDIX F: AUTHOR GUIDELINES: DIE PHARMAZIE

| | | |
|---|---|---|
| **F.1** | Aim | 272 |
| **F.2** | Articles are published in English (preferred) or German and are classified as: | 272 |
| **F.2.1** | Reviews | 272 |
| **F.2.2** | Original articles | 272 |
| **F.2.3** | Short communications | 272 |
| **F.2.4** | Book reviews | 272 |
| **F.3** | Conditions | 272 |
| **F.4** | Preparation of manuscripts | 273 |
| **F.5** | Quotations have to follow the following style: | 275 |
| **F.5.1** | Journal articles: | 275 |
| **F.5.2** | Books/Book chapters | 275 |

## APPENDIX G: THE INTERNATIONAL JOURNAL OF PHARMACEUTICS: GUIDE FOR AUTHORS


| | | |
|---|---|---|
| **G.1** | Introduction | 277 |
| **G.2** | Types of paper | 277 |
| **G.2.1** | Full Length Manuscripts | 277 |
| **G.2.2** | Reviews and Mini-Reviews | 277 |
| **G.3** | Ethics in publishing | 277 |
| **G.4** | Studies in humans and animals | 278 |
| **G.5** | Declaration of interest | 278 |
| **G.6** | Submission declaration and verification | 279 |
| **G.7** | Preprints | 279 |
| **G.8** | Use of inclusive language | 279 |
| **G.9** | Author contributions | 279 |
| **G.10** | Authorship | 280 |
| **G.11** | Changes to authorship | 280 |
| **G.12** | Article transfer service | 280 |
| **G.13** | Copyright | 280 |
| **G.14** | Author rights | 281 |
| **G.15** | Role of the funding source | 281 |
| **G.16** | Funding body agreements and policies | 281 |
| **G.17** | Open access | 282 |
| **G.18** | Elsevier Researcher Academy | 283 |
| **G.19** | Language (usage and editing services) | 283 |
| **G.20** | Submission | 284 |
| **G.21** | Referees | 284 |
| **G.22** | Use of word processing software | 285 |

| | | |
|---|---|---|
| **G.23** | Article structure | 285 |
| **G.23.1** | Subdivision - numbered sections | 285 |
| **G.23.2** | Introduction | 285 |
| **G.23.3** | Material and methods | 285 |
| **G.23.4** | Results | 286 |
| **G.23.5** | Discussion | 286 |
| **G.23.6** | Conclusions | 286 |
| **G.23.7** | Appendices | 286 |
| **G.23.8** | Essential title page information | 286 |
| **G.23.9** | Abstract | 287 |
| **G.23.10** | Graphical abstract | 287 |
| **G.23.11** | Keywords | 287 |
| **G.23.12** | Abbreviations | 287 |
| **G.23.13** | Acknowledgements | 288 |
| **G.23.14** | Formatting of funding sources | 288 |
| **G.23.15** | Units | 288 |
| **G.23.16** | Math formulae | 288 |
| **G.23.17** | Footnotes | 289 |
| **G.23.18** | Image manipulation | 289 |
| **G.24** | Electronic artwork | 289 |
| **G.25** | Formats | 290 |
| **G.25.1** | Color artwork | 290 |
| **G.25.2** | Figure captions | 291 |
| **G.25.3** | Tables | 291 |
| **G.26** | References | 291 |
| **G.26.1** | Citation in text | 291 |

| | | |
|---|---|---|
| **G.26.2** | Reference links | 291 |
| **G.26.3** | Web references | 292 |
| **G.26.4** | Data references | 292 |
| **G.26.5** | References in a special issue | 292 |
| **G.26.6** | Reference management software | 292 |
| **G.26.7** | Reference formatting | 293 |
| **G.26.8** | Reference style | 293 |
| **G.27** | Video | 295 |
| **G.28** | Data visualization | 295 |
| **G.29** | Supplementary material | 295 |
| **G.30** | Research data | 295 |
| **G.30.1** | Data linking | 296 |
| **G.30.2** | Mendeley Data | 296 |
| **G.30.3** | Data in Brief | 297 |
| **G.30.4** | Data statement | 297 |
| **G.31** | Submission checklist | 297 |
| **G.32** | Online proof correction | 298 |
| **G.33** | Offprints | 299 |
| **G.34** | Author inquiries | 299 |

**APPENDIX H: THE INTERNATIONAL JOURNAL OF PHARMACEUTICS: GUIDE FOR AUTHORS**

LANGUAGE EDITING CERTIGICATE ENGLISH

LANGUAGE EDITING CERTIGICATE AFRIKAANS

# LIST OF FIGURES

**CHAPTER 2: FORMULATION AND TRANSDERMAL DELIVERY OF NANO-EMULSIONS COMPARED TO SEMI-SOLID (NANO-EMULGEL) FORMULATIONS CONTAINING STATINS AND APRICOT KERNEL OIL**


| | | |
|---|---|---|
| **Figure 2.1:** | Adapted chemical structural representation of type 1 statin: a) pravastatin and of type 2 statins: b) atorvastatin, c) fluvastatin and d) pitavastatin (Hennessy *et al*., 2016:45). | 16 |
| **Figure 2.2:** | Adapted schematic representation of the human skin layers (Trommer & Neubert, 2006:107. | 20 |
| **Figure 2.3:** | Adapted schematic representation of the epidermis, a) non-viable epidermis and b) viable epidermis (Natarajan *et al.,* 2014). | 20 |
| **Figure 2.4:** | The three transport routes through the skin (Adapted from Lohani, 2014). | 23 |


**CHAPTER 3: A NOVEL HPLC METHOD DEVELOPED AND VALIDATED FOR THE DETECTION AND QUANTIFICATION OF ATORVASTATIN, FLUVASTATIN, PITAVASTATIN AND PRAVASTATIN IN TRANSDERMAL DELIVERY STUDIES**


| | | |
|---|---|---|
| **Figure 1** | HPLC chromatogram indicating the specificity data of: A) atorvastatin, B) fluvastatin, C) pitavastatin and D) pravastatin. (The letters represent the following: a) placebo and b) standard solution with selected statin. The following statin sample solutions were stressed with: c) HCl, d) Milli-Q® water, e) NaOH and f) H2O2 | 54 |
| **Figure 2** | HPLC chromatogram indicating the in vitro skin diffusion study data of: A) fluvastatin, B) pitavastatin, C) atorvastatin and D) pravastatin. The letters represent the following samples with the respective statins: a) standard solution, b) receptor phase (transdermal delivery), c) tape strip (topical delivery) and d) skin sample (topical delivery) | 55 |

**CHAPTER 4: ARTICLE FOR THE PUBLICATION IN THE INTERNATIONAL JOURNAL OF PHARMACEUTICS**


| | | |
|---|---|---|
| **Figure 1:** | Box-plots of the flux values (µg/cm2.h) of **NE1s** and **NEGs** for each statin during the membrane release studies over 6 h | 85 |
| **Figure 2:** | Box-plot presenting the average and median amount per area diffused (µg/cm2) of the **NE1s** and **NEGs** for each statin that diffused through the skin after 12 h | 86 |
| **Figure 3:** | Average concentration (µg/ml) of the **NE1s** and the **NEGs** for each statin present in the SCE and ED | 87 |


## APPENDIX A: VALIDATION OF AN HIGH PERFORMANCE LIQUID CHROMATOGRAPHIC (HPLC) ASSAY FOR ATORVASTATIN, FLUVASTATIN, PITAVASTATIN AND PRAVASTATIN


| | | |
|---|---|---|
| **Figure A.1:** | HPLC used in this study as an analytical instrument (Dionex UltiMate 3000 dual system with ternary gradient pumps, column ovens autosampler and diode array detectors) | 95 |
| **Figure A.2:** | HPLC chromatogram representing the statins' standard solution peaks | 98 |
| **Figure A.3:** | Representation of atorvastatin's standard linear regression curve | 100 |
| **Figure A.4:** | Representation of fluvastatin's standard linear regression curve | 101 |
| **Figure A.5:** | Representation of pitavastatin's standard linear regression curve | 102 |
| **Figure A.6:** | Representation of pravastatin's linear regression curve | 103 |
| **Figure A.7:** | An HPLC chromatogram representative of robustness data for atorvastatin standard solution injected at alternated parameters: a) standard conditions of injection volume (10.00 µl), flow rate (1.0 ml/min), wavelength (240 nm) and gradient (30% ACN); b) at injection volume (10.00 µl), flow rate (1.2 ml/min), wavelength (235 nm) and gradient (35% ACN); c) at injection volume (10.00 µl), flow rate (0.8 ml/min), wavelength (230 nm) and gradient (27% ACN) | 116 |
| **Figure A.8:** | An HPLC chromatogram representative of robustness data for fluvastatin standard solution injected at alternated parameters: a) standard conditions of injection volume (10.00 µl), flow rate (1.0 ml/min), wavelength (240 nm) and gradient (30% ACN); b) at injection volume (10.00 µl), flow rate (1.2 ml/min), wavelength (235 nm) and gradient (35% ACN); c) at injection volume | 117 |

(10.00 µl), flow rate (0.8 ml/min), wavelength (230 nm) and gradient (27% ACN)

**Figure A.9:** An HPLC chromatogram representative of robustness data for pitavastatin standard solution injected at alternated parameters: a) standard conditions of injection volume (10.00 µl), flow rate (1.0 ml/min), wavelength (240 nm) and gradient (30% ACN); b) at injection volume (10.00 µl), flow rate (1.2 ml/min), wavelength (235 nm) and gradient (35% ACN); c) at injection volume (10.00 µl), flow rate (0.8 ml/min), wavelength (230 nm) and gradient (27% ACN) 118

**Figure A.10:** An HPLC chromatogram representative of robustness data for pravastatin standard solution injected at alternated parameters: a) standard conditions of injection volume (10.00 µl), flow rate (1.0 ml/min), wavelength (240 nm) and gradient (30% ACN); b) at injection volume (10.00 µl), flow rate (1.2 ml/min), wavelength (235 nm) and gradient (35% ACN); c) at injection volume (10.00 µl), flow rate (0.8 ml/min), wavelength (230 nm) and gradient (27% ACN) 119

**Figure A.11:** HPLC chromatogram indicating specificity data of atorvastatin: a) placebo, b) standard, c) HCl, d) Milli-Q® water, e) NaOH and f) $H_2O_2$ 127

**Figure A.12:** HPLC chromatogram indicating specificity data of fluvastatin: a) placebo, b) standard, c) HCl, d) Milli-Q® water, e) NaOH and f) $H_2O_2$ 128

**Figure A.13:** HPLC chromatogram indicating specificity data of pitavastatin: a) placebo, b) standard, c) HCl, d) Milli-Q® water, e) NaOH and f) $H_2O_2$ 129

**Figure A.14:** HPLC chromatogram indicating specificity data of pravastatin: a) placebo, b) standard, c) HCl, d) Milli-Q® water, e) NaOH and f) $H_2O_2$ 130

## APPENDIX B: FORMULATION AND STABILITY DETERMINATION OF AN OPTIMISED O/W NANO-EMULSION CONTAINING SELECTED STATINS

**Figure B.1:** Method followed to prepare nano-emulsions (for each individual statin) 142

**Figure B.2:** Nano-emulsions (**NE1** and **NE2**) containing different statins individually: a) **NE1A**, b) **NE2A**, c) **NE1F**, d) **NE2F**, e) **NE1Pi**, f) **NE2Pi**, g) **NE1Pr** and h) **NE2Pr** 143

**Figure B.3:** Mettler Toledo® pH meter (Mettler Toledo, CU) utilised to measure the pH levels of the **NE1s** and **NE2s** 144

| | | |
|---|---|---|
| **Figure B.4:** | Malvern Zetasizer Nano ZS (Malvern Instruments, Worcestershire, UK) utilised to measure the zeta-potential of **NE1s** and **NE2s** | 146 |
| **Figure B.5:** | The average zeta-potential (mV) of the nano-emulsions (**NE1s** and **NE2s**) containing statins: a) **NE1A**, b) **NE2A**, c) **NE1F**, d) **NE2F**, e) **NE1Pi**, f) **NE2Pi**, g) **NE1Pr** and h) **NE2Pr** | 147 |
| **Figure B.6:** | Average droplet size (nm) of the nano-emulsions (**NE1s** and **NE2s**) containing statins: a) **NE1A**, b) **NE2A**, c) **NE1F**, d) **NE2F**, e) **NE1Pi**, f) **NE2Pi**, g) **NE1Pr** and h) **NE2Pr** | 149 |
| **Figure B.7:** | Brookfield Viscometer (DV2T LV Ultra-Middleboro, Massachusetts, USA), linked to a water bath (± 25 °C) was utilised to measure the viscosity of the **NE1** and **NE2** | 150 |
| **Figure B.8:** | TEM micrographs of the **NE1s** and **NE2** each containing a statin: a) **NE1A**, b) **NE2A**, c) **NE1F**, d) **NE2F**, e) **NE1Pi**, f) **NE2Pi**, g) **NE1Pr** and h) **NE2Pr** | 153 |
| **Figure B.9:** | Ultracentrifuge (Beckman Coulter, Optima™ L-100 XP) utilised to rotate **NE1** and **NE2** for the extraction of supernatant | 155 |
| **Figure B.10:** | Prepared nano-emulsions: a) **PNE1**, b) **NE1A**, c) **NE1F**, d) **NE1Pi** and e) **NE1Pr** | 158 |
| **Figure B11:** | The average zeta-potential (mV) for the **PNE1** and **NE1s**: a) **PNE1**, b) **NE1A**, c) **NE1F**, d) **NE1Pi** and e) **NE1Pr** | 161 |
| **Figure B.12:** | The average droplet size (nm) of the **PNE1** and **NE1s**: a) **PNE1**, b) **NE1A**, c) **NE1F**, d) **NE1Pi** and e) **NE1Pr** | 163 |
| **Figure B.13:** | TEM micrographs of **PNE1** compared to those of the **NE1s**: a) **NE1**, b) **NE1A**, | 165 |


## APPENDIX C: FORMULATING AND CHARACTERISATION OF A NANO-EMULGEL COMPARED TO AN OPTIMISED O/W NANO-EMULSION BOTH CONTAINING STATINS IN COMBINATION WITH APRICOT KERNEL OIL


| | | |
|---|---|---|
| **Figure C.1:** | Schematic representation of the method used to prepare the nano-emulgels | 177 |
| **Figure C.2:** | Photographs taken of the different **NEGs** and **NE1s**: a) **NEGA**, b) **NE1A**, c) **NEGF**, d) **NE1F**, e) **NEGPi**, f) **NE1Pi**, g) **NEGPr** and h) **NE1Pr** | 178 |
| **Figure C.3:** | Average zeta-potential (mV) of the different **NEGs** and **NE1s**: a) **NEGA**, b) **NE1A**, c) **NEGF**, d) **NE1F**, e) **NEGPi**, f) **NE1Pi**, g) **NEGPr** and h) **NE1Pr** | 181 |

| | | |
|---|---|---|
| **Figure C.4:** | Average droplet size (nm) of the different **NEGs** and **NE1s**: a) **NEGA**, b) **NE1A**, c) **NEGF**, d) **NE1F**, e) **NEGPi**, f) **NE1Pi**, g) **NEGPr** and h) **NE1Pr** | 183 |
| **Figure C.5:** | Light microscopy micrographs of the **NEGs** compared to TEM micrographs of the **NE1s**: a) **NEGA**, b) **NE1A**, c) **NEGF**, d) **NE1F**, e) **NEGPi**, f) **NE1Pi**, g) **NEGPr** and h) **NE1Pr** | 186 |


## APPENDIX D: DIFFUSION STUDIES OF O/W NANO-EMULSIONS AND NANO-EMULGELS CONTAINING STATINS AND APRICOT KERNEL OIL


| | | |
|---|---|---|
| **Figure D.1:** | The compartments of a Franz diffusion cell | 196 |
| **Figure D.2:** | Grant® water bath (Grant Instruments, UK) | 197 |
| **Figure D.3:** | a) Dow Corning® high vacuum grease, b) horseshoe clamp, c) Parafilm®, d) prepared Franz diffusion cell and e) filled Franz diffusion cells placed in the water bath (37 °C) on a Variomag® magnetic stirring plate (Variomag, USA) | 198 |
| **Figure D.4:** | a) Modified syringes for extraction of receptor phase and b) filled marked vials ready for HPLC analysis | 199 |
| **Figure D.5:** | Average cumulative amount per area (µg/cm$^2$) of **NE1A** that was released through the membranes to indicate the average flux between 2 – 6 h (n = 10) | 204 |
| **Figure D.6:** | Cumulative amount per area (µg/cm$^2$) of **NE1A** that was released through the membranes of each individual Franz cell over 6 h (n = 10) through the membranes to indicate the average flux between 2 – 6 h (n = 10) | 204 |
| **Figure D.7:** | Average cumulative amount per area (µg/cm$^2$) of **NEGA** that was released | 205 |
| **Figure D.8:** | Cumulative amount per area (µg/cm$^2$) of **NEGA** that was released through the membranes of each individual Franz cell over 6 h (n =10) | 205 |
| **Figure D.9:** | Average cumulative amount per area (µg/cm$^2$) of **NE1F** that was released through the membranes to indicate the average flux between 2 – 6 h (n = 11) | 206 |
| **Figure D.10:** | Cumulative amount per area (µg/cm$^2$) of **NE1F** that was released through the membranes each individual Franz cell over 6 h (n = 11) | 206 |
| **Figure D.11:** | Average cumulative amount per area (µg/cm$^2$) of **NEGF** that was released through the membranes to indicate the average flux between 2 – 6 h (n = 10) | 207 |
| **Figure D.12:** | Cumulative amount per area (µg/cm$^2$) of **NEGF** that was released through the membranes of each individual Franz cell over 6 h (n = 10) | 207 |

**Figure D.13:** Average cumulative amount per area (µg/cm$^2$) of **NE1Pi** that was released through the membranes to indicate the average flux between 2 – 6 h (n = 9) 208

**Figure D.14:** Cumulative amount per area (µg/cm$^2$) of **NE1Pi** that was released through the membranes of each individual Franz cell over 6 h (n = 9) 208

**Figure D.15:** Average cumulative amount per area (µg/cm$^2$) of **NEGPi** that was released through the membranes to indicate the average flux between 2 – 6 h (n = 11) 209

**Figure D.16:** Cumulative amount per area (µg/cm$^2$) of **NEGPi** that was released through the membranes of each individual Franz cell over 6 h (n = 11) 209

**Figure D.17:** Average cumulative amount per area (µg/cm$^2$) of **NE1Pr** that was released through the membranes to indicate the average flux between 2 – 6 h (n = 8) 210

**Figure D.18:** Cumulative amount per area (µg/cm$^2$) of **NE1Pr** that was released through the membranes of each individual Franz cell over 6 h (n = 8) 210

**Figure D.19:** Average cumulative amount per area (µg/cm$^2$) of **NEGPr** that was released through the membranes to indicate the average flux between 2 – 6 h (n = 11) 211

**Figure D.20:** Cumulative amount per area (µg/cm$^2$) of **NEGPr** that was released through the membranes of each individual Franz cells over 6 h (n = 11) 211

**Figure D.21:** Box-plots of the flux values (µg/cm$^2$.h) of **NE1s** and **NEG** formulas for each statin during the membrane release studies over 6 h 212

**Figure D.22:** The amount per area of **NE1A** that diffused through skin after a 12 h diffusion study (n = 6) 214

**Figure D.23:** The amount per area of **NEGA** that diffused through skin after a 12 h diffusion study (n = 6) 214

**Figure D.24:** The amount per area of **NE1F** that diffused through skin after a 12 h diffusion study (n = 8) 215

**Figure D.25:** The amount per area of **NEGF** that diffused through skin after a 12 h diffusion study (n = 7) 215

**Figure D.26:** The amount per area of **NE1Pi** that diffused through skin after a 12 h diffusion study (n = 6) 216

**Figure D.27:** The amount per area of **NEGPi** that diffused through skin after a 12 h diffusion study (n = 6) 216

**Figure D.28:** The amount per area of **NE1Pr** that diffused through skin after a 12 h diffusion study (n = 6) 217

| | | |
|---|---|---|
| **Figure D.29:** | The amount per area of **NEGPr** that diffused through skin after a 12 h diffusion study (n = 7) | 217 |
| **Figure D.30:** | Box-plot presenting the average and median amount per area diffused (µg/cm$^2$) of the **NE1s** and **NEGs** for each statin that diffused through the skin after 12 h | 218 |
| **Figure D.31:** | The concentration (µg/ml) of **NE1A** present in the SCE after 12 h | 220 |
| **Figure D.32:** | The concentration (µg/ml) of **NE1A** present in the ED after 12 h | 221 |
| **Figure D.33:** | The concentration (µg/ml) of **NEGA** present in the SCE after 12 h | 221 |
| **Figure D.34:** | The concentration (µg/ml) of **NEGA** present in the ED after 12 h | 222 |
| **Figure D.35:** | The concentration (µg/ml) of **NE1F** present in the SCE after 12 h | 222 |
| **Figure D.36:** | The concentration (µg/ml) of **NE1F** present in the ED after 12 h | 223 |
| **Figure D.37:** | The concentration (µg/ml) of **NEGF** present in the SCE after 12 h | 223 |
| **Figure D.38:** | The concentration (µg/ml) of **NEGF** present in the ED after 12 h | 224 |
| **Figure D.39:** | The concentration (µg/ml) of **NE1Pi** present in the SCE after 12 h | 224 |
| **Figure D.40:** | The concentration (µg/ml) of **NE1Pi** present in the ED after 12 h | 225 |
| **Figure D.41:** | The concentration (µg/ml) of **NEGPi** present in the SCE after 12 h | 225 |
| **Figure D.42:** | The concentration (µg/ml) of **NEGPi** present in the ED after 12 h | 226 |
| **Figure D.43:** | The concentration (µg/ml) of **NE1Pr** present in the SCE after 12 h | 226 |
| **Figure D.44:** | The concentration (µg/ml) of **NE1Pr** present in the ED after 12 h | 227 |
| **Figure D.45:** | The concentration (µg/ml) of **NEGPr** present in the SCE after 12 h | 227 |
| **Figure D.46:** | The concentration (µg/ml) of **NEGPr** present in the ED after 12 h | 228 |
| **Figure D.47:** | Average concentration (µg/ml) of the **NE1s** as well as the **NEGs** for each statin present in the SCE and ED | 229 |

## APPENDIX E: CYTOTOXICITY STUDIES OF O/W NANO-EMULSIONS


| | | |
|---|---|---|
| **Figure E.1:** | Simplified representation of cytotoxic effects on cells: a) normal cell death (apoptosis) and b) cytotoxic cell death (necrosis) (Niles *et al*., 2008:657) | 243 |
| **Figure E.2:** | Cell counting by means of a haemocytometer under a microscope (Provost & Wallert, 2015:1) | 246 |
| **Figure E.3:** | Representation of 96-well plates to be treated | 248 |
| **Figure E.4:** | Illustrative 96-well plate indicating statins dosed in different concentrations for MTT as well as NR | 249 |
| **Figure E.5:** | Illustrative 96-well plate indicating **NE1s** dosed in different concentrations for MTT as well as NR | 250 |
| **Figure E.6:** | Illustrative 96-well plate indicating the excipients together with **PNE1** dosed in different concentrations for MTT as well as NR | 251 |
| **Figure E.7:** | The cytotoxic effects of the statin solutions dosed in different concentrations during the MTT-assay | 253 |
| **Figure E.8:** | Image of a 96-well plate containing cells treated with the statin solutions dosed in different concentrations during the MTT-assay: a) atorvastatin, b) fluvastatin, c) pitavastatin and d) pravastatin | 254 |
| **Figure E.9:** | The cytotoxic effects of the **NE1s** and the **PNE1** dosed in different concentrations during the MTT-assay | 255 |
| **Figure E.10:** | Image of a 96-well plate containing cells treated with different concentrations of the **NE1s** during the MTT-assay: a) **NE1A**, b) **NE1F**, c) **NE1Pi** and d) **NE1Pr** | 256 |
| **Figure E.11:** | The cytotoxic effects of the excipients dosed in different concentrations during the MTT-assay | 258 |
| **Figure E.12:** | Image of a 96-well plate containing cells treated with different concentrations of the excipients during the MTT-assay: a) Tween® 80, b) Span® 60, c) Span® 60-oil and d) **PNE1** (discussed in Section E.3.1.2.2) | 258 |
| **Figure E.13:** | The cytotoxic effects of the statin solutions dosed in different concentrations during the NR-assay | 262 |
| **Figure E.14:** | Image of a 96-well plate containing cells treated with the statin solutions dosed in different concentrations during the NR-assay: a) atorvastatin, b) fluvastatin, c) pitavastatin and d) pravastatin | 262 |

**Figure E.15:** The cytotoxic effects of the **NE1s** and the **PNE1** dosed in different concentrations during the NR-assay 264

**Figure E.16:** Image of a 96-well plate containing cells treated with different concentrations of the **NE1s** during the NR-assay: a) **NE1A**, b) **NE1F**, c) **NE1Pi** and d) **NE1Pr** 264

**Figure E.17:** The cytotoxic effects of the excipients dosed in different concentrations during the NR-assay 266

**Figure E.18:** Image of a 96-well plate containing cells treated with different concentrations of the excipients during the NR-assay: a) Tween® 80, b) Span® 60, c) Span® 60-oil and d) **PNE1** (discussed in Section E.3.2.2.2) 267

# LIST OF TABLES

**CHAPTER 2: FORMULATION AND TRANSDERMAL DELIVERY OF NANO-EMULSIONS COMPARED TO SEMI-SOLID (NANO-EMULGEL) FORMULATIONS CONTAINING STATINS AND APRICOT KERNEL OIL**

**Table 2.1:** Summary of physiochemical properties of statins compared to the idea properties 28

**CHAPTER 3: A NOVEL HPLC METHOD DEVELOPED AND VALIDATED FOR THE DETECTION AND QUANTIFICATION OF ATORVASTATIN, FLUVASTATIN, PITAVASTATIN AND PRAVASTATIN IN TRANSDERMAL DELIVERY STUDIES**

**Table 3.1** Summary of the HPLC's validation parameters and results 53

**CHAPTER 4: ARTICLE FOR THE PUBLICATION IN THE INTERNATIONAL JOURNAL OF PHARMACEUTICS**

**Table 1:** Formula used to prepare **NE1s** and **NEGs** containing statins 82

**Table 2:** LOD (µg/ml) and LOQ (µg/ml) of respective statins 82

**Table 3:** The measured averages during the characterisation of **NE1s** and **NEGs** 83

**Table 4:** The concentration (µg/ml) of the different statins within the formulas that diffused through the skin after 12 h 84

## APPENDIX A: VALIDATION OF AN HIGH PERFORMANCE LIQUID CHROMATOGRAPHIC (HPLC) ASSAY FOR ATORVASTATIN, FLUVASTATIN, PITAVASTATIN AND PRAVASTATIN


| | | |
|---|---|---|
| **Table A.1:** | Summary of analytical method validation guidelines and the results for atorvastatin (Ator), fluvastatin (Flu), pitavastatin (Pita) and pravastatin (Pra) | 97 |
| **Table A.2:** | Retention time (min), area (mAU) and height of the standard solutions (± 20 mg of each statin added up to 100 ml methanol) | 97 |
| **Table A.3:** | Atorvastatin's standard linearity results | 100 |
| **Table A.4:** | Fluvastatin's standard linearity results | 101 |
| **Table A.5:** | Pitavastatin's standard linearity results | 102 |
| **Table A.6:** | Pravastatin's standard linearity results | 103 |
| **Table A.7:** | The mean recovery (%) ranges (APVMA, 2004:5). | 104 |
| **Table A.8:** | Formula for the placebo nano-emulsion (no statins) | 105 |
| **Table A.9:** | Accuracy results of atorvastatin | 106 |
| **Table A.10:** | Statistical analysis of atorvastatin | 106 |
| **Table A.11:** | Accuracy results of fluvastatin | 106 |
| **Table A.12:** | Statistical analysis of fluvastatin | 107 |
| **Table A.13:** | Accuracy results of pitavastatin | 107 |
| **Table A.14:** | Statistical analysis of pitavastatin | 107 |
| **Table A.15:** | Accuracy results of pravastatin | 108 |
| **Table A.16:** | Statistical analysis of pravastatin | 108 |
| **Table A.17:** | The following levels of precision are recommended (APVMA, 2004:5). | 109 |
| **Table A.18:** | Repeatability (intra-day precision) results of atorvastatin | 109 |
| **Table A.19:** | Repeatability (intra-day precision) results of fluvastatin | 110 |
| **Table A.20:** | Repeatability (intra-day precision) results of pitavastatin | 111 |
| **Table A.21:** | Repeatability (intra-day precision) results of pravastatin | 112 |
| **Table A.22:** | Inter-day precision results of atorvastatin | 113 |

| | | |
|---|---|---|
| **Table A.23:** | Inter-day precision results of fluvastatin | 114 |
| **Table A.24:** | Inter-day precision results of pitavastatin | 114 |
| **Table A.25:** | Inter-day precision results of pravastatin | 114 |
| **Table A.26:** | Robustness data for atorvastatin pre- and post-alternations | 116 |
| **Table A.27:** | Robustness data for fluvastatin pre- and post-alternations | 117 |
| **Table A.28:** | Robustness data for pitavastatin pre- and post-alternations | 118 |
| **Table A.29:** | Robustness data for pravastatin pre- and post-alternations | 119 |
| **Table A.30:** | Sample stability parameters for atorvastatin | 121 |
| **Table A.31:** | Sample stability parameters for fluvastatin | 122 |
| **Table A.32:** | Sample stability parameters for pitavastatin | 123 |
| **Table A.33:** | Sample stability parameters for pravastatin | 124 |
| **Table A.34:** | System repeatability of atorvastatin | 125 |
| **Table A.35:** | System repeatability of fluvastatin | 125 |
| **Table A.36:** | System repeatability of pitavastatin | 126 |
| **Table A.37:** | System repeatability of pravastatin | 126 |
| **Table A.38:** | LOD and LOQ results of atorvastatin | 131 |
| **Table A.39:** | LOD and LOQ results of fluvastatin | 132 |
| **Table A.40:** | LOD and LOQ results of pitavastatin | 132 |
| **Table A.41:** | LOD and LOQ results of pravastatin | 133 |
| **Table A.42:** | The LOD and LOQ results of the different statins | 134 |

## APPENDIX B: FORMULATION AND STABILITY DETERMINATION OF AN OPTIMISED O/W NANO-EMULSION CONTAINING SELECTED STATINS


| | | |
|---|---|---|
| **Table B.1:** | Ingredients, suppliers and batch numbers of constituents used to formulate the nano-emulsions | 141 |
| **Table B.2:** | Statin formula codes | 141 |
| **Table B.3:** | The measured pH values for the nano-emulsions (**NE1** and **NE2**) containing statins | 145 |
| **Table B.4:** | Zeta-potential (mV) values of the nano-emulsions (**NE1s** and **NE2s**) containing statins | 146 |
| **Table B.5:** | The average droplet size, as well as the PdI of **NE1** and **NE2** | 148 |
| **Table B.6:** | Viscosity (cP) and torque (%) readings of **NE1s** and **NE2s** (rotation speed at 200 rpm) | 151 |
| **Figure B.7:** | Entrapment efficacy (%EE) of the nano-emulsions (**NE1s** and **NE2s**) containing statins | 155 |
| **Table B.8:** | Formula used to prepare the optimised **NEs** containing statins | 157 |
| **Table B.9:** | Formula used to prepare **PNE1** | 158 |
| **Table B.10:** | The average pH for **PNE1** compared to the **NE1s** | 159 |
| **Table B.11:** | Average zeta-potential (mV) of **PNE1** compared to **NE1s** formulated with different statins | 160 |
| **Table B.12:** | The average droplet size as well as PdI for the **PNE1** and the **NE1s** | 162 |
| **Table B.13:** | Viscosity readings of the **PNE1** compared to the **NE1s** | 164 |

## APPENDIX C: FORMULATING AND CHARACTERISATION OF A NANO-EMULGEL COMPARED TO AN OPTIMISED O/W NANO-EMULSION BOTH CONTAINING STATINS IN COMBINATION WITH APRICOT KERNEL OIL


| | | |
|---|---|---|
| **Table C.1:** | Formula used to prepare nano-emulgel containing statins | 176 |
| **Table C.2:** | The measured average pH of the **NEGs** and **NE1s** | 179 |
| **Table C.3:** | Average zeta-potential (mV) of the **NEGs**, as well as the **NE1s** | 180 |
| **Table C.4:** | The average droplet size and the average PdI values of the **NEGs** and **NE1s** | 183 |
| **Table C.5:** | Viscosity readings of the **NE1s** and the **NEGs** | 185 |


## APPENDIX D: DIFFUSION STUDIES OF O/W NANO-EMULSIONS AND NANO-EMULGELS CONTAINING STATINS AND APRICOT KERNEL OIL


| | | |
|---|---|---|
| **Table D.1:** | The average amount of statins (mg/ml) soluble in *n*-octanol and PBS (pH 7.4) | 202 |
| **Table D.2:** | Determined log D values of the statins | 203 |
| **Table D.3:** | The average %released, the average and median flux (µg/cm$^2$.h) for each formula obtained after a 6 h membrane release study | 212 |
| **Table D.4:** | The average percentage, average amount and median concentration of statins that diffused through skin from each formula (**NE1** and **NEG**) during the *in vitro* skin diffusion studies after 12 h (n = quantity of Franz diffusion cells) | 213 |
| **Table D.5:** | The average and median concentration (µg/ml) of the statins present in the SCE and ED from each formula (**NE** and **NEG**) during tape stripping (n = quantity of Franz diffusion cells) | 220 |
| **Table D.6:** | The p-values of the one-way ANOVAs that were performed on the statin for the different **NE1s** and **NEGs** formulas | 230 |
| **Table D.7:** | Tukey's HSD post-hoc tests of the statins in the different **NE1s** and **NEGs** (separately) according to the homogenous groups (in terms of means) | 231 |
| **Table D.8:** | The p-values of the one-way ANOVA performed on both the **NE1s** and **NEG** that diffused through the skin | 231 |
| **Table D.9:** | Tukey's HSD post-hoc test of the **NE1s** and **NEG** formulas that diffused through the skin, grouped according to their homogenous relationships (respectively) with the cumulative concentrations as a variable | 232 |

**Table D.10:** The p-values of the ANOVA for the effects of the statin, type of formula (**NE1s** and **NEGs**) and the skin layers (ED or SCE) 232

**Table D.11:** The p-values of the one-way ANOVA performed on the statin to compare the type of formula (**NE1s** and **NEGs**) with the skin layer (SCE and ED) 233

**Table D.12:** T-tests for comparisons of the skin layers presented in combinations of the statin and the type of formula 234

**Table D.13:** Tukey's HSD post-hoc of the different formulas (**NE1** and **NEG**) containing statins in combination with the layer of the skin (SCE and ED) the statin presented in 234

## APPENDIX E: CYTOTOXICITY STUDIES OF O/W NANO-EMULSIONS

**Table E.1:** Materials utilised during the *in vitro* cytotoxicity studies 245

**Table E.2:** Statin solutions dosed in different concentrations for MTT as well as NR 249

**Table E.3:** **NE1s** and **PNE1** dosed in different concentrations for MTT as well as NR 250

**Table E.4:** Tween® 80, Span® 60 and Span® 60-oil combination dosed in different concentrations for MTT as well as NR 250

**Table E.5:** The cell viability (%) of the statin solutions dosed in different concentrations during the MTT-assay 253

**Table E.6:** The cell viability (%) of the **NE1s** and the **PNE1** dosed in different concentrations during the MTT-assay 255

**Table E.7:** The cell viability (%) of the excipients dosed in different concentrations during the MTT-assay 257

**Table E.8:** Calculated $IC_{50}$ values of statin solutions, **NE1s**, **PNE1** and the excipients from the MTT-assay results 260

**Table E.9:** The cell viability (%) of the statin solutions dosed in different concentrations during the NR-assay 261

**Table E.10:** The cell viability (%) of the **NE1s** and the **PNE1** dosed in different concentrations during the NR-assay 263

**Table E.11:** The cell viability (%) of the excipients dosed in different concentrations during the NR-assay 266

**Table E.12:** Calculated $IC_{50}$ values of statin solutions, **NE1s**, **PNE1** and the excipients from the NR-assay results 268

# LIST OF EQUATIONS


**CHAPTER 2: FORMULATION AND TRANSDERMAL DELIVERY OF NANO-EMULSIONS COMPARED TO SEMI-SOLID (NANO-EMULGEL) FORMULATIONS CONTAINING STATINS AND APRICOT KERNEL OIL**

**Equation 2.1:** $$\%ionised = \frac{100}{1 + antilog(pKa - pH)}$$ 27

**Equation 2.2:** $$\%unionised = 100 - \%ionised$$ 27

**CHAPTER 3: ARTICLE FOR PUBLICATION IN DIE PHARMAZIE**

**Equation 3.1:** $y = mx + c$ 48

**Equation 3.2:** **LOD =** 3.3 x σ/S 50

**Equation 3.3:** **LOQ =** 10 x σ/S 50

**APPENDIX A: VALIDATION OF AN HIGH PERFORMANCE LIQUID CHROMATOGRAPHIC (HPLC) ASSAY FOR ATORVASTATIN, FLUVASTATIN, PITAVASTATIN AND PRAVASTATIN**

**Equation A.1:** $y = mx + c$ 99

**Equation A.2:** DL = 3.3 x σ/S 133

**Equation A.3:** QL = 10 x σ/S 133

**APPENDIX B: FORMULATION AND STABILITY DETERMINATION OF AN OPTIMISED O/W NANO-EMULSION CONTAINING SELECTED STATINS**

**Equation B.1:** %EE = [(Ct – Cf)/Ct] x 100 154

## APPENDIX D:

**Equation D.1** $$Log\ D\ =\ Log\left(\frac{concentration\ statin\ -\ octanol}{concentration\ statin\ PBS}\right)$$ 203

## APPENDIX E: CYTOTOXICITY STUDIES OF O/W NANO-EMULSIONS

**Equation E.1:** $C_1V_1 = C_2V_2$ 247

**Equation E.2:** $$\%live/viable\ cells\ =\ \frac{(Sample_{560\,-\,630})\,-\,(Blank_{560\,-\,630})}{(Negative\ control_{560\,-\,630})\,-\,(Blank_{560\,-\,630})}$$ 252

**Equation E.3:** $y = mx + c$ 259

# ABBREVIATIONS

| | |
|---|---|
| **%EE** | Entrapment efficiency |
| **%RSD** | Percentage relative standard deviation |
| **A*β*** | Amyloid-*Beta* |
| **ACN** | Acetonitrile |
| **AFB** | Aktiewe farmaseutiese bestanddele |
| **ANOVA** | Analysis of variance |
| **API** | Active pharmaceutical ingredient |
| **APVMA** | Australian Pesticides and Veterinary Medicines Authority |
| **ATL** | Analytical Technology Laboratory |
| **CHD** | Coronary heart disease |
| **$CO_2$** | Carbon dioxide |
| **CVD** | Cardiovascular disease |
| **CYP** | Cytochrome P (Hepatic enzyme) |
| **DMEM** | Dulbecco's Modified Eagle Medium |
| **DMSO** | Dimethyl sulfoxide |
| **DNA** | Deoxyribonucleic acid |
| **ED** | Epidermis-dermis |
| **EDTA** | Trypsin-Versene® |
| **FBS** | Foetal bovine serum |
| **FDA** | Food and Drug Administration |
| **FC** | Franz cells |
| **FH** | Familial hypercholesterolemia |
| **H+** | Hydrogen ions |
| **$H_2O_2$** | Hydrogen peroxide |

| | |
|---|---|
| **HaCaT** | Human keratinocytes / menslike keratinosiete |
| **HBA** | Hydrogen ion acceptor bonds |
| **HBD** | Hydrogen ion donor bonds |
| **HCl** | Hydrochloric acid |
| **HDL** | High density lipoprotein |
| **HDVC** | Hoëdrukvloeistofchromatografiese |
| **HLB** | Hydrophilic-lipophilic balance |
| **HMG-CoA** | 3-hydroxy-3-methyl-glutaryl-coenzyme A |
| **HPLC** | High performance liquid chromatographic |
| **HRTEM** | High-resolution transmission electron microscopy |
| **HSD** | Honestly significant difference |
| **HTN** | Hydrogel-thickened nano-emulsion |
| **$IC_{50}$** | Concentration to which compounds inhibited 50% of the cell growth |
| **ICH** | International Conference of Harmonisation |
| **IDL** | Intermediate-density lipoprotein |
| **$KH_2PO_4$** | Potassium dihydrogen orthophosphate |
| **LAMB** | Laboratory for Applied Molecular Biology |
| **LDH** | Lactate dehydrogenase |
| **LDL** | Low density lipoprotein |
| **LOQ** | Limit of quantification |
| **LOD** | Limit of detection |
| **Log D** | Octanol-buffer distribution coefficient |
| **Log P** | Octanol-water partition coefficient |
| **MTT** | Methylthiazol tetrazolium |
| **NaOH** | Sodium hydroxide |
| **NE** | Nano-emulsion |

| | |
|---|---|
| **NE1** | O/w nano-emulsion with a Tween® 80:Span® 60 ratio of 3:3 |
| **NE1A** | 2% atorvastatin in nano-emulsion |
| **NE1F** | 2% fluvastatin in nano-emulsion |
| **NE1Pi** | 2% pitavastatin in nano-emulsion |
| **NE1Pr** | 2% pravastatin in nano-emulsion |
| **NE2** | O/w nano-emulsion with a Tween® 80:Span® 60 ratio of 2:3 |
| **NEG** | Nano-emulgel (Optimised nano-emulsion with Carbopol® Ultrez 20) |
| **NEGA** | 2% atorvastatin in nano-emulgel |
| **NEGF** | 2% fluvastatin in nano- emulgel |
| **NEGPi** | 2% pitavastatin in nano- emulgel |
| **NEGPr** | 2% pravastatin in nano- emulgel |
| **$NH_4OH$** | Ammonia |
| **NR** | Neutral red |
| **NRF** | National Research Foundation |
| **NWU** | North-West University |
| **NCEP** | National Cholesterol Education Program |
| **OH-** | Hydroxide ions |
| **O/w** | Oil-in-water / olie-in-water |
| **OECD** | Organisation for Economic Co-operation and Development |
| **OM** | Optical microscopy |
| **PBS** | Phosphate buffer solution |
| **PCS** | Photon correlation spectroscopy |
| **PdI** | Polydispersity index |
| **Pen/Strep** | Penicillin/Streptomycin |
| **PNE1** | Optimised o/w nano-emulsion placebo |
| **PVDF** | Polyvinylidene fluoride |

| | |
|---|---|
| **SCE** | Stratum corneum-epidermis |
| **SC** | Spindle (cylindrical) |
| **SD** | Standard deviation |
| **TC** | Total cholesterol |
| **TEM** | Transmission electron microscopy |
| **THF** | Tetrahydrofuran |
| **USP** | United States Pharmacopeia |
| **UV** | Ultra violet |
| **v/v** | Volume per volume |
| **VLDL** | Very low density protein |
| **W/o** | Water-in-oil |
| **w/v** | Weight per volume |
| **w/w** | Weight per weight |

# CHAPTER 1

INTRODUCTION, RESEARCH PROBLEM AND AIMS

## 1.1 Introduction

Cholesterol is an insoluble lipid molecule present in human body cells, especially the liver, brain and kidneys (Scherr & Zidenberg-Cherr, 2016:1). These lipid molecules help to maintain a healthy life as they are essential to sustain cellular structure, aid the syntheses of hormones (oestrogen and testosterone), bile acids, vitamin D (Scherr & Zidenberg-Cherr, 2016:1) and uphold brain function and development (Zhang & Liu, 2015:254).

Cholesterol requires specific transporters to travel in the bloodstream (Crawford, 1996:341). These transporters, known as lipoproteins, are produced by the liver and intestines (Onwe *et al.,* 2015:24) and facilitate lipid movement from the intestine to the liver and between the liver and cells in the body (Onwe *et al.,* 2015:24). Lipoproteins are classified into three categories according to the density of their particles (Rohilla *et al.,* 2012:15), namely very low-density lipoprotein (VLDL), low-density lipoprotein (LDL) and high-density lipoprotein (HDL), also known as lipoprotein-cholesterol lipids (Rohilla *et al*., 2012:15). Elevated blood cholesterol, particularly transported by LDL, also identified as "bad" cholesterol, can cause health risks such as cardiovascular diseases (CVDs) (Onwe *et al.,* 2015:24).

Elevated blood cholesterol can be revealed with a lipid profile serum test to detect the amount of triglycerides and cholesterol (HDL & LDL) present in the bloodstream (Onwe *et al.,* 2015:24), which assists in diagnosis of hyperlipidaemia (hypercholesterolemia) and appropriate medical treatment (Onwe *et al.,* 2015:24).

There are five main classed medications utilised to treat primary hyperlipidaemia, namely statins, nicotinic acid, cholesterol absorption inhibitors, fibric acid and bile acid binding resins (Braamskamp *et al.,* 2012:759; Hasani-Ranjbar *et al.,* 2010:2935; Rohilla *et al.,* 2012:16). Statins, the first-line treatment for primary hyperlipidaemia due to their ability to lower LDL as well as triglycerides (Robinson & Goldberg, 2011:19), are classified as 3-hydroxy-3-methyl-glutaryl-coenzyme A (HMG-CoA) reductase inhibitors, with both anti-atherosclerotic and obstructive tumour-cell growth abilities (Stancu & Sima, 2001:385).

Statins as are administered orally (Robinson & Goldberg, 2011:19). Oral administration of medicine has many advantages overall, however there are inadequacies that occur where statins are concerned. These inadequacies include reduced systemic bioavailability as a result of either extensive clearance of statins by means of liver enzymes (hepatic clearance),

or statin-stomach content interaction (Marrow *et al*., 2007:37; Naik *et al*., 2000:319). Given that the bioavailability of statins is low, drug interactions that affect statin metabolism can increase serum levels, escalating the risk of side effects, especially in patients with liver disease (Piepho, 2000:36). Statins can also be responsible for side effects such as elevated serum aminotransferase levels and an increased risk of hepatic toxicity (McKenney *et al.,* 2007:89), and can cause gastro-intestinal side-effects, i.e. flatulence, nausea and vomiting, difficulty swallowing, indigestion, diarrhoea, constipation and abdominal cramps (Mancini *et al.,* 2013:1553). Due to these inadequacies and side effects of oral administered statins, an alternative administration route, more specifically transdermal delivery route will be investigated.

Effective transdermal delivery of active pharmaceutical ingredients (APIs) requires permeation of APIs through the skin to achieve systematic circulation by applying a preparation topically (Kala & Juyal, 2018:2190). The skin is the largest and heaviest organ of the human body, with a surface area of roughly 2 $m^2$ and a weight of up to 5 kg (Godin & Touitou, 2007:1153). This organ has various functions, mainly to serve as an obstruction mechanism to protect the human body from external environmental elements (Flynn, 2002:188). Although there are many contradictions in literature, Foldvari (2000:417), among others, classifies the human skin into three closely stacked layers: the epidermis, dermis and hypodermis. The epidermis is divided into two sub-sections (outside to inside), the non-viable epidermis (stratum corneum) and the viable epidermis with sub-layers as stratum granulosum, stratum spinosum and stratum basale (Kute & Saudagar, 2013:272; Ng & Lau, 2015:2). The stratum corneum is known as the rate-limiting barrier (El Maghraby *et al*., 2008:204), which also serves as the protective shield of the skin (Bouwstra & Ponec, 2006:2081; Venus *et al*., 2011:471). This structure complicates the process of permeation for transdermal delivery of both hydrophilic and lipophilic APIs (Baibhav *et al*., 2011:66). To address this challenge, APIs need to comply with ideal physiochemical characteristics (Naik *et al.,* 2000:319) with regards to partition coefficient (log P), molecular weight, melting point, aqueous solubility, diffusion coefficient, pKa (Williams, 2013:682), pH and polarity (Rastogi & Yadav, 2012:165).

The statins utilised in this study are not completely compliant with the ideal physiochemical characteristics for transdermal delivery, as a result the APIs need to be formulated within a carrier system to improve skin permeation (Gabera *et al.,* 2017:75). Various carrier systems are available of which nano-emulsions (Gabera *et al.,* 2017:75) will be utilised for the purpose of this study for transdermal delivery of statins.

Nano-emulsions consist of two phases, the oil phase and the water phase, in which either one is dispersed into another in the form of droplets within the nanometre scale (100 – 500 nm) (Nalini *et al.,* 2017:1453). As a result of the combination of two immiscible liquid phases (oil phase and water phase) (Kumar, 2014:1), surfactants are a necessity in the formulation of nano-emulsions to ease the dispersion process and ensure stability (Mason *et al.,* 2006:37; Nalini *et al.,* 2017:1453), since they have the ability to decrease interfacial tension between the two phases and enhance phase compatibility.

Nano-emulsions possess high degrees of stability and low tendencies to form precipitant or creaming (Shah *et al.,* 2010:25). In addition, nano-emulsions have a major advantage, as they are able to penetrate the skin (Shah *et al.,* 2010:25). To complete the formulation of the nano-emulsions and further penetration of statins in the formula, a penetration enhancer will be included.

Penetration enhancers alter and lessen challenges that the barrier of the skin present, consequently enhancing permeation and absorption of APIs (Alexander et al., 2012:29; Boglarka et al., 2016:1135). Penetration enhancers are classified into six categories, namely physical enhancers, particulate systems, drug vehicle based, biochemical approach, natural penetration enhancers and chemical enhancers (Lakshmi *et al.,* 2017:10). In this study, apricot kernel oil, classified as a natural penetration enhancer, will be studied. Natural penetration enhancers are dominant penetration enhancers as they interact with cellular corneocytes to eliminate matters of lamellar bodies by disrupting lipophilic bilayers (Wang *et al.,* 2003:1612; Williams, 2013:694), thus enhancing flux of APIs across the stratum corneum (Vermaak *et al.,* 2011:922). Apricot kernel oil, originating from cold pressed dried kernels of apricots, appears as a light coloured oily substance with a nutty odour (Healthguidance, 2017). Apricot kernel oil is widely used in skin products (Healthguidance, 2017) and contains similar fatty acids present in the human skin (Wang, 2012:1745); this occurrence lowers the probability of skin irritations (Vermaak *et al.,* 2011:922). Apricot kernel oil is also used in massage therapy for its moisturising and soothing effect on dry, irritated, sensitive and premature aging skin (Healthguidance, 2017).

In this study, an oil-in-water (o/w) nano-emulsion will be formulated, which will be compared to a nano-emulgel. A nano-emulgel is simply a nano-emulsion with a gelling agent, also known as thickening agents, added to the formulation (Basera *et al.,* 2015:1872; Chellapa, 2015:45; Eid *et al.,* 2014:1). These gel-like formulations decrease interfacial and surface tension even more than nano-emulsions, which tend to enhance the viscosity (Chellapa, 2015:45) and increase skin permeability (Chellapa, 2015:44, Eid *et al.,* 2014:1).

## 1.2 Research problem

The first research problem is oral administration of statins encounter hepatic first-pass clearance and increases the risk for hepatic toxicity (McKenney *et al.,* 2007:89). In addition, gastro-intestinal side effects, such as flatulence, nausea and vomiting, difficulty swallowing, indigestion, diarrhoea, constipation and abdominal cramps, may occur (Mancini *et al.,* 2013:1553).

The second research problem is the transdermal delivery of statins. Drug penetration and permeation through the skin are significantly affected by the physical properties of the skin layers (Ng & Lau, 2015:2). Furthermore, the stratum corneum is lipophilic and the subsequent layers hydrophilic, therefore, it forms a barrier preventing API penetration through the skin (Foldvari, 2000:418).

## 1.3 Aims and objectives

The aim of this study will be to examine transdermal delivery of statins through the formulation of nano-emulsions, compared to nano-emulgels, with apricot kernel oil as a penetration enhancer.

The objectives of this study will be to:

- Obtain and validate an HPLC (high performance liquid chromatography) method for transdermal statin delivery analysis.
- Determine statin aqueous solubility and octanol-buffer distribution coefficient (log D).
- Develop and formulate a single optimal nano-emulsion and nano-emulgel formula in which 2% statin (atorvastatin, fluvastatin, pravastatin and pitavastatin) will be stable.
- Physical and chemical characterisation of the formulas, i.e. visual inspection, pH, zeta-potential, droplet size, viscosity and morphology.
- Establish the release rate of statins from the nano-emulsion dispersions compared to nano-emulgel formulations by means of membrane release studies.
- Determine transdermal delivery of statins from nano-emulsion dispersions compared to nano-emulgel formulations through the process of tape stripping.
- Evaluate the cytotoxic effect of statin solutions, statin formulated in nano-emulsions, placebo nano-emulsion and excipients (surfactants and apricot kernel oil) on human skin keratinocytes cell lines (HaCaT) by means of methylthiazol tetrazolium (MTT) and neutral red (NR) assays.

**References**


Alexander, A., Dwivedi, S., Ajazuddin, Giri, T.K., Saraf, S., Saraf. S. & Tripathi, D.K. 2012. Approaches for breaking the barrier of drug permeation through transdermal drug delivery. *Journal of controlled release,* 164:26-40.

Baibhav, J., Gurpreet, S., Rana, A.C., Seema, S. & Vikas, S. 2011. Emulgel: a comprehensive review on the recent advances in topical drug delivery. *International research journal of pharmacy*, 2:66-70.

Basera, K., Bhatt, G., Kothiyal, P. & Gupta, P. 2015. Nanoemulgel: a novel formulation approach for topical delivery of hydrophobic drugs. *World journal of pharmacy and pharmaceutical sciences*, 4:1871-1886.

Boglarka, B., Gabor, V., Szilvia, B., Maria, B., Andras, K., Balint, S., Krisztina, T., Piroska, S. & Erzsebet, C. 2016. Investigation of the efficacy of transdermal penetration enhancers through the use of human skin and a skin mimic artificial membrane. *Journal of pharmaceutical sciences,* 105:1134-1140.

Braamskamp, M.J., Wijburg, F.A. & Wiegman, A. 2012. Drug therapy of hypercholesterolaemia in children and adolescents*. Drugs,* 72:759-72.

Bouwstra, J.A. & Ponec, M. 2006. The skin barrier in healthy and diseased state. *Biochimica et Biophysica Acta*, 1758:2080-2095.

Chellapa, P., Mohamed, A.T., Keleb, E.I., Elmahgoubi, A., Eid, A.M., Issa, Y.S. & Elmarzugi, N.A. 2015. Nanoemulsion and nanoemulgel as a topical formulation. *IOSR journal of pharmacy*, 5(10):43-47.

Eid, A.M., El–Enshasy, H.A., Aziz, R. & Elmarzugi, N.A. 2014. Preparation, characterization and anti–inflammatory activity of Swietenia macrophylla nanoemulgel. *Journal of nanomedicine and nanotechnology*, 5:1-10.

El Maghraby, G.M., Barry, B.W. & Williams, A.C. 2008. Liposomes and skin: from drug delivery to model membranes. *European Journal of Pharmaceutical Sciences*, 34:203-222.

Flynn, G.L. 2002. Cutaneous and transdermal delivery - processes and system of delivery. (*In* Banker, G.S. & Rhodes, C.T., eds. Modern pharmaceutics. 4th ed. New York: Marcel Dekker. p. 187-235).

Foldvari, M. 2000. Non-invasive administration of drugs through the skin: challenges in delivery system design. *Pharmaceutical Science & Technology Today*, 3(12):417-425.

Gabera, M., Medhata, W., Hanya, M., Sahera, N., Fang, J., Elzoghby, A. 2017. Protein-lipid nanohybrids as emerging platforms for drug and gene delivery: Challenges and outcomes. *Journal of Controlled Release,* 254:75-91.

Godin, B. & Touitou, E. 2007. Transdermal skin delivery: Predictions for humans from in vivo, ex vivo and animal models. *Advanced drug delivery reviews,* 59:1158.

Hasani-Ranjbar, S., Nayebi, N., Moradi, L., Mehri, A., Larijani, B. & Abdollahi, M. 2010. The efficacy and safety of herbal medicines used in the treatment of hyperlipidemia; a systematic review. *Current Pharmaceutical Design,* 16:2935-47.

Healthguidance. 2017. http://www.healthguidance.org/entry/1807/1/Benefits-of-Apricot-Kernel -Oil.html Date of access: 12 June 2017.

Kala, S., Juyal, D. 2018. Recent developments on natural transdermal penetration enhancers. *International journal of pharmaceutical sciences and research*, 9(6):2190-2196.

Kute, S.B. & Saudagar, R.B. 2013. Emulsified gel: a novel approach for delivery of hydrophobic drugs: An overview. *Journal of Advanced Pharmacy Education and Research,* 3:368-376.

Lakshmi, P.K., Samratha, K.D., Prasanthi, B., Veeresh, A.C. 2017. Oil as penetration enhancers for improved transdermal drug delivery. *International Research Journal of Pharmacy,* 8(4):9-17.

Mancini, G.B.J., Tashakkor, A.Y., Baker, S., Bergeron, J., Fitchett, D., Frohlich, J., Genest, J., Gupta, M., Hegele, R.A., Ng, D.S., Pearson, G.J., Pope, J. 2013. Diagnosis, prevention, and management of statin adverse effects and intolerance: Canadian working group consensus update. *Canadian journal of cardiology,* 29:1553-1568.

Marrow, D.I.J., McCarron, P.A., Woolfson, A.D. & Donnelly, R.F. 2007. Innovative strategies for enhancing topical and transdermal drug delivery. *The Open Drug Delivery Journal*, 1:36-59.

Mason, T.J., Wilking, J.N., Meleson, K., Chang, C.B & Graves, S.M. 2006. Nanoemulsions: Normation, structure and physical properties. *Journal of Physics-Condensed Matter*, 18:636-43.

McKenney, J.M. Davidson, M.H. Jacobson, T.A. Guyton, J.R. 2006. National lipid association statin safety assessment task force. *American journal of cardiology*, 97(8A):89C-94C.

Nalini, T., Kumari, V.S. & Basha S.K. 2017. Novel nanosystems for herbal drug delivery. *World journal of pharmacy and pharmaceutical sciences*, 6(5):1447-1463.

Naik, A., Kalia, Y.N. & Guy, R.H. 2000. Transdermal drug delivery: overcoming the skin's barrier function. *Pharmaceutical Science and Technology Today*, 3(9):318-326.

Ng, K.W., Lau, W.M. 2015. Skin deep: The basics of human skin structure and drug penetration. file:///C:/Users/22819509/Downloads/ng-2015-skin-deep.pdf. Date of access: 5 Oct. 2018.

Onwe, P.E., Folawiyo, M.A., Okike, P.I., Balogun, M.E., Umahi, G., Besong, E.E., Okorocha, A.E & Afoke, A.O. 2015. Lipid Profile and the growing concern on lipid related diseases. *Journal of Pharmacy and Biological Sciences,* 10(5):22-27.

Piepho, R.W. 2000. The Pharmacokinetics and Pharmacodynamics of Agents Proven to Raise High-Density Lipoprotein Cholesterol. The American journal of cardiology, 86(12A): 35L-40L.

Rastogi , V., Yadav, P. 2012. Transdermal drug delivery system: An overview. *Asian journal of pharmaceutics,* 161-170.

Robinson, JG. & Goldberg, AC. 2011. Treatment of adults with Familial Hypercholesterolemia and evidence for treatment*:* Recommendations from the National Lipid Association Expert Panel on Familial Hypercholesterolemia. *Journal of clinical lipidology,* 5:S18–S29.

Rohilla, A., Dagar, N., Rohilla, S., Dahiya, A. & Kushnoor, A. 2012. Hyperlipidemia- A deadly pathological condition*. International journal of current pharmaceutical research,* 4(2):15-18.

Scherr, R.E., Zidenberg-Cherr, S. 2016. Nutrition and health info sheet: Cholesterol. https://nutrition.ucdavis.edu/sites/g/files/dgvnsk426/files/content/infosheets/fact-consumer-cholesterol.pdf. Date off access: 17 Oct 2018.

Shah, P., Bhalodia, D. & Shelat, P. 2010. Nanoemulsions: a pharmaceutical review. *Systemic reviews in pharmacy*, 1:24-31.

Stancu, C & Sima, A. 2001. Statins: mechanism of action and effects. *Journal of cellular and molecular medicine* 5(4):378-387.

Venus, M., Waterman, J. & McNab, I. 2011. *Basic physiology of the skin. Surgery* (Oxford), 29:471-474.

Vermaak, I., Kamatou, G.P.P., Komane-Mofokeng, B., Viljoen, A.M. & Beckett, K. 2011. African seed oils of commercial importance: cosmetic application. *South African journal of botany*, 77:920-933.

Wang, W. 2012. Evaluation of siberian apricot (Prunus sibirica L.) germplasm variability for biodiesel properties. *Journal of American oil chemists' society*, 89:1743-1747.

Wang, Y., Fan, Q., Song, Y. & Michnaik, B. 2003. Effects of fatty acids and iontophoresis on the delivery of midodrine hydrochloride and the structure of human skin. *Pharmaceutical research*, 20:1612-1618.

Williams, A.C. 2013. Topical and transdermal drug delivery. *In* Aulton, M.E., *ed*. Aulton's pharmaceutics: the design and manufacture of medicines. 3rd ed. London: Churchill Livingstone. p. 675-697.

Zhang, J., Liu, Q. 2015. Cholesterol metabolism and homeostasis in the brain. *Protein & cell,* 6(4):254-264.

# CHAPTER 2

FORMULATION AND TRANSDERMAL DELIVERY OF NANO-EMULSIONS COMPARED TO SEMI-SOLID (NANO-EMULGEL) FORMULATIONS CONTAINING STATINS AND APRICOT KERNEL OIL

## 2.1 Introduction

Cholesterol is a lipid compound, produced by the liver, which forms an essential part of body cells, particularly the cell walls. Here it provides cell stability and assists cell communication to ensure that body cells perform as a unit (Scherr & Zidenberg-Cherr, 2016:1). Cholesterol is a core component in the brain, which contains up to 20% of the body's cholesterol (Zhang & Liu, 2015:254), identifying it as the highest cholesterol containing organ (Ferris *et al*., 2017:1189). There is great importance in the maintenance of brain cholesterol levels, as cholesterol aids with the growth and development of dendrites, synapses and neurons to sustain normal brain function and development and assist with axonal regulation (Zhang & Liu, 2015:254). Furthermore, cholesterol serves as a forerunner of corticosteroids, sex hormones, bile acids and vitamin D produced in the body (Scherr & Zidenberg-Cherr, 2016:1).

Although cholesterol is essential for normal body and mind function, an unusual elevation of blood cholesterol levels can occur, known as hypercholesterolemia or hyperlipidaemia. This occurrence has extensively been connected to health complications, for example atherosclerosis and CVDs. Elevated blood cholesterol can be revealed with lipid profile serum tests, which is a diagnostic method used to determine the appropriate medical therapy (Onwe *et al*., 2015:24).

The medical therapy currently available to treat hyperlipidaemia are statins, nicotinic acid, cholesterol absorption inhibitors, fibric acid and bile acid binding resins (Braamskamp *et al.,* 2012:759; Hasani-Ranjbar *et al.,* 2010:2935; Rohilla *et al.,* 2012:16). Statins are the first-line treatment (Robinson & Goldberg, 2011:19; Schierwagen *et al.,* 2017:G407) as this pharmacological class inhibits the enzyme responsible for endogenous cholesterol (Schierwagen *et al.,* 2017:G407), earning them the identity of 3-hydroxy-3-methyl-glutaryl-coenzyme A (HMG-CoA) reductase inhibitors (Fong, 2016:663).

Statins are currently registered as an oral treatment (Robinson & Goldberg, 2011:19), however, oral administered statins present with inadequacies, such as gastrointestinal side effects (flatulence, nausea and vomiting, difficulty swallowing, indigestion, diarrhoea, constipation and abdominal cramps) (Mancini *et al.*, 2013:1553), and reduced systemic

bioavailability. The last mentioned is a result of either extensive clearance of statins by means of liver enzymes (cytochrome P-450) or statin-stomach content interaction (Marrow *et al.,* 2007:37; Naik *et al*., 2000:319). The occurrence of drug interactions can increase statin levels in the circulatory system, which can induce adverse effects (Piepho, 2000:36). Orally administered statins can also be responsible for side effects such as elevated serum aminotransferase levels, consequently, increasing the risk of hepatic toxicity (McKenney *et al.*, 2007:89; Schierwagen *et al*., 2017:G407).

Due to these inadequacies and side effects of oral administered statins, the transdermal delivery route will be investigated as a more suitable pathway of administration. This route entails drug delivery across the skin layers and into the circulatory system (Kala & Juyal, 2018:2190). One of the major factors to consider when investigating this route is the physical properties of the skin layers, since it influences drug delivery across the skin (Ng & Lau, 2015:2). The human skin consists of different layers, each constructed with various cells to perform specific roles (Ng & Lau, 2015:2). These layers are classified into three categories, e.g. the epidermis, dermis and underlying hypodermis (Ng & Lau, 2015:2). The epidermis is further divided into sub-layers, of which the stratum corneum is the most specialised layer (Baibhav *et al.*, 2011:66). The stratum corneum is the rate-limiting barrier known for its hydrophilic and lipophilic construction, which mainly poses challenges to APIs absorption (Baibhav *et al*., 2011:66).

Resulting from these challenges, literature has provided ideal physiochemical characteristics an API should possess to accomplish successful transdermal delivery (Naik *et al.,* 2000:319). Statins utilised in this study are non-compliant to many of the ideal physiochemical requirements for transdermal delivery (Naik *et al.,* 2000:319) with regard to log P or log D, molecular weight, melting point, aqueous solubility, diffusion coefficient, pKa (Williams, 2013:682), pH and polarity (Rastogi & Yadav, 2012:165). Consequently, statins need to be formulated within a carrier system to overcome the barrier posed by the skin (Gabera *et a*l., 2017:75).

Various carrier systems exist of which nano-emulsions (sonicated conventional emulsions), liposomes and nano-capsules are most frequently used for their eco-friendly, non-immunogenic and biocompatible nature (Gabera *et al.,* 2017:75). In addition, these systems are able to bypass hepatic metabolism, enhance absorption, prolong half-lives and reduce toxicity (Gabera *et al*., 2017:75). Nano-emulsions are the carrier system that will be researched for the transdermal delivery of the statins, which will be compared to nano-emulgels formulated from the optimised nano-emulsion formula.

A nano-emulgel is simply a nano-emulsion with a gelling-agent added to it (Basera *et al*., 2015:1872; Chellapa, 2015:45; Eid *et al*., 2014:1). These gel-like formulations decrease interfacial and surface tension even more than nano-emulsions, which tend to improve formulation viscosity (Chellapa, 2015:45) and increase skin permeability (Chellapa, 2015:44, Eid *et al*., 2014:1).

To further the improvement of skin permeability and API absorption, penetration enhancers (also known as sorption accelerants) are required in the formula (Kala & Juyal, 2018:2190). Penetration enhancers improve permeation and absorption of APIs by reversibly altering the challenges presented by the skin (Alexander *et al*., 2012:29; Boglarka *et al*., 2016:1135; Kala & Juyal, 2018:2190). Penetration enhancers are classified into six categories, namely physical enhancers, particulate systems, drug vehicle based, biochemical approach, natural penetration enhancers and chemical enhancers (Lakshmi *et al*., 2017:10).

Apricot kernel oil (*Prunus armeniaca*) was the chosen natural penetration enhancer and will be included in the formula as the oil phase, thus it has a double function, which includes serving as an oil phase, as well as having the function of enhanced penetration. Apricot kernel oil, procured from cold pressed dried kernels of apricots, presents as a light, oily substance with a nutty aroma (Healthguidance, 2017). Apricot kernel oil possesses pleiotropic healing benefits towards atopic dermatitis and inflammation (Hoag, 2018:17). This oil classifies as a natural penetration enhancer that disrupts the lipophilic bilayers of the skin by interfering with cellular corneocytes to eliminate matters of lamellar bodies (Wang *et al*., 2003:1612; Williams, 2013:694), which subsequently enhances the flux of APIs across the stratum corneum (Vermaak *et al*., 2011:922).

### 2.2 Defining cholesterol

Cholesterol is a fatlike molecule also known as lipids in the human bloodstream (Scherr & Zidenberg-Cherr, 2016:2). Cholesterol is insoluble in blood, therefore, it requires specific transporters to travel in the bloodstream (Rohilla *et al*., 2012:15). These transporters, known as lipoproteins, consist of a central part made up of cholesterol and triglycerides, with an exterior surface that contains protein (Rohilla *et al*., 2012:15). Lipoprotein particles are produced by the liver and some intestines to facilitate lipid transport from intestines to the liver and between the liver and functioning body cells (Jonas, 2002:483). Lipoprotein particles are classified according to their densities, as the density of these particles determine lipoprotein-cholesterol bindings. The lipoprotein-cholesterol lipids are classified as HDL, LDL and VLDL (Rohilla *et al*., 2012:15).

### 2.2.1 High density lipoprotein

HDL (good cholesterol) inhibits excess fat binding on artery walls. It binds and transports cholesterol to the liver to be metabolised (Rohilla *et al*., 2012:15). Ideal HDL levels are > 60 mg/dl, whereas < 40 mg/dl indicates a great risk for CVD. Elevated HDL levels may imply that the heart is healthy (Rohilla *et al*., 2012:15). HDL is also researched as topical wound-healing administration, since it has the pleiotropic effects aside from arterial functions to serve as an anti-inflammatory, atheroprotective cell protector with healing properties to the body (Gordts *et al*., 2014:419).

### 2.2.2 Low density lipoprotein

LDL transports hepatic and intestinal cholesterol to the rest of the body (Rohilla *et al*., 2012:15), more specific the organs, tissue, muscles and the heart (Onwe *et al.,* 2015:22). The ideal LDL level is < 100 mg/dl and can descend to 50 – 70 mg/dl, while levels of 160 – 189 mg/dl are referred to as elevated (Onwe *et al.,* 2015:24). Elevated levels of LDL, heightens the risk of CVDs and atherosclerosis (Mahmood *et al.,* 2009:14; Onwe *et al.,* 2015:23).

### 2.2.3 Very low-density lipoprotein

VLDL transports cholesterol similar to LDL and consists predominantly of fat (Onwe *et al.,* 2015:23). High concentrations of VLDL and triglycerides are also linearly linked to CVDs and atherosclerosis (Onwe *et al*., 2015:23). Surplus alcohol, sugar or calories are transformed to triglycerides to be transported by VLDL, where it accumulates in the fat cells of the body enhancing the risk of diabetes (Smelt, 2010:1625). The accepted triglyceride concentration is < 150 mg/dl, whereas values between 200 and 499 mg/dl are regarded as elevated, but concentration levels of 500 mg/dl and above, are regarded as abnormal and increase the risk of CVD (Onwe *et al.,* 2015:22).

Lipoprotein-cholesterols classified above, all contribute to the total cholesterol (TC). Guidelines of the National Cholesterol Education Programme (NCEP) specified the desired TC levels as < 200 mg/dl (adults) and < 180 mg/dl (children). The risk of cardiac episodes reduces when TC levels decline to 150 mg/dl, hence levels higher than 240 mg/dl represents hyperlipidaemia (Rohilla *et al*., 2012:15).

## 2.3 Hyperlipidaemia

Hyperlipidaemia is a chronic illness defined as an unusual high level of lipids detected in the blood plasma (Churchill-Livingstone's Dictionary, 2008). This illness, which has a mortality figure of approximately 4.4 million people annually, has been linked to CVDs, dominating with the highest mortality rate worldwide (Santaniello & Giannini, 2015:1).

### 2.3.1 Pathophysiology of hyperlipidaemia

Hyperlipidaemia is classified into two categories namely primary hyperlipidaemia and secondary hyperlipidaemia (Rohilla *et al*., 2012:16).

#### 2.3.1.1 Primary hyperlipidaemia

Primary hyperlipidaemia, also known as familial hypercholesterolemia (FH) is a congenital metabolic disorder resultant of a LDL receptor gene-coding defect. This defect causes elevated serum LDL cholesterol (Rohilla *et al*., 2012:16), which contributes to the growth of xanthomas, cholesterol accumulation in peripheral tissues, atherosclerosis (cholesterol residue on arterial walls) and coronary heart disease (CHD) (Fahed & Nemer, 2011:23).

#### 2.3.1.2 Secondary hyperlipidaemia

Secondary hyperlipidaemia is caused by underlying illnesses such as diabetes mellitus (due to high production of VLDL), hypothyroidism (caused by the reduction of cholesterol degradation), hyperadrenocorticism (result of induced VLDL production), polycystic ovary syndrome and elevated oestrogen levels in females, liver illness hypercholesterolemia and nephrotic syndrome (as a consequence of increased cholesterol production) (Rohilla *et al*., 2012:16).

In addition to the categories of hyperlipidaemia, an unhealthy lifestyle (high saturated fat diets), passiveness, obesity, alcohol abuse, menopause and medication (thiazide diuretics, beta-blockers, oral contraceptives, glucocorticosteroids, cyclosporine and retinoic acid) can also contribute to elevated cholesterol levels (Fatima *et al.,* 2017:118).

Although various categories of hyperlipidaemia exist, primary hyperlipidaemia is the elevated lipid abnormality focused on during this study.

### 2.3.2 Diagnoses of primary hyperlipidaemia

A lipid profile is a serum test performed to detect the amount of triglycerides and cholesterol (HDL and LDL) in the blood. The results of these serum tests accompanied by the patient's

risks for CVDs and other illnesses such as diabetes type 2 will determine the appropriate medical treatment (Onwe *et al.,* 2015:24).

### 2.3.3 Medical treatment of primary hyperlipidaemia

Five main classed medications are currently used to treat hyperlipidaemia namely statins, nicotinic acid, cholesterol absorption inhibitors, fibric acid and bile acid binding resins (Braamskamp *et al*., 2012:759; Hasani-Ranjbar *et al*., 2010:2935; Rohilla *et al.*, 2012:16).

To this day, statins persist as the preferred medical treatment for hyperlipidaemia for their ability to reduce LDL. Rare incidents have occurred where individuals' LDL levels do not reduce to the required level. In these uncommon cases, statins are prescribed in combination with nicotinic acid, cholesterol absorption inhibitors, fibric acid and bile acid binding resins to reach desirable LDL levels; however, combination therapy may result in severe myopathy and rhabdomyolysis (Zodda *et al.*, 2018:1).

Recent studies have also revealed two new lipid-reducing alternatives, namely lomitapide and mipomersen, for the treatment of FH by lowering LDL levels and in turn decreasing CVDs. However, the financial aspect of these novel alternatives remains to be of issue. Therefore, statins remain as the first line medical treatment for hyperlipidaemia (Zodda *et al.*, 2018:1).

## 2.4 Statins

Statins classified as HMG-CoA reductase inhibitors (Fong, 2016:663) are a major prescribed medicinal treatment worldwide, treating over 40 million patients who suffer from elevated cholesterol levels (Hennessy *et al.*, 2016:3). HMG-CoA reductase is responsible for the catalyses of the transformation of HMG-CoA to mevalonate to produce cholesterol (Fong, 2016:663). Statins are seen as one of the most significant medical discoveries of the 20$^{th}$ century (Hennessy *et al.*, 2016:3; Santaniello & Giannini, 2015:1) as they have the ability to decrease the cholesterol generated in the liver by reducing HMG-CoA reductase (Fong, 2016:663; Hennessy *et al.*, 2016:3). As a result, a lower intracellular cholesterol concentration causes an increased expression of LDL receptors on the surface of hepatocytes. LDL present in the blood will bind to these increased LDL-receptors, consequently lowering blood LDL concentrations (Fong, 2016:663). An additional advantage of the increased expression of LDL receptors is the lowering LDL precursors (VLDL and IDL (Intermediate-density lipoprotein)) (Zodda *et al.*, 2018:2). Statins can also increase the concentrations of HDL and reduce triglyceride concentration, which make them even more beneficial (Fong, 2016:663).

Since elevated cholesterol levels are related to atherosclerosis and CVDs (Fatima *et al.* 2017:120), statins have been able to reduce the occurrence of CVDs in high risk patients (Fatima *et al.* 2017:120; Fong, 2016: 663). This first line medical treatment has a dual function, unrelated to lipid altering effects. Statins have the ability to reduce the production of nonsteroidal isoprenoid complexes, derived from mevalonic acid (Fong, 2016:663), which inhibits inflammatory processes and promotes immunomodulatory and anti-microbial functions (Hennessy *et al.*, 2016:3).

Statins may also be connected to lowering the occurrence of vascular dementia, since some isoprenoid complexes are suggested to contribute to vascular dementia development (Schultz *et al.*, 2018:9). Statins have also proved promising effects towards lowering brain ischemia, due to their ability to reduce cell proliferation and platelet accumulation, as well as inhibition of LDL oxidation (Schultz *et al.*, 2018:9).

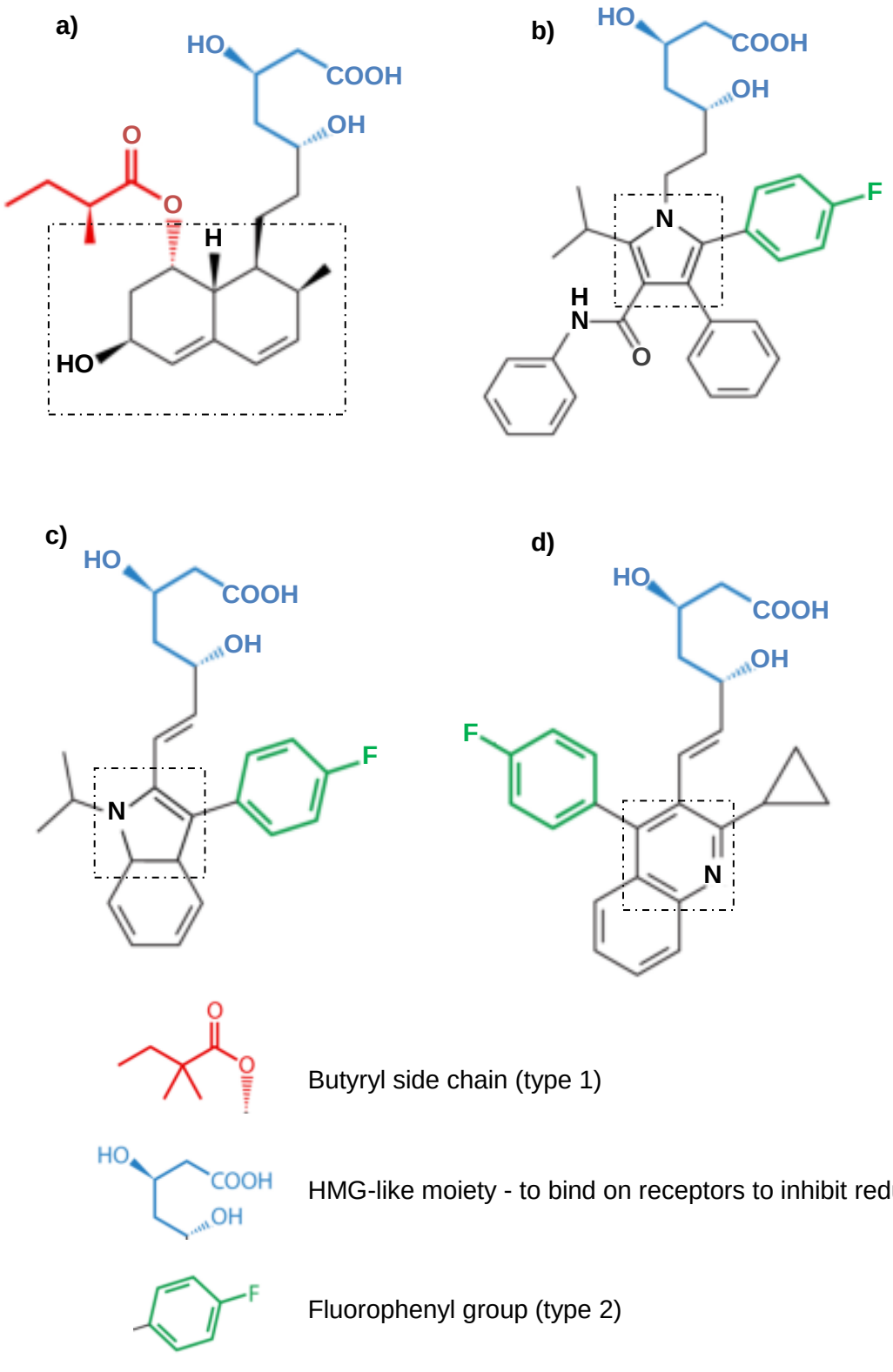


**Figure 2.1:** Adapted chemical structural representation of type 1 statin: a) pravastatin and of type 2 statins: b) atorvastatin, c) fluvastatin and d) pitavastatin (Hennessy *et al*., 2016:45).

Recent studies have proposed that a reduced risk of developing Alzheimer's disease and dementia in patients using statin therapy exist. Alzheimer's disease can be caused by the gathering of abundance amyloid-*β* (A*β*) peptide in crucial sections of the brain affecting cognition and memory (contributing factors are still unidentified). Since a decrease of 24S-hydroxycholesterol in the brain is linked to amyloid-*β* (A*β*) peptide reductase, statins may serve as a potential therapy for Alzheimer's disease; however, statins may cause reversible cognitive impairment (Schultz *et al.*, 2018:9).

The first statin, mevastatin, a metabolic product of *Penicillium citrinum* was discovered in 1976. Since then nine statins have been typified, hence, the Food and Drug Association of America (FDA) permitted seven statins to treat patients with elevated serum cholesterol levels (Hennessy *et al*., 2016:3). These approved statins are either developed from fermentation (lovastatin, pravastatin and simvastatin) or solely synthetic (atorvastatin, fluvastatin, pitavastatin and rosuvastatin) (Santaniello & Giannini, 2015:1).

Statins are separated into two classes according to their chemical structure (Hennessy *et al*., 2016:3). Type 1 statins (lipophilic) contain a decalin ring in their chemical structure (Santaniello & Giannini, 2015:1) with a butyryl side chain, and structurally bear a resemblance to mevastatin (Hennessy *et al*., 2016:3). Type 1 statins include lovastatin, pravastatin and simvastatin (Hennessy *et al*., 2016:3). Type 2 statins (lipophobic) contain a pyrimidinyl central ring connected to a fluorophenyl group instead of a butyryl side chain (type 1), and generally own longer side chains than type 1 statins (Hennessy *et al*., 2016:3). Type 2 statins include atorvastatin, cerivastatin (discontinued because of muscle toxicity), fluvastatin, pitavastatin and rosuvastatin (Hennessy *et al*., 2016:3).

For the purpose of this study atorvastatin, fluvastatin, pitavastatin and pravastatin will be investigated.

### 2.4.1 Administration of statins

Statins are currently only administered orally in tablet form to be taken at night as cholesterol synthesis mainly occurs during early morning hours (Cruz *et al*., 2008:E99). Although oral administration of medicine is the preferred route due to patient compliance, this route has various impediments regarding statins.

### 2.4.2 Impediments of oral treatment with statins

Oral administration of medicine has its advantages, although there are limitations that can occur where statins are concerned. These limitations include reduced bioavailability (Atorvastatin (12%), fluvastatin (10 - 35%), pitavastatin (> 60%) and pravastatin (18%)) as a result of either the major hepatic first-pass clearance of statins by CYP 450 liver enzymes (Atorvastatin (CYP 450 3A4), fluvastatin (CYP 450 2C9), pitavastatin (CYP 450 2C9) and pravastatin (CYP 450 3A4)) (Sahebzamani *et al*., 2014:3) or interaction with stomach content (Marrow *et al*., 2007:37; Naik *et al*., 2000:319; Zodda *et al.*, 2018:3). The occurrence of drug interactions, where drugs that inhibit CYP 450 liver enzymes are combined with statin therapy, can cause elevated statin levels in the circulatory system. Elevated circulatory statin levels can increase the possibility of adverse effects, especially in patients with liver disease (Piepho, 2000:36; Zodda *et al.*, 2018:3).

Statins can also be responsible for side effects such as an increased risk for hepatic toxicity resultant of elevated serum aminotransferase levels (McKenney *et al.,* 2007:89). Furthermore, oral administered statins can cause gastrointestinal side effects, i.e. flatulence, nausea and vomiting, difficulty swallowing, indigestion, diarrhea, constipation and abdominal cramps (Mancini *et al.,* 2013:1553).

Statins with the exception of pravastatin have great affinity for plasma proteins and are highly bound (atorvastatin 98%, fluvastatin 98% and pitavastatin 96%) resulting in low exposure to active, unbound drug and reduction in pharmacological effect (Fong, 2016:24; Zodda *et al.*, 2018:3). The low plasma protein binding of pravastatin (50%) allows the unbound drug to be up to 10-times higher than other statins, hence the hydrophilic nature of pravastatin ensures limited distribution (Zodda *et al.*, 2018:3).

Diverse effects of statin therapy, such as myopathy and/or rhabdomyolysis (Zodda *et al.*, 2018:1), are not regarded as limitations to overcome during this study, since this phenomenon is independent of the administration route.

The impediments mentioned regarding the oral treatment of statins, with the exception of myopathy and/or rhabdomyolysis, lead to the investigation of an alternative route of administration.

### 2.4.3 Alternative route of administration of statins

Due to these limitations and side effects, alternative administration routes should be researched; hence, this study will focus on the transdermal delivery route.

## 2.5 Transdermal route

The transdermal route of delivery was the primary route for drug administration centuries ago and includes delivering drugs systematically by applying a preparation on integrated skin (Kala & Juyal, 2018:2190). Transdermal delivery of drugs can enhance patient compliance, as it is non-invasive and can produce fewer gastrointestinal adverse effects (flatulence, nausea and vomiting, difficulty swallowing, indigestion, diarrhoea, constipation and abdominal cramps), since the administration route avoids hepatic metabolism (Rastogi & Yadav, 2012:163). Furthermore, the transdermal route delivers constant plasma concentrations for extended time periods, lessen inter-/intra-variations between patients (Kala & Juyal, 2018:2190) and tolerates the possibility of intervention, such as removal of the APIs applied on integrated skin to steer clear of overdosing (Rastogi & Yadav, 2012:163). Additionally, the skin has a rather large surface area for application of transdermal formulations (Rastogi & Yadav, 2012:163).

## 2.6 The human skin

The skin is classified as the largest, heaviest organ of the human body with a surface area of roughly 2 $m^2$ with a weight of approximately 5 kg (Godin & Touitou, 2007:1153). This organ acts as a protective barrier between the human organs and the external environment, as it retains body tissue and fluids (Flynn, 2002:188). The skin further prevents dehydration, regulates fat-soluble substance uptake and provides protection against UV-rays. The regulation of body temperature and blood pressure (by means of circulation) also adds to the importance of the skin. In addition, the skin aids in metabolism and synthesis, such as vitamin D production, and comprises antimicrobial together with anti-oxidative properties (Flynn, 2002:188; Mostafa *et al.,* 2015:795).

Drug penetration and permeation through the skin are significantly affected by the physical properties of the skin layers (Ng & Lau, 2015:2). The human skin consists of different layers, categorised as the epidermis, dermis and underlying hypodermis (Ng & Lau, 2015:2).

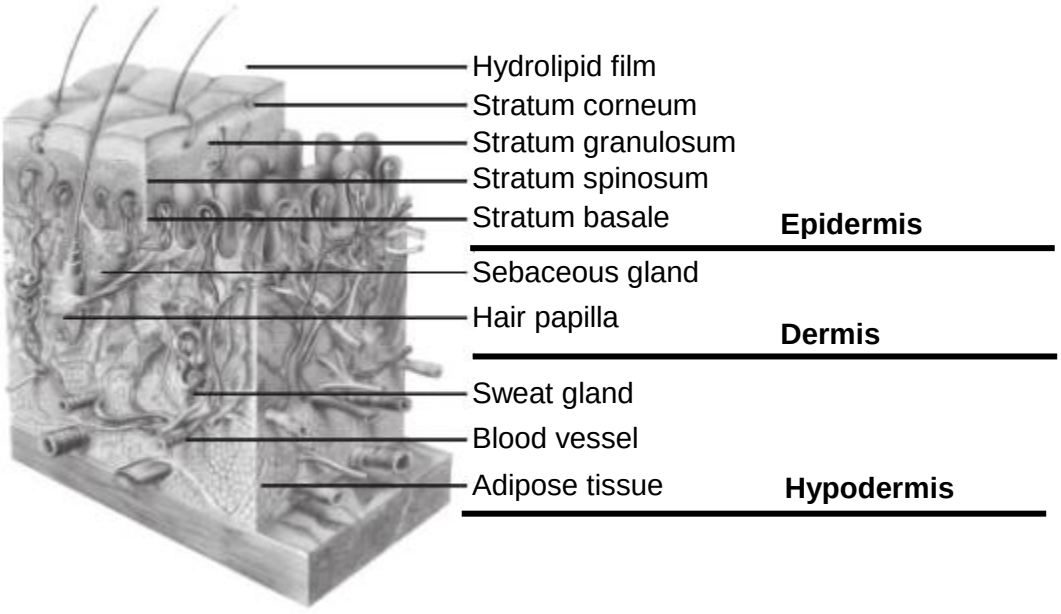


**Figure 2.2:** Adapted schematic representation of the human skin layers (Trommer & Neubert, 2006:107)

The epidermis is sectioned into two sub-sections (outside to inside), namely the non-viable epidermis (stratum corneum) and the viable epidermis with sub-layers (stratum granulosum, stratum spinosum and stratum basale) (Kute & Saudagar, 2013:272; Ng & Lau, 2015:2). The epidermis also includes appendageal elements such as sweat ducts and hair follicles (Ng & Lau, 2015:2).

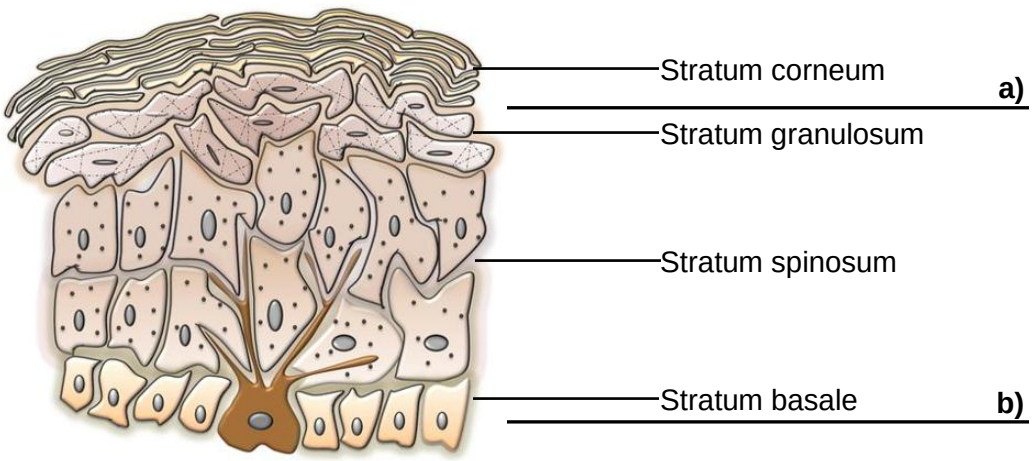


**Figure 2.3:** Adapted schematic representation of the epidermis, a) non-viable epidermis and b) viable epidermis (Natarajan *et al.,* 2014)

### 2.6.1 Viable epidermis (stratum granulosum, stratum spinosum and stratum basale)

The viable epidermis is a hydrophilic layer between the non-viable epidermis and the dermis and mainly consists of protein, water (Jepps *et al.,* 2013:155; Kute & Saudagar, 2013:372), keratinocytes and smaller quantities of Merkel cells, Langerhans cells and melanocytes (Geerligs, 2006:6). As the keratinocytes travel from the stratum basale to the surface of the skin (stratum corneum), they start to adjust in size, form and physical characteristics (Geerligs, 2006:7). The migration process begins in the stratum basale, where the cells start to divide (Geerligs, 2006:7). After cell division, these cells migrate to the stratum spinosum, but not before they transform to larger, three dimensional (polyhedral) cells (Geerligs, 2006:5). In the stratum spinosum, polyhedral cells start to flatten as they migrate further to the stratum granulosum (Geerligs, 2006:5). Here, the process of mitochondrial and nucleic deterioration occurs and by the time they reach the stratum corneum, they are completely transformed to non-viable (Geerligs, 2006:5). The stratum corneum is constantly restored as cells on the surface are replaced by new cells from deeper within the stratum corneum, and old cells are discarded, also referred to as shedding (Geerligs, 2006:5). This process occurs over a period of 6 to 30 days (Geerligs, 2006:5).

### 2.6.2 Non-viable epidermis

The stratum corneum, 25 – 45 µm in diameter and 0.3 – 0.7 µm in thickness, includes 15 – 25 layers of hydrophilic corneocytes (thickness of ~ 10 – 25 µm and intercellular spacing of 0.1 – 0.3 µm), which are flat cells (excluding a nucleus), coated with lipids (lipophilic) and desmosomes (Geerligs, 2006:5). Desmosomes (corneosomes) are protein-formed links between corneocytes, which in collaboration with lipids sustain stratum corneum integrity (Geerligs, 2006:5). Together these elements are generally stated as a brick-and-mortar construction (Geerligs, 2006:5). This brick-and-mortar construction, poses challenges to hydrophilic and lipophilic absorption (Baibhav *et al.*, 2011:66). Lipids surrounding the corneocytes function as the primary barrier to water loss from beneath the epidermis and consist of long chain fatty acids, cholesterol and ceramides with additional small quantities of glucosylceramides and phospholipids (Geerligs, 2006:5; Menon *et al*., 2012:4; Williams, 2013:677). The lipids surrounding the corneocytes, especially long chain fatty acids play a major role in the skin's barrier properties (Gaur *et al*., 2014:1812), therefore, the stratum corneum is accountable for the control of API transport (flux) through skin (Marrow, 2007:36) and is also known as the rate-limiting barrier (El Maghraby *et al*., 2008:204; Jepps *et al*., 2013:153).

### 2.6.3 Dermis

The dermis (thickness of 3 – 5 mm), located between the epidermis and the hypodermis (Jepps *et al*., 2013:677; Kute & Saudagar, 2013:372), consists of elastin and collagen fibrils surrounded by a thick hydrophilic mucopolysaccharide gel (Geerligs, 2006:8; Jepps *et al*., 2013:677; Williams, 2013:677). The dermis has a mechanical, as well as a protective function as elastic fibres ensure protection of cells and vessels, and contribute to the healing process (Geerligs, 2006:8). The dermis also sustains the epidermis (Geerligs, 2006:8) and includes blood vessels, lymph vessels and nerve endings (Foldvari, 2000:418).

### 2.6.4 Hypodermis

The hypodermis (thickness differs with age, race, gender, anatomical location, etc.), is the fat (adipose) tissue layer located beneath the dermis and above the muscles (Geerligs, 2006:8). The adipose tissue is connected to the dermis with vascular and nerve complexes, as well as epidermal appendages (hair and nerve endings) (Geerligs, 2006:9). The adipose tissue includes adipocytes (one third), comprised in a collagen fibre network (Geerligs, 2006:9). The residual two thirds contain fibroblastic tissue, macrophages, leukocytes and premature adipocytes (Geerligs, 2006:9). The hypodermis has sufficient blood supply for the adipocytes to operate effectively (Geerligs, 2006:9). The key purpose of the hypodermis is to shield the body against physical trauma, stores high-energy molecules and offers isolation against temperature variations (Williams, 2013:677).

## 2.7 Transport of APIs through the skin

When a formulation is applied to skin, the API molecules diffuse from the optimal formulation towards the skin surface (stratum corneum). The stratum corneum is responsible for the regulation of API transport (flux) through the skin (Marrow, 2007:36); hence, to overcome the challenges that this barrier poses for the API to reach the systemic circulation, investigation into transport routes through the stratum corneum is necessary. There are three transport routes through the skin, e.g. the follicular, transcellular and intercellular route (Wiechers, 2008:7).

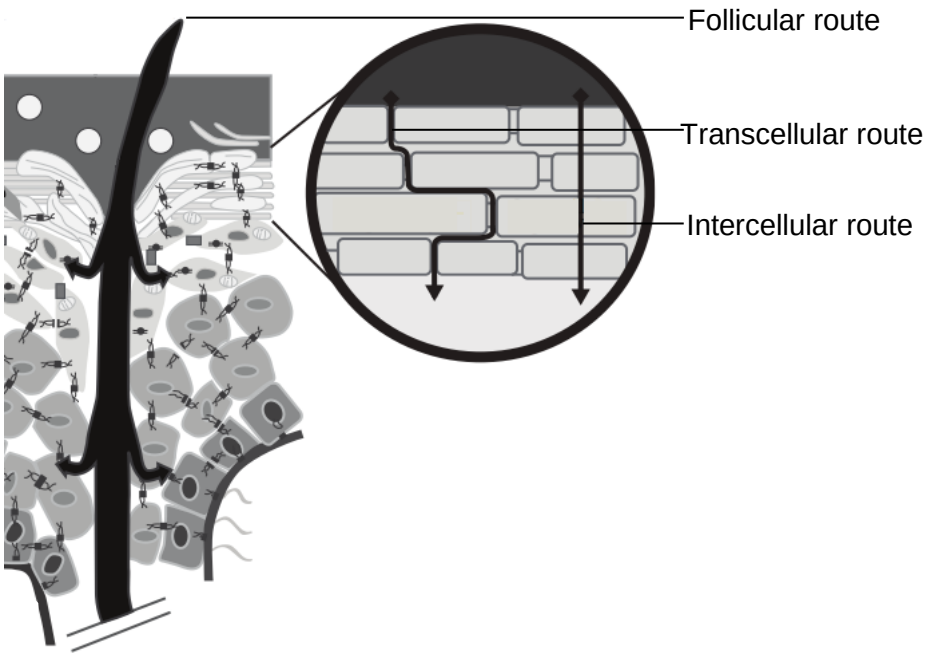


**Figure 2.4:** The three transport routes through the skin (Adapted from Lohani, 2014).

### 2.7.1 Follicular route

During this route, also known as the transappendageal route or shunt route, the API, permeates through the channels of sweat, apocrine glands and hair follicles (sebaceous glands), (Gaur *et al.,* 2014:1813; Williams, 2003:678). By following this route, the API (lipophilic) completely avoids the challenges of the stratum corneum (Marrow *et al*., 2007:38; Williams, 2003:31); hence, these channels only exist in approximately 0.1% of the skin surface and as a result, this route is unpopular (Gaur *et al.,* 2014:1813; Jepps *et al.,* 2013:160; Marrow *et al.,* 2007:38).

### 2.7.2 Transcellular route

This route requires the API to transport (partition and diffusion) through the layers of hydrophilic corneocytes (consist of hydrated keratin), as well as in the lipid coatings (lipophilic) of the stratum corneum (Ng & Lau, 2015:9; Rastogi & Yadav, 2012:163). Seen as the corneocytes are in abundance within the stratum corneum, this route is favourable for hydrophilic APIs; hence, challenges occur because of the lipophilic nature of lipid coatings (Marrow *et al*., 2007:38).

### 2.7.3 Intercellular route

During this route, the API moves through the continuous lipophilic lipid coatings of the stratum corneum (Marrow *et al*., 2007:38; Williams, 2003:38). Although this route is favourable for non-polar (uncharged) APIs, as the lipid coatings are also non-polar (Geethu *et al*., 2014:1813), it is still challenging for APIs to move through (Marrow *et al*., 2007:38; Ng & Lau, 2015:9), as API must diffuse across and partition in the continuous aqueous, as well as lipid environment (Rastogi & Yadav, 2012:163).

The skin limits the permeation of APIs (Williams, 2013:680) and affects the API flux directly (Williams, 2013:680), thus for an API to overcome the challenges that the skin presents and to sufficiently penetrate the skin through the routes mentioned before, the API needs to possess specific ideal characteristics (Rastogi & Yadav, 2012:165).

## 2.8 Physiochemical characteristics

The ideal physicochemical characteristics that are required from the APIs to successfully permeate the skin are log P or log D, molecular weight, melting point, aqueous solubility, diffusion coefficient, pKa (Williams, 2013:682), pH and ionisation (Rastogi & Yadav, 2012:165).

### 2.8.1 Log P and log D

The partition coefficient of an API is indicative of its division between the lipophilic- and the hydrophilic phase (Williams, 2013:676). When taking the brick (hydrophilic) and mortar (lipophilic) structure of the stratum corneum into consideration, the log P or log D value will be of assistance to determine the API distribution (Williams, 2013:676). If the API is highly lipophilic, it is to remain in the lipophilic part of the stratum corneum, and if it is too hydrophilic, it will be unable to penetrate the stratum corneum when applied (Sharma *et al.,* 2011:74). Although lipophilic APIs permeate the skin with more efficiency (Williams, 2003:37), its ideal for an API to own lipophilic and hydrophilic properties for effective skin permeation (Naik *et al.,* 2000:319; Williams. 2003:37).

The required log P or log D of an API is $1 < 3$, indicating both water and oil solubility (Subedi *et al*., 2010:339; Williams, 2003:36). Atorvastatin (1.11), pitavastatin (1.49) and fluvastatin (1.27) are lipophilic in nature and succeed to the ideal log P value, however, pravastatin (-0.84) will not be able to penetrate the skin surface as it hydrophilic and does not own a log P value within the required range (Sahebzamani *et al.,* 2014:3).

### 2.8.2 Molecular weight

It is proposed that molecular weight can influence API flux through the skin (Barry, 2002:513; Williams 2003:36), thus molecular weight and size of the API molecules affects transdermal permeation (Williams, 2003:36). The API's molecular weight and size should not exceed 500 g/mol (Naik *et al*., 2000:319; Williams, 2013:675). Due to skin characteristics, larger molecules will be blocked by the barrier of the stratum corneum (Williams, 2013:680). Fluvastatin (411.47 g/mol), pitavastatin (421.46 g/mol) and pravastatin (446.52 g/mol) have molecular weights below 500 g/mol (Ruan *et al.,* 2012:512), hence, atorvastatin (1155.34 g/mol) (Al-Adl *et al.,* 2017:1) does not succeed to the required parameter.

### 2.8.3 Melting point

The melting point is the specific temperature to which a solid material changes to a liquid state at atmospheric pressure (Reddy *et al*., 2016:975). A direct relationship exists between an API's aqueous solubility and its melting point (Williams, 2003:37), thus the higher the melting point the lower the aqueous solubility (Williams, 2003:37). The required melting point for APIs to acquire transdermal delivery is < 200 °C (Naik *et al*., 2000:319). Atorvastatin (± 151 °C) (Satpute *et al.,* 2018:14171), fluvastatin (194 – 197 °C) (LKT labs, 2018a), pitavastatin (190 – 192 °C) (Van der Schaaf *et al.,* 2006) and pravastatin (171.2 – 173 °C) (LKT labs, 2018b), succeed in the required melting point parameter.

### 2.8.4 Aqueous solubility

Solubility is referred to as the ability of a chemical compound (solid, liquid or gas) also called salute, to dissolve in a solvent (solid, liquid or gas) to produce a solution (homogenous) (Savjani *et al*., 2012:1). In this study, a solid (API) will be dissolved within a liquid and the solubility measure will indicate whether the APIs are able to dissolve in the solvent and result in skin permeation (Steele & Austin, 2009:24). According to the Encyclopaedia Britannica (2016), solubility is a vital physicochemical characteristic of an API, allegedly there is a close correlation which links solubility and permeability of the skin, therefore, higher solubility produces better skin penetration, thus aqueous solubility will be affected by lipophilic APIs (Williams, 2003:37).

The required aqueous solubility of an API to penetrate the skin effectively is > 1 mg/ml (Naik *et al*., 2000:319). Literature states that atorvastatin has an aqueous solubility of 0.190 mg/ml (Phosphate buffered solution (PBS) at pH 6.8) (Rodde *et al*., 2014:3), fluvastatin of 0.2 mg/ml (PBS at pH 7.2) (Cayman chemical, 2010), pitavastatin of 0.5 mg/ml (PBS at pH 7.2) (Cayman

chemical, 2014) and pravastatin of 10 mg/ml (PBS at pH 7.2) (Cayman chemical, 2015). Therefore, only pravastatin succeeds in the required parameter.

### 2.8.5 Diffusion coefficient

Diffusion is known as the relocation of molecules from a high concentration (initially concentrated) to a low concentration (area without/low concentration) (Comsol, 2017; Williams, 2003:27). The diffusion coefficient is the extent of the molecule flux across a plane (high concentration gradient) to another plane with a different concentration gradient (low) (Comsol, 2017). Diffusion coefficient data progresses linearly over time, therefore has a unit of area ($cm^2$) per time (h or s) (Comsol, 2017; Williams, 2003:27). When a porous medium is involved, diffusion becomes more complicated as the molecules must steer through porous material; this is where Fick's laws for passive diffusion is applicable (Comsol, 2017). Fick's law is therefore utilised to determine passive diffusion of APIs through the skin (Williams, 2013:675). As mentioned before, the stratum corneum has a complicated structure, which leads to restriction of the diffusion process (Barry, 2002:512). Diffusion rate can be affected by the phase of the formulation (Barry, 2002:512), whereas diffusivity is dependent on the amount of hydrogen ($H^+$) bonds present in the API's chemical structure (Williams, 2013:680) amongst other aspects. The requested amount of hydrogen ($H^+$) bonds of the structure to diffuse effectively is ≤ 5 donor $H^+$-bonds (HBD) and ≤ 10 acceptor $H^+$-bonds (HBA) (Ammar, 2017:3). Utilising Molinspiration (computational tool), atorvastatin (HBD = 4, HBA = 7), fluvastatin (HBD = 3, HBA = 5), pitavastatin (HBD = 3, HBA = 5) (De Brito, 2011:802) and pravastatin (HBD = 4, HBA = 7) (IUPHAR/BPS Guide to pharmacology, 2017) are within the $H^+$-bond requirements (HBD & HBA) , thus the statins' $H^+$-bonds should not interfere with the diffusion ability.

### 2.8.6 pH, pKa and ionisation

The skin displays an acidic environment (pH ± 5) (Ng & Lau, 2015:8; Williams, 2013:678). It has been suggested that pH values below 3 or above 9 may cause irritation and harm towards the skin and also affect skin penetrability (Akula *et al.,* 2018:1; Naik *et al.,* 2000:319). The pH has the ability to affect the ratios to which weakly acidic and basic APIs dissociates, which is reliant on the pKa or pKb values of the API (Akula *et al.,* 2018:1; Barry, 2002:511). Ionisation is extremely important due to the barrier (lipophilic) posed by the skin (Williams, 2003:38).

It has been suggested that API penetration across the dermis is affected by ionic state, thus species of ionised nature permeate inadequately compared to unionised species (Akula *et al.,*

2018:1). Consequently, an increased amount of unionised API can enhance skin permeability (Akula *et al.,* 2018:1). The hypothesis is thus that unionised species permeate through the lipid layers of the skin more effectively than ionised species, which are mostly unable to penetrate the stratum corneum (Barry, 2002:511; Williams, 2003:38).

An altered Henderson-Hasselbalch equation (Equations 2.1 and 2.2) was utilised to determine the ionisation of an API or formulation.

$$\%ionised = \frac{100}{1 + antilog(pKa - pH)} \qquad \textbf{Equation 2.1}$$

$$\%unionised = 100 - \%ionised \qquad \textbf{Equation 2.2}$$

Statins investigated portrayed the following pKa values (acids and bases): atorvastatin (4.6), fluvastatin (5.5), pitavastatin (4.7) and pravastatin (4.7) (Fong, 2016:23); due to these pKa values, the unionised species of the statins were calculated. At a pH of 5 (pH of the skin), atorvastatin (28.475%), pitavastatin (33.386%) and pravastatin (33.386%) displayed low unionised species with the exception of fluvastatin (75.975%), which displayed a higher amount of unionised species. Due to the ionic state of the atorvastatin, pitavastatin and pravastatin, which could result in inadequate penetration of the skin, APIs will be formulated with penetration enhancers within a drug delivery system (transport system) in attempt to overcome this inadequacy.

### 2.8.7 Requirements for specific statins

Table 2.1 indicates that statins used in this study do not comply with all the ideal physicochemical characteristics, consequently statins will not be able to overcome this barrier and penetrate the skin without the assistance of a carrier system also known as transport agents (Gabera *et al.,* 2017:75).

**Table 2.1:** Summary of physiochemical properties of statins compared to the idea properties

| | | Atorvastatin | Fluvastatin | Pitavastatin | Pravastatin | Ideal properties |
|---|---|---|---|---|---|---|
| **Log P** | | 1.11[a] | 1.27[a] | 1.49[a] | - 0.84[a] | **1 – 3[b]** |
| **Molecular weight (Da)** | | 1155.34[c] | 411.47[d] | 421.46[d] | 446.52[d] | **< 500[e]** |
| **Melting point (°C)** | | ± 151[f] | 194 – 197[g] | 190 – 192[h] | 171.2 – 173[i] | **< 200[r]** |
| **Aqueous solubility (mg/ml)** | | 0.190 (pH 6.8)[j] | 0.2 (pH 7.2)[k] | 0.5 (pH 7.2)[l] | 10 (pH 7.2)[m] | **> 1[e]** |
| **Diffusion coefficient** | **HBD** | 4[n] | 3[n] | 3[n] | 4[n] | **≤ 5[s]** |
| | **HBA** | 7[n] | 5[n] | 5[n] | 7[n] | **≤10[s]** |
| **pKa** | | 4.6[p] | 5.5[p] | 4.7[p] | 4.7[p] | **< 4 (Acids)[e]** |
| **Non-ionised species (%)** | | 28.475 | 75.975 | 33.386 | 33.386 | **High[q]** |

a) Sahebzamani *et al*., 2014:3, b) Subedi *et al*., 2010:339; Williams, 2003:36, c) Al-Adl *et al*., 2017:1, d) Ruan *et al*., 2012:512, e) Naik *et al*., 2000:319; Williams, 2013:675, f) Satpute *et al*., 2018:14171, g) LKT labs, 2018a, h) Van der Schaaf *et al*., 2006, i) LKT labs, 2018b, j) Rodde *et al*., 2014:3, k) Cayman chemical, 2010, l) Cayman chemical, 2014, m) Cayman chemical, 2015, n) IUPHAR/BPS Guide to pharmacology, 2017, o) Ashford, 2013:324, p) Fong, 2016:23, q) Akula *et al*., 2018:1, r) Naik et al., 2000:319 and s) Ammar, 2017:3.

## 2.9 Transport agents

The most frequently used transport agents are required to be biodegradable, non-immunogenic and biocompatible (Gabera *et al.,* 2017:75). Although numerous transport agents exist, nano-emulsions are the transport agent to be researched for transdermal delivery of statins.

## 2.10 Nano-emulsions

Nano-emulsions are transport systems described as modifying two immiscible liquid phases (oil phase and water phase) to create a single phase formulation; this system has been in existence from the 1940's (Kumar, 2014:1-2). Nano-emulsions can be categorised into three groups dependent of their composition, which is oil droplets dispersed in a water medium called oil in water (o/w) nano-emulsions, water droplets dispersed in an oil medium (water in oil (w/o) nano-emulsions) and bicontinuous nano-emulsions, where water, as well as oil droplets are dispersed and surrounded by a continuous system (Kumar, 2014:2; Verma *et al.,* 2018:374). For the purpose of this study, o/w nano-emulsions were formulated.

Nano-emulsions are utilised in cosmetic preparations, as well as the pharmaceutical industry to serve as delivery systems for antibiotics, topical formulations, vaccines, Deoxyribonucleic acid (DNA) encoded medications administered among different administration pathways such as oral, transdermal, intra-nasal and pulmonary routes (Verma *et al.,* 2018:374).

Nano-emulsions, also known as nano-dispersed systems, ultrafine-emulsions, mini-emulsions or submicron-emulsions (Kumar, 2014:1), are generally seen as a harmless, effective option for cosmetic or pharmaceutical formulation development (Chime *et al*., 2014:95-98). Nano-emulsions are isotropic systems, since they measure the same property values when inspected from different angles (Kumar, 2014:1) with high thermodynamic (Kumar, 2014:1), as well as physical stability (Abolmaali *et al*., 2011:140; Lu *et al*., 2014:826; Tadros *et al*., 2004:303). Nano-emulsions enhance the solubility of lipophilic APIs and are able to transport both hydrophilic and lipophilic constituents (Verma *et al.,* 2018:376). These transport systems are responsible for fewer side effects due to a reduced required dose (Verma *et al.,* 2018:376). The occurrence of flocculation, sedimentation and creaming are also in the minority, as nano-emulsions tend to maintain their satisfactory aesthetic form (Lu *et al*., 2014:826; Tadros *et al*., 2004:303). This phenomenon is a result of a nano-emulsion's droplet size range (100 – 500 nm) (Nalini *et al*., 2017:1453), which decreases tension between the oil and water particles' surfaces, no gravitational interference and limited size distribution (Kumar, 2014:1). The tiny particles cross skin barriers with less effort and provide a larger surface area when applied, therefore, increasing the permeation of APIs, increasing its bioavailability (Kela & Kaur, 2013:9206; Klang *et al*., 2015:258; Lu *et al*., 2014:826; Nalini *et al*., 2017:1453; Tadros *et al.,* 2004:304). To produce nano-scale size droplets within a nano-emulsion, emulsification methods are required (Abolmaali *et al*., 2011:141; Tadros *et al*., 2004:307; Verma *et al.,* 2018:376).

### 2.11 Emulsification

Two principle methods are validated to formulate nano-emulsions, namely high energy emulsification (sonication and high amplitude ultrasonic emulsification (Ochoa *et al*., 2016:80), microfluidisation, jet dispersion (Kumar, 2014:4), high-pressure homogenisation, membrane emulsification and high-energy stirring emulsification) and low energy emulsification (spontaneous emulsification, phase inversion temperature emulsification and emulsion inversion point emulsification) (Verma *et al.,* 2018:379). In this study, a high energy emulsification method was followed by means of an ultrasonicator.

### 2.11.1 High energy emulsification

An ultrasonicator equipped with a probe, which when inserted into a formulation creates mechanical vibrations causing cavitation (breakdown of particles in a formulation) (Kumar, 2014:4). The breakdown of these particles produce significant tremors throughout the whole formulation and as a result, dispersed droplets are spread through the solution into smaller droplets (nano-particles) (Kumar, 2014:4), which for the purpose of this study is droplet size range of 100 – 500 nm. Nano-particles cross skin barriers effortlessly and increase skin penetration of APIs. To enhance penetration of APIs further, agents known as penetration enhancers are included in formulations.

## 2.12 Penetration enhancers

Penetration enhancers are included in formulations to achieve exactly as named, penetration enhancement. These agents also enhance the permeation rate to achieve the required therapeutic effect and aid the permeation of non-permeable APIs through the skin, consequently increasing transdermal formula absorption (Kala & Juyal, 2018:2192). However, the amount and type of penetration enhancers varies with the APIs used (Kala & Juyal, 2018:2192).

There are suggested suitable properties that penetration enhancers should bare. Penetration enhancers are required to be non-irritating, non-toxic and non-allergenic, they should also have the ability to act instantaneously, and deliver expected, reproducible results. These agents should be pharmacologically inactive once inside the body and only act one-directional, as it can enhance penetration of APIs into the body, but not reversed. Once penetration enhancers have been removed from the skin, the skin layers and its properties ought to return fully to a homeostatic state within a short time. Penetration enhancers should be congruent with other compounds in the formula, as well as the API (Parhi *et al.,* 2012:219).

Penetration enhancers are mainly classified into six categories, namely physical enhancers, particulate systems, drug vehicle based, biochemical approach, natural penetration enhancers and chemical enhancers (Lakshmi *et al.,* 2017:10). A natural penetration enhancer was chosen for this study, which will be discussed further.

### 2.12.1 Natural penetration enhancers

Natural penetration enhancers are the most utilised penetration enhancers. These penetration enhancers interact with cellular corneocytes by disrupting the lipophilic bilayers of the skin (Wang *et al.,* 2003:1612; Williams, 2013:694). Due to this interaction, the API flux

across the stratum corneum increases (Vermaak *et al.,* 2011:922). The phenomenon is made possible by the fatty acids within the chemical structure of natural penetration enhancers, which are known to increase the rate of API-skin permeation by means of intercellular lipid structure modification of the stratum corneum to decrease the barrier's resistance (Kala & Juyal, 2018:2194). Fatty acids can enhance skin permeation of both hydrophilic, as well as lipophilic APIs, although the flux of ionised APIs is higher (Kala & Juyal, 2018:2194). Long chain unsaturated fatty acids ($C_{18}$) are very advantageous as they increase penetration enhancing effects significantly (Kala & Juyal, 2018:2192). Natural penetration enhancers containing these long chain unsaturated fatty acids ($C_{18}$), such as oleic and linoleic fatty acids, are the most beneficial to transdermal delivery as these acids are also present in the human skin (Wang, 2012:1745), which lowers the probability of skin irritations ad easing the disruption process (Vermaak *et al.,* 2011:922). Apricot kernel oil is the natural penetration enhancer utilised in this study.

#### 2.12.1.1 Apricot kernel oil as a natural penetration enhancer

Apricot kernel oil is an oily substance extracted from cold pressed dried kernels of apricots (Healthguidance, 2017). Similar to other natural penetration enhancers, apricot kernel oil contains fatty acids also present in the human skin (oleic acid: 58 – 68%, and linoleic acid 22 – 31%, unsaturated, 18-carbon fatty acids) (Wang, 2012:1745). Consequently, apricot kernel oil is widely incorporated in cosmetic and skin nourishing formulations (Healthguidance, 2017). This nourishing effect is resultant of the abundance of vitamins A and E present in this natural oil, thus serving perfectly as a massage therapy product for its vibrant, moisturising and soothing effect on dry, irritated, sensitive and premature aging skin (Healthguidance, 2017). To aid formulation and enhance compatibility between the apricot kernel oil, APIs and aqueous phase appropriate surfactants should be included in the formula.

### 2.13 Surfactants

Surfactants serve as an interfacial film between the phases of a formulation (Kumar, 2014:1), to stabilise the system to which it is applied by decreasing surface tension, enhance emulsification (Baibhav *et al*., 2011:68; Hyma *et al*., 2014:4), easing the process of droplet splitting (reduced particle size) (Huyn, 2012:111) and enhancing nano-emulsion stability (Setya *et al*., 2014:2218-2219). Surfactants comprise two segments, namely the head, which is lyophilic therefore, interacts with the water phase, and the tail, which is lyophobic and interacts with the oil phase, which combined forms an amphipathic molecule (Huyn, 2012:111).

There are different types of surfactants of which the superior is the non-ionic surfactants, with more advantages towards compatibility, toxicity and stability in comparison to cationic, anionic and amphoteric structured surfactants (Kumarn *et al*., 2011:209). Non-ionic surfactants have a reduced irritable effect on cells, are less haemolytic and tend to sustain a pH value near the physiological pH value (Kumarn *et al*., 2011:209).

For formulation compatibility and stability, hydrophilic-lipophilic balance (HLB) are required to be between the values of 8 and 19 (Eid *et al*., 2014:4; Setya *et al*., 2014:2218). A high diversity of surfactants prevails, however for purpose of this study, Span® 60 (sorbitan monostearate) and Tween® 80 (polysorbate 80) were utilised.

Span® 60 possesses an HLB value of 4.7 (> 10), therefore has to be added in the oil phase, as it classifies as an oil soluble surfactant (Reddy *et al*., 2013:87; Zhang, 2009b:6780). Span® 60 is non-ionic and serves as a wetting agent and enhances dispersion, emulsification (Zhang, 2009b:675) and stability (Baibhav *et al*., 2011:68; Zhao *et al*., 2013:1834). Span surfactants are formed through sorbitol dehydration. Span® 60 is also known to alter physical characteristics of formulations through reduced interfacial surface tension, droplet size distribution and enhanced viscosity (Zhao *et al*., 2013:1837).

Tween® 80, a general used non-ionic surfactant derived from oleic acid and polyethoxylated sorbitan, possesses an HLB value of 15 (> 10) (Zhang, 2009a:550-551); therefore, it classifies as a water soluble surfactant (Koocheki *et al*., 2011:1149; Reddy *et al*., 2013:87) and is also soluble in methanol, ethanol and ethyl acetate. Water-soluble surfactants enhance the stability of formulations and reduce the energy level requested to produce a nano-emulsion (Chime *et al*., 2014:91). Tween® 80 present as a thick, yellowish fluid and is widely utilised in food and cosmetic products (non-toxic) to serve as an emulsifier, as it provides a smooth texture and increase endurance to melting (Huyn, 2012:111). Tween® 80 also reduces interfacial tension and increases the speed of surfactant absorption by emulsion droplets, therefore lowering droplet sizes and enhancing the viscosity (Koocheki *et al*., 2011:1153).

These surfactants not only have solubilising, wetting, emulsification and permeability enhancing properties, but also serve as P-glycoprotein inhibitors, to aid the absorption of APIs (Kumarn *et al*., 2011:209). Although surfactants have many advantages, solubility of the API in oil still plays a crucial role in the formulation (Debnath *et al*., 2011:74; Reddy *et al*., 2013:87; Setya *et al*., 2014:2218). Surfactants are not only utilised in nano-emulsions, but also in other transport systems namely and semi-solid formulations, such as emulgels, ointments and creams.

## 2.14 Semi-solid formulations

Semi-solid formulations, e.g. gels, creams and ointments, are convenient and beneficial in the development and delivery of medications to be applied to the skin. These formulations have a tendency to be non-irritating and are easily applied and removed from the skin. Semi-solid formulations also have the advantage to be adequately stable enough to escape the necessity of repeated application (Brown *et al.,* 2018:2). A semi-solid formulation further presents direct contact when applied on the skin, and as a result has the double function of aiding API delivery, as well as operating as a carrier system (Gupta & Garg, 2002:144). In this study, the chosen semi-solid formulation that was formulated and investigated was a nano-emulgel.

### 2.14.1 Nano-emulgel

A nano-emulgel formulation can be defined as the creation of a nano-emulsion-based-hydrogel, by merging a nano-emulsion with a hydrogel medium (Chellapa, 2015:44). These formulations are classified among semi-solid dosage systems with a consistency between a liquid and a solid (Kaur *et al*., 2013:202), and are known to enhance permeability when applied to the skin (Chellapa, 2015:44). A nano-emulgel (nano-emulsion based hydrogel) displays characteristics of nano-emulsions, as well as gels (Kaur *et al.,* 2017:1) as they present with limited size distribution (Kumar, 2014:1) and consist of droplet sizes between 100 and 500 nm (Nalini *et al.,* 2017:1453).

A nano-emulgel acts as a drug storage system, which affects the delivery of APIs from the inner-to the outer phase of the system; however, the specific delivery of a nano-emulgel rests on the arrangement of the polymer bindings of the structure, as well as the crosslink density (Chellapa, 2015:44). The ability of the API to penetrate the skin effectively, and be delivered successfully, depends on the affinity of the API to diffuse from out the nano-emulgel (Chellapa, 2015:44). As nano-emulgels contact the human skin, it releases the dispersed oil drops from the gel-structure, which will then permeate through the stratum corneum and release the API and not through the aqueous phase as seen in nano-emulsions (Chellapa, 2015:44). By combining an optimal nano-emulsion with a gelling agent, interfacial-and surface tension decreases even more than those of nano-emulsions. Consequently, swelling of water phase is of result, and a formulation with higher viscosity is produced (Chellapa, 2015:45; Mahalingam *et al*., 2008:293; Mitsui, 1997:138). The enhancement of the water phase's viscosity further enhances skin permeability (Chellapa, 2015:44; Eid *et al*., 2014:1).

### 2.14.2 Gelling agents

Gelling agents consists of high molecular weights (Mahalingam *et al*., 2008:293), which improves the stability of the formulation by preventing particle separation (Mitsui, 1997:138). Nano-emulgels consist of a higher stability than nano-emulsions, as the oil droplets, which encapsulate the lipophilic APIs, are dispersed more effectively in the gel-structure, which extends the efficacy of limited half-life APIs, as this gel-structure regulates the release of the APIs (Chellapa, 2015:45). Formulations of nano-emulgels also increase patient compliance (Pund *et al*., 2015:152; Williams, 2013:687), as they are more effortlessly applied and removed from the skin, compared to other topical formulations for example creams and ointments (Chellapa, 2015:45). The gelling-agent utilised in this study was Carbopol® 20.

### 2.14.3 Carbopol® Ultrez 20

Carbopol® Ultrez 20 is a whitish snow-like powder, which is used effortlessly as it wets and dissolves rapidly (Lubrizol, 2018). This gelling-agent has many other advantages such as swelling, which results in a higher viscosity and in turn enhances the stability of the formulation. Carbopol® Ultrez 20 has the ability to maintain stable over wide pH range, which leads to less challenges during the formulation process. This gelling-agent also helps to dissolve substances in the formulation and when added to a formulation, it presents with a glowing rich appearance, which makes it favourable to use widely in gels, creams, lotions, shampoos, etc. (Lubrizol, 2018). Carbopol® Ultrez 20 has been utilised to raise the viscosity of nano-emulsions, as well as enhance permeability of formulations when applied topically (Chudasama, 2011:35).

Nano-emulgels are also more stable than nano-emulsions as the oil droplets, which contain lipophilic APIs, are dispersed more effectively in the gel-structure, and therefore extend the effectiveness of limited half-life APIs as this structure regulates the release of the APIs (Chellapa, 2015:45).

Nano-emulgels also shows enhanced adhesion characteristics when applied on the skin and furthermore consist of an induced solubilisation capability, which result in a higher concentration gradients of API and in turn, a higher concentration of API can penetrate the skin (Chellapa, 2015:45).

## 2.15 Conclusion

Elevated blood cholesterol, known as hypercholesterolemia or hyperlipidaemia is connected to atherosclerosis and CVDs. Statins are the first-line medical therapy to treat hyperlipidaemia. This first-line medical therapy is currently only available as an oral treatment, which has shown to produce a reduced systemic bioavailability. Consequently, the transdermal delivery route, as an alternative, will be investigated in an attempt to find a sufficient pathway.

The physiochemical properties of statins utilised in this study are non-compliant for transdermal delivery, thus carrier systems such as nano-emulsions will be researched to encapsulate statins for transdermal delivery. A penetration enhancer is to be included in the formula to improve permeation and absorption of the statins through reversibly altering the challenges presented by the skin's multifaceted structure. Apricot kernel oil is the chosen natural penetration enhancer to attempt to disorder the lipophilic bilayers of the skin to enhance the flux of APIs across the stratum corneum. An optimised nano-emulsion formula suitable for statins utilised in this study will be modified to produce an optimised nano-emulgel for the purpose of viscosity improvement and skin permeability enhancement. The formulated nano-emulsions and nano-emulgel formulations are to be compared regarding transdermal delivery.

**References**


Abolmaali, S.S., Tamaddon, A.M., Farvadi, F.S., Daneshamuz, S. & Moghimi, H. 2011. Pharmaceutical nanoemulsions and their potential topical and transdermal applications. *Iranian journal of pharmaceutical sciences*, 7:139-150.

Akula, P., Lakshmi P.K. 2018. Effect of pH on weakly acidic and basic model drugs and determination of their ex vivo transdermal permeation routes. *Brazilian journal of pharmaceutical sciences,* 54(2):1-8.

Al-Adl, S.M., Abdel-Aziz, L.M., Mohamed, M.A.M. 2017. Spectrophotometric determination of atorvastatin calcium and rosuvastatin calcium in bulk and dosage form using P-Dimethylaminobenzaldehyde. *Journal of applied pharmacy,* 9(1):1-7.

Alexander, A., Dwivedi, S., Ajazuddin, Giri, T.K., Saraf, S., Saraf. S. & Tripathi, D.K. 2012. Approaches for breaking the barrier of drug permeation through transdermal drug delivery. *Journal of Controlled Release,* 164:26-40.

Ammar, O. 2017. In silico pharmacodynamics, toxicity profile and biological activities of the Saharan medicinal plant *Limoniastrum feei. Brazilian journal of pharmaceutical sciences,* 53(3):1-10.

Baibhav, J., Gurpreet, S., Rana, A.C., Seema, S. & Vikas, S. 2011. Emulgel: a comprehensive review on the recent advances in topical drug delivery. *International research journal of pharmacy*, 2:66-70.

Barry, B. 2002. Transdermal drug delivery. (*In* Aulton, M.E., ed. Pharmaceutics: the science of dosage form design. 2nd ed. London: Churchill Livingstone. p. 499-533).

Basera, K., Bhatt, G., Kothiyal, P. & Gupta, P. 2015. Nanoemulgel: a novel formulation approach for topical delivery of hydrophobic drugs. *World journal of pharmacy and pharmaceutical sciences*, 4:1871-1886.

Boglarka, B., Gabor, V., Szilvia, B., Maria, B., Andras, K., Balint, S., Krisztina, T., Piroska, S. & Erzsebet, C. 2016. Investigation of the efficacy of transdermal penetration enhancers through the use of human skin and a skin mimic artificial membrane. *Journal of Pharmaceutical Sciences,* 105:1134-1140.

Braamskamp, M.J., Wijburg, F.A. & Wiegman, A. 2012. Drug therapy of hypercholesterolaemia in children and adolescents. *Drugs,* 72:759-72.

Brown, T.L., Hiu, S.P., Chan, T., Angove, M.J., Tucci, J. 2018. Semi-solid and solid dosage forms for the delivery of phage therapy to epithelia. *Pharmaceuticals*, 11(26):1-12.

Cayman chemical. 2010. Fluvastatin (sodium salt) (Material safety data sheet). https://s3-us-west-2.amazonaws.com/drugbank/msds/DB01095.pdf?1374296087. Date of access: 18 Oct 2018.

Cayman chemical. 2014. Pitavastatin calcium salt (Product information 15414) https://www.caymanchem.com/pdfs/15414.pdf Date of access: 18 Oct 2018.

Cayman chemical. 2015. Pravastatin (sodium salt) (Material safety data sheet). https://www.caymanchem.com/msdss/10010343m.pdf Date of access: 18 Oct 2018.

Chudasama, A., Patel, V., Nivsarkar, M., Vasu, K. & Shishoo, C. 2011. Investigation of microemulsion system for transdermal delivery of itraconazole. *Journal of advanced pharmaceutical technology & research*, 2(1):30-38.

Chellapa, P., Mohamed, A.T., Keleb, E.I., Elmahgoubi, A., Eid, A.M., Issa, Y.S. & Elmarzugi, N.A. 2015. Nanoemulsion and nanoemulgel as a topical formulation. *IOSR journal of pharmacy*, 5(10):43-47.

Chime, S.A., Kenechukwu, F.C. & Attama, A.A. 2014. Nanoemulsions: advances in formulation, characterization and application in drug delivery. (*In* Sezer, A.D., ed. Application of nanotechnology in drug delivery. p. 77-126). http://cdn.intechopen.com/pdfs-wm/47116.pdf Date of access: 20 Dec. 2017.

Churchill-Livingstone's Dictionary of Sport and Exercise Science and Medicine. 2008. Hyperlipidaemia. http://medical-dictionary.thefreedictionary.com/browse/hyperlipidaemia Date of access: 29 March 2017.

Comsol, 2017. Diffusion coefficient. https://www.comsol.com/multiphysics/diffusion-coefficient Date of access: 8 Oct 2018.

Cruz, M.P., Küstner, E.C., Vicente, J.A.G., Ferrero, X.M., Thio, E.B., López, J.L. 2008. Adverse side effects of statins in the oral cavity. *Medicina oral patologia oral y cirugia bucal,*13(2):E98-101.

De Brito, M.A. 2011. Pharmacokinetic study with computational tools in the medicinal chemistry course. *Brazilian journal of pharmaceutical sciences,* 47(4):797-805.

Debnath, S., Satayanarayana & Kumar, G.V. 2011. Nanoemulsion-a method to improve the solubility of lipophilic drugs. *Pharmanest: an international journal of advances in pharmaceutical sciences*, 2:72-83.

Eid, A.M., El–Enshasy, H.A., Aziz, R. & Elmarzugi, N.A. 2014. Preparation, characterization and anti–inflammatory activity of Swietenia macrophylla nanoemulgel. *Journal of nanomedicine and nanotechnology*, 5:1-10.

El Maghraby, G.M., Barry, B.W. & Williams, A.C. 2008. Liposomes and skin: from drug delivery to model membranes. *European journal of pharmaceutical sciences*, 34:203-222.

Encyclopaedia Britannica. 2016. Partition coefficient. http://global.britannica.com/science/partition-coefficient Date of access: 8 Oct 2018.

Fahed, A.C., Nemer, G.M. 2011. Familial hypercholesterolemia: The lipids or the genes? *Nutrition & metabolism*, 8:23.

Fatima, T., Ansari, M., Naaz, H., Banu, H., Mehveen, Z. 2017. Hyperlipidemia- A critical pathological condition. *International journal of pharmacy and pharmaceutical research,* 8(3):110-124.

Ferris, H.A., Perry, R.J., Moreira, G.V., Shulman, G.I., Horton, J.D., Kahn, C.R. 2017. Loss of astrocyte cholesterol synthesis disrupts neuronal function and alters whole-body metabolism. *Journal of the national academy of sciences,* 114(5):1189-1194.

Flynn, G.L. 2002. Cutaneous and transdermal delivery - processes and system of delivery. (*In* Banker, G.S. & Rhodes, C.T., eds. Modern pharmaceutics. 4th ed. New York: Marcel Dekker. p. 187-235).

Foldvari, M. 2000. Non-invasive administration of drugs through the skin: challenges in delivery system design. *Pharmaceutical sciences and technology today*, 3:417-425.

Fong, C. 2016. Statins in therapy: Understanding their hydrophilicity, lipophilicity, binding to 3-hydroxy-3-methylglutaryl-CoA reductase, ability to cross the blood brain barrier and metabolic stability based on electrostatic molecular orbital studies. *European journal of medicinal chemistry,* 85:661-674.

Fong, C. 2016. Statins in therapy: Cellular transport, side effects, drug-drug interactions and cytotoxicity -the unrecognized role of lactones. https://hal.archives-ouvertes.fr/hal-01185910/document. Date of access: 5 Nov 2018.

Gabera, M., Medhata, W., Hanya, M., Sahera, N., Fang, J., Elzoghby, A. 2017. Protein-lipid nanohybrids as emerging platforms for drug and gene delivery: Challenges and outcomes. *Journal of Controlled Release,* 254:75-91.

Gaur, S., Garg, A., Yadav, D., Beg, M. & Gaur, K. 2014. Nanoemulsion gel as novel oil based colloidal nanocarrier for topical delivery of bifonazole. *Indian research journal of pharmacy and science*, 1:36-54.

Geerligs, M. 2006. In vitro mechanical characterization of human skin layers: stratum corneum, epidermis and hypodermis. http://www.mate.tue.nl/mate/pdfs/11389.pdf. Date of access: 5 Oct. 2018.

Geethu, V.S., Manikandan, P., Nethaji, R., Surenderan, N.S. & Babu, G. 2014. A review on: transdermal drug delivery systems. *Indo American journal of pharmaceutical research*, 4:1809-1824.

Godin, B. & Touitou, E. 2007. Transdermal skin delivery: Predictions for humans from in vivo, ex vivo and animal models. *Advanced drug delivery reviews,* 59:1158.

Gordts, S.C., Muthuramu, I., Amin, R., Jacobs, F., De Geest, B. 2014. The impact of lipoproteins on wound healing: topical HDL therapy corrects delayed wound healing in apolipoprotein E deficient mice. *Pharmaceuticals,* 7:419-432.

Gupta, P. & Garg, S. 2002. Recent advances in semisolid dosage forms for dermatological application. *Pharmaceutical technology*, 144-162.

Hasani-Ranjbar, S., Nayebi, N., Moradi, L., Mehri, A., Larijani, B. & Abdollahi, M. 2010. The efficacy and safety of herbal medicines used in the treatment of hyperlipidemia; a systematic review. *Current Pharmaceutical Design,* 16:2935-47.

Healthguidance. 2017. http://www.healthguidance.org/entry/1807/1/Benefits-of-Apricot-Kernel -Oil.html Date of access: 12 June 2017.

Hennessy, E., Adams, C., Reen, F.J., O'Gara, F. 2016. Statins inhibit bacterial growth and virulence. *Antimicrobial agents and chemotherapy,* 1-44.

Hoag, G.E. 2018. Topical analgesic pain relief formulations manufacture and methods of use thereof. United States patent application publication, 1-24.

Huynh, P.T. 2012. Solvent-free beta-carotene nanoparticles for food fortification. The State University of New Jersey: New Jersey. (Dissertation-PhD).

Hyma, P., Jahan, N., Raheemunissa, Sreelekha, G. & Babu, K. 2014. Emulgel: a review. *International journal of pharmaceutical archive*, 3:1-11.

IUPHAR/BPS. 2017. Guide to pharmacology. http:www.guidetopharmacology.org/GRAC/LigandDisplayForward?ligandId=2953. Date of access: 5 Oct. 2018.

Jepps, O.W., Dancik, Y., Anissimov, Y.G. & Roberts, M.S. 2013. Modelling the human skin barrier - towards a better understanding of dermal absorption. *Advanced drug delivery reviews*, 65:152-168.

Jonas, A. 2002. Lipoprotein structure. (*In* Vance, D.E. & Vance, J.E., eds. Biochemistry of lipids, lipoproteins and membranes. 4th ed. Urbana: Illinois. p. 483-504).

Kala, S & Juyal, D. 2018. Recent developments on natural transdermal penetration enhancers. *International journal of pharmaceutical sciences and research*, 9(6):2190-2196.

Kela, S.K. & Kaur, C.D. 2013. Pharmaceutical nanoemulsions an ardent carrier for drug delivery. *Indo American journal of pharmaceutical research*, 3:9202-9212.

Klang, V., Schwarz, J.C. & Valenta, C. 2015. Nanoemulsions in dermal drug delivery. (*In* Dragicevic-Curic, N. & Maibach, H.I., eds. Percutaneous penetration enhancers: chemical methods in penetration enhancement: drug manipulation strategies and vehicle effects. Heidelberg: Springer. p. 255-266).

Koocheki, A., Kadkhodaee, R. 2011. Effect of alyssum homolocarpum seed gum, Tween 80 and NaCl on droplets characteristics, flow properties and physical stability of ultrasonically prepared corn oil-in-water emulsions. *Food hydrocolloids*, 25:1149-1157.

Kumar, S. 2014. Role of nano-emulsion in pharmaceutical sciences. *A review Asian journal of research in pharmaceutical sciences and biotechnology* 2(1):1-15.

Kumarn, G.P., Rajeshwarrao, P. & Padmavathi, T. 2011. India college of pharmacy, nonionic surfactant vesicular systems for effective drug delivery-an overview. *Acta pharmaceutica sinica B*, 1(4):208-219.

Kute, S.B. & Saudagar, R.B. 2013. Emulsified gel: a novel approach for delivery of hydrophobic drugs: an overview. *Journal of advanced pharmacy education and research*, 3:368-376.

Lakshmi, P.K., Samratha, K.D., Prasanthi, B., Veeresh, A.C. 2017. Oil as penetration enhancers for improved transdermal drug delivery. *International Research Journal of Pharmacy,* 8(4):9-17.

LKT labs. 2018a. Fluvastatin sodium (93957-55-2). https://www.lktlabs.com/product/fluvastatin-sodium/. Date of access: 5 Nov 2018.

LKT labs. 2018b. Pravastatin sodium (81131-70-6). https://www.lktlabs.com/product/pravastatin-sodium/. Date of access: 5 Nov 2018.

Lohani, A., Verma, A., Joshi, H., Yadav, N., Karki, N. 2014. Nanotechnology-based cosmeceuticals. *International scholarly research notices*: *Dermatology,* 1-14.

Lu, W., Chiang, B., Haung, D. & Li, P. 2014. Skin permeation of D-limonene-based nanoemulsions as a transdermal carrier prepared by ultrasonic emulsification. *Ultrasonics sonochemistry*, 21:826-832.

Lubrizol. 2018. Carbapol® Ultrez 20 polymer. http://www.lubrizol.com Date of access: 27 Aug 2018.

Mahalingam, R., Li, X. & Jasti, B.R. 2008. Semisolid dosages: ointments, creams and gels. (*In* Gad, S.C., ed. Pharmaceutical manufacturing handbook: production and processes. New Jersey: John Wiley & Sons. p. 267-309).

Mahmood, Z.A., Ahmed, S.W., Sualeh, M., Mahmood, S.B.Z. 2009. Hyperlipidemia development and consequences. *Medical channel,* 15(3):14-17.

Mancini, G.B.J., Tashakkor, A.Y., Baker, S., Bergeron, J., Fitchett, D., Frohlich, J., Genest, J., Gupta, M., Hegele, R.A., Ng, D.S., Pearson, G.J., Pope, J. 2013. Diagnosis, prevention, and management of statin adverse effects and intolerance: Canadian working group consensus update. *Canadian journal of cardiology,* 29:1553-1568.

Marrow, D.I.J., McCarron, P.A., Woolfson, A.D. & Donnelly, R.F. 2007. Innovative strategies for enhancing topical and transdermal drug delivery. *The open drug delivery journal*, 1:36-59.

McKenney, J.M. Davidson, M.H. Jacobson, T.A. Guyton, J.R. 2006. National lipid association statin safety assessment task force. *American journal of cardiology*, 97(8A):89C-94C.

Menon, G.K., Cleary, G.W. & Lane, M.E. 2012. The structure and function of the stratum corneum. *International journal of pharmaceutics*, 435:3-9.

Mitsui, T. 1997. Polymers. (*In* Mitsui, T., ed. New cosmetic science. Netherlands: Elsevier. p. 138-140).

Mostafa, W.Z., Hegazy, R.A. 2015. Vitamin D and the skin: Focus on a complex relationship. *Journal of advanced research*, 6:793-804.

Naik, A., Kalia, Y.N. & Guy, R.H. 2000. Transdermal drug delivery: overcoming the skin's barrier function. *Pharmaceutical science and technology today*, 3:318-325.

Nalini, T., Kumari, V.S. & Basha S.K. 2017. Novel nanosystems for herbal drug delivery. *World journal of pharmacy and pharmaceutical sciences*, 6(5):1447-1463.

Natarajan, V.T., Ganju, P., Ramkumar, A., Grover, R., Gokhale, R.S. 2014. Multifaceted pathways protect human skin from UV radiation. https://media.nature.com/lw926/nature-assets/nchembio/journal/v10/n7/images/nchembio.1548-F1.jpg. Date of access: 5 Nov 2018.

Ng, K.W., Lau, W.M. 2015. Skin deep: The basics of human skin structure and drug penetration. file:///C:/Users/22819509/Downloads/ng-2015-skin-deep.pdf. Date of access: 5 Oct. 2018.

Ochoa, A.A., Hernandez-Becerra, J.A., Cavazos-Garduno, A., Vernon-Carte, E.J., Garc, H.S. 2016. Preparation and characterization of curcumin nanoemulsions obtained by thin-film hydration emulsification and ultrasonication methods. http://www.scielo.org.mx/pdf/rmiq/v15n1/1665-2738-rmiq-15-01-00079.pdf. Date of access: 28 Sept. 2018.

Onwe, P.E., Folawiyo, M.A., Okike, P.I., Balogun, M.E., Umahi, G., Besong, E.E., Okorocha, A.E., Afoke, A.O. 2015. Lipid profile and the growing concern on lipid related diseases. *Journal of pharmacy and biological sciences,* 10(5):22-27.

Parhi, R., Suresh, P., Mondal, S., Kumar, P.M. 2012. Novel penetration enhancers for skin applications. *Current drug delivery*, 9:219-230.

Piepho, R.W. 2000. The Pharmacokinetics and Pharmacodynamics of Agents Proven to Raise High-Density Lipoprotein Cholesterol. *The American journal of cardiology*, 86(12A): 35L-40L.

Pund, S., Pawar, S., Gangurde, S. & Divate, D. 2015. Transcutaneous delivery of leflunomide nanoemulgel: mechanistic investigation into physicomecanical characteristics, in vitro anti-psoriatic and anti-melonoma activity. *International journal of pharmaceutics*, 487:148-156.

Rastogi , V., Yadav, P. 2012. Transdermal drug delivery system: An overview. *Asian journal of pharmaceutics,* 161-170.

Reddy, C.S.K., Khan, K.K.A., Nagaraja. 2016. A review on the determination of melting point measurement system. *International journal of advance research electrical electronics and instrumentation engineering,* 5(2):975-979.

Reddy, A.K., Debnath, S. & Babu, M.N. 2013. Nanoemulsions a novel approach for lipophilic drugs - a review*. Asian journal of pharmaceutical research*, 3:84-92.

Robinson, JG. & Goldberg, AC. 2011. Treatment of adults with Familial Hypercholesterolemia and evidence for treatment*:* Recommendations from the National Lipid Association Expert Panel on Familial Hypercholesterolemia. *Journal of Clinical Lipidology,* 5:S18-S29.

Rodde, M.S., Divase, G.T., Devkar, T.B., Tekade, A.R. 2014. Solubility and bioavailability enhancement of poorly aqueous soluble atorvastatin: *in vitro*, *ex vivo*, and *in vivo* studies. *BioMed research international*, 1-11.

Rohilla, A., Dagar, N., Rohilla, S., Dahiya, A., Kushnoor, A. 2012. Hyperlipidemia- A deadly pathological condition. *International journal of current pharmaceutical research,* 4(2):15-18.

Ruan, F., Zheng, Q., Wang, J. 2012. Mechanisms of bone anabolism regulated by statins. *Bioscience reports,* 32:511-519.

Sahebzamani, F.M., Munro, C.L., Marroquin, O.C., Diamond, D.M., Keller, E., Kip, K.E. 2014. Examination of the FDA warning for statins and cognitive dysfunction. *Journal of pharmacovigilance,* 2(4):1-9.

Santaniello, M. & Giannini, G. 2015. Statins solubilized in fish oil: Versatile and simple combinations by innovative formulations. *Nutrition and food technology,* 1(1):1-10.

Satpute, V.M., Shirsat, M.K., Dhobale, A.V., Wani, R.M., Kharde, S.N. 2018. Formulation and evaluation of atorvastatin calcium oral dispersible tablet*. International journal of current advanced research*, 7:14170-14174.

Savjani, K.T., Gajjar, A.K., Savjani, J.K. 2012. Drug solubility: Importance and enhancement techniques. *International scholarly research network: Pharmaceutics*, 2012:1-10.

Setya, S., Talegaonkar, S. & Razdab, B.K. 2014. Nanoemulsions: formulation methods and stability aspects. *World journal of pharmacy and pharmaceutical sciences*: 3:2214-2228.

Sharma, N., Agarwal, G., Rana, A.C., Bhat, Z.A., Kumar, D. 2011. Trasderma drug deivery system: A too for ove drug deivery system. *Iteratioa oura for drug deveopmet & research,* 3(3):70-84.

Scherr, R.E., Zidenberg-Cherr, S. 2016. Nutrition and health info sheet: Cholesterol. https://nutrition.ucdavis.edul>factsheets.pdf. Date off access: 17 Oct 2018.

Schierwagen, R., Trebicka, J., Uschner, F.E., Magdaleno, F., Klein, S. 2017. Rationale for the use of statins in liver disease. *American journal of physiology gastrointestinal and liver physiology,* 312:G407-G412.

Schultz, G., Patten, D.K., Berlau, D.J. 2018. The role of statins in both cognitive impairment and protection against dementia. *Translatioal neurogeneration,* 7(5):1-11.

Smelt, A.H.M. 2010. Triglycerides and gallstone formation. *Clinica chimica acta,* 411:1625-1631.

Steele, G. & Austin, T. 2009. Preformulation investigations using small amounts of compound as an aid to candidate drug selection and early development. (*In* Gibson, M., ed. Pharmaceutical preformulation and formulation: a practical guide from candidate drug selection to commercial dosage form. 2nd ed. New York: Informa Healthcare. p. 17-128).

Subedi, R.K., Oh, S.Y., Chun, M. & Choi, H. 2010. Recent advantages in transdermal drug delivery. *Archives of pharmacal research*, 33:339-351.

Tadros, T., Izquierdo, P., Esquena, J. & Solans, C. 2004. Formation and stability of nano-emulsions. *Advances in colloid and interface science*, 108(19):303-318.

Trommer, H., Neubert,R.H.H. 2006. Overcoming the stratum corneum: The modulation of skin penetration. Skin pharmacology and physiology, 19:106-121.

Van Der Schaaf, P.A., Blatter, F., Szelagiewicz, M., Oberwil, S. 2006. United States patent application publication https://patentimages.storage.googleapis.com/5f/33/53/12e51d9490de73/US20060142582A1.pdf. Date of access: 5 Nov 2018.

Verma, S., Kumar, N., Kumar, U., Jain, G. 2018. Nanoemulsion: an exceptional mode for delivery of poorly soluble drug. *World journal of pharmacy and pharmaceutical sciences,* 7(2):374-392.

Vermaak, I., Kamatou, G.P.P., Komane-Mofokeng, B., Viljoen, A.M. & Beckett, K. 2011. African seed oils of commercial importance: cosmetic application. *South African Journal of Botany*, 77:920-933.

Wang, Y., Fan, Q., Song, Y. & Michnaik, B. 2003. Effects of fatty acids and iontophoresis on the delivery of midodrine hydrochloride and the structure of human skin. *Pharmaceutical Research*, 20:1612-1618.

Wang, W. 2012. Evaluation of siberian apricot (Prunus sibirica L.) germplasm variability for biodiesel properties. *Journal of American Oil Chemists' Society*, 89:1743-1747.

Wiechers, J.W. 2008. Skin delivery: what it is and why we need it. (*In* Wiechers, J.W., ed. Science and applications of skin delivery systems. Carol Stream, IL: Allured Publishing. p. 1-21).

Williams, A.C. 2003. Structure and function of human skin. (*In* Williams, A.C., ed. Transdermal and topical drug delivery: from theory to clinical practice. London: Pharmaceutical Press. p. 1-26).

Williams, A.C. 2013. Topical and transdermal drug delivery. (*In* Aulton, M.E., *ed*. Aulton„s pharmaceutics: the design and manufacture of medicines. 4th ed. London: Churchill Livingstone. p. 675-697).

Zhang, D. 2009a. Polyoxyethylene sorbitan fatty acid esters. (*In* Rowe, R.C., Sheskey, P.J. & Quinn, M.E., eds. Handbook of pharmaceutical excipients. 6th ed. USA: Pharmaceutical Press. p. 549-553).

Zhang, D. 2009b. Sorbitan esters. (In Rowe, R.C., Sheskey, P.J. & Quinn, M.E., eds. Handbook of pharmaceutical excipients. 6th ed. USA: Pharmaceutical Press. p. 675-678).

Zhang, J., Liu, Q. 2015. Cholesterol metabolism and homeostasis in the brain. *Protein & cell,* 6(4):254-264.

Zhao, Q., Kuang, W., Long, Z., Fang, Liu, D., Yang, B., Zhao, M. 2013. Effect of sorbitan monostearate on the physical characteristics and whipping properties of whipped cream. *Food chemistry*, 141:1834-1840.

Zodda, D., Giammona, R., Schifilliti, S. 2018. Treatment strategy for dyslipidaemia in cardiovascular disease prevention: focus on old and new drugs. *Pharmacy,* 6(10):1-16.

# CHAPTER 3

Chapter 3 is written for the purpose of publication in Die Pharmazie. This Chapter follows the author guidelines and format of this journal (provided in Appendix F). This manuscript is written in Arial 10 and UK English was used.

Centre of Excellence for Pharmaceutical Sciences, North-West University, Private Bag X6001, Potchefstroom, 2520, South Africa

**A novel HPLC method developed and validated for the detection and quantification of atorvastatin, fluvastatin, pitavastatin and pravastatin in transdermal delivery studies**

**Authors**: Sumari Maree, Jan L. du Preez, Lissinda H. du Plessis, Jeanetta du Plessis and Minja Gerber*

* Corresponding author: Centre of Excellence for Pharmaceutical Sciences (Pharmacen™), North-West University, Private Bag X6001, Potchefstroom, 2520, South Africa. Tel.: +2718 299 2328; Fax: +2787 231 5432. E-mail address: Minja.Gerber@nwu.ac.za

**Abstract**

A novel HPLC method with UV detection for the identification and quantification of atorvastatin, fluvastatin, pitavastatin and pravastatin during *in vitro* transdermal delivery studies has been developed and validated. The method proved to be most effective with a Restek Ultra C18, 250 x 4.6 mm, 5 µm (Restek, Bellefonte, PA) column with a flow rate of 1.0 ml/min of statins at 240 nm UV detection with the injection volume set at 10 µl. The mobile phase was determined as acetonitrile/Milli-Q® water (Milli-Q® Academic water purification system, Merck-Millipore, Midrand, RSA) with 0.1% orthophosphoric acid, which starts at 30% acetonitrile and increases linearly to 70% after 4 min; subsequently it is held at 70% for up to 10 min and then re-equilibrated to start conditions. This HPLC method indicated linearity within the concentration range of 0.05-200.00 µg/ml with a correlation coefficient ($R^2$) of 1 and an average recovery of 98-103%. Limit of detection (LOD) and limit of quantification (LOQ) values showed that statins could still be identified at concentrations 0.004-0.006 µg/ml with the exception of atorvastatin (0.116 µg/ml) which was quantified at a concentration of 0.013-0.035 µg/ml. Specificity evaluation performed during method validation confirmed method suitability for accurate detection and quantification of statins when combined with excipients included in formulations of transdermal delivery systems.

**1. Introduction**

Cholesterol, produced by the liver, is present in all body cells; particularly in cell walls. Here it has the important function of providing cell stability and assisting cell interaction to ensure that the body cells perform as a unit [Scherr and Zidenberg-Cherr, 2016]. Cholesterol is also a core component in the brain to sustain normal brain function and development, which contains up to 20% of the body's cholesterol [Zhang and Liu, 2015]; hence, identifying it as the highest cholesterol containing organ [Ferris et al. 2017]. Elevated blood cholesterol, which can be detected with a lipid profile serum test, are linked to health risks such as cardiovascular diseases (CVDs) [Onwe et al. 2015], which is the leading cause of death in the world [AHA, 2018]. Statins, the first-line treatment for primary hyperlipidaemia (due to their ability to lower low density lipoproteins (LDL) and triglycerides [Schierwagen et al. 2017]) are classified as 3-hydroxy-3-methyl-glutaryl-coenzyme A (HMG-CoA) reductase inhibitors, with both anti-atherosclerotic and obstructive tumour-cell growth abilities [Stancu and Sima, 2001]. Statins have the ability to restrict the enzymes responsible for endogenous cholesterol, as well as isoprenoid formation [Schierwagen et al. 2017] earning them the identity of HMG-

CoA [Fong, 2016]. Statins are currently registered as an oral treatment [Robinson and Goldberg, 2011]; however, oral administered statins present inadequacies such as gastro-intestinal side-effects (flatulence, nausea and vomiting, difficulty swallowing, indigestion, diarrhoea, constipation and abdominal cramps) [Mancini et al. 2013] and reduced systemic bioavailability, as a result of either extensive clearance of statins by means of liver enzymes (cytochrome P450) for those who experience hepatic clearance or statin-stomach content interaction [Marrow et al. 2007; Naik et al. 2000].

In the attempt to overcome or bypass these inadequacies and side-effects of oral administered statins, the transdermal delivery route was investigated as a more suitable pathway of administration. A novel HPLC method was developed and validated for atorvastatin, fluvastatin, pitavastatin and pravastatin to adhere to requirements that *in vitro* skin permeation studies require; a sensitive, suitable and accurate method to detect exceptionally small concentrations.

**2. Investigations, results and discussion**

The method was validated according to required parameters known as linearity, accuracy, precision (both inter-day and intra-day), system stability, specificity, LLOD (lowest limit of detection) and LLOQ (lowest limit of quantification) (see Table 1).

The linearity was performed through preparation of a standard solution (±20 mg in 100 ml methanol (0.02%)) for each of the statins; where after 5 ml of the standard solution was transferred to a separate volumetric flask and made up to volume (100 ml) with methanol. Volumes of the standard as well as the dilution were transferred to HPLC vials, which was injected and analysed (in replicate) at injection volumes of 2.5 µl, 5.0 µl, 7.5 µl and 10.0 µl. From the different concentration ranges obtained, analytical response plots (peak areas against analyte concentration (µg/ml)) were generated to produce standard linear regression curves for each statin. The linearity of the data is presented through the linear regression equation (see Eq. 1), where the *y*-unit represents the peak area of the analyte (statin); the *x*-unit, the concentration analyte (statin) present in the sample; *c*, the y-intercept and *m,* the slope [Paithankar, 2013]. The linear regression equation obtained for each statin was used to calculate the correlation coefficient ($R^2$). The $R^2$ for each statin was calculated as 1 (see Table 1), which signified a strong relationship between the peak areas and analyte concentration (µg/ml) within the evaluated concentration range.

$$y = mx + c \qquad \textbf{Eq. 3.1}$$

Accuracy is reported as recovery (%) and can be described as the relationship between the noted results to the results expected [APVMA, 2004]. The expected recovery is influenced by the analyte concentration, the sample placebo and the method with which the sample is prepared [APVMA, 2004]. The accuracy results of atorvastatin (99.2%), fluvastatin (103.0%), pitavastatin (98.0%) and pravastatin (100.2%) proved to be accurate and within acceptable limits, since the mean recovery (%) ranged between 90-110% [APVMA, 2004] with consistent relative standard deviations (%RSD) of 0.7-0.9%.

Precision, defined as the degree of variation (%RSD) between the data obtained from numerous measurements under certain conditions utilising a main sample [APVMA, 2004] was determined in terms of intra-day (repeatability performed in one day) and inter-day (intermediate precision performed

over three consecutive days) precision. When assessing precision, a %RSD value is calculated [APVMA, 2004] on a minimum of nine samples [ICH, 2005]. Prior to testing the precision, standard solutions, a placebo nano-emulsion and spiked solutions (±400 mg statin added up to 100 ml methanol) for each statin were prepared. Intra-day and inter-day precision were determined in triplicate. Samples to be tested were prepared to contained 0.16%, 0.18% and 0.20% spiked solution and 0.60%, 0.80% and 1.00% placebo transdermal formulation, respectively which were made up to volume with methanol. A volume of each prepared sample was transferred to vials, which was injected in the HPLC to be compared to injected standards of each statin. Note that for inter-day precision, only the intermediate concentrations were analysed from days 2-3. The %RSD values calculated during intra-day, as well as inter-day precision for statins were satisfactory, as they remained lower than 5% respectively [APVMA, 2004; Paithankar, 2013] (see Table 1).

System stability assesses the ability of the validation method to determine compounds when degradation products are present [Huber, 2007]. This experiment measures in hourly intervals over a selected time period [Huber, 2007] of 24 h. A standard sample was prepared containing ±20 mg (200 µg/ml) of each statin added up to volume (100 ml) with methanol. A small quantity was transferred to an HPLC vial to be injected and analysed. Sample stability results (%RSD) for statins qualified as stable as the degradation value was less than 2% [Paithankar, 2013] (see Table 1).

Repeatability in terms of accuracy and precision was prepared similar to the method used to determine system stability. Each sample was injected six consecutive times into the HPLC, to determine retention times and peak areas of samples under the same conditions in one day. System repeatability of statins succeeded in the criteria, since the %RSD was less than 2% for the peak area and the retention times [Paithankar, 2013] (see Table 1).

To determine the specificity, tests are performed to accurately establish the reaction of the tested active pharmaceutical ingredient's (API's) peak in the presence of impurities (other components) [Huber, 2007] using the specific analytical method [ICH, 2005]. Specificity is required to consider the analytical method as acceptable and when no peak hindrances appear with the retention times of the API, the method is regarded as specific [Snyders et al. 1997]. Specificity was determined through preparation of five samples each containing approximately 20 mg of each statin added up to volume (100 ml) with methanol. A small quantity was transferred to a vial to be injected and analysed by the HPLC as a standard (b). Additional vials were prepared containing only methanol, which served as the placebos (a) for each statin. A volume of 1 ml of the standard solution containing the selected statin was transferred to four separate test tubes, where each of these test tubes were spiked with a volume of 200 µl of hydrochloric acid (HCl) (c), Milli-Q® water (d), sodium hydroxide (NaOH) (e) and hydrogen peroxide ($H_2O_2$) (f). A small quantity was transferred to an HPLC vial to be injected and analysed. Figures 1 (A – D) indicates that degradation peaks detected caused by additives ((c)-(f)) in the samples. Peak retention times of statins remained unaltered and were 4.84, 5.84, 8.53 and 8.95 min for pitavastatin, pravastatin, atorvastatin and fluvastatin, respectively.

The LOD of an analytical method represents the sensitivity and is described as the lowest detectable analyte in a sample; this is not necessarily a definite value [APVMA, 2004, Snyder et al. 1997]. On the

contrary to the LOD, the LOQ is described as the lowest detectable amount of analyte present in a sample under specific conditions, this value can be accurately determined [APVMA, 2004]. To establish the LOD and LOQ values, each statin was weighed (±5 mg) individually. These weighed statins were then dissolved in different 100 ml volumetric flasks with methanol and made up to volume. A volume of 1 ml of each solution was extracted and further diluted to 100 ml with methanol. HPLC vials were filled with 1 ml of diluted solution for each statin. Each vial was injected six consecutive times at four different injection volumes (2.5, 5.0, 7.5 and 10.0 µl). The LOD and LOQ of the statins were established through the calculation of regression through data analysis, where σ indicates the standard variation of the *y*-intercept and *S* indicates the gradient of the slope. Eq. 2 and Eq. 3 were used to calculate the LOD and LOQ, respectively [Swartz and Krull, 2012]. The LOD and LOQ results of statins were within accepted parameters, as the LOD's %RSD values were less than 15%, and LOQ's %RSD measured below 20% [FDA, 2001; Rathmann et al. 2015].

**LOD** = 3.3 x σ/S **Eq. 3.2**

**LOQ** = 10 x σ/S **Eq. 3.3**

Subsequent to the validation of the analytical method, skin diffusion and tape stripping studies were performed. Analysis of the statins in the receptor phase, tape strips and skin samples were performed utilising the newly validated method (see Fig. 2).

**3. Experimental**

To develop the HPLC method used in this study, an analytical instrument (Dionex UltiMate 3000 dual system with ternary gradient pumps, column ovens, an autosampler and diode array detectors) was used. This analytical instrument operated on Chromeleon 7.2 instrument control and data analysis software (Thermo Fisher Scientific Inc., Waltham, MA) for optimal processing of data. A Restek Ultra $C_{18}$, 250 x 4.6 mm, 5 µm (Restek, Bellefonte, PA) column was inserted, with a flow rate of 1.0 ml/min at 240 nm UV detection with the injection volume set at 10 µl. The mobile phase was determined as acetonitrile/Milli-Q® water (Milli-Q® Academic water purification system, Merck-Millipore, Midrand, RSA) with 0.1% orthophosphoric acid, which starts at 30% acetonitrile and increases linearly to 70% after 4 min, which is held at 70% for up to 10 min and then re-equilibrated to start conditions. The solvent used during method development and validation was methanol. The retention times were reported as 4.84, 5.84, 8.53 and 8.95 min for pitavastatin, pravastatin, atorvastatin and fluvastatin, respectively with a stop time of 15 min.

**Acknowledgements**

This study was executed with the funding from The South African National Research Foundation (NRF): Competitive Support for Unrated Researchers (CSUR) (Grants no. 105913) and The Centre of Excellence for Pharmaceutical Sciences (Pharmacen™) of the North-West University, Potchefstroom Campus, South Africa.

**Disclaimer**

The authors proclaim no conflict of interest. Any opinion, findings and conclusions, or recommendations expressed in this material are those of the authors and therefore the NRF does not accept any liability in regard thereto.

**References**


AHA (American heart association). 2018. Heart disease and stroke statistics 2018 at a glance. https://www.heart.org/-/media/data-import/downloadables/heart-disease-and-stroke-statistics-2018---at-a-glance-ucm_498848.pdf. Date of access: 21 Oct 2018.

APVMA (Australian pesticides and veterinary medicines authority). 2004. Guidelines for the validation of analytical methods for active constituents, agricultural and veterinary chemical products. http://apvma.gov.au/sites/default/files/docs/guideline-69-analytical-methods.pdf Date of access: 14 Dec. 2017.

FDA (Food and drug administration). 2001. Guidance for Industry: bioanalytical method validation. http://www.fda.gov/downloads/drugs/guidancecomplianceregulatoryinformation/guidances/ucm368107.pdf Date of access: 19 Dec. 2017.

Ferris HA, Perry RJ, Moreira GV, Shulman GI, Horton JD, Kahn CR (2017) Loss of astrocyte cholesterol synthesis disrupts neuronal function and alters whole-body metabolism. Journal of the national academy of sciences, 114(5):1189-1194.

Fong C (2016) Statins in therapy: Understanding their hydrophilicity, lipophilicity, binding to 3-hydroxy-3-methylglutaryl-CoA reductase, ability to cross the blood brain barrier and metabolic stability based on electrostatic molecular orbital studies. Eur J Med Chem, 85:661-674.

Huber L (2007) Validation of Analytical Methods. https://www.agilent.com/cs/library/primers/public/5990-5140EN.pdf. Date of access: 13 Dec. 2017.

ICH (International Conference of Harmonisation). 2005. Validation of analytical procedures: text and methodology Q2 (R1). http://www.ich.org/fileadmin/Public_Web_Site/ICH_Products/Guidelines/Quality/Q2_R1/Step4/Q2_R1__Guideline.pdf Date of access: 13 Dec. 2017.

Mancini GBJ, Tashakkor AY, Baker S, Bergeron J, Fitchett D, Frohlich J, Genest J, Gupta M, Hegele, RA, Ng DS, Pearson GJ, Pope J (2013) Diagnosis, prevention, and management of statin adverse effects and intolerance: Canadian working group consensus update. Can J Cardiol, 29:1553-1568.

Marrow DIJ, McCarron PA, Woolfson AD, Donnelly RF (2007) Innovative strategies for enhancing topical and transdermal drug delivery. The open drug delivery journal, 1:36-59.

Naik A, Kalia YN, Guy RH (2000) Transdermal drug delivery: overcoming the skin's barrier function.

Pharm. Sci. Technol. Today, 3(9):318-326.

Onwe PE, Folawiyo MA, Okike PI, Balogun ME, Umahi G, Besong EE, Okorocha AE, Afoke AO (2015) Lipid Profile and the growing concern on lipid related diseases. IOSR J Pharm Biol Sci, 10(5):22-27.

Paithankar HV (2013) HPLC method validation for pharmaceuticals. International journal of universal pharmacy and bio sciences, 2(4):229-240.

Rathmann D, Rijntjes E, Lietzow J, Köhrle J (2015) Quantitative analysis of thyroid hormone metabolites in cell culture samples using LC-MS/MS. Eur Thyroid J, 4:51-58.

Robinson JG, Goldberg AC (2011) Treatment of adults with Familial Hypercholesterolemia and evidence for treatment: Recommendations from the National Lipid Association Expert Panel on Familial Hypercholesterolemia. J Clin Lipidol, 5:S18-S29.

Scherr RE, Zidenberg-Cherr S (2016) Nutrition and health info sheet: Cholesterol. https://nutrition.ucdavis.edu/sites/g/files/dgvnsk426/files/content/infosheets/fact-consumer-cholesterol.pdf. Date off access: 17 Oct 2018.

Schierwagen R, Trebicka J, Uschner FE, Magdaleno F, Klein S (2017) Rationale for the use of statins in liver disease. Am. J. Physiol. Gastrointest. Liver Physiol., 312:G407-G412.

Snyder LR, Kirkland JJ, Glajch JL (1997) Completing the method: validation and transfer. In Snyder, L.R., Kirkland, J.J. & Glajch, J.L., eds. Practical HPLC method development. 2nd ed. New York: John Wiley & Sons. p. 685-713.

Stancu C, Sima A (2001) Statins: mechanism of action and effects. J. Cell. Mol. Med., 5(4):378-387.

Swartz ME, Krull IS (2012) Handbook of analytical validation. Boca Raton: CRC Press.

Zhang J, Liu Q (2015) Cholesterol metabolism and homeostasis in the brain. Protein & cell, 6(4):254-264.

**Table 3.1:** Summary of the HPLC's validation parameters and results

| Validation parameters | | Accepted parameters | Atorvastatin | Fluvastatin | Pitavastatin | Pravastatin |
|---|---|---|---|---|---|---|
| **Linearity** | | $R^2$>0.98 | $R^2$=1 | $R^2$=1 | $R^2$=1 | $R^2$=1 |
| **Accuracy** | | Recovery (90-110%) | 99.2% | 103.0% | 98.0% | 100.2% |
| **Precision** | Intra-day | RSD≤5% | 0.68% | 1.56% | 0.83% | 2.48% |
| | Inter-day | | 0.72% | 0.90% | 0.78% | 3.35% |
| **System stability** | | RSD<2% | 0.94% | 0.77% | 0.27% | 0.65% |
| **System repeatability** | Peak area | RSD<2% | 0.78% | 0.25% | 0.20% | 0.31% |
| | Retention time (min) | RSD<2% | 0.05% | 0.03% | 0.06% | 0.06% |
| **Specificity** | | Fig. 1 specificity | | | | |
| **LOD (µg/ml)** | | RSD<15% | 0.116 | 0.006 | 0.005 | 0.004 |
| **LOQ (µg/ml)** | | RSD<20% | 0.035 | 0.019 | 0.015 | 0.013 |

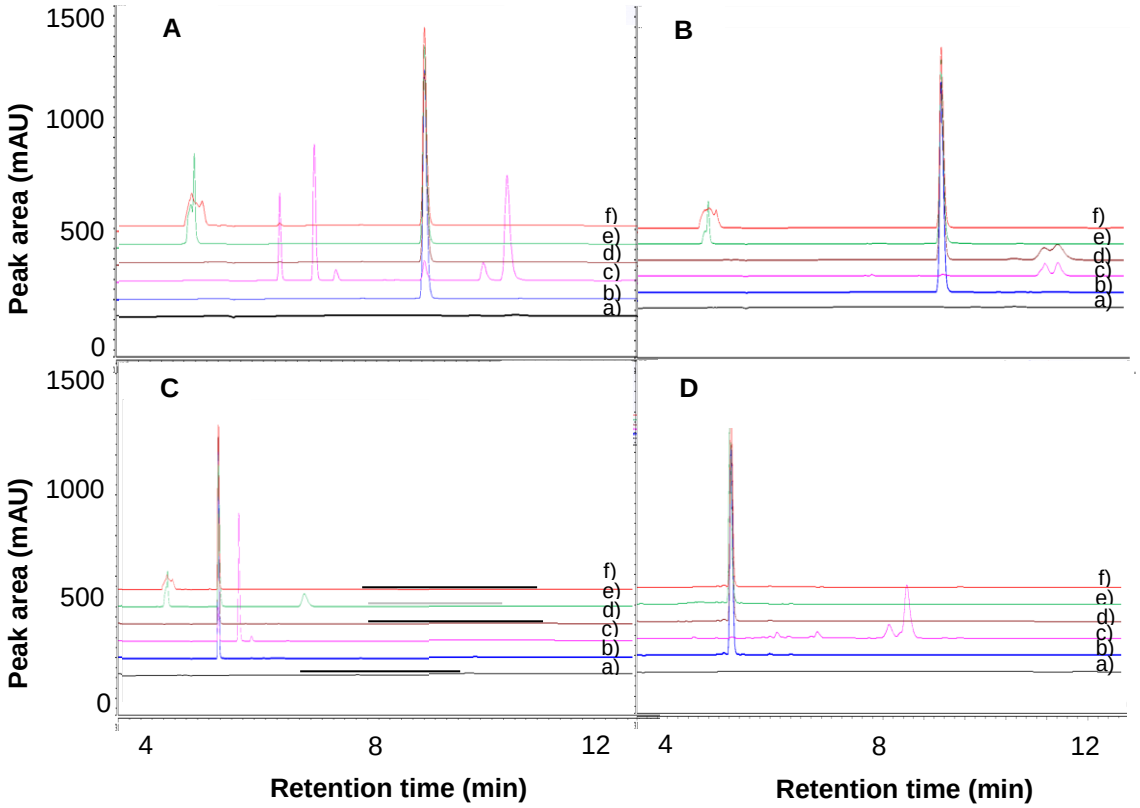


**Fig. 3.1:** HPLC chromatogram indicating the specificity data of: A) atorvastatin, B) fluvastatin, C) pitavastatin and D) pravastatin. (The letters represent the following: a) placebo and b) standard solution with selected statin. The following statin sample solutions were stressed with: c) HCl, d) Milli-Q® water, e) NaOH and f) $H_2O_2$

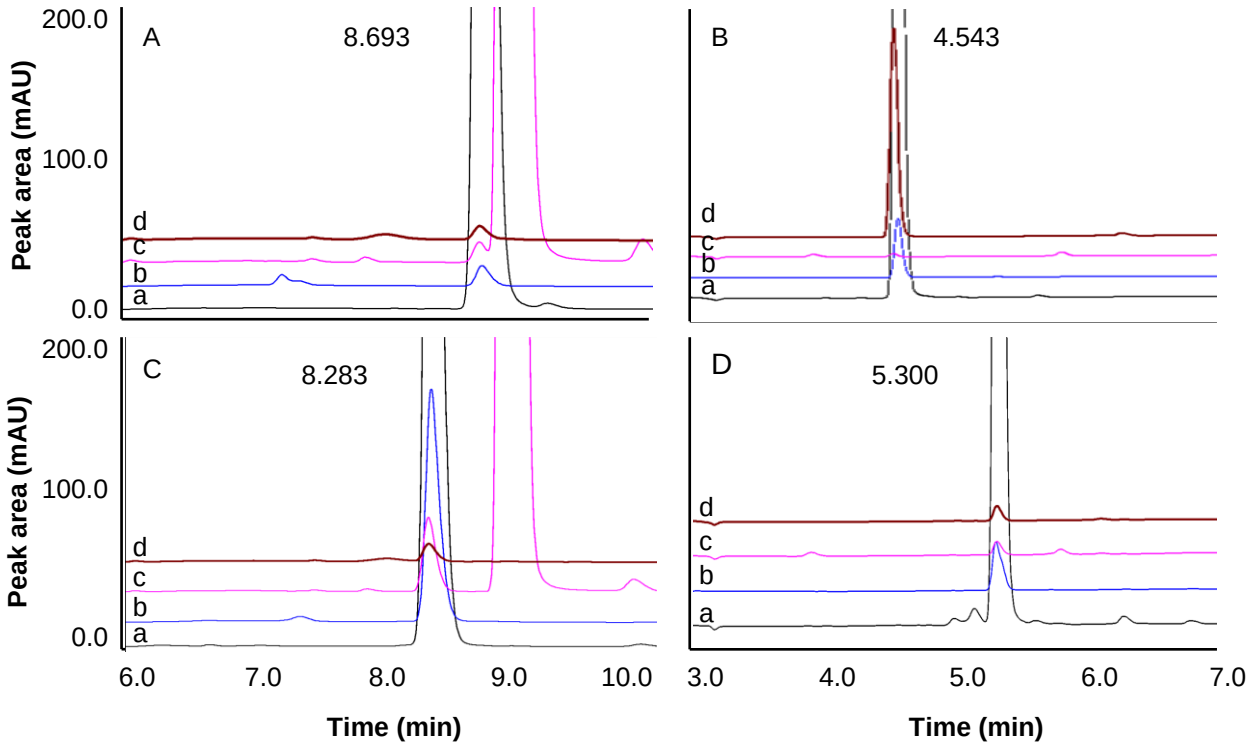


**Fig. 3.2:** HPLC chromatogram indicating the *in vitro* skin diffusion study data of: A) fluvastatin, B) pitavastatin, C) atorvastatin and D) pravastatin. The letters represent the following samples with the respective statins: a) standard solution, b) receptor phase (transdermal delivery), c) tape strip (topical delivery) and d) skin sample (topical delivery)

# CHAPTER 4

ARTICLE FOR THE PUBLICATION IN THE INTERNATIONAL JOURNAL OF PHARMACEUTICS

This Chapter is written for publication in The International Journal of Pharmaceutics (in article form). The paragraphs of this chapter have been justified for the ease of reading. The authors have decided to write in UK English, as the author's guide accepts both UK and US English. The complete author's guide is listed in Appendix G.

# Transdermal delivery of selected statins formulated in nano-emulsions to be compared to nano-emulgels

Sumari Maree, Jeanetta du Plessis, Lissinda H du Plessis and Minja Gerber*

Centre of Excellence for Pharmaceutical Sciences, North-West University, Private Bag X6001, Potchefstroom 2520, South Africa

*Corresponding author. Tel.: +2718 299 2328; Fax: +2787 231 5432. E-mail address: Minja.Gerber@nwu.ac.za (M Gerber).

**Abstract**

Statins are the primary active pharmaceutical ingredient (API) in the oral treatment of hyperlipidaemia. Oral-administered statins supposedly have gastro-intestinal side-effects, and low bioavailability due to hepatic clearance. The goal was to formulate statins within nano-formulas for transdermal delivery.

Characterisation techniques were performed on nano-formulas to confirm formula stability, where after cytotoxicity studies were conducted on the pre-malignant human immortalised keratinocytes (HaCaT) to determine whether HaCaT cell lines were affected by statins and other compounds in the nano-formulas.

Membrane release studies for the determination of statins released from formulas were conducted, followed by *in vitro* skin diffusion studies and tape stripping, to evaluate the transdermal and/or topical delivery of statins. Statistical analyses were performed to analyse the variances between the means of data obtained from afore-mentioned studies.

Membrane release studies concluded that the nano-emulsion had the higher median flux values compared to nano-emulgels, with the exception of pravastatin nano-emulgel which prevailed among all the nano-formulas. Skin diffusion studies indicated that nano-emulgels persist with higher median concentration of statins diffused through skin than their respective nano-emulsions. Tape stripping results revealed that statin concentrations were higher in the skin layers than that which had diffused through the skin.

*Keywords:* nano-emulsion, nano-emulgel, plasma concentrations, statins, transdermal delivery, cytotoxicity

**Graphical Abstract**

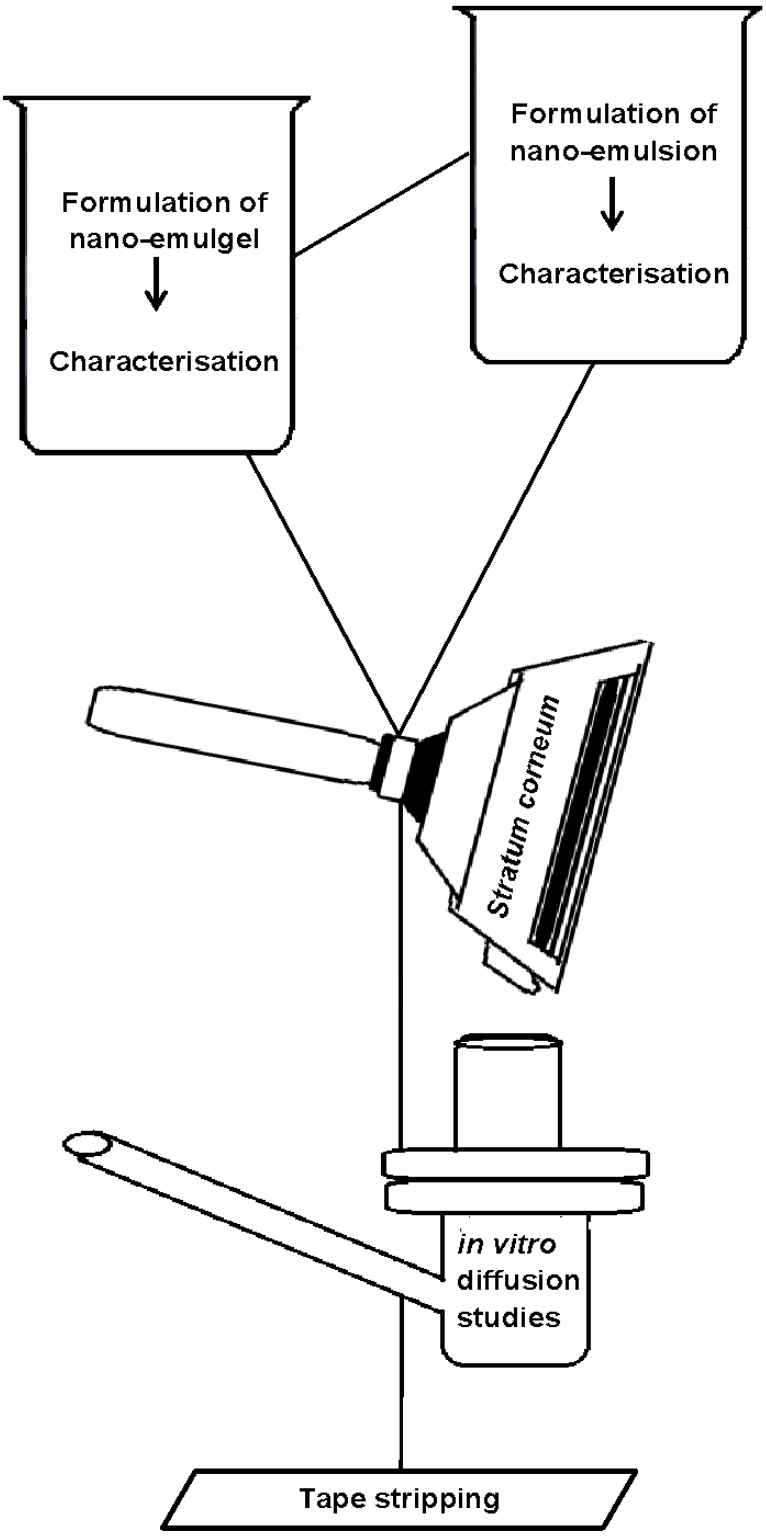

## 1 Introduction

Cholesterol - a fatty compound generated in the liver - plays a vital role in the cell walls of the body, where it supports cell stability and promotes cell interaction to ensure that body cells function as a unit (Scherr & Zidenberg-Cherr, 2016). Cholesterol is also crucial to maintain brain function, as this organ contains up to 20% of the human body's cholesterol (Zhang & Liu, 2015). Elevated blood cholesterol, also known as hypercholesterolemia or hyperlipidaemia have repeatedly been associated as a cause of chronic illnesses such as atherosclerosis and cardiovascular diseases (CVDs). Statins, classified as HMG-CoA (as 3-hydroxy-3-methyl-glutaryl-CoA) reductase inhibitors (Fong, 2016) are registered as the first-line medical treatment of hyperlipidaemia (Zodda *et al.*, 2018; Robinson & Goldberg, 2011) as they have the ability to lower low density lipoprotein (LDL) concentrations present in the blood stream (Fong, 2016). Statins are only available as an oral administration, which presents with adverse effects such as gastro-intestinal side-effects (flatulence, nausea and vomiting, difficulty swallowing, indigestion, diarrhoea, constipation and abdominal cramps) (Mancini *et al.,* 2013). In addition, statins show reduced systemic bioavailability as a result of either extensive hepatic clearance of the cytochrome P-450 liver enzyme, statin-stomach content interaction (Marrow *et al.,* 2007; Naik *et al.,* 2000) or the occurrence of statin-drug interactions (Piepho, 2000). Due to the side-effects and interactions of oral administered statins, the transdermal delivery route will be investigated as an alternative.

The transdermal delivery route involves the delivery of a drug through the skin layers to reach the circulatory system (Kala & Juyal, 2018). The human skin comprises various layers, each constructed with a variety of cells, which perform certain roles (Ng & Lau, 2015). Skin layers are classified as the epidermis, dermis and underlying hypodermis (Ng & Lau, 2015). The epidermis is further sub-divided, of which the stratum corneum (the outmost layer of the human skin) is the most specialised (Baibhav *et al.,* 2011). The stratum corneum is known as the rate-limiting barrier of the skin and since its construction consists of both hydrophilic and lipophilic properties, this sub-layer mostly opposes APIs absorption (Baibhav *et al.,* 2011).

Investigated statins (atorvastatin, fluvastatin, pitavastatin and pravastatin) are non-compliant to a number of ideal physiochemical requirements for transdermal delivery (Naik *et al.,* 2000) with regard to partition coefficient (log P), octanol buffer distribution coefficient (log D), molecular weight, melting point, aqueous solubility, diffusion coefficient, pKa (Williams, 2013), pH and polarity (Rastogi & Yadav, 2012). Consequently, statins need to be formulated within a carrier system to overcome the barrier posed by the skin (Gabera *et al.,* 2017).

The carrier system in this study is nano-emulsions, for their ability to avoid hepatic metabolism, enhance absorption, prolong half-lives and reduce toxicity (Gabera *et al.,* 2017). Nano-emulsions will be compared to nano-emulgels (gelling-agents containing nano-emulsion) formulated from the optimised nano-emulsion formula.

Gelling-agents as additives tend to decrease interfacial and surface tension more than nano-emulsions to produce a more viscous formulation (Chellapa, 2015), which have shown to increase in skin permeability (Chellapa, 2015, Eid *et al.,* 2014).

Skin permeability and active pharmaceutical ingredient (API) absorption can be further improved with penetration enhancers (Kala & Juyal, 2018), by reversibly modifying the challenges posed by the stratum corneum (Boglarka *et al.,* 2016; Kala & Juyal, 2018). Apricot kernel oil is the chosen penetration enhancer, with the dual function of serving as an oil phase in the formulas. Apricot kernel oil contains long chain fatty acids (oleic acid (58-68%) and linoleic acid (22-31%), unsaturated, 18-carbon fatty acids) (Wang, 2012) also present in the human skin, which reduces the occurrence of skin irritations (Vermaak *et al.,* 2011). Rich in vitamins, apricot kernel oil nourishes dry skin when applied. Natural penetration enhancers alter the lipophilic bilayers of the skin by disrupting the cellular corneocytes (Wang *et al.,* 2003; Williams, 2013); in turn increasing the flux of APIs across the stratum corneum (Vermaak *et al.,* 2011).

The aim of the study was to evaluate whether optimised statins, incorporated within apricot kernel oil droplets of nano-emulsions and nano-emulgels, succeeded in transdermal delivery, and if so, which formulas prevailed. In addition, the concentrations of statins to diffuse through the skin to achieve circulation were compared to that of literature regarding oral administered

statins. These comparisons evaluate the efficiency of the transdermal route by use of nano-emulsions and nano-emulgels.

## 2 Materials and Methods

### 2.1 Materials

Statins (atorvastatin, fluvastatin, pitavastatin and pravastatin) were obtained from DB Fine Chemicals (Johannesburg, RSA); apricot kernel oil (natural oil) was attained from CJP Chemicals (Johannesburg, RSA); sorbitan monostearate, the lipophilic surfactant (Span® 60), polyoxyethylene 20 sorbitan fatty acid ester, the hydrophilic surfactant (Tween® 80) and Carbopol®20 Ultrez 20 (thickening agent) were obtained from Sigma & Aldrich (Johannesburg, RSA). The phosphate buffer solution (PBS) was made up with sodium hydroxide (NaOH) and potassium dihydrogen orthophosphate ($KH_2PO_4$), both provided by Sigma-Aldrich (Johannesburg, RSA). The mobile phase preparation, HPLC grade acetonitrile and orthophosphoric acid were supplied by Sigma-Aldrich (Johannesburg, RSA) and used in combination with Milli-Q® water (deionised) attained from a Milli-Q® Academic water purification system (Merck-Millipore, Midrand, RSA). Only HPLC grade chemicals were utilised.

### 2.2 Methods

#### 2.2.1 Formulation of statin nano-emulsions and nano-emulgels

Different surfactant ratios were tested during formulation of the nano-emulsions, to determine which formula was the most stable and sufficient regarding dissolution of statins to be used as the optimised formula. Nano-emulsions were prepared by heating 40 ml Milli-Q® water in a glass beaker (containing magnetic stirrer) on a pre-heated hot plate equipped with a magnetic stirrer. A pipetted volume of Tween® 80 (surfactant) was added to the heated Milli-Q® water, producing the water phase. The oil phase was then prepared by adding a weighed amount of Span® 60 (surfactant) to the apricot kernel oil in a separate glass beaker (containing magnetic stirrer) and placed onto a pre-heated hot plate equipped with a magnetic stirrer. After adequate surfactant-phase mixing, a weighed amount of statin was added to the oil phase. Stirring continued to the point of complete dissolution of the statin in the oil phase.

Subsequently, the oil phase was added drop wise to the water phase, while stirring continued to ensure appropriate emulsification. The newly formed emulsion was kept at room temperature (25°C) to cool down after proper emulsification, after which it was sonicated with an ultrasonicator (Model UP200St, Hielscher Ultrasonics, Teltow, DE) for 3 min in 1 min intervals to produce a nano-emulsion. This formulation process was performed for the preparation of all the involved statins' nano-emulsions. Nano-emulgels were prepared separately for each statin following a similar method used to prepare nano-emulsions, with the exception of adding a weighed amount of Carbopol® Ultrez 20 to the water phase, after proper mixing of Tween® 80 and water phase. The water phase containing Tween® 80 and Carbopol® Ultrez 20 remained on the hot plate until it presented with a thickened presence and Carbopol® Ultrez 20 was no longer visible. The adequately mixed oil phase containing the statin and Span® 60, was then poured drop wise into the thickened water phase (on hot plate), while stirred rapidly by means of homogenisation (±750 rpm). Afterwards, the emulgel was transferred to the ultrasonicator to be sonicated for 3 min in 1 min intervals to produce a nano-emulgel. The optimised nano-emulsion formula (**NE1**) for statins was named atorvastatin **NE1A**, fluvastatin **NE1F**, pitavastatin **NE1Pi** and pravastatin **NE1Pr**. The nano-emulgels (**NEGs**) for the respective statins were named atorvastatin **NEGA**, fluvastatin **NEGF**, pitavastatin **NEGPi** and pravastatin **NEGPr** (Table 1).

Table 1:

Formula used to prepare **NE1s** and **NEGs** containing statins

### 2.2.2 Analysis of statins

An HPLC analytical method was developed and validated at the North-West University (NWU), Potchefstroom Campus, South Africa, in the Analytical Technology Laboratory (ATL). A Dionex UltiMate 3000 dual system with ternary gradient pumps, column ovens, an autosampler and diode array detectors was utilised to develop the HPLC method. This analytical instrument operated on Chromeleon 7.2 instrument control and data analysis software (Thermo Fisher Scientific Inc., Waltham, MA) for optimal processing of data. The

detection wavelength was set at 240 nm. The column used was a Restek Ultra $C_{18}$, 250 x 4.6 mm, 5 µm (Restek, Bellefonte, PA). The mobile phase was determined as acetonitrile/Milli-Q® water (Milli-Q® Academic water purification system, Merck-Millipore, Midrand, RSA) with 0.1% orthophosphoric acid, which starts at 30% acetonitrile and increases linearly to 70% after 4 min, held at 70% up to 10 min and then re-equilibrated to start conditions. The runtime consists of 15 min, with a flow rate of 1.0 ml/min at an injection volume of 10 µl. The retention times of statins were established as pitavastatin (±4.84 min), pravastatin (±5.84 min), atorvastatin (±8.53 min) and fluvastatin (±8.95 min), with HPLC grade methanol as the solvent. The limit of detection (LOD) and limit of quantification (LOQ) values of statins were calculated. Analytical tests were executed within a controlled environment (25°C).

### 2.2.3 Standard preparation

- The standard solution was prepared by adding ±20 mg statin in a 100 ml volumetric flask and filled up to volume with methanol. A volume of 5 ml of the standard statin was diluted to 50 ml with methanol; this step was repeated to prepare a second dilution from the first dilution.

### 2.2.4 Physicochemical properties

#### 2.2.4.1 Aqueous solubility

A volume of 10 ml PBS (7.4) was poured into separate test tubes, where after the PBS was saturated separately with individual statins to the point of precipitation. Test tubes were well shaken and placed in a preheated water bath (32°C) for 24 h. Test tubes were observed repeatedly to ensure saturation was maintained. After 24 h, the test tubes were removed from the water bath and centrifuged for 15 min. PBS (containing dissolved statin) was extracted from each test tube and filtered through 0.45 µm nylon membrane filters into HPLC vials for analysis (triplicate).

#### 2.2.4.2 Octanol-buffer distribution coefficient (log D)

The solubility of *n*-octanol solubility experiments had to be performed prior to log D determination. These experiments were performed to establish the appropriate amount of statins (mg/ml) to be added to the saturated phases during the log D determination

experiments. The technique used to determine the log D value of compounds is known as the shake flask method. Equal volumes of PBS (pH 7.4) (phase 1) and *n*-octanol (phase 2) were mixed in a separating funnel and kept still to equilibrate for 24 h to ensure co-saturation of the both phases. Phase 1, the bottom layer (pre-saturated PBS), and phase 2 (pre-saturated n-octanol) were drained into separate beakers. A weighed amount of ±40 mg of each statin was added to their own 20 ml pre-saturated octanol-volumetric flask. A volume of 3 ml of each saturated octanol-statin solution was extracted and added to 3 ml of pre-saturated PBS (pH 7.4) (triplicate). The test tubes were placed into a shaker water bath at 32°C for 8 h. The test tubes were then removed and 1 ml octanol phase of each test tube (top layer) was transferred to separate 10 ml volumetric flasks and made up to volume with methanol. The volumetric flasks were mixed adequately and volumes transferred separately to HPLC vials. PBS (containing dissolved statin), was extracted from each test tube and directly transferred to separate HPLC vials. Vials obtained from log D determination experiments were analysed by means of HPLC.

### 2.3 Characterisation of optimal statin nano-emulsions and nano-emulgels

Characterisation of the formulas was performed by means of visual inspection, pH, zeta-potential, droplet size, distribution and viscosity.

#### 2.3.1 Visual inspection

Visual inspection was performed to detect visible presence of sedimentation and flocculation in the formulas.

#### 2.3.2 pH

A calibrated Mettler Toledo® pH meter (Mettler Toledo, CU), equipped with a Mettler Toledo® InLab® 410 electrode (Mettler Toledo, CU) was used to determine the pH of nano-emulsions and nano-emulgels in triplicate.

### 2.3.3 Zeta-potential

To determine the zeta-potential of the formulas, a Malvern Zetasizer Nano ZS (Malvern Instruments, Worcestershire, UK) was used. An extracted volume of each nano-emulsion was diluted separately with Milli-Q® water (1:100) and mixed thoroughly by rotating the flask while holding it. The solutions were then transferred, each in their own clear disposable zeta cell. Each sample's measurement was performed in triplicate.

### 2.3.4 Droplet size and distribution

A Malvern Zetasizer Nano ZS (Malvern Instruments, Worcestershire, UK) was utilised to determine the droplet size and distribution of the formulas. The method of sample preparation was identical to the method used in testing zeta-potential (see Section 2.4.3). Each sample's measurement was performed in triplicate.

### 2.3.5 Viscosity

To measure the viscosity of formulas, a Brookfield Viscometer (DV2T LV Ultra-Middleboro, Massachusetts, USA), linked to a water bath (±25°C) was used. To reach the appropriate temperature, formulas were placed into the water bath one hour prior to viscosity testing. A cylindrical spindle (SC4-18) rotating at a speed of 200 rpm was used to measure the viscosity of nano-emulsions, and T-bar spindles, rotating at a speed of 20 to 30 rpm, were used to measure the viscosity of nano-emulgels. Viscosity readings were measured in centipoise (cP), in 10-sec intervals for 50 sec. Rheocalc T 1.2.19 software was used to collect multipoint data, in order to analyse and calculate average viscosity values.

## 2.4 Diffusion studies

Diffusion studies entailed membrane release studies and *in vitro* skin diffusion, which were performed by means of the Franz cell method.

### 2.4.1 Membrane release studies

Prior to membrane release studies, Franz cells were prepared by smearing the donor and receptor compartments with vacuum grease. A small magnetic stirrer was placed into each receptor compartment, where after polyvinylidene fluoride (PVDF) (Pall® Life Sciences, Michigan, USA) membranes 25 mm in diameter and a pore size of 0.45 µm were placed on

the receptor compartment. The vacuum greased donor compartments were positioned on the receptor compartments and the rims of these cells were sealed with vacuum grease. Finally, horseshoe clamps were fastened over the cells.

Preheated Grant® water baths (Grant Instruments, UK) were used to heat PBS (7.4) (37°C) and formulas (32°C) an hour prior to performing membrane release studies. Receptor compartments were filled with 2 ml PBS and a volume of 1 ml formula was transferred to each donor compartment, where after these compartments were enclosed with Parafilm®. The filled Franz cells were placed in a preheated water bath (37°C) on a Variomag® magnetic stirring plate (Variomag, USA).

The receptor phases were extracted individually via the sampling port in the same order as filled, and refilled with PBS (37°C). The extraction and refilling of the receptor compartments were performed in 1 h intervals for six consecutive hours. Each hour's receptor content was transferred into separate HPLC vials. All the vials were inserted into the HPLC and injected in duplicate, along with a standard (injection volumes of 2.5, 5.0, 7.5 and 10.0 µl) to produce a linear regression line for analysis.

### 2.4.2 Skin preparation

The skin utilised for diffusion studies was Caucasian female skin, attained from abdominoplasty. Ethical approval was acquired from the Research Ethics Committee of the North-West University (NWU-00111-17-A1-01) for experimental use of biological material for *in vitro* transdermal drug delivery studies. Signed informed consent forms were obtained from surgeons as well as donor patients. The collected skin was transported in a cooler stored in a freezer (-20°C). Prior to skin diffusion studies, the skin was defrosted to be dermatomed (400 µm). Dermatomed skin was spread out on Whatman® filter paper and cut into circles. Subsequently, skin circles were visually inspected before covered with aluminium foil and returned to the freezer (-20°C).

### 2.4.3 Skin diffusion studies

A method similar to membrane release studies (see Section 2.5.1) was utilised during *in vitro* skin diffusion studies, except that skin circles, instead of PVDF membrane filters, were used.

Circular cut dermatomed skin was placed with the stratum corneum facing upwards on the receptor compartment. Receptor compartments were filled with 2 ml PBS (pH 7.4) and instead of extracting the receptor phase hourly, extractions were performed once after 12 h. Samples of extractions were analysed identically to those of membrane release studies along with a standard.

### 2.4.4 Tape stripping

Tape stripping was performed after completion of diffusion studies, to determine the concentration statin present in the stratum corneum-epidermis (SCE) and epidermis-dermis (ED). Franz cells were disassembled and circles of dermatomed skin were removed from receptor compartments and pinned to the Parafilm®. Surplus formula on skin was dabbed off with paper towel, where after the stratum corneum layer of each circle of dermatomed skin was removed with 16 different tape strips. After disposing of the first strip, the 15 remaining strips (SCE) were placed in a single polytop containing 5 ml methanol and the residual skin (ED) was detached from the Parafilm® and placed into a separate polytop containing 5 ml methanol. These polytops were stored in the fridge (4°C) for ±8 h. Finally, each polytop's content was extracted and filtered, using 0.45 µm nylon membrane filters, into HPLC vials for analysis.

## 2.5 Data analysis

During membrane release studies, cumulative concentrations of each cell were determined from HPLC results of receptor extractions over a period of 6 h. Average cumulative amount per area (µg/cm$^2$) of cells for each hour were calculated and graphed against time (h). The linear section (specified hours) of this graph was used to obtain a linear equation of which the slope (*m*) value indicated the average flux value. The average percentages released from the formulas were also calculated. This method was followed for nano-emulsions as well as nano-emulgels.

During skin diffusion studies, the total amount of statin diffused per area (µg/cm$^2$) through the skin after 12 h of each cell was plotted. Concentration (µg/ml) statin present in SCE and ED of each cell after 12 h were also calculated and plotted, respectively. The average percentage

statin diffused through the skin, and the average area concentration (µg/ml) statin present in SCE and ED after 12 h were determined for nano-emulsions as well as nano-emulgels.

### 2.6 Statistical analysis

Statistical analysis was performed on the results of cumulative concentrations of statins released from formulas during membrane release studies, as well as total concentrations diffused during skin diffusion studies and concentration statin present in SCE and ED after skin diffusion studies (tape stripping). Statistical analysis was performed with statistical methods such as ANOVA (analyse the variance) and t-tests.

## 3 Results and Discussion

### 3.1 Formulation of nano-emulsions and nano-emulgels

The optimal formulas of nano-emulsions and nano-emulgels each contained 2% of an individual statin.

### 3.2 Analysis of statins

The concentrations of the statins present in the receptor phase (average concentration diffused (µg/ml) through the skin) of **NE1s** and **NEGs** were higher than the LOD and LOQ values, with the exception of **NE1A**, and could therefore be quantified and analysed (Table 2).

Table 2:

LOD (µg/ml) and LOQ (µg/ml) of respective statins

### 3.3 Physicochemical properties

#### 3.3.1 Aqueous solubility

The solubility of atorvastatin (0.596 mg/ml), fluvastatin (0.529 mg/ml), pitavastatin (0.452 mg/ml) and pravastatin (0.882 mg/ml) was determined with PBS (pH 7.4) as a solvent. Since the ideal aqueous solubility for substances to cross the skin is >1 mg/ml (Naik *et al.,* 2000), atorvastatin, fluvastatin, pitavastatin and pravastatin did not succeed to this required solubility parameter.

### 3.3.2 Log D

The log D values calculated for atorvastatin (1.238), fluvastatin (1.358) and pitavastatin (1.034) presented within the ideal log D values (1-3), however for pravastatin a log D value of -0.394 determined.

### 3.3.3 Characterisation of NEGs and NE1s

Results obtained from the visual inspection, pH, surface potential zeta-potential, droplet size and distribution, and viscosity are summarised in Table 3.

Table 3:

The measured averages during the characterisation of **NE1s** and **NEGs**

**NEGs** compared to **NE1s** through visual inspection, presented with a shiny, smooth, white gel-like appearance. The **NEGs** also appeared to be higher in viscosity when compared to the **NE1s**, which presented with a whitish-milky fluidic appearance. Both the **NEGs** and the **NE1s** showed absence of sedimentation, flocculation and visible oil droplets. The average pH levels of the **NEGs** varied between the values of 4 and 6, which was lower than the pH levels of **NE1s** (6-8). Carbopol® Ultrez 20 is an acidic polymer, which supports the decrease of the pH levels after being included in the formula (Lubrizol, 2009:2). To reach maximum viscosity, the Carbopol® Ultrez 20-containing formulation's pH level is ideally between 6 and 7, thus **NEGs'** pH levels for each statin had to be modified (neutralised) (Lubrizol, 2009:2) with NaOH. Since the human skin tolerates substances with pH values of 3-9 (Barry, 2002:512), it can be concluded that all the formulas' pH values were within these parameters and therefore should not act as an irritant towards the skin when applied topically. At a pH of 5, atorvastatin (28.475%), pitavastatin (33.386%) and pravastatin (33.386%) displayed low unionised species with the exception of fluvastatin (75.975%). Molecules of a mainly ionised nature penetrate the stratum corneum weakly (Barry, 2002:511; Williams, 2003:38) and could affect diffusion of API through the skin tremendously.

The zeta-potential of the **NEGs** and the **NE1s** were compared and in all comparisons, the **NEGs** presented with higher zeta-potential values than its respective **NE1**, indicating that the

**NEGs** are more stable than its **NE1**-counterpart. The ideal zeta-potential values were higher than ±20 mV (Kumar, 2014:5), therefore it can be concluded that the **NEGs** and **NE1s** were all well within the accepted range of stability parameters.

When the average polydispersity-index (PdI) of the **NEGs** were compared to the average PdI of the **NE1s**, it was detected that the **NEGs** had insignificantly higher PdI values than their respective **NE1s**, except for **NEGA**, which presented with a slightly smaller PdI value than and **NE1A**. This agreed with literature that Carbopol® Ultrez 20 containing **NEGs** do not have significant PdI value variations compared to **NE1s** (Eid *et al.,* 2014:5).

The **NEGs** presented with significantly larger viscosity readings than the **NE1s**, which agreed with literature that combining an optimal nano-emulgel with a gelling agent enhances the water phase's viscosity, as it reduces interfacial and surface tension even more than nano-emulsions (Chellapa, 2015:45). Since the **NEGs** pH levels were modified (neutralised) (Lubrizol, 2009:2) with NaOH to a level of 6-7, the viscosity was increased drastically.

### 3.4 Membrane release studies

The median flux values of the **NE1** and **NEG** membrane release studies (Fig. 1) indicated that **NE1F** (367.1524 µg/cm$^2$.h) prevailed with the highest median flux compared to **NE1Pi** (150.3878 µg/cm$^2$.h), **NE1A** (102.9833 µg/cm$^2$.h) and **NE1Pr** (93.3947 µg/cm$^2$.h). **NEGs'** median flux values revealed that the **NEGPr** (393.3500 µg/cm$^2$.h) had the highest median flux value, followed by **NEGF** (111.5819 µg/cm$^2$.h), **NEGPi** (107.3441 µg/cm$^2$.h) and lastly, **NEGA** (101.1957 µg/cm$^2$.h). Median flux values of **NE1s** were higher for **NE1A**, **NE1F** and **NE1Pi**, compared to its **NEG**-counterparts, however **NEGPr** was the only **NEG** formula to show higher median flux values compared to its **NE1**-counterpart.

Fig 1: Box-plots of the flux values (µg/cm$^2$.h) of **NE1s** and **NEGs** for each statin during the membrane release studies over 6 h

### 3.5 Diffusion experiments

The median concentrations of statins diffused through skin as well as statins concentrations in the SCE and ED were investigated for **NE1s** and **NEGs** of each statin.

### 3.5.1 Skin diffusion studies

The mean and medians of the total amount (µg/cm$^2$) of statins to diffuse through the skin from **NE1s** and **NEGs** after 12 h were presented and investigated (Fig. 2).

Fig. 2: Box-plot presenting the average and median amount per area diffused (µg/cm$^2$) of the **NE1s** and **NEGs** for each statin that diffused through the skin after 12 h

It was found that **NE1Pi** (0.3865 µg/cm$^2$) was the **NE1** with the highest median amount per area diffused through skin, followed by **NE1Pr** (0.2845 µg/cm$^2$), **NE1F** (0.1250 µg/cm$^2$) and lastly, **NE1A** (0.0530 µg/cm$^2$). The **NEG** formula with the highest median amount statin per area diffused was **NEGF** (2.8070 µg/cm$^2$), followed by **NEGPr** (1.1350 µg/cm$^2$), **NEGPi** (0.7220 µg/cm$^2$) and **NEGA** (0.0735 µg/cm$^2$).

The **NEGs** (**NEGA**, **NEGF**, **NEGPi** and **NEGPr**) presented with higher median amounts per area diffused than their **NE1**-counterparts (**NE1A**, **NE1F**, **NE1Pi** and **NE1Pr**). In formula, Carbopol® Ultrez 20 has the ability to either increase or decrease diffusion of APIs through the skin (Nastiti *et al.,* 2017:11). In this study, an increase in transdermal diffusion results was observed for **NEGs**. The **NE1** that prevailed with the highest median amount per area diffused through skin was pitavastatin. **NE1A** and **NEGA** presented with the lowest median amount per area diffused through skin. When Carbopol® Ultrez 20 was included in **NE1s** were to produce **NEGs**, fluvastatin was the statin that prevailed compared to all the formulas.

Plasma concentrations after oral administration of statins were compared to transdermal delivery of statins obtained in this study and indicated that **NE1A** and **NEGA**, **NE1Pr** and **NEGPr** had substantially higher concentrations during transdermal delivery and **NEGPi** only slightly higher. However, fluvastatin **NE1Pi**, **NE1F** and **NEGF** showed lower concentrations to reach circulation than that of the oral administration compared to the oral route of administration.

Table 4:

The concentration (µg/ml) of the different statins within the formulas that diffused through the skin after 12 h

### 3.6 Tape stripping

#### 3.6.1 Stratum corneum-epidermis

The median concentration **NE1s** and **NEGs** in SCE were investigated (Fig. 3). It was found that **NE1A** (7.0865 µg/ml) prevailed with the highest median concentration in the SCE, followed by **NE1Pi** (1.6720 µg/ml), **NE1Pr** (1.0540) and **NE1F** (0.4148 µg/ml). With inspection of the SCE regarding **NEGs**, the statin formula that prevailed with the highest median concentration was **NEGPr** (1.5076 µg/ml), followed by **NEGPi** (1.2155 µg/ml), **NEGA** (0.7189 µg/ml) and **NEGF** (0.3871 µg/ml).

**NE1s** were then compared to the **NEG**-counterparts and it was revealed that **NE1A**, **NE1Pi** and **NE1F** had higher median concentrations in the SCE than its respective **NEGs** (**NEGA**, **NEGPi** and **NEGF**). The exception was **NEGPr**, which indicated a higher median concentration than its **NE1** formula (**NE1Pr**).

Fig. 3: Average concentration (µg/ml) of the **NE1s** and the **NEGs** for each statin present in the SCE and ED

#### 3.6.2 Epidermis-dermis

The median concentration in ED regarding **NE1s** and **NEGs** were then investigated. The order of **NE1s** revealed to be **NE1A** (24.5545 µg/ml) > **NE1Pi** (6.4808 µg/ml) > **NE1F** (2.6555 µg/ml) > **NE1Pr** (2.4706 µg/ml) and for **NEGs**, the order presented as **NEGPi** (9.7714 µg/ml) > **NEGA** (3.8193 µg/ml) > **NEGPr** (1.8380 µg/ml) > **NEGF** (1.0510 µg/ml). With inspection of the median concentration in ED, **NE1s** was compared to its **NE-**counterpart, **NE1A** > **NEGA**, **NE1F** > **NEGF**, **NE1Pr** > **NEGPr** except for pitavastatin, where the **NEGPi** presented with a higher median concentration compared to its **NE1Pi**.

The median concentration of statins in the SCE and ED was higher than the median amount statin diffused through skin, with the exception of **NEGPi**, which dominated with a higher median concentration diffused through the skin than present in the SCE, hence lower than median concentration present in the ED. This implies that the amount of statins that achieved the receptor phase was lower than the amount of statins present in the SCE and ED.

The median amount of statins diffused (µg/ml) through the skin was higher for **NE1s** and **NEGs** for statins compared to the LOD and LOQ values tabled in Section 3.2, with the exception of **NE1A**, thus it could be quantified.

### 3.7 Statistical analysis

#### 3.7.1 Membrane release studies

Statistical analysis was performed on membrane release studies by means of ANOVA, t-tests and Tukey's tests.

A two-way ANOVA was performed on **NE1s** and **NEGs**. The interaction between the type of formula (**NE1**/**NEG**) and the statins revealed a p-value of <0.001; therefore, indicative of a statistical significant interaction. Due to this statistical significant interaction, a one-way ANOVA was performed for each of the **NE1s** and **NEGs** to compare the statins. The results indicated that when the means of the **NE1s** were compared with each other, and the means of the **NEGs** were compared with each other, differences between the actual means of the statins presented as significant ($p<0.001$ and $<0.05$) for both the means of the **NE1s** and the means of the **NEGs**. Tukey's honestly significant difference (HSD) post-hoc tests were performed for each formula type to compare the means of the statins pairwise. Here it was suggested that the **NE1s** of atorvastatin and pravastatin were homogenously grouped, hence fluvastatin and pitavastatin had no similarities regarding their means as **NE1F** and **NE1Pi** were separately grouped, respectively. With inspection of the **NEGs**, **NEGA**, **NEGF** and **NEGPi** shared similar properties, whilst **NEGPr** was grouped individually.

#### 3.7.2 Skin diffusion studies

Statistical analysis was performed on skin diffusion studies by means of ANOVA, t-tests and Tukey's test. The results were categorised as statin diffused through the skin and statin present in skin layers (SCE-ED). Here, statistical data reflected biased distribution; therefore, logarithmic transformation was performed in advance to produce near to normal distribution.

### 3.7.3 Statin diffusion through the skin

A two-way ANOVA was performed on the **NE1s** and **NEGs** of statin diffused through the skin. An interaction between the type of formula (**NE1/NEG**) and statin occurred and indicated a p-value of 0.025, which presented with a statistical significant interaction. Consequently, a one-way ANOVA was performed for each of the **NE1s** and **NEGs** to compare statins.

The log-cumulative concentrations of **NE1s** and the means of the log-cumulative concentrations of the **NEGs** were compared. The p-values were below 0.05 (<0.001 and 0.003 respectively), indicating statistical significant variances were obtained.

Tukey's HSD post-hoc test of the **NE1s** and **NEGs** that diffused through the skin suggested that **NE1F**, **NE1Pr** and **NE1Pi** had homogenous relationships; however, **NE1A** was in a separate group where similar properties to **NE1F** were observed. A similar pattern was revealed for the **NEGs**; though, **NEGPi** presented as the formula that related to **NEGPr** and **NEGF**, and **NEGA** as a separate group.

### 3.7.4 Tape stripping

The ANOVA of statins present in skin layers was performed by means of statistical analysis. The interactions between the statins and the skin layers, and the statins and the type of formula, presented as 0.013 and <0.001, respectively, which indicated statistical significant interactions. Hence, p-values of the skin layers and the type of formula interactions, and the statin-skin layers-type of formula interactions were above 0.05 (0.619 and 0.497, respectively), which indicated statistical insignificant interactions.

Since significant interactions occurred, one-way ANOVAs were performed to compare statins on each of the combinations of the skin layer and the type of formula, which was followed by t-tests to compare SCE with ED for each formula containing a statin.

The p-values of each compared group (SCE vs. **NE1**, ED vs. **NE1**, SCE vs. **NEG** and ED vs. **NEG**) were lower than 0.05 (<0.001, <0.001, 0.030 and <0.001, respectively). This suggests that statistical significant variations were present for each comparison.

To obtain specific data of interactions indicated by ANOVAs, t-tests were performed. Here the p-values for t-tests of **NE1A**, **NEGA**, **NE1F**, **NEGF**, **NE1Pi** and **NEGPi** in respective combinations with skin layers (SCE-ED) were below 0.05, indicating that statistical significant variations occurred. However, **NEGPr** present in the layers of the skin, presented with a p-value of 0.259, which indicated a statistical insignificant variation, while **NEGPr** was nearly significant (p=0.06).

Tukey's HSD post-hoc tests were then performed to determine homogenous relationships between the specified statins formulated in a specified type of formula (**NE1**/**NEG**) compared to the layer (SCE/ED) of the skin in which the statin presented. **NE1Pr** and **NE1Pi** presented with a homogenous relationship in each of the combinations, with the exception of the ED and respective **NEG** combinations. It was observed that **NE1A** and **NE1F** were only partly homogenous in combinations of SCE-**NEG** and ED-**NEG**, however, regarding **NE1s** present in skin layers respectively, non-relatable properties occurred.

## 4 Conclusion

The median amount per area that diffused through the skin was evaluated and revealed that atorvastatin (**NE1A**) had the lowest concentrations in the receptor phase for the **NE1s**, as well as the **NEGs**. The large concentration of atorvastatin present in the SCE and ED of **NE1A** might be ascribed to its high molecular weight (1155.34 g/mol), blocking penetration through the skin (Jia *et al.,* 2017:2). **NEGA** exhibited low concentrations of atorvastatin in the **SCE**, as well as diffused through the skin, hence in the ED it was delivered moderately. The aforementioned might suggest that **NEGA** was caught in this layer or favoured the ED, which could have progressed to the lower concentration of atorvastatin diffused through the skin.

The concentration of diffused fluvastatin (**NEGF**) prevailed in the receptor phase, but presented as the lowest in the SCE and ED when compared to all the formulas (**NE1s** and **NEGs**). This may suggest that the **NEG** formula was absolute for the transdermal delivery of fluvastatin, as high concentrations diffused through the skin and low concentrations in the SCE and ED suggest ideal targeting. **NE1F** concentrations were low in both the receptor phase as

well as the SCE, confirming the statement that by adding a gelling agent to the **NE1** formula may have contributed to the targeted delivery of **NEGF**.

Pravastatin (**NEGPr**) was revealed as the second highest concentration of statin diffused through the skin, and the second lowest concentration in the ED among **NE1s** and **NEGs**. The concentration pravastatin (**NEGPr**) present in the **SCE** prevailed among **NEGs** (ranked the highest of all the **NEGs**), and third highest among all the tested formulas. It can be proposed that the release of **NEGPr** from the SCE was lagged; hence, the **NEG** improved the release of pravastatin from the ED to the receptor phase indicative of high transdermal delivery. **NE1Pr** offered low to average concentrations in the SCE, ED and the receptor phase. Therefore, it can be assumed that the **NEG** certainly affected the transdermal delivery of pravastatin.

The concentration **NEGPi** in the receptor phase was ranked the third highest of all the formulas. **NEGPi** compared to the **NEGs** presented with the second highest concentration in the SCE and attained the fourth highest concentration compared to **NE1s** as well as **NEGs**. **NEGPi** had the highest concentration amongst the **NEGs** in the ED, and ranked the second highest concentration when compared to all the formulas in the ED. It can be proposed that **NEGPi** permeated promptly to the ED from the SCE, subsequently delivering high concentrations through the skin. **NE1Pi** persevered with the highest concentrations delivered to the receptor phase among the **NE1s** and the fourth highest concentrations diffused through the skin when compared to all the formulas. **NE1Pi** obtained the second highest concentration in the SCE among all the formulas, and offered the second highest delivery among the **NE1s** in the ED, and the third highest concentration when compared to all the formulas. Thus, it can be suggested that by modifying the formula of **NEGPi**, transdermal delivery of pitavastatin may improve and targeting could be achieved.

It is however evident that when investigating the transdermal and topical results, the **NE1s** (in general) improved the topical (SCE and ED) delivery of the statins when compared to its **NEG**-counterparts, whereas **NEGs** furthered the delivery of the statins transdermally (receptor phase); this might also be the motivation why the **NE1s** had higher concentrations topically than the **NEGs**, since the **NEGs** increased penetration of statins through the skin, into the systemic circulation (receptor phase). The occurrence of **NEGs** presenting with lower median concentrations in the SCE can be attributed to the addition of a gelling-agent (Carbopol® Ultrez 20). This agent initiates swelling of the **NE1s** and produces formulations with higher viscosity (Mahalingam *et al.,* 2008:293; Mitsui, 1997:138) thus, increasing the permeation of APIs through the skin (Eid *et al.,* 2014:1).

**Acknowledgements**

The authors express their appreciation towards the South African National Research Foundation (NRF) (Grant number: 105913) and also the Centre of Excellence for Pharmaceutical Sciences (Pharmacen™) at the North-West University, Potchefstroom Campus, South Africa, for their financial assistance. Any opinion, findings and conclusions, or recommendations expressed in this material are those of the authors and therefore the NRF does not accept any liability in regard thereto. A special word of appreciation to Prof F Steyn, at Statistical Consultation Services of the North-West University, Potchefstroom Campus, South Africa, for the statistical analysis of data obtained.

**Conflict of Interest**

The authors declare no conflict of interest.

**References**

Baibhav, J., Gurpreet, S., Rana, A.C., Seema, S. & Vikas, S. 2011. Emulgel: a comprehensive review on the recent advances in topical drug delivery. *International research journal of pharmacy*, 2:66-70.

Barry, B. 2002. Transdermal drug delivery. (*In* Aulton, M.E., *ed*. Pharmaceutics: the science of dosage form design. 2nd ed. London: Churchill Livingstone. p. 499-533.

Boglarka, B., Gabor, V., Szilvia, B., Maria, B., Andras, K., Balint, S., Krisztina, T., Piroska, S. & Erzsebet, C. 2016. Investigation of the efficacy of transdermal penetration enhancers through the use of human skin and a skin mimic artificial membrane. J. Pharm. Sci., 105:1134-1140.

Chellapa, P., Mohamed, A.T., Keleb, E.I., Elmahgoubi, A., Eid, A.M., Issa, Y.S. & Elmarzugi, N.A. 2015. Nanoemulsion and nanoemulgel as a topical formulation. IOSR J Pharm, 5(10):43-47.

Eid, A.M., El–Enshasy, H.A., Aziz, R. & Elmarzugi, N.A. 2014. Preparation, characterization and anti–inflammatory activity of Swietenia macrophylla nanoemulgel. J Nanomed Nanotechnol, 5:1-10.

Fong, C. 2016. Statins in therapy: Cellular transport, side effects, drug-drug interactions and cytotoxicity -the unrecognized role of lactones. https://hal.archives-ouvertes.fr/hal-01185910/document. Date of access: 5 Nov 2018.

Gabera, M., Medhata, W., Hanya, M., Sahera, N., Fang, J., Elzoghby, A. 2017. Protein-lipid nanohybrids as emerging platforms for drug and gene delivery: Challenges and outcomes. J Control Release, 254:75-91.

Gadkari, P.N., Patil, P.B.,Saudagar, R.B. 2018. A review on nanoemulsion based gel. European j. biomed. pharm. sci., 5(4):914-921.

Hennessy, E., Adams, C., Reen, F.J., O'Gara, F. 2016. Statins inhibit bacterial growth and virulence. Antimicrob. Agents Chemother., 1-44.

Kala, S & Juyal, D. 2018. Recent developments on natural transdermal penetration enhancers. Int J Pharm Sci Res, 9(6):2190-2196.

Kumar, S. 2014. Role of nano-emulsion in pharmaceutical sciences - a review. Asian journal of research in pharmaceutical sciences and biotechnology, 2(1):1-15.

Lubrizol. 2009. Viscosity of carbopol® polymers in aqueous systems. http://www.lubrizol.com>lubrizol>Techicaldatasheet Date of access: 27 Aug 2018.

Mancini, G.B.J., Tashakkor, A.Y., Baker, S., Bergeron, J., Fitchett, D., Frohlich, J., Genest, J., Gupta, M., Hegele, R.A., Ng, D.S., Pearson, G.J., Pope, J. 2013. Diagnosis, prevention, and management of statin adverse effects and intolerance: Canadian working group consensus update. Can J Cardiol, 29:1553-1568.

Marrow, D.I.J., McCarron, P.A., Woolfson, A.D. & Donnelly, R.F. 2007. Innovative strategies for enhancing topical and transdermal drug delivery. *The open drug delivery journal*, 1:36-59.

Naik, A., Kalia, Y.N. & Guy, R.H. 2000. Transdermal drug delivery: overcoming the skin's barrier function. Pharm. Sci. Technol. Today, 3:318-325.

Nastiti, C.M.M.R., Ponto, T., Abd, E., Grice, J.E., Benson, H.A.E., Roberts, M.S. 2017. Topical nano and microemulsions for skin delivery. *Pharmaceutics*, 9(37):2-25.

Ng, K.W., Lau, W.M. 2015. Skin deep: The basics of human skin structure and drug penetration. file:///C:/Users/22819509/Downloads/ng-2015-skin-deep.pdf. Date of access: 5 Oct. 2018.

Piepho, R.W. 2000. The Pharmacokinetics and Pharmacodynamics of Agents Proven to Raise High-Density Lipoprotein Cholesterol. Am. J. Cardiol., 86(12A): 35L-40L.

Rastogi, V., Yadav, P. 2012. Transdermal drug delivery system: An overview. Asian J Pharm, 161-170.

Robinson, JG. & Goldberg, AC. 2011. Treatment of adults with Familial Hypercholesterolemia and evidence for treatment: Recommendations from the National Lipid Association Expert Panel on Familial Hypercholesterolemia. J Clin Lipidol, 5:S18-S29.

Scherr, R.E., Zidenberg-Cherr, S. 2016. Nutrition and health info sheet: Cholesterol. https://nutrition.ucdavis.edul>factsheets.pdf. Date off access: 17 Oct 2018.

Vermaak, I., Kamatou, G.P.P., Komane-Mofokeng, B., Viljoen, A.M. & Beckett, K. 2011. African seed oils of commercial importance: cosmetic application. S Afr J Bot, 77:920-933.

Wang, Y., Fan, Q., Song, Y. & Michnaik, B. 2003. Effects of fatty acids and iontophoresis on the delivery of midodrine hydrochloride and the structure of human skin. Pharm Res, 20:1612-1618.

Williams, A.C. 2013. Topical and transdermal drug delivery. (*In* Aulton, M.E., *ed*. Aulton„s pharmaceutics: the design and manufacture of medicines. 4th ed. London: Churchill Livingstone. p. 675-697).

Zhang, J., Liu, Q. 2015. Cholesterol metabolism and homeostasis in the brain. *Protein & cell,* 6(4):254-264.

Zodda, D., Giammona, R., Schifilliti, S. 2018. Treatment strategy for dyslipidaemia in cardiovascular disease prevention: focus on old and new drugs. *Pharmacy,* 6(10):1-16.

**Tables**

Table 1:

Formula used to prepare **NE1s** and **NEGs** containing statins

| Phase | Constituent | NE1 | NEG |
|---|---|---|---|
| **Water phase** | Milli-Q® water | 87.0% | 86.5% |
| | Tween® 80 | 6.0% | 6.0% |
| | Carbopol® Ultrez 20 | - | 0.5% |
| **Oil phase** | Apricot kernel oil | 8.0% | 80.% |
| | Span® 60 | 6.0% | 6.0% |
| | Statin | 2.0% | 2.0% |

Table 2:

LOD (µg/ml) and LOQ (µg/ml) of respective statins

| Statin | LOD | LOQ |
|---|---|---|
| **Atorvastatin** | 0.116 | 0.035 |
| **Fluvastatin** | 0.006 | 0.019 |
| **Pitavastatin** | 0.005 | 0.015 |
| **Pravastatin** | 0.004 | 0.013 |

Table 3:

The measured averages during the characterisation of **NE1s** and **NEGs**

| Formula | pH | Zeta-potential (mV) | Droplet size (nm) | Viscosity (cP) |
|---|---|---|---|---|
| **NE1A** | 6.57 | -43.7 | 137.40 | 4.45 |
| **NEGA** | 5.49 | -53.1 | 212.87 | 2937.67 |
| **NE1F** | 7.81 | -55.7 | 165.40 | 5.79 |
| **NEGF** | 5.67 | -62.5 | 201.73 | 5935.67 |
| **NE1Pi** | 6.54 | -40.1 | 130.73 | 4.28 |
| **NEGPi** | 4.90 | -48.9 | 256.03 | 3612.50 |
| **NE1Pr** | 7.21 | -48.3 | 114.23 | 3.59 |
| **NEGPr** | 5.11 | -62.1 | 267.53 | 1911.00 |

Table 4:

The concentration (µg/ml) of the different statins within the formulas that diffused through the skin after 12 h

| | **Concentration (µg/ml)** |
|---|---|
| **Atorvastatin plasma concentration (oral dosage)** | 0.0009[a] |
| **NE1A** | 0.0330 |
| **NEGA** | 0.0670 |
| **Fluvastatin plasma concentration (oral dosage)** | 1.7300[b] |
| **NE1F** | 0.0810 |
| **NEGF** | 1.3830 |
| **Pitavastatin plasma concentration (oral dosage)** | 0.3000[c] |
| **NE1Pi** | 0.2870 |
| **NEGPi** | 0.4190 |
| **Pravastatin plasma concentration (oral dosage)** | 0.0641[d] |
| **NE1Pr** | 0.1770 |
| **NEGPr** | 0.4920 |

a) DeGorter *et al*., 2013, b) Routes, 2004, c) Therapeutic goods administration, 2013, d) Clarke *et al.,* 2011:1947

**Figures:**

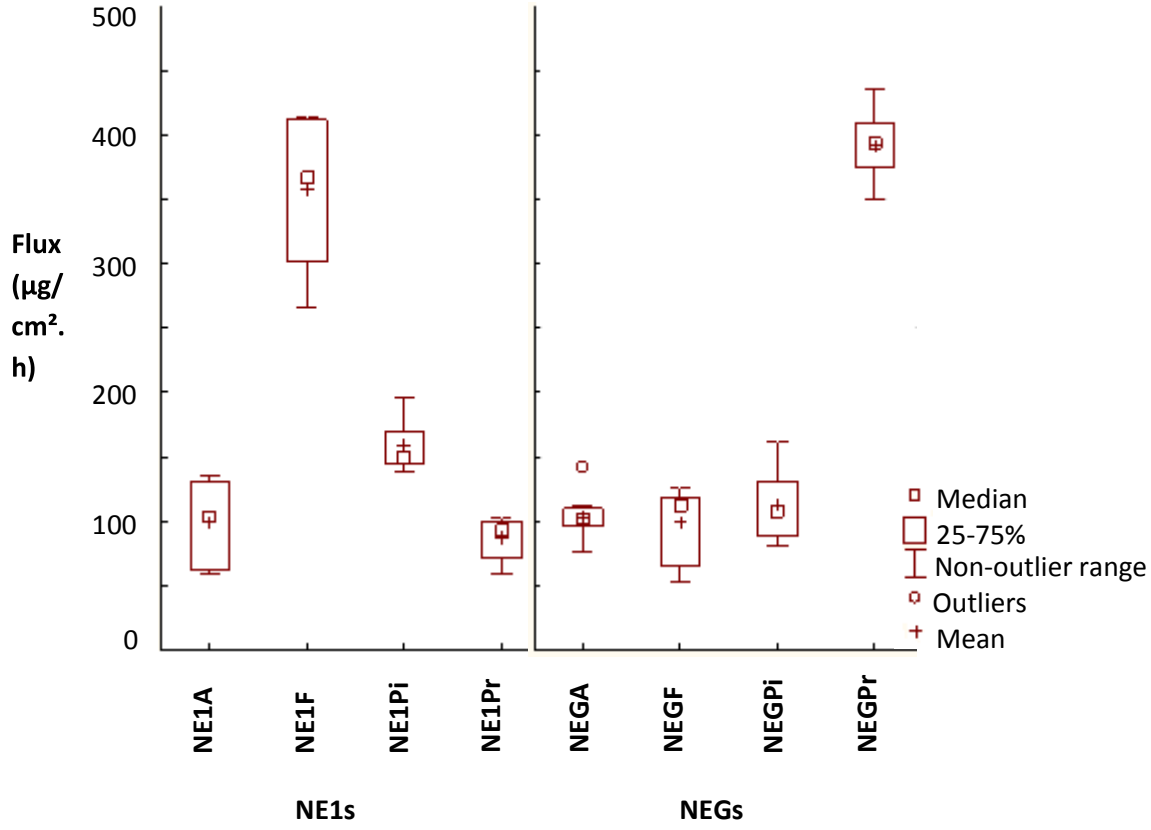


Fig 1: Box-plots of the flux values (µg/cm$^2$.h) of **NE1s** and **NEGs** for each statin during the membrane release studies over 6 h

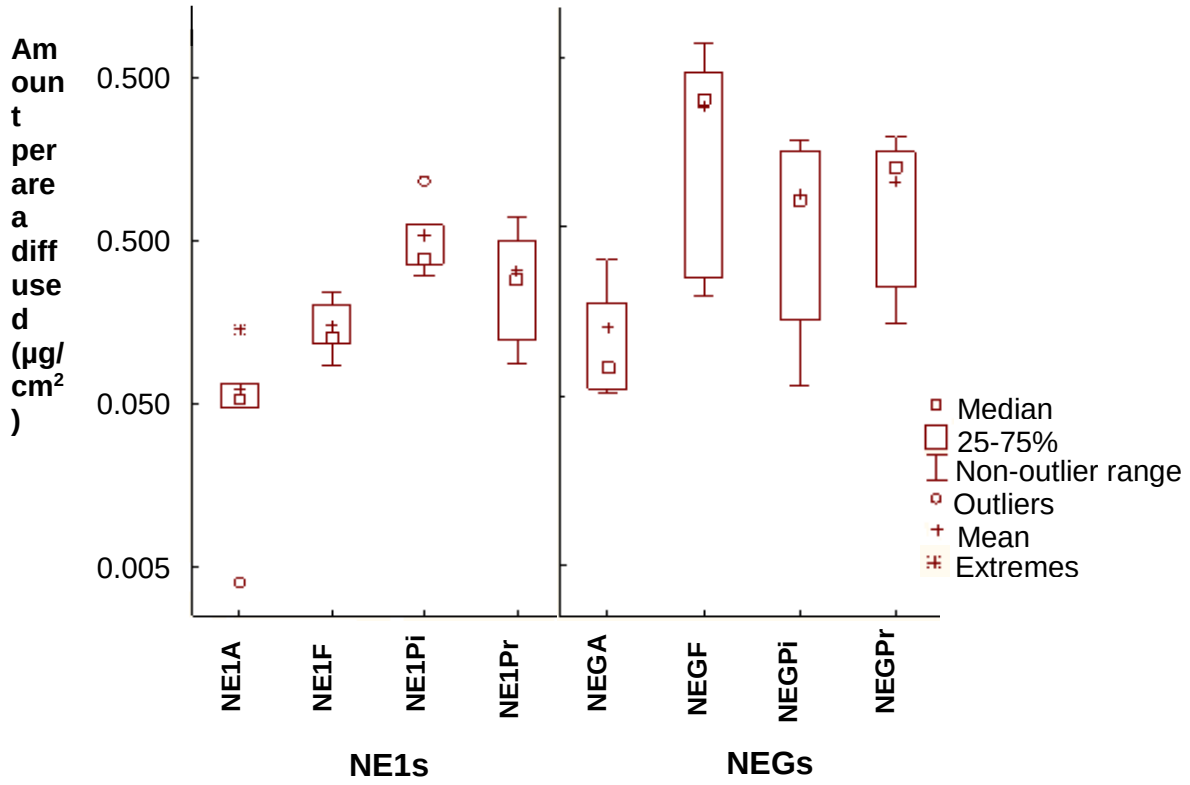


Fig. 2: Box-plot presenting the average and median amount per area diffused (µg/cm$^2$) of the **NE1s** and **NEGs** for each statin that diffused through the skin after 12 h

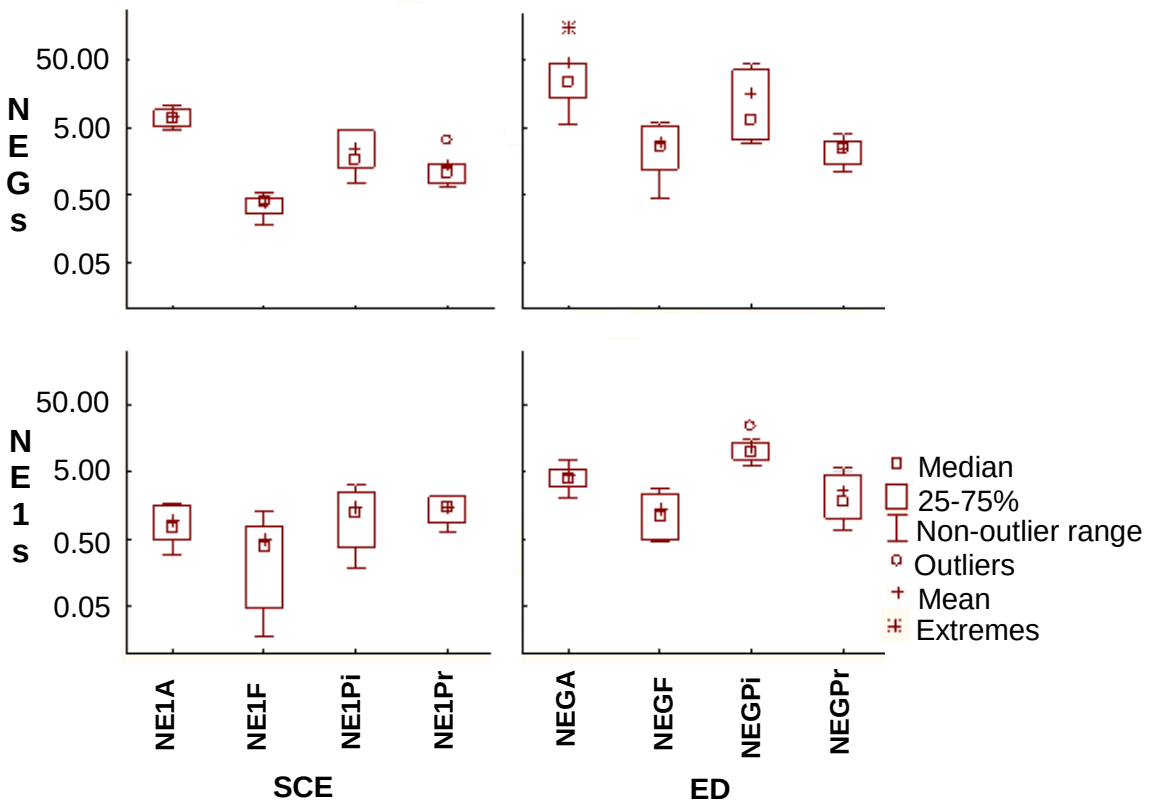


Fig. 3: Average concentration (µg/ml) of the **NE1s** and the **NEGs** for each statin present in the SCE and ED

# CHAPTER 5

CONCLUSION AND PROSPECTS FOR THE FUTURE

Cardiovascular diseases are responsible for 17.3 million deaths globally each year and are the leading contribution to mortality rates in South Africa after AIDS, as 215 individuals die from CVDs each day (HSFSA, 2016:1). CVDs have frequently been linked to elevated blood cholesterol (hyperlipidaemia) (Onwe *et al.,* 2015:24), since blood cholesterol tends to accumulate in the walls of arteries; particularly cholesterol transported by LDL (Schultz *et al.,* 2018:9). Currently, oral administered statins are the first-line medical therapy for hyperlipidaemia (Zodda *et al.,* 2018:1), since this therapy has the ability to lower LDL cholesterol as they decrease HMG-CoA reductase (Fong, 2016:663; Hennessy *et al.,* 2016:3).

Statins as a therapy are favourable; however, the route of administration (oral route) presents with obstacles such as gastro-intestinal side-effects and low bioavailability due to first-pass metabolism (CYP450 liver enzymes) (Sahebzamani *et al.,* 2014:3; Zodda *et al.,* 2018:3). In attempt to overcome these hindrances, the transdermal delivery of statins was investigated. Nano-emulsions and nano-emulgels were selected as transport systems to investigate their ability to penetrate and cross the complicated skin layers, more specifically, the stratum corneum. Atorvastatin, fluvastatin, pitavastatin and pravastatin were the selected statins, and apricot kernel oil was used as a penetration enhancer.

Objectives were set as:

- Development and validation of an HPLC method for analysis of transdermal statin delivery.
- Determination of statin solubility and log D.
- Formulation of an optimised nano-emulsion and nano-emulgel formula in which 2% atorvastatin, fluvastatin, pravastatin and pitavastatin (separately) would be stable.
- Stability testing of formulas by means of characterisation techniques (physical and chemical), i.e. visual inspection, pH, zeta-potential, droplet size, viscosity and morphology.
- Establishing the release rate of the statins from the nano-emulsions compared to nano-emulgels through membrane release studies.
- Determining transdermal and/or topical delivery of the statins from the nano-emulsions compared to nano-emulgels by means of skin diffusion and tape stripping.

- Evaluation of cytotoxic effects of the statin solutions, nano-emulsions containing the selected statins, placebo nano-emulsion and excipients (Span® 60, Tween® 80 and apricot kernel oil) on HaCaT cell lines by use of MTT- and NR-assays.

An HPLC analytical method was developed and validated and the method proved to be reliable, accurate and reproducible.

Statin solubility was determined: atorvastatin (0.596 ± 0.024 mg/ml), fluvastatin (0.529 ± 0.088 mg/ml), pitavastatin (0.452 ± 0.038 mg/ml) and pravastatin (0.882 ± 0.003 mg/ml). These solubility values correlated with the literature (atorvastatin: 0.190 mg/ml (Rodde *et al.,* 2014:3), fluvastatin: 0.200 mg/ml (Cayman chemical, 2010:2) and pitavastatin: 0.500 mg/ml (Cayman chemical, 2014)) in the sense that these statins were lipophilic, with the exception of pravastatin (10.00 mg/ml) (Cayman Chemical, 2015:4). Pravastatin is described as more hydrophilic than lipophilic; however, large differences occurred between solubility values obtained in the literature compared to the solubility values in this study. The differences in solubility values can be due to pH and temperature differences. Log D values of statins were determined as 1.238 ± 0.001 (atorvastatin), 1.358 ± 0.003 (fluvastatin), 1.034 ± 0.030 (pitavastatin) and - 0.394 ± 0.005 (pravastatin). Log D values (in terms of lipophilicity) provided confirmation to the solubility results, which indicates that atorvastatin, fluvastatin and pitavastatin presented as lipophilic, while pravastatin was more hydrophilic.

Pre-formulation of the nano-emulsions were performed to establish the appropriate surfactant-surfactant ratio in which 2% statins (separately) could be formulated. The most stable formula ratio was Tween® 80:Span® 60 (3:3) (**NE1**), proved by the physical and chemical characterisation of the competing formulas. These optimised nano-emulsions formulas were named atorvastatin (**NE1A**), fluvastatin (**NE1F**), pitavastatin (**NE1Pi**) and pravastatin (**NE1Pr**). Nano-emulgel (**NEG**) formulations were formulated from the optimised nano-emulsion by adding Carbopol® Ultrez 20 (gelling agent) to the **NE1** of each statin and was referred to as atorvastatin (**NEGA**), fluvastatin (**NEGF**), pitavastatin (**NEGPi**) and pravastatin (**NEGPr**), which was also characterised. Characterisation techniques involved visual inspection, pH, zeta-potential, droplet size, viscosity and morphology. Visual inspection confirmed that the **NE1** of each statin presented with a smooth, milk-like appearance, where the **NEGs** presented as thick, white and shiny. No sedimentation or visible oil droplets were present in either the **NE1s** or **NEGs**. After modification of **NEG's** pH values, **NE1s** and **NEGs** presented with pH values between 4 and 8, thus acceptable for transdermal administration, since the skin (pH 5) can endure pH values of 3 – 9 (Barry, 2002:512).

Zeta-potential values confirmed stability, as the **NE1s** and **NEGs** presented with values above - 40 mV, which were well within the required parameter of ± 20 mV (Kumar, 2014:5). All the **NE1s** and **NEGs** abided to required parameters for droplet sizes (< 500 nm) (Nalini *et al.,* 2017:1453) and PdI (< 0.5) (Elmataeeshy *et al.,* 2018:24), which was confirmed with transmission electron microscopy (TEM) for **NE1s**, and microscopy for **NEGs**. Viscosity measures (cP) between the **NE1s** and the **NEGs** varied significantly due to the gelling agent included in **NEGs**; therefore, the **NEGs** presented with substantially higher viscosity measures.

Membrane release studies revealed that **NE1F** presented with the highest flux among the **NE1s** (**NE1Pi**, **NE1A** and **NE1Pr**) and **NEGPr** among the **NEGs** (**NEGF**, **NEGPi** and **NEGA**). **NEGPr** was also the only **NEG** to show faster release of the statin compared to its **NE1**.

Skin diffusion studies revealed that the concentration diffused through skin for **NEGs** was higher than each of the respective **NE1s**. The **NE1s** displayed that **NE1A** prevailed with the highest median concentration in the SCE, while the **NEGs** presented **NEGPr** as the statin formula with the highest median concentration in the SCE. **NEGPr** was also the only **NEG** to dominate its **NE1**-counterpart. Conclusively, **NEGs** (except for except for **NEGF**, **NE1F** and **NE1Pi**) showed higher bioavailability for statins compared to oral administration of statins, therefore could be very promising to the future of transdermal statin therapy.

Cytotoxicity assays were performed with higher concentrations of statins and excipients than used in transdermal diffusion studies. The concentration values to which these compounds inhibited 50% of the cell growth ($IC_{50}$) for MTT results of statin solutions indicated that fluvastatin presented more cytostatic to the cells compared to atorvastatin, pitavastatin and pravastatin. NR-assay results for $IC_{50}$ values of statin solutions showed that atorvastatin and fluvastatin presented more cytostatic towards cells than pitavastatin and pravastatin. The **NE1s**, as well as **PNE1** indicated cytostatic effects on the cells during MTT-assays at high treatment concentrations; however, the **PNE1** presented as the most cytostatic. The **NE1A** presented as more cytostatic compared to **NE1F**, **NE1Pi** and **NE1Pr**, which again presented as the least toxic among the statins. The NR-assay results for the **NE1s** and the **PNE1** showed cytostatic effects on cells at high concentrations, of which the **PNE1** showed the lowest toxicity. The **NE1F** was the most cytostatic towards cells compared to **NE1Pi**, **NE1A** and **NE1Pr**. The MTT- and NR-assay for excipients indicated that Tween® 80, Span® 60 and Span® 60-apricot kernel oil treatments presented with cytostatic effects on cells at high concentrations. Span® 60 and Tween® 80 had comparable $IC_{50}$ values measured up to Span® 60-apricot kernel oil, which was displayed as the least cytostatic with the highest $IC_{50}$ value. In conclusion, statins and excipients are non-toxic toward cells at concentrations used

in transdermal studies.

Prospects for the future:

- The transdermal route utilising **NEGs** can be investigated as the alternative administration route for other APIs with the same difficulties as statins (especially hepatic metabolism, gastro-intestinal side-effects and drug interactions with stomach content), such as anti-retroviral APIs and anti-fungal APIs, e.g. itraconazole, fluconazole, etc., as statins incorporated in the **NEGs** showed higher bioavailability than oral administered statins.
- Other natural oils as penetration enhancers can be investigated and compared to the bioavailability produced by apricot kernel oil.
- Investigate other formulations of statins (i.e. self-heating patches) to evaluate whether statins diffused through the skin are higher than that of **NEGs**.
- Investigating atorvastatin as a topical delivery system, for its anti-inflammatory properties.

**References**


Barry, B. 2002. Transdermal drug delivery. (*In* Aulton, M.E., ed. Pharmaceutics: the science of dosage form design. 2nd ed. London: Churchill Livingstone. p. 499-533.

Cayman chemical. 2010. Fluvastatin (sodium salt) (Material safety data sheet). https://s3-us-west-2.amazonaws.com/drugbank/msds/DB01095.pdf?1374296087. Date of access: 18 Oct 2018.

Cayman chemical. 2014. Pitavastatin calcium salt (Product information 15414) https://www.caymanchem.com/pdfs/15414.pdf Date of access: 18 Oct 2018.

Cayman chemical. 2015. Pravastatin (sodium salt) (Material safety data sheet). https://www.caymanchem.com/msdss/10010343m.pdf Date of access: 18 Oct 2018.

Elmataeeshy, M.E., Sokar, M.S., Bahey-El-Din, M.B. & Shaker, D.S. 2018. Enhanced transdermal permeability of terbinafine through novel nanoemulgel formulation. *Future journal of pharmaceutical sciences*, 4(1):18-28.

Fong, C. 2016. Statins in therapy: Understanding their hydrophilicity, lipophilicity, binding to 3-hydroxy-3-methylglutaryl-CoA reductase, ability to cross the blood brain barrier and metabolic stability based on electrostatic molecular orbital studies. *European journal of medicinal chemistry,* 85:661-674.

Hennessy, E., Adams, C., Reen, F.J., O'Gara, F. 2016. Statins inhibit bacterial growth and virulence. *Antimicrobial agents and chemotherapy,* 1-44.

HSFSA *see* Heart and Stroke Foundation South Africa. 2016. Cardiovascular diseases in South-Africa. http://www.heartfoundation.co.za/wp-content/uploads/2017/10/CVD-stats-reference-document-2016-for-media-1.pdf. Date of access: 13 Oct. 2018.

Kumar, S. 2014. Role of nano-emulsion in pharmaceutical sciences. *A review Asian journal of research in pharmaceutical sciences and biotechnology* 2(1):1-15.

Nalini, T., Kumari, V.S. & Basha S.K. 2017. Novel nanosystems for herbal drug delivery. *World journal of pharmacy and pharmaceutical sciences*, 6(5):1447-1463.

Onwe, P.E., Folawiyo, M.A., Okike, P.I., Balogun, M.E., Umahi, G., Besong, E.E., Okorocha, A.E., Afoke, A.O. 2015. Lipid profile and the growing concern on lipid related diseases. *Journal of pharmacy and biological sciences*, 10(5):22-27.

Rodde, M.S., Divase, G.T., Devkar, T.B., Tekade, A.R. 2014. Solubility and bioavailability enhancement of poorly aqueous soluble atorvastatin: *in vitro*, *ex vivo*, and *in vivo* studies. *BioMed research international*, 1-11.

Sahebzamani, F.M., Munro, C.L., Marroquin, O.C., Diamond, D.M., Keller, E., Kip, K.E. 2014. Examination of the FDA warning for statins and cognitive dysfunction. *Journal of pharmacovigilance,* 2(4):1-9.

Schultz, G., Patten, D.K., Berlau, D.J. 2018. The role of statins in both cognitive impairment and protection against dementia. *Translational neurogeneration*, 7(5):1-11.

Zodda, D., Giammona, R., Schifilliti, S. 2018. Treatment strategy for dyslipidaemia in cardiovascular disease prevention: focus on old and new drugs. *Pharmacy,* 6(10):1-16.

# APPENDIX A

VALIDATION OF AN HIGH PERFORMANCE LIQUID CHROMATOGRAPHIC (HPLC) ASSAY FOR ATORVASTATIN, FLUVASTATIN, PITAVASTATIN AND PRAVASTATIN

## A.1 Purpose of validation

Method validation, also known as the procedure of presenting recorded confirmation that the method performs as intended (Shabir, 2003:57), is a requirement in most guidelines and quality criteria associated with laboratories (Huber, 2007:2). Validation of analytical methods is critical for analytical assays for the main principle of acquiring precise, constant and reliable results (Huber, 2007:2). The results of a validated method offer confirmation for reliability, creditability and accuracy (Huber, 2007:2), which plays an essential role in good analytical practice (Huber, 2007:2).

## A.2 Chromatographic conditions

A high-performance liquid chromatographic (HPLC) analytical method was developed and validated at the North-West University (NWU), Potchefstroom campus, with the assistance of Professor Jan du Preez in the Analytical Technology Laboratory (ATL). To develop an HPLC method effectively, some acceptance criteria should be determined. Assay optimisation and pre-validation were performed to establish the influence of the assay conditions and sample elements on the assay performance.

To develop the HPLC method used in this study an analytical instrument (Dionex UltiMate 3000 dual system with ternary gradient pumps, column ovens, an autosampler and diode array detectors) was used. This analytical instrument operated on Chromeleon 7.2 instrument control and data analysis software (Thermo Fisher Scientific Inc., Waltham, MA) for optimal processing of data. The HPLC method developed to perform the analysis on the statins utilised in this study was as follows:

**Column:** Restek Ultra C18, 250 x 4.6 mm, 5 um (Restek, Bellefonte, PA)

**Flow rate:** 1.0 ml/min

**Injection volume:** 10 µl

**Detection wavelength (nm):** UV at 240 nm

**Retention time pitavastatin:** ± 4.84 min

**Retention time pravastatin:** ± 5.84 min

**Retention time atorvastatin:** ± 8.53 min

**Retention time fluvastatin:** ± 8.95 min

**Stop time:** 15.00 min

**Solvent:** Methanol

**Mobile phase:** Acetonitrile/water with 0.1% orthophosphoric acid

The mobile phase was determined as acetonitrile (ACN)/Milli-Q® water (Milli-Q® Academic water purification system, Merck-Millipore, Midrand, RSA) with 0.1% orthophosphoric acid, which started at 30% acetonitrile and increased linearly to 70% after 4 min and then held at 70% up to 10 min and then re-equilibrated at start conditions.


**Figure A.1:** HPLC used in this study as an analytical instrument (Dionex UltiMate 3000 dual system with ternary gradient pumps, column ovens autosampler and diode array detectors)

### A.3 Guidelines to the method validation

According to the USP (2009), laboratory testing is required for analytical method validation and the results of the method should meet the prerequisites for the specified analytical guidelines (parameters). Thus, method validation requires specific wide-ranging laboratory validation tests, which have been categorised into different groups by national, as well as universal boards (Huber, 2007:14; Paithankar, 2013:232). The required parameters are usually displayed in terms of correlation coefficient ($R^2$), relative standard deviation (RSD) or standard deviation (SD).

Huber (2007) combined The International Conference for Harmonization (ICH), The United States Pharmacopeia (USP) and the general requirements for the competence of testing and calibration laboratories (ISO/IEC 17025) and summarised the parameters as follows:

- Linearity
- Accuracy
- Precision
    - Repeatability (intra-day)
    - Intermediate precision (inter-day)
    - Reproducibility
- Ruggedness and robustness
- System stability
- Specificity
- Limit of detection (LOD)
- Limit of quantitation (LOQ)

**Table A.1:** Summary of analytical method validation guidelines and the results for atorvastatin (Ator), fluvastatin (Flu), pitavastatin (Pita) and pravastatin (Pra)

| Validation parameters | | Accepted parameters | Ator | Flu | Pita | Pra |
|---|---|---|---|---|---|---|
| **Linearity** | | $R^2 \geq 0.999$ | $R^2 = 1$ | $R^2 = 1$ | $R^2 = 1$ | $R^2 = 1$ |
| **Accuracy** | | Recovery (90.0 – 110.0%) | 99.2% | 103.0% | 98.0% | 100.2% |
| **Precision** | Intra-day | %RSD ≤5.00% | 0.68% | 1.56% | 0.83% | 2.48% |
| | Inter-day | | 0.72% | 0.90% | 0.78% | 3.35% |
| **Robustness** | | See Section A.3.3 | | | | |
| **System stability** | | %RSD < 2.00% | 0.94% | 0.77% | 0.27% | 0.65% |
| **System repeatability** | Peak area | %RSD < 2.00% | 0.78% | 0.25% | 0.20% | 0.31% |
| | Retention time (min) | %RSD < 2.00% | 0.05% | 0.03% | 0.06% | 0.06% |
| **Specificity** | | See Section A.3.6 | | | | |
| **LOD (µg/ml)** | | %RSD < 15.000% | 0.116 | 0.006 | 0.005 | 0.004 |
| **LOQ (µg/ml)** | | %RSD < 20.000% | 0.035 | 0.019 | 0.015 | 0.013 |

**Table A.2:** Retention time (min), area (mAU) and height of the standard solutions (± 20 mg of each statin added up to 100 ml methanol)

| Statins | Retention time (min) | Area (mAU) (mAU x min) | Height (mAU) |
|---|---|---|---|
| **Atorvastatin** | 8.507 | 89.868 | 877.747 |
| **Fluvastatin** | 8.920 | 130.085 | 1183.913 |
| **Pitavastatin** | 4.547 | 128.288 | 2713.035 |
| **Pravastatin** | 5.400 | 94.248 | 1632.613 |

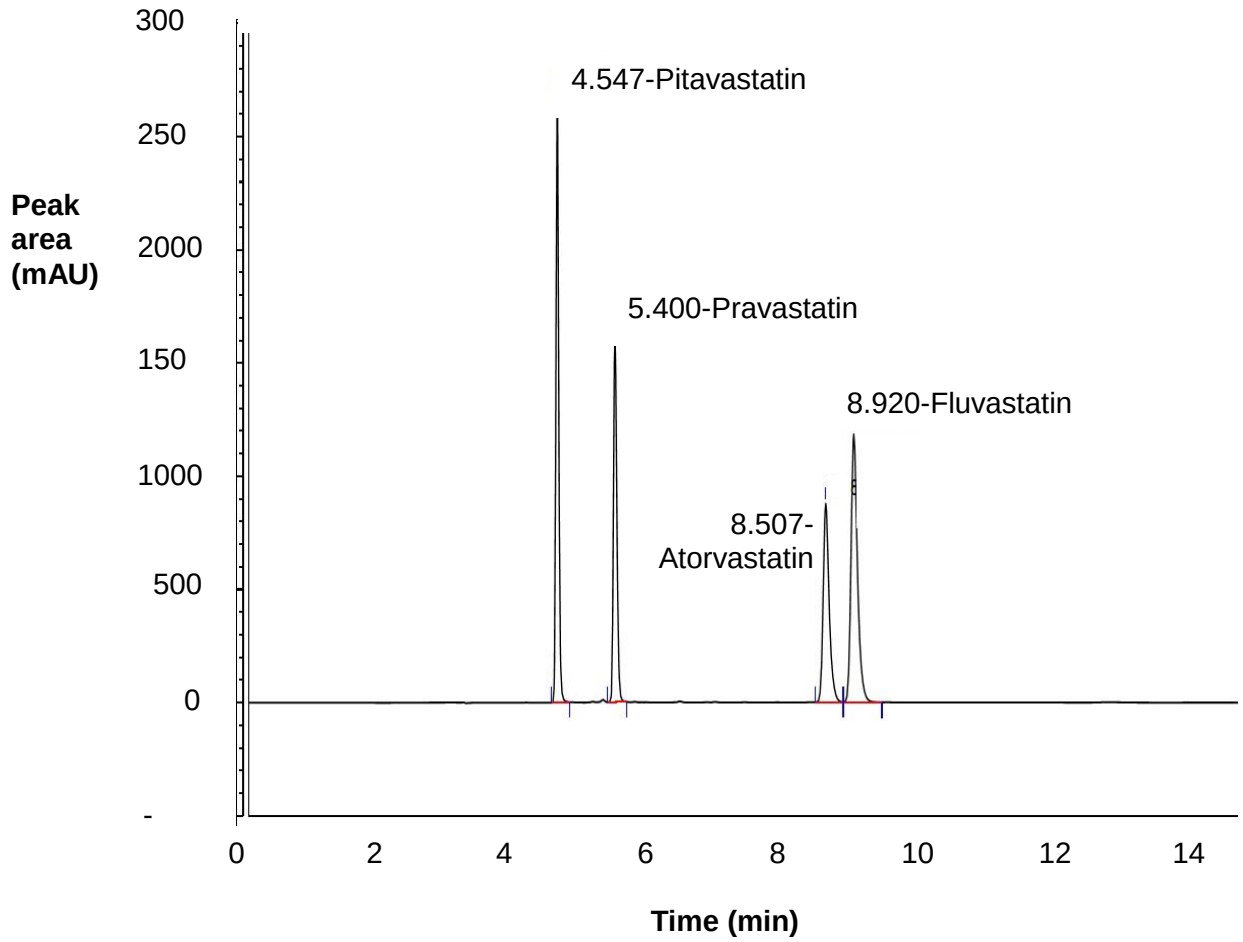


**Figure A.2:** HPLC chromatogram representing the statins' standard solution peaks

### A.3.1 Linearity

Linearity refers to the capability of the analytical procedure to produce results (on a specific scale) that correspond with the amount of analyte present in the given sample (ICH, 2005:5; Paithankar, 2013:234); linearity testing may be performed by diluting the stock solution directly (Huber, 2007:19).

To determine linearity, six or more standards should be prepared with concentrations between the suspected concentration ranges (APVMA, 2004:4). A linear relationship is to be established through visual examination of the analytical response plot (peak areas) against analyte concentration (µg/ml), where *y*-unit represents the peak area of the analyte (statin) and *x*-unit the concentration analyte (statin) present in the sample, and *c* is the y-intercept (Snyder *et al.*, 1997a:644). The slope (*m*) should present as a straight regression line (Snyder *et al.,* 1997b:691) to calculate the correlation coefficient ($R^2$) for each analyte individually; if the value of this coefficient exceeds 0.98, it is an indication of a strong relationship between analyte concentration and response (Paithankar, 2013:235; Snyder et al., 1997b:691).

The linearity of the data is presented through the linear regression equation (Paithankar, 2013:235; Snyder et al., 1997a:644).

$y = mx + c$ **Equation A.1**

### A.3.1.1 Linearity method

A standard solution containing ± 20 mg statins was weighed separately in a 100 ml volumetric flask. These flasks were then filled up to volume (100 ml) with the solvent (methanol). To ensure the statins were thoroughly dissolved, the flasks were shaken manually and placed on an Elma Transonic EL540 ultrasonic bath; a volume of 1 ml of each statin solution was transferred to marked HPLC vials to be evaluated.

A volume of 5 ml of each standard statin solution was diluted with methanol to a volume of 50 ml and marked as the first dilution; a volume of 1 ml of each statin's first dilution was transferred to marked HPLC vials to be evaluated.

A second dilution was prepared by obtaining a volume of 5 ml of each statin's first dilution and adding methanol up to a volume of 50 ml; a volume of 1 ml of each statin's second dilution was then withdrawn and injected into a marked HPLC vials.

All the marked vials were inserted into the HPLC and injected in duplicate with injection volumes of 2.5, 5.0, 7.5 and 10.0 µl to determine the linear regression.

**Table A.3:** Atorvastatin's standard linearity results

| Concentration (µg/ml) | Area 1 (mAU) | Area 2 (mAU) | Mean area (mAU) |
|---|---|---|---|
| 0.619 | 0.227 | 0.227 | 0.2 |
| 1.238 | 0.437 | 0.439 | 0.4 |
| 1.857 | 0.665 | 0.664 | 0.7 |
| 2.476 | 0.886 | 0.883 | 0.9 |
| 6.190 | 2.122 | 2.115 | 2.1 |
| 12.380 | 4.279 | 4.279 | 4.3 |
| 18.570 | 6.432 | 6.432 | 6.4 |
| 24.760 | 8.592 | 8.583 | 8.6 |
| 61.900 | 22.303 | 22.248 | 22.3 |
| 123.800 | 44.884 | 44.865 | 44.9 |
| 185.700 | 67.385 | 67.275 | 67.3 |
| 247.600 | 89.831 | 89.902 | 89.9 |

| | |
|---|---|
| **$R^2$** | 1 |
| **y-intercept** | - 0.1386 |
| **Slope** | 0.3633 |

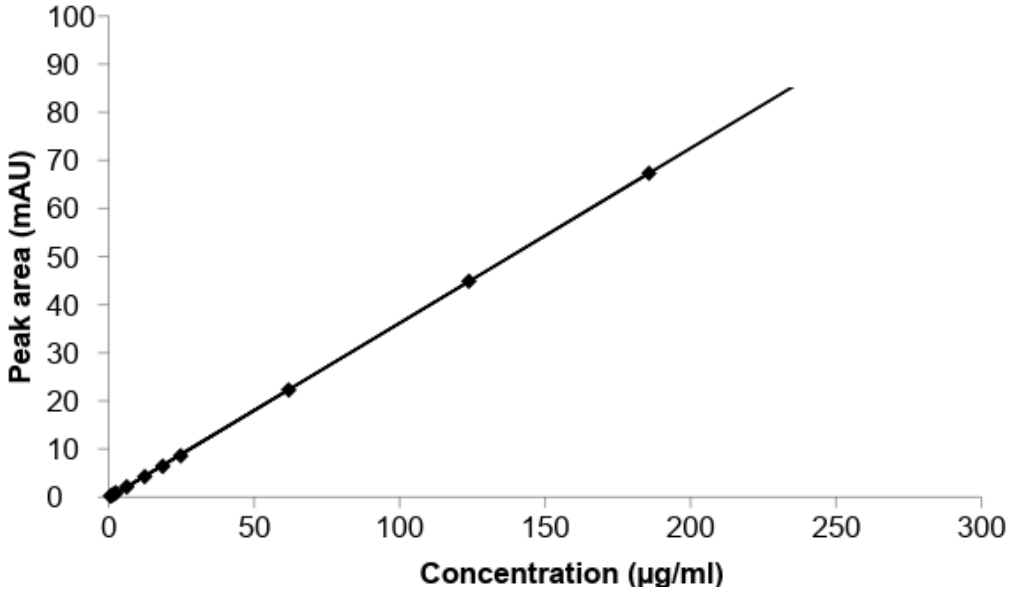


**Figure A.3:** Representation of atorvastatin's standard linear regression curve

Atorvastatin standard solution's linearity results were calculated as $R^2 = 1$, which signified a strong relationship between analyte concentration and response, as this value exceeded 0.999 (Paithankar, 2013:235). The slope also presented as a straight regression line (APVMA,

2004:4; Snyder *et al.,* 1997b:691) as required (Figure A.3).

**Table A.4:** Fluvastatin's standard linearity results

| Concentration (µg/ml) | Area 1 (mAU) | Area 2 (mAU) | Mean area (mAU) |
|---|---|---|---|
| 0.625 | 0.331 | 0.331 | 0.3 |
| 1.250 | 0.660 | 0.653 | 0.7 |
| 1.874 | 0.975 | 0.972 | 1.0 |
| 2.499 | 1.286 | 1.284 | 1.3 |
| 6.248 | 3.092 | 3.080 | 3.1 |
| 12.495 | 6.204 | 6.203 | 6.2 |
| 18.743 | 9.303 | 9.303 | 9.3 |
| 24.990 | 12.416 | 12.420 | 12.4 |
| 62.475 | 32.277 | 32.214 | 32.2 |
| 124.950 | 65.017 | 64.917 | 65.0 |
| 187.425 | 97.414 | 97.180 | 97.3 |
| 249.900 | 130.027 | 130.108 | 130.1 |

| $R^2$ | 1 |
|---|---|
| y-intercept | -0.1906 |
| Slope | 0.5207 |

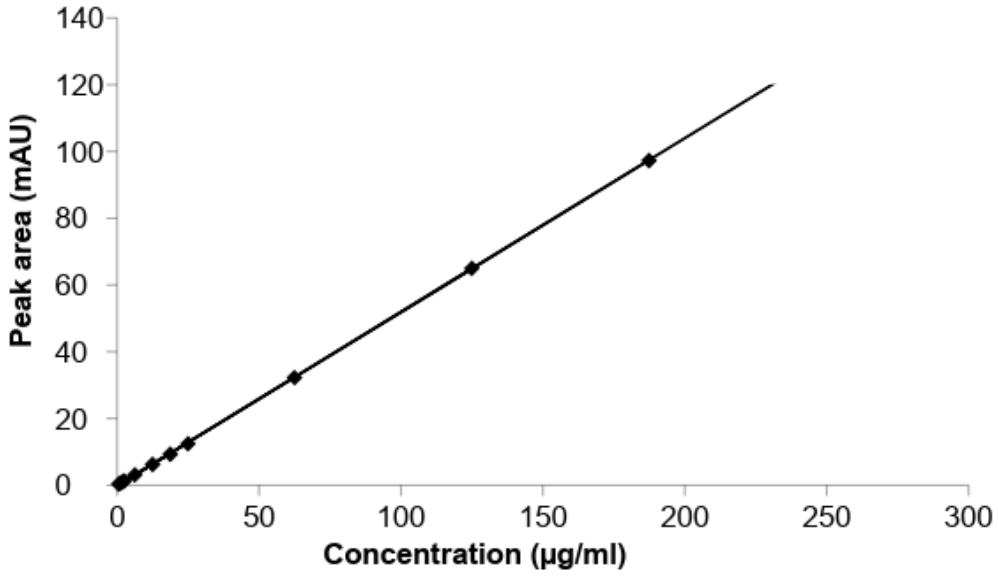


**Figure A.4:** Representation of fluvastatin's standard linear regression curve

Fluvastatin standard solution's linearity results specified $R^2 = 1$, which indicated a strong correlation between analyte concentration and response as this value exceeded 0.999 (Paithankar, 2013:235). The slope also displayed a straight regression line (APVMA, 2004:4; Snyder *et al.,* 1997b:691) as requested (Figure A.4).

**Table A.5:** Pitavastatin's standard linearity results

| Concentration (µg/ml) | Area 1 (mAU) | Area 2 (mAU) | Mean area (mAU) |
|---|---|---|---|
| 0.596 | 0.316 | 0.316 | 0.3 |
| 1.191 | 0.634 | 0.633 | 0.6 |
| 1.787 | 0.958 | 0.959 | 1.0 |
| 2.382 | 1.270 | 1.272 | 1.3 |
| 5.955 | 3.083 | 3.073 | 3.1 |
| 11.910 | 6.216 | 6.200 | 6.2 |
| 17.865 | 9.288 | 9.288 | 9.3 |
| 23.820 | 12.412 | 12.449 | 12.4 |
| 59.550 | 32.265 | 32.101 | 32.2 |
| 119.100 | 64.503 | 64.800 | 64.7 |
| 178.650 | 96.247 | 95.636 | 95.9 |
| 238.200 | 127.536 | 127.729 | 127.6 |

| | |
|---|---|
| **$R^2$** | 1 |
| **y-intercept** | -0.0557 |
| **Slope** | 0.5375 |

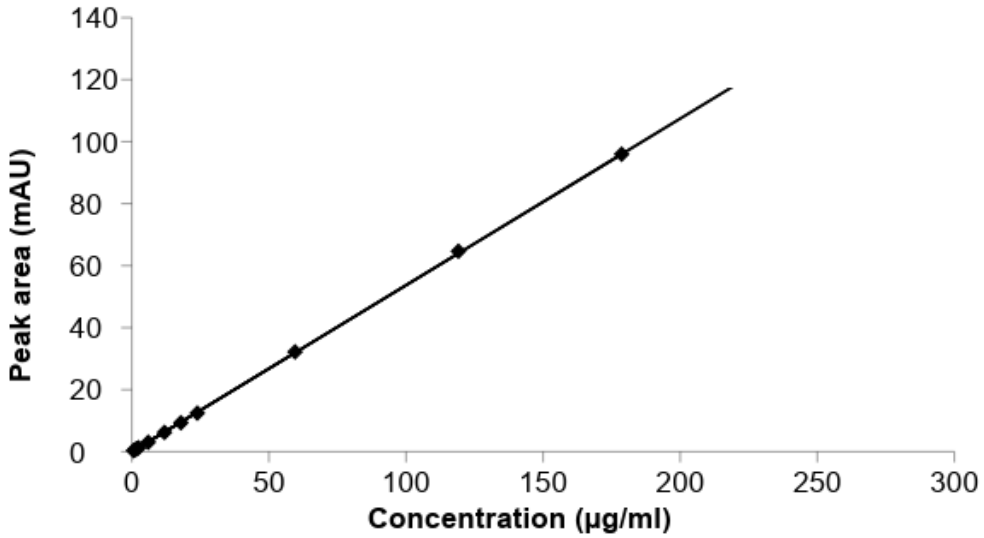


**Figure A.5:** Representation of pitavastatin's standard linear regression curve

Pitavastatin standard solution's linearity results quantified $R^2 = 1$, which indicated a strong

relationship between analyte concentration and response as this value exceeded 0.999 (Paithankar, 2013:235). The slope presented a straight regression line (APVMA, 2004:4; Snyder *et al.,* 1997b:691) as required (Figure A.5).

**Table A.6:** Pravastatin's standard linearity results

| Concentration (µg/ml) | Area 1 (mAU) | Area 2 (mAU) | Mean area (mAU) |
|---|---|---|---|
| 0.601 | 0.233 | 0.233 | 0.233 |
| 1.202 | 0.469 | 0.469 | 0.469 |
| 1.803 | 0.705 | 0.706 | 0.706 |
| 2.404 | 0.939 | 0.938 | 0.939 |
| 6.010 | 2.279 | 2.285 | 2.282 |
| 12.020 | 4.605 | 4.600 | 4.603 |
| 18.030 | 6.928 | 6.928 | 6.928 |
| 24.040 | 9.246 | 9.237 | 9.241 |
| 60.100 | 23.905 | 23.843 | 23.874 |
| 120.200 | 47.962 | 48.028 | 47.995 |
| 180.300 | 71.362 | 71.179 | 71.271 |
| 240.400 | 94.374 | 94.651 | 94.512 |

| | |
|---|---|
| **$R^2$** | 1 |
| **y-intercept** | -0.0271 |
| **Slope** | 0.3948 |

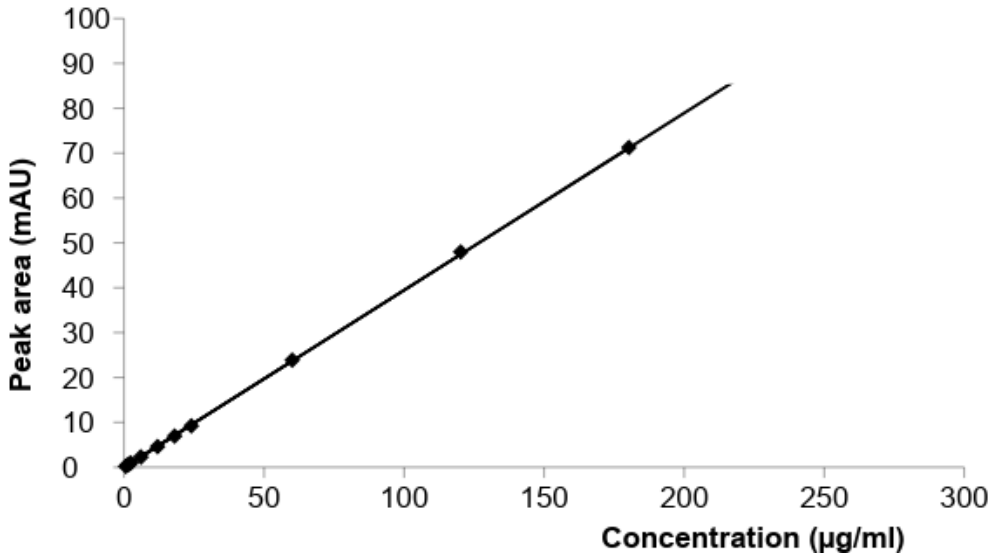


**Figure A.6:** Representation of pravastatin's linear regression curve

Pravastatin standard solution's linearity results indicated $R^2 = 1$, which suggested a strong relationship between analyte concentration and response as this value exceeded 0.999 (Paithankar, 2013:235). The slope presented as a straight regression line (APVMA, 2004:4; Snyder *et al.,* 1997b:691) as required (Figure A.6).

### A.3.2 Accuracy

Accuracy is described as the magnitude to which the accepted value (reference) of analyte in the sample compares to the actual measured value (APVMA, 2004:4; Paithankar, 2013:236). A sample containing pure solvent with a specified weighed concentration is acceptable as a reference value (Huber, 2007:19; Paithankar, 2013:236) and will therefore serve as the accepted value in this study. This method of accuracy is highly influenced by the preparation of samples, thus, the preparation of samples should be identical to each other (Huber, 2007:19; Paithankar, 2013:236).

The accuracy of methods may vary over certain assay values, thus a minimum of nine samples are recommended, with three different concentrations in the specified range (APVMA, 2004:5; ICH, 2005:4); therefore, three concentrations each in triplicate. Accuracy is reported as recovery (%) and can be described as the relationship between the noted results and the result expected (APVMA, 2004:5; Paithankar, 2013:236). The recovery expected is influenced by the analyte concentration, the sample placebo and the method in which the sample was prepared (APVMA, 2004:5).

**Table A.7:** The mean recovery (%) ranges (APVMA, 2004:5).

| Active content (%) | Acceptable recovery mean |
|---|---|
| ≥ 10.0 | 98 – 102% |
| ≥ 1.0 | 90 – 110% |
| 0.1 – 1.0 | 80 – 120% |
| < 0.1 | 75 – 125% |

For the purpose of this study, the spiked placebo recovery method was utilised. Spiked placebo solutions were prepared by adding ± 400 mg of the statin (active constituent) to a volumetric flask, which was made up to volume (100 ml) with methanol. This process was performed separately for each statin.

**Table A.8:** Formula for the placebo nano-emulsion (no statins)

| Phase 1: Water phase | Quantity |
|---|---|
| **Water** | 40.000 ml |
| **Tween 80®** | 2.804 ml |
| **Phase 2: Oil phase** | **Quantity** |
| **Apricot kernel oil** | 4.350 ml |
| **Span 60®** | 3.000 g |

Nine volumetric flasks were used for each statin:

- Three flasks were prepared with 3 ml spiked solution and 0.6 ml placebo nano-emulsion.
- Three flasks were prepared with 4 ml spiked solution and 0.8 ml placebo nano-emulsion.
- Three flasks were prepared with 5 ml spiked solution and 1.0 ml placebo nano-emulsion.

These flasks were filled up to volume (100.0 ml) with methanol and mixed thoroughly in an ultrasonic bath. Small quantities of each flask were then transferred into vials, which were injected into the HPLC.

Standard solutions were prepared by weighing roughly 20 mg of each statin (active constituent) in separate volumetric flasks, adding methanol up to volume (100.0 ml) and each statin dissolved thoroughly. A small quantity of the standard was then transferred to an HPLC vial to be injected. The vials were subsequently assayed and the results thereof were compared to the expected results.

**Table A.9:** Accuracy results of atorvastatin

| Concentration spiked (µg/ml) | Area 1 (mAU) | Area 2 (mAU) | Mean area (mAU) | Recovery (µg/ml) | Recovery (%) |
|---|---|---|---|---|---|
| 119.8 | 46.031 | 47.003 | 47 | 118.7 | 99.1 |
| 119.8 | 46.618 | 46.643 | 47 | 119.0 | 99.3 |
| 119.8 | 46.899 | 46.951 | 47 | 119.7 | 99.9 |
| 159.7 | 60.877 | 62.149 | 62 | 156.9 | 98.3 |
| 159.7 | 61.835 | 60.501 | 61 | 156.0 | 97.7 |
| 159.7 | 63.358 | 62.783 | 63 | 160.9 | 100.8 |
| 199.6 | 77.984 | 77.986 | 78 | 198.9 | 99.7 |
| 199.6 | 76.877 | 77.691 | 77 | 197.2 | 98.8 |
| 199.6 | 78.279 | 77.131 | 78 | 198.2 | 99.3 |

**Table A.10:** Statistical analysis of atorvastatin

| Statistical analysis | |
|---|---|
| Mean recovery (%) | 99.2 |
| SD | 0.8 |
| %RSD | 0.9 |

The accuracy results of atorvastatin were within acceptable limits, since the mean recovery (%) was 99.2%, thus ranged between 90 – 110% (APVMA, 2004:5).

**Table A.11:** Accuracy results of fluvastatin

| Concentration spiked (µg/ml) | Area 1 (mAU) | Area 2 (mAU) | Mean area (mAU) | Recovery (µg/ml) | Recovery (%) |
|---|---|---|---|---|---|
| 119.7 | 66.003 | 65.784 | 66 | 124.3 | 103.9 |
| 119.7 | 65.679 | 65.735 | 66 | 124.0 | 103.6 |
| 119.7 | 65.446 | 64.871 | 65 | 122.9 | 102.7 |
| 159.6 | 87.577 | 87.638 | 88 | 165.3 | 103.6 |
| 159.6 | 86.987 | 86.940 | 87 | 164.1 | 102.8 |
| 159.6 | 87.682 | 87.540 | 88 | 165.3 | 103.6 |
| 199.5 | 108.554 | 108.586 | 109 | 204.8 | 102.7 |
| 199.5 | 108.639 | 108.619 | 109 | 205.0 | 102.7 |
| 199.5 | 106.649 | 107.908 | 107 | 202.4 | 101.4 |

**Table A.12:** Statistical analysis of fluvastatin

| Statistical analysis | |
|---|---|
| Mean recovery (%) | 103.0 |
| SD | 0.7 |
| %RSD | 0.7 |

The accuracy of fluvastatin (103.0%) was within acceptable limits, since the mean recovery (%) ranged between 90 – 110% (APVMA, 2004:5).

**Table A.13:** Accuracy results of pitavastatin

| Concentration spiked (µg/ml) | Area 1 (mAU) | Area 2 (mAU) | Mean area (mAU) | Recovery (µg/ml) | Recovery (%) |
|---|---|---|---|---|---|
| 120.0 | 63.157 | 63.350 | 63 | 118.8 | 99.0 |
| 120.0 | 63.330 | 63.307 | 63 | 118.9 | 99.1 |
| 120.0 | 62.908 | 62.754 | 63 | 118.0 | 98.3 |
| 160.0 | 83.146 | 83.358 | 83 | 156.3 | 97.7 |
| 160.0 | 83.058 | 82.956 | 83 | 155.9 | 97.4 |
| 160.0 | 83.726 | 83.910 | 84 | 157.4 | 98.4 |
| 200.1 | 103.902 | 104.087 | 104 | 195.3 | 97.6 |
| 200.1 | 103.902 | 104.087 | 104 | 195.3 | 97.6 |
| 200.1 | 103.265 | 103.281 | 103 | 193.9 | 96.9 |

**Table A.14:** Statistical analysis of pitavastatin

| Statistical analysis | |
|---|---|
| Mean recovery (%) | 98.0 |
| SD | 0.7 |
| %RSD | 0.7 |

The accuracy of pitavastatin ranged between 90 – 110% and was within acceptable limits, since the mean recovery (%) was 98.0% (APVMA, 2004:5).

**Table A.15:** Accuracy results of pravastatin

| Concentration spiked (µg/ml) | Area 1 (mAU) | Area 2 (mAU) | Mean area (mAU) | Recovery (µg/ml) | Recovery (%) |
|---|---|---|---|---|---|
| 120.1 | 49.518 | 49.528 | 50 | 121.4 | 101.1 |
| 120.1 | 49.146 | 49.613 | 49 | 121.0 | 100.8 |
| 120.1 | 48.800 | 49.222 | 49 | 120.1 | 100.0 |
| 160.1 | 65.801 | 65.837 | 66 | 161.3 | 100.7 |
| 160.1 | 66.210 | 66.213 | 66 | 162.3 | 101.3 |
| 160.1 | 65.952 | 65.985 | 66 | 161.7 | 101.0 |
| 200.2 | 80.400 | 81.121 | 81 | 198.0 | 98.9 |
| 200.2 | 80.549 | 81.070 | 81 | 198.1 | 99.0 |
| 200.2 | 81.107 | 80.951 | 81 | 198.6 | 99.2 |

**Table A.16:** Statistical analysis of pravastatin

| Statistical analysis | |
|---|---|
| Mean recovery (%) | 100.2 |
| SD | 0.9 |
| %RSD | 0.9 |

The accuracy of pravastatin presented within acceptable limits, since the mean recovery (%) was 100.2% (90 – 110%) (APVMA, 2004:5).

### A.3.3 Precision

Precision of an analytical method is defined as the degree of variation (standard deviation) between data obtained from numerous measurements under certain conditions, utilising a main sample (APVMA, 2004:5; Paithankar, 2013:235). Precision is measured on three levels namely repeatability (intra-day precision), intermediate precision (inter-day precision) and reproducibility (Huber, 2007:18; ICH, 2005:4; Paithankar, 2013:235). Only repeatability (intra-day precision) and intermediate precision (inter-day precision) will be calculated and discussed here, while reproducibility will be explained under ruggedness. When precision is determined a minimum of five (replicate) samples are required (APVMA, 2004:5). When analysed, the %RSD value is calculated (APVMA, 2004:5; Paithankar, 2013:236).

**Table A.17:** The following levels of precision are recommended (APVMA, 2004:5).

| Constituent in sample | Precision (%RSD) |
|---|---|
| > 10.0% | ≤ 2% |
| 1.0 Up to 10.0% | ≤ 5% |
| 0.1 Up to 1.0% | ≤ 10% |
| < 0.1% | ≤ 20% |

### A.3.3.1 Repeatability (intra-day precision)

Repeatability, also known as intra-assay precision, conveys precision, as results are measured over a short period under similar conditions (ICH, 2005:4) in the same laboratory (Huber, 2007:18). When assessing repeatability, nine (minimum) samples are required, therefore three different sample concentrations are injected in triplicate and evaluated on the HPLC in one day (ICH, 2005:10). The preparation method is similar to the preparation method used in accuracy.

**Table A.18:** Repeatability (intra-day precision) results of atorvastatin

| Concentration spiked (µg/ml) | Peak area | | | Recovery | |
|---|---|---|---|---|---|
| | 1 | 2 | Average | (mg/100 ml) | % |
| 119.979 | 46.965 | 46.294 | 46.6 | 118.5 | 98.8 |
| 119.979 | 46.497 | 45.803 | 46.2 | 117.3 | 97.7 |
| 119.979 | 47.193 | 46.250 | 46.7 | 118.7 | 98.9 |
| 159.972 | 62.539 | 62.590 | 62.6 | 159.0 | 99.4 |
| 159.972 | 62.021 | 62.203 | 62.1 | 157.8 | 98.7 |
| 159.972 | 62.206 | 61.816 | 62.0 | 157.6 | 98.5 |
| 199.965 | 76.605 | 77.462 | 77.0 | 195.7 | 97.9 |
| 199.965 | 77.724 | 77.744 | 77.7 | 197.5 | 98.8 |
| 199.965 | 75.939 | 76.837 | 76.4 | 194.1 | 97.1 |
| | | | | **Mean** | 0.98 |
| | | | | **SD** | 0.01 |
| | | | | **%RSD** | 0.68 |

The %RSD value calculated (intra-day precision) for atorvastatin was 0.68%, hence smaller than the recommended level of precision, which was indicated as 5% (APVMA, 2004:5; Paithankar, 2013:236).

**Table A.19:** Repeatability (intra-day precision) results of fluvastatin

| Concentration spiked (µg/ml) | Peak area | | | Recovery | |
|---|---|---|---|---|---|
| | 1 | 2 | Average | (mg/100 ml) | % |
| 120.015 | 63.227 | 64.484 | 63.9 | 120.8 | 100.7 |
| 120.015 | 62.448 | 62.536 | 62.5 | 118.2 | 98.5 |
| 120.015 | 63.704 | 64.280 | 64.0 | 121.1 | 100.9 |
| 160.020 | 84.720 | 86.043 | 85.4 | 161.5 | 101.0 |
| 160.020 | 85.915 | 85.929 | 85.9 | 162.6 | 101.6 |
| 160.020 | 83.217 | 85.397 | 84.3 | 159.5 | 99.7 |
| 200.025 | 110.013 | 111.205 | 110.6 | 209.3 | 104.6 |
| 200.025 | 105.998 | 105.565 | 105.8 | 200.1 | 100.1 |
| 200.025 | 107.392 | 106.219 | 106.8 | 202.1 | 101.0 |
| | | | | **Mean** | 1.01 |
| | | | | **SD** | 0.02 |
| | | | | **%RSD** | 1.56 |

The %RSD value calculated (intra-day precision) for fluvastatin was 1.56%, which was less than the 5% the recommended level of precision (APVMA, 2004:5; Paithankar, 2013:236).

**Table A.20:** Repeatability (intra-day precision) results of pitavastatin

| Concentration spiked (µg/ml) | Peak area | | | Recovery | |
|---|---|---|---|---|---|
| | 1 | 2 | Average | (mg/100 ml) | % |
| 120.030 | 63.264 | 62.956 | 63.1 | 122.2 | 101.8 |
| 120.030 | 62.644 | 62.801 | 62.7 | 121.5 | 101.2 |
| 120.030 | 63.024 | 62.901 | 63.0 | 121.9 | 101.6 |
| 160.040 | 82.934 | 82.907 | 82.9 | 160.6 | 100.3 |
| 160.040 | 82.790 | 82.954 | 82.9 | 160.5 | 100.3 |
| 160.040 | 82.434 | 82.333 | 82.4 | 159.5 | 99.7 |
| 200.050 | 103.288 | 103.058 | 103.2 | 199.8 | 99.9 |
| 200.050 | 102.998 | 103.689 | 103.3 | 200.1 | 100.0 |
| 200.050 | 102.481 | 102.615 | 102.5 | 198.6 | 99.3 |
| | | | | **Mean** | 100.45 |
| | | | | **SD** | 0.83 |
| | | | | **%RSD** | 0.83 |

The %RSD value calculated (intra-day precision) for pitavastatin was 0.83%, therefore under the recommended level of precision, which was indicated as 5% (APVMA, 2004:5; Paithankar, 2013:236).

**Table A.21:** Repeatability (intra-day precision) results of pravastatin

| Concentration spiked (µg/ml) | Peak area | | | Recovery | |
|---|---|---|---|---|---|
| | 1 | 2 | Average | (mg/100 ml) | % |
| 120.1 | 38.838 | 39.385 | 39.1 | 119.0 | 99.1 |
| 120.1 | 38.746 | 38.677 | 38.7 | 117.8 | 98.1 |
| 120.1 | 38.566 | 38.791 | 38.7 | 117.7 | 98.0 |
| 160.1 | 52.887 | 53.140 | 53.0 | 161.3 | 100.8 |
| 160.1 | 53.447 | 53.853 | 53.6 | 163.3 | 102.0 |
| 160.1 | 50.855 | 50.333 | 50.6 | 154.0 | 96.2 |
| 200.2 | 68.017 | 68.462 | 68.2 | 207.7 | 103.8 |
| 200.2 | 67.340 | 67.464 | 67.4 | 205.1 | 102.5 |
| 200.2 | 67.626 | 67.871 | 67.7 | 206.2 | 103.0 |
| | | | | **Mean** | 100.37 |
| | | | | **SD** | 2.49 |
| | | | | **%RSD** | 2.48 |

The %RSD value calculated (intra-day precision) for pravastatin was 2.48%, thus smaller than the recommended level of precision, which was indicated as 5% (APVMA, 2004:5; Paithankar, 2013:236).

### A.3.3.2 Intermediate precision (inter-day precision)

Intermediate precision can be described as the degree of comparison between multiple measurements obtained under similar conditions using identical methods (ICH, 2005:5), completed over a few days in the same laboratory (Huber,2007:18). The objective is to confirm that future results will be comparable, given the method is performed in the same laboratory (Huber, 2007:18). In this study, intermediate precision was established utilising HPLC, over a period of three days, by analysing three homogenous samples containing similar concentrations.

**Day 1**

Repeatability results were used.

**Day 2**

On the second day the following samples were prepared:

- Three flasks with 4.0 ml (16 mg) spiked solution and 0.8 ml placebo nano-emulsion, made up to volume (100.0 ml) with methanol for each statin. These flasks were mixed thoroughly on an ultrasonic bath. Small quantities of each flask were then transferred to vials to be injected (duplicate) by the HPLC.
- A standard solution for each statin (active constituent) was prepared containing 20 mg active constituent with methanol added to volume (100.0 ml).

**Day 3**

On the third day the following samples were prepared:

- Three flasks with 4.0 ml (16 mg) spiked solution and 0.8 ml placebo nano-emulsion made up to volume (100.0 ml) with methanol for each statin. These flasks were mixed thoroughly in an ultrasonic bath. Small quantities of each flask were then transferred to vials to be injected (in duplicate) by the HPLC.
- A standard solution for each statin (active constituent) was prepared containing 20 mg active constituent with methanol added to volume (100.0 ml).

**Table A.22:** Inter-day precision results of atorvastatin

| Days | %Recovery | | | Mean | SD | %RSD |
|---|---|---|---|---|---|---|
| **Day 1** | 99.4 | 97.6 | 98.5 | 98.87 | 0.39 | 0.39 |
| **Day 2** | 98.7 | 97.5 | 97.4 | 97.43 | 0.12 | 0.12 |
| **Day 3** | 98.5 | 97.3 | 97.6 | 97.84 | 0.50 | 0.51 |
| **Between days:** | | | | 98.05 | 0.71 | 0.72 |

The %RSD value calculated (inter-day precision) for atorvastatin was 0.72%, which was smaller than the 5% recommended level of precision (APVMA, 2004:5; Paithankar, 2013:236).

**Table A.23:** Inter-day precision results of fluvastatin

| Days | %Recovery | | | Mean | SD | %RSD |
|---|---|---|---|---|---|---|
| **Day 1** | 101.0 | 102.2 | 102.5 | 100.74 | 0.79 | 0.79 |
| **Day 2** | 101.6 | 102.4 | 102.6 | 102.03 | 0.34 | 0.34 |
| **Day 3** | 99.7 | 101.6 | 102.6 | 102.56 | 0.07 | 0.07 |
| **Between days:** | | | | 101.78 | 0.91 | 0.90 |

The %RSD value calculated (inter-day precision) for fluvastatin was 0.90%, less than the proposed level of precision, which was indicated as 5% (APVMA, 2004:5; Paithankar, 2013:236).

**Table A.24:** Inter-day precision results of pitavastatin

| Days | %Recovery | | | Mean | SD | %RSD |
|---|---|---|---|---|---|---|
| **Day 1** | 100.3 | 100.3 | 100.3 | 100.09 | 0.29 | 0.29 |
| **Day 2** | 100.3 | 100.3 | 98.3 | 100.09 | 0.29 | 0.29 |
| **Day 3** | 99.7 | 99.7 | 98.4 | 98.97 | 0.91 | 0.91 |
| **Between days:** | | | | 99.72 | 0.78 | 0.78 |

The %RSD value calculated (inter-day precision) for pitavastatin was 0.78%, therefore under the advised level of precision, which was indicated as 5% (APVMA, 2004:5; Paithankar, 2013:236).

**Table A.25:** Inter-day precision results of pravastatin

| Days | %Recovery | | | Mean | SD | %RSD |
|---|---|---|---|---|---|---|
| **Day 1** | 100.8 | 102 | 96.20 | 99.62 | 2.50 | 2.51 |
| **Day 2** | 94.10 | 94.50 | 93.80 | 94.16 | 0.26 | 0.28 |
| **Day 3** | 93.30 | 92.8 | 93.30 | 93.12 | 0.23 | 0.25 |
| **Between days:** | | | | 99.72 | 0.78 | 3.35 |

The %RSD value calculated (inter-day precision) for pravastatin was 3.35%, hence smaller than the recommended level of precision, which was indicated as 5% (APVMA, 2004:5; Paithankar, 2013:236).

### A.3.3 Robustness

Numerous definitions of robustness and ruggedness exist in the context of validation, which are very similar and regularly utilised as synonyms, but the most frequent description for robustness is the constancy of an analytical procedure's measurements after deliberate alterations of certain parameters (ICH, 2005:5; Paithankar, 2013:238). The United States Pharmacopeia (USP, 2011) individualised these two terms by defining ruggedness as the level to which results are reproducible under certain different standard test conditions, for example variation of laboratories, materials, elapsed times of assay, operators, reagent batches, assay temperatures and days (Huber, 2007:26).

Ruggedness will therefore not be performed in this study as there is access to one only laboratory with HPLC equipment.

As stated before, robustness is the constancy of an analytical procedure's measurements after deliberate alternations of certain parameters (ICH, 2005:5; Paithankar, 2013:238). The measurements obtained will be an indication if the samples' retention time peaks on the chromatograms were affected by the alternations of the parameters (Paithankar, 2013:238; Snyders *et al*., 1997b:702). These chromatograms compared to chromatograms of procedures without any alternations of parameters will indicate if the analytical procedure is reliable (ICH, 2005:5; Paithankar, 2013:238). The data from this experiment will determine if revalidation of a method is necessary should parameters change (Huber, 2007:26; Paithankar, 2013:238). When using HPLC, typical alternations are (ICH, 2005:13):

- Alternations of the pH in the mobile phase
- Alternations of the composition of the mobile phase
- Variation of columns
- Alternation in temperature
- Alternation in flow rate
- Wavelength alteration
- Gradient alteration

In this study, robustness was established by the alternation of flow rate, wavelength and gradient. A standard solution was prepared containing ± 20 mg of each statin (separately) in a 100 ml volumetric flask. These flasks were then filled up to volume (100 ml) with the solvent (methanol).

The statins were thoroughly mixed in the flasks and placed on an Elma Transonic EL540 ultrasonic bath and a volume of 1 ml of each statin flask were then withdrawn and injected into marked HPLC vials to be evaluated.

The four standard solutions were injected under normal chromatographic conditions (Tables A.26 – A.29 see, sample a) and different chromatographic conditions (Tables A.26 – A.29 see, samples b and c), to determine if the changes would influence the sample and its retention time.

**Table A.26:** Robustness data for atorvastatin pre- and post-alternations

| Sample | Alterations to HPLC parameters | | | | | |
|---|---|---|---|---|---|---|
| | Injection volume (µl) | Flow rate (ml/min) | Wavelength (nm) | Gradient (ACN) | Peak area (mAU) | Retention time (min) |
| **a)** | 10.00 | 1.0 | 240 | 30% | 77.49 | 8.28 |
| **b)** | 10.00 | 1.2 | 235 | 35% | 60.27 | 7.21 |
| **c)** | 10.00 | 0.8 | 230 | 27% | 86.26 | 9.72 |

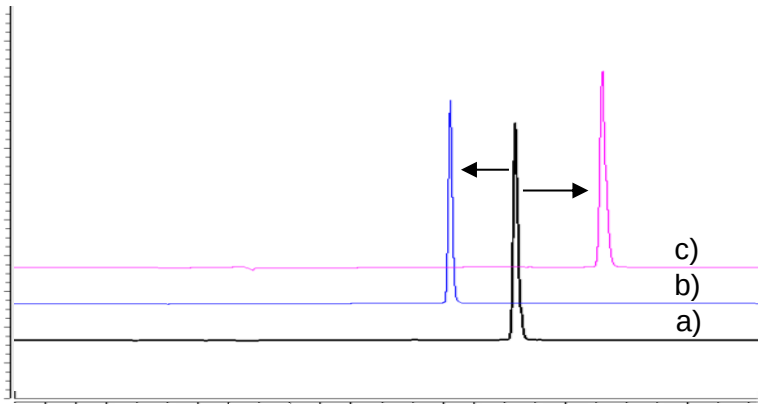


**Figure A.7:** An HPLC chromatogram representative of robustness data for atorvastatin standard solution injected at alternated parameters: a) standard conditions of injection volume (10.00 µl), flow rate (1.0 ml/min), wavelength (240 nm) and gradient (30% ACN); b) at injection volume (10.00 µl), flow rate (1.2 ml/min), wavelength (235 nm) and gradient (35% ACN); c) at injection volume (10.00 µl), flow rate (0.8 ml/min), wavelength (230 nm) and gradient (27% ACN)

In Table A.26 and Figure A.7 the robustness data (pre- and post-alternations) for atorvastatin suggested that under different chromatographic conditions, sample b) reduced the retention time, while c) took longer to emerge compared to a).

Although altered parameters of the HPLC conditions affected the retention times of the peaks compared to the standard (normal conditions, a), the retention times differed minimally, thus this method can be regarded as reliable.

**Table A.27:** Robustness data for fluvastatin pre- and post-alternations

| Sample | Alterations to HPLC parameters | | | | | |
|---|---|---|---|---|---|---|
| | Injection volume (µl) | Flow rate (ml/min) | Wavelength (nm) | Gradient (ACN) | Peak area (mAU) | Retention time (min) |
| **a)** | 10.00 | 1.0 | 240 | 30% | 100.45 | 8.67 |
| **b)** | 10.00 | 1.2 | 235 | 35% | 84.12 | 7.50 |
| **c)** | 10.00 | 0.8 | 230 | 27% | 124.12 | 10.23 |

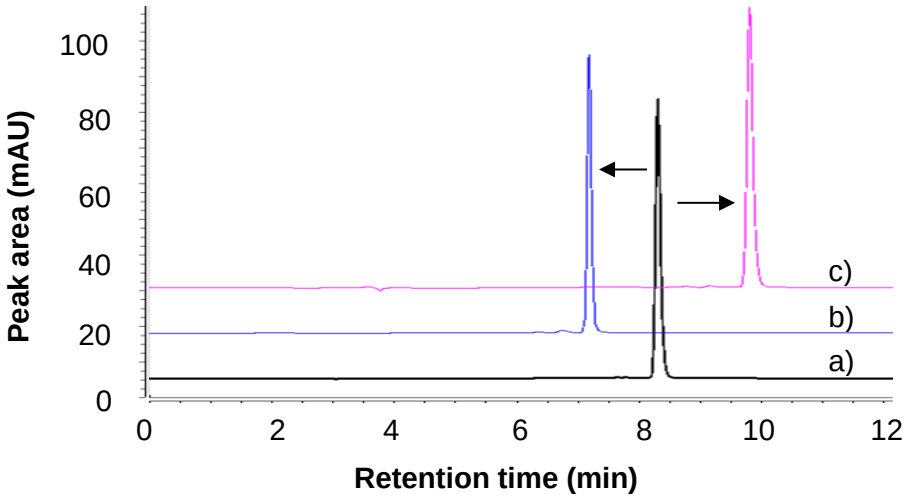


**Figure A.8:** An HPLC chromatogram representative of robustness data for fluvastatin standard solution injected at alternated parameters: a) standard conditions of injection volume (10.00 µl), flow rate (1.0 ml/min), wavelength (240 nm) and gradient (30% ACN); b) at injection volume (10.00 µl), flow rate (1.2 ml/min), wavelength (235 nm) and gradient (35% ACN); c) at injection volume (10.00 µl), flow rate (0.8 ml/min), wavelength (230 nm) and gradient (27% ACN)

From Table A.27 and Figure A.8 the robustness data (pre- and post-alternations) for fluvastatin indicated that sample b) appeared sooner, while with c), the retention time was

increased when compared to the standard a) (normal chromatographic conditions).

Altered parameters of the HPLC conditions influenced the retention times of the peaks marginally compared to the standard, therefore, this method can be regarded as reliable.

**Table A.28:** Robustness data for pitavastatin pre- and post-alternations

| Sample | Alterations to HPLC parameters | | | | | |
|---|---|---|---|---|---|---|
| | Injection volume (µl) | Flow rate (ml/min) | Wavelength (nm) | Gradient (ACN) | Peak area (mAU) | Retention time (min) |
| **a)** | 10.00 | 1.0 | 240 | 30% | 99.68 | 4.33 |
| **b)** | 10.00 | 1.2 | 235 | 35% | 68.40 | 3.08 |
| **c)** | 10.00 | 0.8 | 230 | 27% | 101.94 | 5.51 |

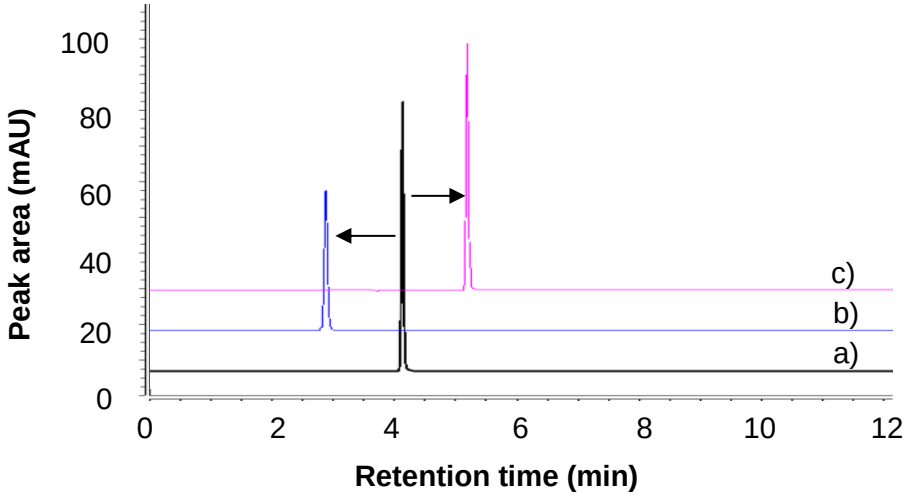


**Figure A.9:** An HPLC chromatogram representative of robustness data for pitavastatin standard solution injected at alternated parameters: a) standard conditions of injection volume (10.00 µl), flow rate (1.0 ml/min), wavelength (240 nm) and gradient (30% ACN); b) at injection volume (10.00 µl), flow rate (1.2 ml/min), wavelength (235 nm) and gradient (35% ACN); c) at injection volume (10.00 µl), flow rate (0.8 ml/min), wavelength (230 nm) and gradient (27% ACN)

From Table A.28 and Figure A.9 the robustness data (pre- and post-alternations) for pitavastatin indicated that sample b) reduced the retention time when compared to a), while with c) the retention time was delayed.

Varied parameters of the HPLC conditions affected the retention times of the peaks slightly compared to the standard (a), consequently this method can be considered as reliable.

**Table A.29:** Robustness data for pravastatin pre- and post-alternations

| Sample | Alterations to HPLC parameters | | | | | |
|---|---|---|---|---|---|---|
| | Injection volume (µl) | Flow rate (ml/min) | Wavelength (nm) | Gradient (ACN) | Peak area (mAU) | Retention time (min) |
| **a)** | 10.00 | 1.0 | 240 | 30% | 80.16 | 5.28 |
| **b)** | 10.00 | 1.2 | 235 | 35% | 65.83 | 4.20 |
| **c)** | 10.00 | 0.8 | 230 | 27% | 88.31 | 6.42 |

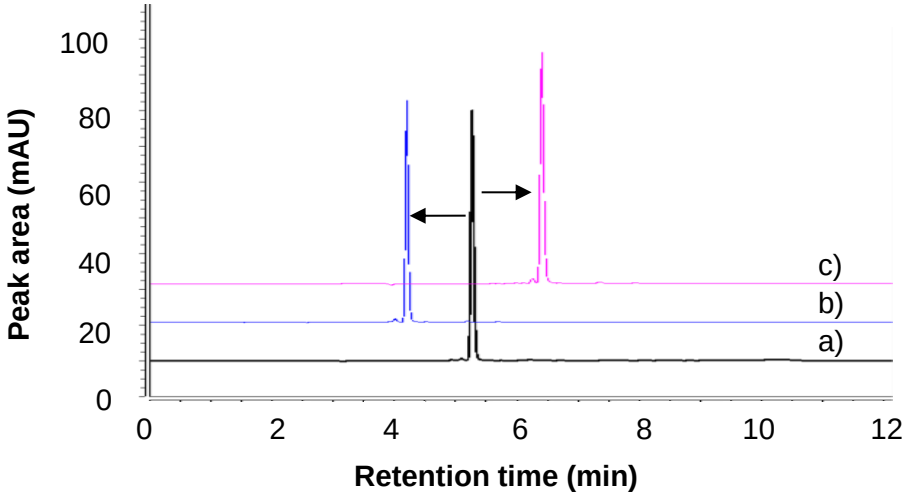


**Figure A.10:** An HPLC chromatogram representative of robustness data for pravastatin standard solution injected at alternated parameters: a) standard conditions of injection volume (10.00 µl), flow rate (1.0 ml/min), wavelength (240 nm) and gradient (30% ACN); b) at injection volume (10.00 µl), flow rate (1.2 ml/min), wavelength (235 nm) and gradient (35% ACN); c) at injection volume (10.00 µl), flow rate (0.8 ml/min), wavelength (230 nm) and gradient (27% ACN)

From Table A.29 and Figure A.10 the robustness data (pre- and post-alternations) for pravastatin indicated that under varied chromatogram conditions, b) and c) reduced and increased the retention time, respectively, with regard to sample a) (the standard under normal chromatographic conditions).

Altered parameters of the HPLC conditions affected the retention times of the peaks slightly compared to the standard, as a result this method can be counted as reliable.

### A.3.4 System stability

Chemicals can degrade during storage, sample preparation, etc., consequently the stability of the standards, as well as the analyte should be determined. System stability determines if the validation method in use can accurately detect compounds when degradation products are present (Huber, 2007:27). This method therefore measures the biasness in outcomes of the experiment, which is performed with stock solutions containing an identified concentration of the chemical compound in a suitable solvent measured in hourly intervals over a selected time (Huber, 2007:27).

In this study, a sample containing ± 20 mg (200 µg/ml) of a single statin was prepared and added up to volume (100 ml) with methanol. A small quantity was transferred to an HPLC vial to be injected and analysed by the HPLC. The sample was injected in 1 h intervals for 24 h. A solution with a degradation value higher than 2% indicates the sample is unstable and therefore cannot be utilised from the time of degradation (Paithankar, 2013:238).

**Table A.30:** Sample stability parameters for atorvastatin

| Time (h) | Peak area | %Remaining |
|---|---|---|
| **0** | 74.017 | 100.0 |
| **1** | 72.790 | 98.3 |
| **2** | 72.721 | 98.2 |
| **3** | 72.433 | 97.9 |
| **4** | 72.366 | 97.8 |
| **5** | 72.228 | 97.6 |
| **6** | 72.057 | 97.4 |
| **7** | 71.905 | 97.1 |
| **8** | 71.918 | 97.2 |
| **9** | 71.643 | 96.8 |
| **10** | 71.742 | 96.9 |
| **11** | 71.676 | 96.8 |
| **12** | 71.644 | 96.8 |
| **13** | 71.535 | 96.6 |
| **14** | 71.348 | 96.4 |
| **15** | 71.456 | 96.5 |
| **16** | 71.396 | 96.5 |
| **17** | 71.250 | 96.3 |
| **18** | 71.316 | 96.4 |
| **19** | 71.263 | 96.3 |
| **20** | 71.210 | 96.2 |
| **21** | 71.243 | 96.3 |
| **22** | 71.203 | 96.2 |
| **23** | 70.864 | 95.7 |
| **24** | 71.063 | 96.0 |
| **Mean** | 71.8 | 97.6 |
| **SD** | 0.68 | 0.92 |
| **%RSD** | 0.95 | 0.94 |

Sample stability results (%RSD) for atorvastatin (0.94%), which is qualified as stable as the degradation value was less than 2% (Paithankar, 2013:238).

**Table A.31:** Sample stability parameters for fluvastatin

| Time (h) | Peak area | %Remaining |
|---|---|---|
| **0** | 103.463 | 100.0 |
| **1** | 102.942 | 99.5 |
| **2** | 102.756 | 99.3 |
| **3** | 102.510 | 99.1 |
| **4** | 102.536 | 99.1 |
| **5** | 102.273 | 98.9 |
| **6** | 102.085 | 98.7 |
| **7** | 102.035 | 98.6 |
| **8** | 101.951 | 98.5 |
| **9** | 101.900 | 98.5 |
| **10** | 101.713 | 98.3 |
| **11** | 101.503 | 98.1 |
| **12** | 101.313 | 97.9 |
| **13** | 101.368 | 98.0 |
| **14** | 101.353 | 98.0 |
| **15** | 101.126 | 97.7 |
| **16** | 101.276 | 97.9 |
| **17** | 101.013 | 97.6 |
| **18** | 100.928 | 97.6 |
| **19** | 100.970 | 97.6 |
| **20** | 100.801 | 97.4 |
| **21** | 100.747 | 97.4 |
| **22** | 100.670 | 97.3 |
| **23** | 100.732 | 97.4 |
| **24** | 100.587 | 97.2 |
| **Mean** | 101.6 | 98.2 |
| **SD** | 0.78 | 0.75 |
| **%RSD** | 0.77 | 0.77 |

Sample stability results (% RSD) for fluvastatin degradation value was 0.77%, therefore the sample succeeded with stability, as it was lower than 2% (Paithankar, 2013:238).

**Table A.32:** Sample stability parameters for pitavastatin

| Time (h) | Peak area | %Remaining |
|---|---|---|
| **0** | 109.848 | 100.0 |
| **1** | 109.810 | 100.0 |
| **2** | 109.740 | 99.9 |
| **3** | 109.495 | 99.7 |
| **4** | 109.675 | 99.8 |
| **5** | 109.493 | 99.7 |
| **6** | 109.535 | 99.7 |
| **7** | 109.511 | 99.7 |
| **8** | 109.580 | 99.8 |
| **9** | 109.513 | 99.7 |
| **10** | 109.429 | 99.6 |
| **11** | 109.431 | 99.6 |
| **12** | 109.370 | 99.6 |
| **13** | 109.281 | 99.5 |
| **14** | 109.312 | 99.5 |
| **15** | 109.431 | 99.6 |
| **16** | 109.352 | 99.5 |
| **17** | 108.946 | 99.2 |
| **18** | 109.272 | 99.5 |
| **19** | 108.962 | 99.2 |
| **20** | 109.183 | 99.4 |
| **21** | 108.805 | 99.1 |
| **22** | 109.071 | 99.3 |
| **23** | 108.719 | 99.0 |
| **24** | 109.071 | 99.3 |
| **Mean** | 109.4 | 99.5 |
| **SD** | 0.29 | 0.27 |
| **%RSD** | 0.27 | 0.27 |

Sample stability results (% RSD) for pitavastatin degradation value was 0.27%, qualifying as stable, as it was under 2% (Paithankar, 2013:238).

**Table A.33:** Sample stability parameters for pravastatin

| Time (h) | Peak area | %Remaining |
|---|---|---|
| **0** | 94.227 | 100.0 |
| **1** | 93.804 | 96.7 |
| **2** | 94.018 | 99.8 |
| **3** | 92.403 | 98.1 |
| **4** | 93.990 | 99.7 |
| **5** | 93.852 | 99.6 |
| **6** | 93.772 | 99.5 |
| **7** | 93.900 | 99.7 |
| **8** | 93.853 | 99.6 |
| **9** | 93.789 | 99.5 |
| **10** | 93.717 | 99.5 |
| **11** | 93.510 | 99.2 |
| **12** | 93.583 | 99.3 |
| **13** | 93.508 | 99.2 |
| **14** | 93.443 | 99.2 |
| **15** | 93.523 | 99.3 |
| **16** | 93.258 | 99.0 |
| **17** | 93.343 | 99.1 |
| **18** | 93.229 | 98.9 |
| **19** | 93.176 | 98.9 |
| **20** | 93,309 | 99.0 |
| **21** | 93.177 | 98.9 |
| **22** | 93.125 | 98.8 |
| **23** | 93.551 | 99.3 |
| **24** | 93.590 | 99.3 |
| **Mean** | 93.5 | 99.2 |
| **SD** | 0.37 | 0.64 |
| **%RSD** | 0.40 | 0.65 |

Sample stability results (% RSD) for pravastatin degradation value was 0.65%, which qualified as stable since it was beneath 2% (Paithankar, 2013:238).

### A.3.5 System repeatability

Repeatability, in terms of accuracy and precision, was prepared similar to the method used to determine system stability. Each sample was injected six consecutive times into the HPLC to determine retention times and peak areas of samples under the same conditions in one day.

To succeed in the criteria, the %RSD should be less than 2% for the peak area, as well as the retention times (Paithankar, 2013:235).

**Table A.34:** System repeatability of atorvastatin

| Injection | Peak area | Retention time (min) |
|---|---|---|
| **1** | 74.08 | 8.23 |
| **2** | 74.10 | 8.22 |
| **3** | 72.81 | 8.22 |
| **4** | 73.35 | 8.22 |
| **5** | 72.88 | 8.22 |
| **6** | 72.78 | 8.22 |
| **Mean** | 73.33 | 8.22 |
| **SD** | 0.57 | 0.00 |
| **%RSD** | 0.78 | 0.05 |

System repeatability of atorvastatin was determined as 0.78% and 0.05% for peak area and retention time respectively, and therefore succeeded in the criteria since the %RSD was less than 2% for the peak area, as well as the retention times (Paithankar, 2013:235).

**Table A.35:** System repeatability of fluvastatin

| Injection | Peak area | Retention time (min) |
|---|---|---|
| **1** | 101.85 | 8.61 |
| **2** | 101.70 | 8.61 |
| **3** | 101.67 | 8.61 |
| **4** | 101.80 | 8.60 |
| **5** | 101.71 | 8.61 |
| **6** | 102.42 | 8.60 |
| **Mean** | 101.86 | 8.61 |
| **SD** | 0.26 | 0.00 |
| **%RSD** | 0.25 | 0.03 |

System repeatability of fluvastatin was determined as 0.25% and 0.03% for peak area and retention time respectively, and therefore succeeded in the criteria since the %RSD should be less than 2% for the peak area, as well as the retention times (Paithankar, 2013:235).

**Table A.36:** System repeatability of pitavastatin

| Injection | Peak area | Retention time (min) |
|---|---|---|
| **1** | 102.01 | 4.48 |
| **2** | 101.81 | 4.47 |
| **3** | 101.83 | 4.47 |
| **4** | 101.36 | 4.47 |
| **5** | 101.79 | 4.47 |
| **6** | 101.59 | 4.47 |
| **Mean** | 101.73 | 4.47 |
| **SD** | 0.21 | 0.00 |
| **%RSD** | 0.20 | 0.06 |

System repeatability of pitavastatin was determined as 0.20% and 0.06% for peak area and retention time respectively, which was beneath 2% for the peak area, as well as the retention times and succeeded in the criteria since the %RSD is less than 2% (Paithankar, 2013:235).

**Table A.37:** System repeatability of pravastatin

| Injection | Peak area | Retention time (min) |
|---|---|---|
| **1** | 82.847 | 5.263 |
| **2** | 81.878 | 5.260 |
| **3** | 82.047 | 5.257 |
| **4** | 82.331 | 5.263 |
| **5** | 82.059 | 5.257 |
| **6** | 82.137 | 5.263 |
| **Mean** | 82.22 | 5.26 |
| **SD** | 0.31 | 0.00 |
| **%RSD** | 0.38 | 0.06 |

System repeatability of pravastatin was determined as 0.38% and 0.057% for peak area and retention time respectively, and therefore succeeded in the criteria since the %RSD should be less than 2% for the peak area, as well as the retention times (Paithankar, 2013:235).

### A.3.6 Specificity

To determine specificity, tests are performed to accurately establish the reaction of the tested compound's peak in the presence of impurities (other components) (Huber, 2007:15) using the specific analytical method (ICH, 2005:4). Specificity is required to consider the analytical method as acceptable, and when no peak hindrances appear with retention times of the API, the method is regarded as specific (Snyders *et al.,* 1997b:696-700).

Specificity was determined through preparation of five samples each containing approximately 20 mg of each statin and added up to volume (100 ml) with methanol. A small quantity was transferred to an HPLC vial to be injected and analysed by the HPLC as a standard (b). Additional vials were prepared containing only methanol, which served as the placebo (a) for each statin.

A volume of 1 ml of each statin standard solution was transferred to four separate test tubes, which were spiked with a volume of 200 µl of c) hydrochloric acid (HCl) d) Milli-Q® water, e) sodium hydroxide (NaOH) and f) hydrogen peroxide ($H_2O_2$); each statin should be spiked separately with each aforementioned compound. A small quantity was transferred to an HPLC vial to be injected and analysed by the HPLC.

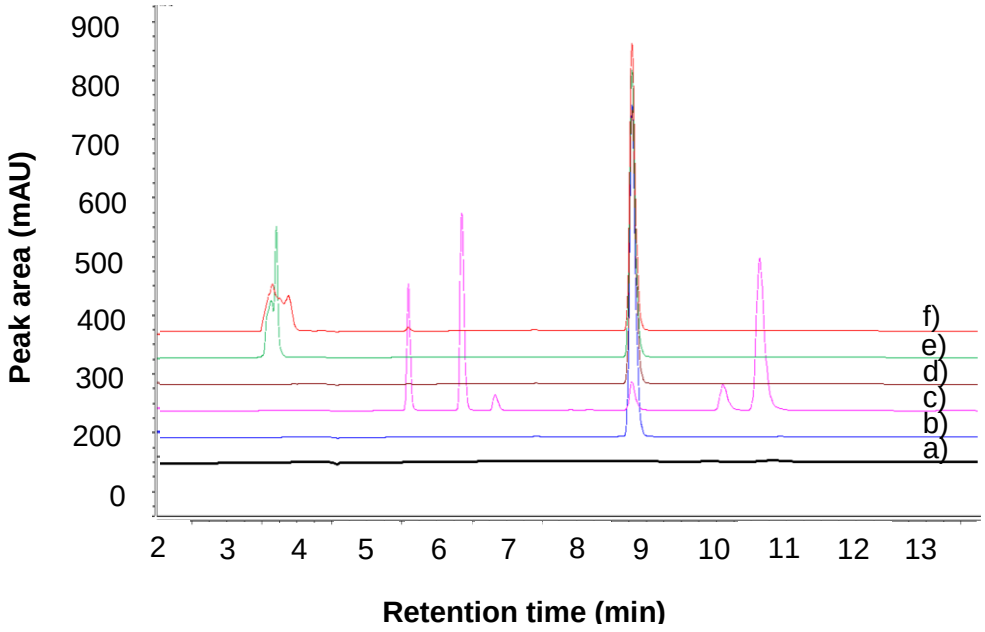


**Figure A.11:** HPLC chromatogram indicating specificity data of atorvastatin: a) placebo, b) standard, c) HCl, d) Milli-Q® water, e) NaOH and f) $H_2O_2$

Figure A.11 indicated that no peak hindrances appeared with the retention times of atorvastatin when c) HCl, d) Milli-Q® water, e) NaOH and f) $H_2O_2$ were added to the samples in comparison with the standard; however, c) HCl degraded atorvastatin as the peak was significantly smaller compared to the standard (b) and peaks of degradation products were visible, but did not interfere with the atorvastatin peak.

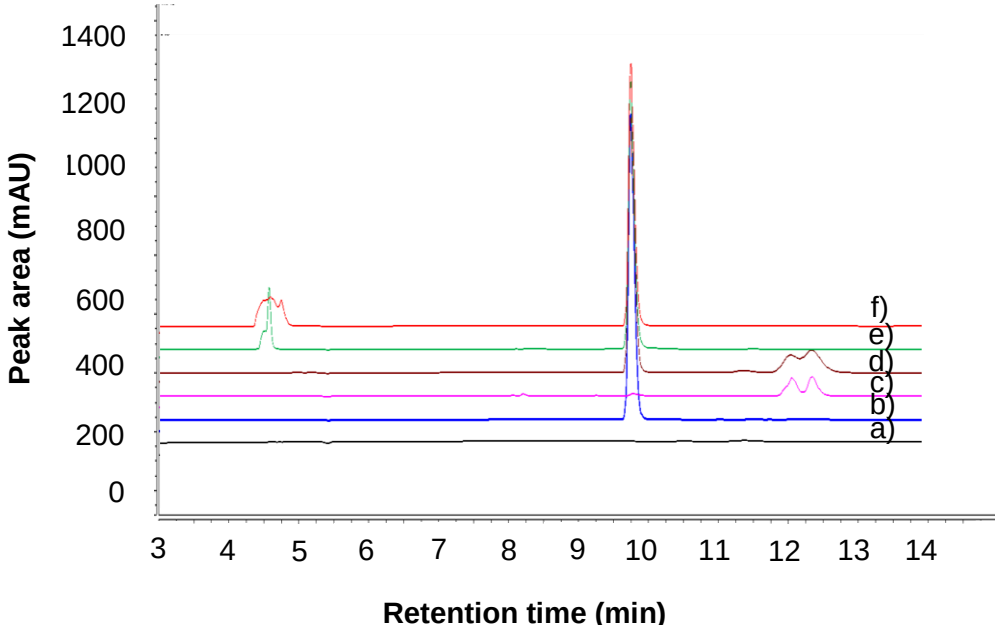


**Figure A.12:** HPLC chromatogram indicating specificity data of fluvastatin: a) placebo, b) standard, c) HCl, d) Milli-Q® water, e) NaOH and f) $H_2O_2$

Figure A.12 indicated there were no peak interferences with the retention times of fluvastatin when c) HCl, d) Milli-Q® water, e) NaOH and f) $H_2O_2$ were included in the samples; however, the HCI in c) affected fluvastatin, as the peak was minute compared to the standard (b) and degradation products' peaks presented. However peaks of degradation products had no interference with fluvastatin's peak.

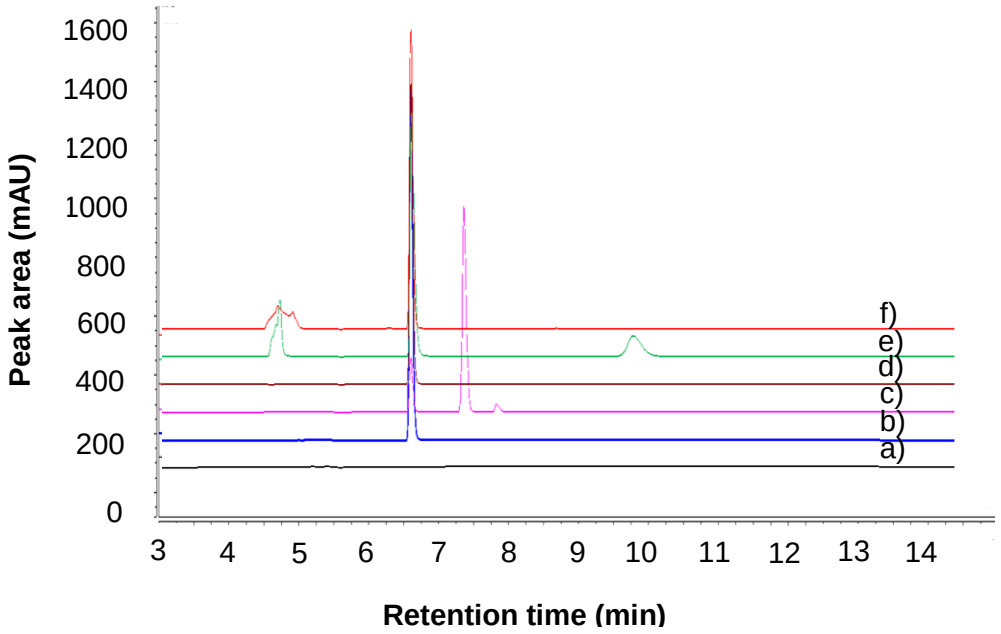


**Figure A.13:** HPLC chromatogram indicating specificity data of pitavastatin: a) placebo, b) standard, c) HCl, d) Milli-Q® water, e) NaOH and f) $H_2O_2$

Figure A.13 indicated there were no peak variations with the retention times of pitavastatin when c) HCl, d) Milli-Q® water, e) NaOH and f) $H_2O_2$ were included in the samples; in spite of this, when compared to the standard (b), HCl affected pitavastatin as the peak was small and degradation products' peaks appeared, hence degradation products' peaks indicated no peak interference regarding pitavastatin.

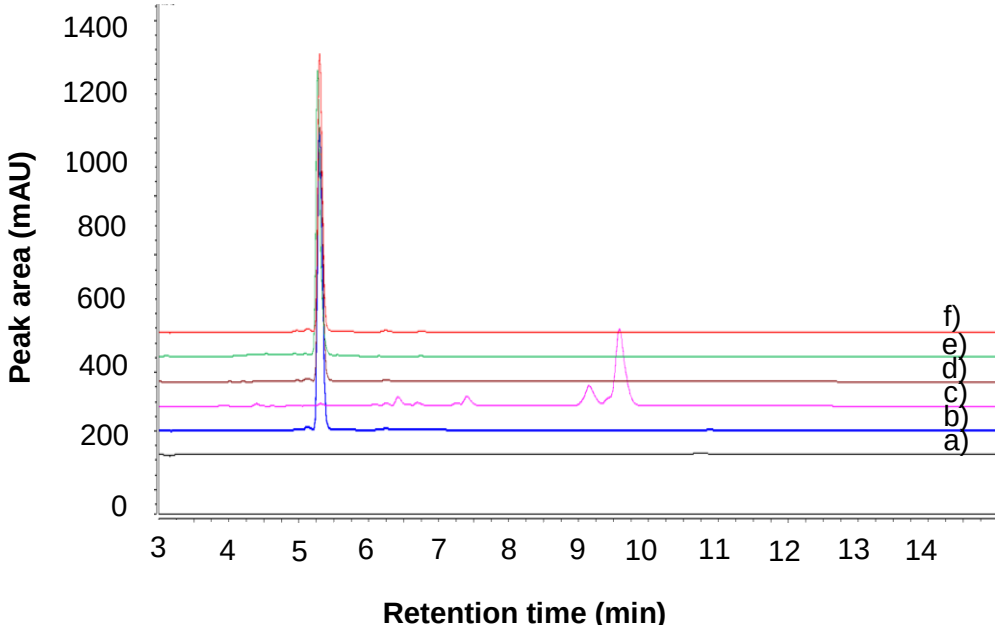


**Figure A.14:** HPLC chromatogram indicating specificity data of pravastatin: a) placebo, b) standard, c) HCl, d) Milli-Q® water, e) NaOH and f) $H_2O_2$

Figure A.14 indicated there was no occurrence of peak variations with the retention times of pravastatin when c) HCl, d) Milli-Q® water, e) NaOH and f) $H_2O_2$ were included in the samples, although when compared to the standard (b), HCl affected pravastatin as the peak was minute and there were peaks of degradation products. Detected degradation products did not interfere with pravastatin's peak.

### A.3.7 Limit of detection

Limit of detection of an analytical method represents the sensitivity and is described as the lowest detectable analyte in a sample, this is not necessarily a definite value (APVMA, 2004:4, Snyder *et al*., 1997b:659). The LOD is calculated through analysing samples with noted analyte concentrations and through determination of lowest level (lowest calibration standard) of analyte, which can be accurately detected under specific analytical conditions (APVMA, 2004:4, Snyder *et al*., 1997b:659). The peak response of the lowest calibration standard, which corresponds with the analyte, is normally measured six to ten times (APVMA, 2004:4). A maximum LOD %RSD of 15.00% is regarded as acceptable (FDA, 2001:10; Rathmann *et al.,* 2015:54).

### A.3.8 Limit of quantitation

Limit of quantitation is described as the lowest detectable amount of analyte present in a sample under specific conditions, a value that can be accurately determined (APVMA, 2004:4). LOQ, used as a guideline for analytical procedures, is utilised specifically for detecting impurities, products of degradation and active constituents especially in low quantities (APVMA, 2004:4). The stock solution sample (estimate LOQ value) should be injected six to 10 times (APVMA, 2004:4). A maximum LOQ %RSD of 20.00% is the preferred parameters (FDA, 2001:10; Rathmann *et al.,* 2015:53).

To establish the LOD and LOQ values, each statin was weighed (± 5 mg) individually. These statins were then dissolved in different 100 ml volumetric flasks with methanol and made up to volume. A volume of 1 ml of each solution was extracted and further diluted to 100 ml with methanol. HPLC vials were filled with 1 ml of diluted solution for each statin. Each vial was injected six times at four different injection volumes (2.5, 5.0, 7.5, and 10.0) respectively.

**Table A.38:** LOD and LOQ results of atorvastatin

| **Injection volume** | | **2.5** | **5.0** | **7.5** | **10.0** |
|---|---|---|---|---|---|
| **Concentration (µg/ml)** | | 0.1225 | 0.245 | 0.3675 | 0.49 |
| **Area** | **1** | 0.058 | 0.121 | 0.184 | 0.250 |
| | **2** | 0.057 | 0.121 | 0.186 | 0.246 |
| | **3** | 0.057 | 0.122 | 0.188 | 0.249 |
| | **4** | 0.058 | 0.120 | 0.179 | 0.248 |
| | **5** | 0.057 | 0.121 | 0.185 | 0.248 |
| | **6** | 0.058 | 0.121 | 0.183 | 0.249 |
| **Area mean** | | 0.06 | 0.12 | 0.18 | 0.25 |
| **SD** | | 0.00 | 0.00 | 0.00 | 0.00 |
| **%RSD** | | 0.80 | 0.44 | 1.52 | 0.44 |

**Table A.39:** LOD and LOQ results of fluvastatin

| Injection volume | | 2.5 | 5.0 | 7.5 | 10.0 |
|---|---|---|---|---|---|
| Concentration (µg/ml) | | 0.12525 | 0.2505 | 0.37575 | 0.501 |
| Area | 1 | 0.082 | 0.169 | 0.247 | 0.337 |
| | 2 | 0.083 | 0.168 | 0.249 | 0.331 |
| | 3 | 0.082 | 0.168 | 0.250 | 0.325 |
| | 4 | 0.083 | 0.158 | 0.246 | 0.326 |
| | 5 | 0.080 | 0.178 | 0.250 | 0.326 |
| | 6 | 0.084 | 0.167 | 0.246 | 0.329 |
| Area mean | | 0.08 | 0.17 | 0.25 | 0.33 |
| SD | | 0.00 | 0.01 | 0.00 | 0.00 |
| %RSD | | 1.66 | 3.51 | 0.72 | 1.24 |

**Table A.40:** LOD and LOQ results of pitavastatin

| Injection volume | | 2.5 | 5.0 | 7.5 | 10.0 |
|---|---|---|---|---|---|
| Concentration (µg/ml) | | 0.124 | 0.248 | 0.372 | 0.496 |
| Area | 1 | 0.079 | 0.159 | 0.238 | 0.320 |
| | 2 | 0.079 | 0.159 | 0.237 | 0.321 |
| | 3 | 0.079 | 0.159 | 0.238 | 0.321 |
| | 4 | 0.078 | 0.158 | 0.237 | 0.320 |
| | 5 | 0.079 | 0.157 | 0.239 | 0.321 |
| | 6 | 0.078 | 0.159 | 0.239 | 0.321 |
| Area mean | | 0.08 | 0.16 | 0.24 | 0.32 |
| SD | | 0.00 | 0.00 | 0.00 | 0.00 |
| %RSD | | 0.46 | 0.42 | 0.23 | 0.15 |

**Table A.41:** LOD and LOQ results of pravastatin

| Injection volume | | 2.5 | 5.0 | 7.5 | 10.0 |
|---|---|---|---|---|---|
| Concentration (µg/ml) | | 0.134 | 0.268 | 0.402 | 0.536 |
| Area | 1 | 0.068 | 0.140 | 0.210 | 0.281 |
| | 2 | 0.067 | 0.140 | 0.210 | 0.281 |
| | 3 | 0.066 | 0.140 | 0.210 | 0.280 |
| | 4 | 0.070 | 0.139 | 0.211 | 0.278 |
| | 5 | 0.070 | 0.140 | 0.209 | 0.280 |
| | 6 | 0.069 | 0.139 | 0.207 | 0.281 |
| Area mean | | 0.07 | 0.14 | 0.21 | 0.28 |
| SD | | 0.00 | 0.00 | 0.00 | 0.00 |
| %RSD | | 2.11 | 0.49 | 0.62 | 0.35 |

The LOD and LOQ of the statins were established through the calculation of regression through data analysis to determine the standard error of the y-intercept and the gradient of the slope. Equation A.2 was used to calculate the LOD (Swartz & Krull, 2012:70), while Equation A.3 calculated the LOQ (Swartz & Krull, 2012:71).

$DL = 3.3 \times \sigma/S$ **Equation A.2**

$QL = 10 \times \sigma/S$ **Equation A.3**

Where $\sigma$ indicates the standard variation of the y-intercept and $S$ indicates the gradient of the slope.

**Table A.42:** The LOD and LOQ results of the different statins

| Statin | LOD (µg/ml) | LOQ (µg/ml) |
|---|---|---|
| **Atorvastatin** | 0.116 | 0.035 |
| **Fluvastatin** | 0.006 | 0.019 |
| **Pitavastatin** | 0.005 | 0.015 |
| **Pravastatin** | 0.004 | 0.013 |

The LOD and LOQ results of statins were within accepted parameters, since the %RSD values for both LOD and LOQ were less than 15.00% and 20.00%, respectively.

### A.3.8 Conclusion

The HPLC method for statins (atorvastatin, fluvastatin, pitavastatin and pravastatin) was completed and validated; this method proved to be precise, constant and reliable. The results of this validated method offered verification for reliability, credibility and accuracy, thus suitable to detect and analyse the statins in the dispersions and formulations (nano-emulsion and nano-emulgels, respectively). This HPLC method for statins was also applied for the testing of membrane and *in vitro* skin diffusion studies.

**References**


APVMA ***see*** Australian Pesticides and Veterinary Medicines Authority

Australian pesticides and veterinary medicines authority. 2004. Guidelines for the validation of analytical methods for active constituents, agricultural and veterinary chemical products. http://apvma.gov.au/sites/default/files/docs/guideline-69-analytical-methods.pdf Date of access: 14 Dec. 2017.

Cowley, A. 2012. The effect of selected natural oils on the permeation of flurbiprofen through human skin. Potchefstroom: NWU. (Dissertation - MSc).

FDA ***see*** Food and Drug Administration

Food and drug administration. 2001. Guidance for Industry: bioanalytical method validation. http://www.fda.gov/downloads/drugs/guidancecomplianceregulatoryinformation/guidances/ucm368107.pdf Date of access: 19 Dec. 2017.

Huber, L. 2007. Validation of Analytical Methods. Agilent technologies: USA. 1-76p.

ICH *see* International Conference of Harmonisation. 2005. Validation of analytical procedures: text and methodology Q2 (R1). http://www.ich.org/fileadmin/Public_Web_Site/ICH_Products/Guidelines/Quality/Q2_R1/Step4/Q2_R1__Guideline.pdf Date of access: 13 Dec. 2017.

Paithankar, H.V. 2013. HPLC method validation for pharmaceuticals. *International journal of universal pharmacy and bio sciences,* 2(4):229 – 240.

Rathmann, D., Rijntjes, E., Lietzow, J. & Köhrle, J. 2015. Quantitative analysis of thyroid hormone metabolites in cell culture samples using LC-MS/MS. *European thyroid journal*, 4:51-58.

Shabir, G.A. 2003. Validation of high-performance liquid chromatography methods for pharmaceutical analysis Understanding the differences and similarities between validation requirements of the US Food and Drug Administration, the US Pharmacopeia and the International Conference on Harmonization. *Journal of chromatography,* 987(1-2):57-66.

Snyder, L.R., Kirkland, J.J. & Glajch, J.L. 1997a. Quantitation (Including trace analysis). (*In* Snyder, L.R., Kirkland, J.J. & Glajch, J.L., *eds*. Practical HPLC method development. 2nd ed. New York: John Wiley & Sons. p. 643-684).

Snyder, L.R., Kirkland, J.J. & Glajch, J.L. 1997b. Completing the method: validation and transfer. (*In* Snyder, L.R., Kirkland, J.J. & Glajch, J.L., *eds*. Practical HPLC method development. 2nd ed. New York: John Wiley & Sons. p. 685-713).

Swartz, M.E. & Krull, I.S. 2012. Handbook of analytical validation. Boca Raton: CRC Press.

USP ***see*** United States Pharmacopeia

United States Pharmacopeia. 2009. Validation of compendial methods. https://hmc.usp.org>c1225_1susp40.pdf Date of access: 26 Feb. 2018.

USP ***see*** United States Pharmacopeia

United States Pharmacopeia. 2011. Validation of compendial procedures.http://www.drugfuture.com/pharmacopoeia/usp35/pdf/08770882%20[1225]%20validation%20of%20compendial%20procedures.pdf Date of access: 16 Dec. 2017.

# APPENDIX B

FORMULATION AND STABILITY DETERMINATION OF AN OPTIMISED O/W NANO-EMULSION CONTAINING SELECTED STATINS

## B.1 Introduction

Statins are the preferred therapy to treat hyperlipidaemia for its lowering LDL effect (Smith 2001:1583). Statins, classified as HMGCoA reductase inhibitors (Fong, 2016:663) are only available in oral preparations. However, this preferred therapy presents with gastro-intestinal side effects (Mancini *et al*., 2013:1553) and reduced systemic bioavailability. The occurrence of the last-mentioned is resultant of either major hepatic first-pass clearance (CYP450 enzymes), stomach content-drug or statin-drug interaction (Marrow *et al*., 2007:37; Naik *et al*., 2000:319). Due to the complications of oral administered statins, the transdermal delivery of statins will be investigated.

Transdermal delivery is a complicated process as the human skin's multifarious structure restricts the process of permeation of both hydrophilic and lipophilic APIs (Baibhav *et al*., 2011:66). To overcome the barrier that the skin poses, APIs need to comply with ideal physiochemical characteristics of transdermal delivery (Naik *et al.,* 2000:319). Given that statins are non-compliant to these ideal physiochemical characteristics, a carrier system must be utilised to improve skin permeation (Gabera *et al.,* 2017:75). The chosen carrier system for this study was nano-emulsions.

Nano-emulsions, also known as nano-dispersed systems, ultrafine-emulsions, mini-emulsions or submicron-emulsions (Kumar, 2014:1), are safe and effective options used in the development of cosmetic and pharmaceutical preparations (Chime *et al*., 2014:95-98). Nano-emulsions persist with high thermodynamic (Kumar, 2014:1) and physical stability (Abolmaali *et al.,* 2011:140; Lu *et al*., 2014:826; Tadros *et al.,* 2004:303), which reduces the occurrence of flocculation, sedimentation and creaming to maintain a satisfactory aesthetic form (Lu *et al.,* 2014:826; Tadros *et al*., 2004:303). The aforementioned is a result of a nano-emulsion's droplet size, which ranges between 100 and 500 nm (Nalini *et al.,* 2017:1453) and has a limited size distribution (Kumar, 2014:1). To obtain nano-scale size droplets, emulsification methods are required during the formulation process (low-or high energy) (Abolmaali *et al.,* 2011:141; Tadros *et al.,* 2004:307). Hence, a high energy emulsification method was followed.

High energy emulsification methods include microfluidisation, jet dispersion (Kumar, 2014:4), high pressure homogenisation, sonication and high amplitude ultrasonication (Ochoa *et al*.,

2016: 80). An ultrasonicator (Model UP200St, Hielscher Ultrasonics, Teltow, DE) was utilised to emulsify nano-emulsions. This ultrasonicator involves a probe inserted into the formulation to create vibrations (mechanical) in order to produce cavitation (the main principle on which ultrasonication is based on) (Kumar, 2014:4). These vibrations reduce the particles/droplet size within the formulation to produce a nano-emulsion (Kumar, 2014:4).

Nano-emulsions are isotropic systems that entail two immiscible liquid phases (oil phase and the water phase) combined to produce one phase (Kumar, 2014:1). There are three types of nano-emulsions, namely oil in water (o/w – oil droplets are dispersed in the water phase), water in oil (w/o – water are dispersed in the oil phase) and bicontinuous nano-emulsions (water, as well as oil droplets are dispersed and surrounded by a continuous system) (Kumar, 2014:2). In this study, o/w nano-emulsions were formulated.

### B.1.1 The oil phase

The oil phase of the nano-emulsion alters the challenges of the skin barrier, more specifically the stratum corneum (Baibhav *et al*., 2011:68) to enhance permeation and absorption of the APIs (Alexander *et al*., 2012:29).

A wide variety of natural oils are commonly utilised in topical pharmaceutical preparations (Cizinauskas *et al*., 2017:1), apricot kernel oil (natural oil) was used as the main constituent in the oil phase. Apricot kernel oil, which is safe to use in pharmaceutical, cosmetic and food products (Kaya *et al*., 2008:2597), contains fatty acids such as oleic (58 – 68%) and linoleic acid (22 – 31%) of which both are unsaturated 18-carbon fatty acids, similar to those found in the human skin (Cizinauskas *et al*., 2017:1). Due to the shared fatty acids found in both apricot kernel oil and human skin, apricot kernel oil may serve as a non-irritable penetration enhancer (Baibhav *et al*., 2011:68).

Important considerations when attempting to achieve an optimised o/w nano-emulsion, are the selection of an appropriate oil phase to obtain maximum API solubility (see Section B.2) (Kaur *et al*., 2017:2) and the degree to which the oil assists the process of emulsification (Debnath *et al*., 2011:74; Reddy *et al*., 2013:87; Setya *et al.,* 2014:2218).

### B.1.2 Water phase

In this study, o/w nano-emulsions were formulated, where the water phase was to be the majority phase. In an o/w nano-emulsion, the water phase can include water or various alcohols (Hyma *et al*., 2014:4) and executes a vital role as a solvent (Silva *et al.,* 2012:857). The solvent used as the water phase in the formulations during this study was Milli-Q® water.

### B.1.3 Surfactants

Surfactants that serve as an interfacial film between these two phases (Kumar, 2014:1) possess various chemical properties, therefore surfactants with appropriate hydrophilic-lipophilic balance (HLB) value are essential (Kaur *et al*., 2017:2). The appropriate HLB value is between 8 and 19 (Eid *et al*., 2014:4; Setya *et al.,* 2014:2218). A high diversity of surfactants prevails, however, for purpose of this study, Span® 60 (sorbitan monostearate) and Tween® 80 (polysorbate 80) were utilised.

Span® 60 possesses an HLB value of 4.7 (> 10), which has be added to the oil phase since it classifies as an oil soluble surfactant (Reddy *et al.,* 2013:87; Zhang, 2009b:6780). Span® 60 is non-ionic and operates as a wetting agent, as well as a dispersion enhancer as it eases the process of emulsification (Zhang, 2009b:675), in turn increasing formulation stability (Baibhav *et al*., 2011:68; Zhao *et al*., 2013:1834). Span® 60 is also known to alter physical characteristics of formulations through reduced interfacial surface tension, droplet size distribution and enhanced viscosity (Zhao *et al.*, 2013:1837).

Tween® 80, a non-ionic surfactant widely exploited in the food and cosmetic industry for its non-toxic advantages, is derived from oleic acid and polyethoxylated sorbitan and possesses an HLB value of 15 (> 10) (Zhang, 2009a:550-551), which classifies it as a water-soluble surfactant (Koocheki *et al*., 2011:1149; Reddy *et al*., 2013:87). Water-soluble surfactants enhance the stability of the formulations and reduce the energy level requested to produce a nano-emulsion (Chime *et al.*, 2014:91). Tween® 80 presents as a thick, yellowish fluid to serve as an emulsifier, as it provides a smooth texture and increase endurance to melting. Tween® 80 also reduces interfacial tension and increases the speed of surfactant absorption by emulsion droplets, therefore lowering droplet sizes and enhancing the viscosity (Koocheki *et al*., 2011:1153).

These surfactants not only have solubilising, wetting, emulsification and permeability properties, but also serve as P-glycoprotein inhibitors, which aid the absorption of APIs (Kumarn *et al.,* 2011:209). Although surfactants have many advantages, the solubility of the API in oil still plays a crucial role in the formulation (Debnath *et al.,* 2011:74; Reddy *et al.,* 2013:87; Setya *et al.,* 2014:2218). Therefore, the oil and water solubility of statins in apricot kernel oil had to be determined prior to the formulation process.

## B.2 Method to determine the solubility of API in apricot kernel oil

### B.2.1 Preparation of samples

A volume of 5 ml apricot kernel oil was placed into 13 separate test tubes, three test tubes for each statin (atorvastatin, fluvastatin, pitavastatin and pravastatin) and the remaining test tube only contained apricot kernel oil. Test tubes were marked clearly to avoid confusion. Each oil-containing test tube was oversaturated with the indicated statin, as marked on the test tube, and then placed into an Elma Transsonic EL540 ultrasonic bath to be dissolved, before putting all 13 test tubes into a water bath for 24 h at 32 °C.

After 24 h, test tubes were removed and centrifuged for 15 min at 45 000 rpm. A volume of 1 ml the content of each test tube was transferred to separate volumetric flasks, weighed and noted. Volumetric flasks were then filled up to volume (25 ml) with tetrahydrofuran (THF) and mixed well until thoroughly dissolved. A volume of 1 ml THF solution was withdrawn from each statin flask, and injected into separate marked HPLC vials and analysed by HPLC.

### B.2.2 Standard

Separate standard solutions were prepared; each contained a single statin (roughly 5 mg) dissolved in THF (25 ml). A volume of 1 ml of each standard solution was transferred to four separate marked HPLC vials and analysed by HPLC.

### B.2.3 Placebo

A volume of 1 ml of the remaining test tube containing only apricot kernel oil was weighed and diluted to a volume of 25 ml utilising THF. A volume of 1 ml of the placebo was placed into a marked HPLC vial and analysed by HPLC.

After data analysis, calculated results stated that atorvastatin produced an apricot kernel oil solubility of 0.146 mg/ml, fluvastatin 0.082 mg/ml, pitavastatin 0.388 mg/ml and pravastatin 0.541 mg/ml. Since the tested formulas contained 4 – 6 ml apricot kernel oil, the chosen weight was determined as 2 g of each statin in its formulation.

## B.3 Goal of formulation

The objective was to establish a main formula, in which all four statins presented stability and complied with the required physical property parameters, which in turn enhanced credibility, reduced variables and created an opportunity for comparability.

Prior to the formulation process, relatable studies and literature regarding nano-emulsion formulation, surfactant ratios, nano-emulgels, etc. were investigated. The next step was to start the formulation process to try to formulate an optimised nano-emulsion.

**Table B.1:** Ingredients, suppliers and batch numbers of constituents used to formulate the nano-emulsions

| Constituent | Supplier | Batch number |
|---|---|---|
| Atorvastatin | DB Fine | 20170518 |
| Fluvastatin | DB Fine | 1701108447 |
| Pitavastatin | DB Fine | AFM-170502 |
| Pravastatin | DB Fine | 0651001 |
| Span® 60 | Sigma & Aldrich | 5361721034 |
| Tween® 80 | Sigma & Aldrich | BCBV7863 |
| Apricot kernel oil | 1512E036197 | CJP Chemicals |

### B.4 Formula and formulation method used to prepare the nano-emulsions

During this step, different surfactant ratios were tested in the formulations to detect which were the most stable and sufficient concerning dissolution. The following ratios were investigated: nano-emulsion containing Tween® 80:Span® 60 (3:3), which was named **NE1** and a nano-emulsion containing Tween® 80:Span® 60 (2:3), which was named **NE2**. These nano-emulsions were then formulated with statins, followed by characterisation and allocation of the codes, as in Table B.2.

**Table B.2:** Statin formula codes

| Statin | Formula | Code |
|---|---|---|
| Atorvastatin | **NE1** | **NE1A** |
| | **NE2** | **NE2A** |
| Fluvastatin | **NE1** | **NE1F** |
| | **NE2** | **NE2F** |
| Pitavastatin | **NE1** | **NE1Pi** |
| | **NE2** | **NE2Pi** |
| Pravastatin | **NE1** | **NE1Pr** |
| | **NE2** | **NE2Pr** |

Table B.2 gives the formula used to formulate **NE1** and **NE2** as well as the individualised codes.

A step-wise illustration of the process used during the manufacturing of the **NE1** and **NE2** is presented in Figure B.1; eight nano-emulsions were formulated.

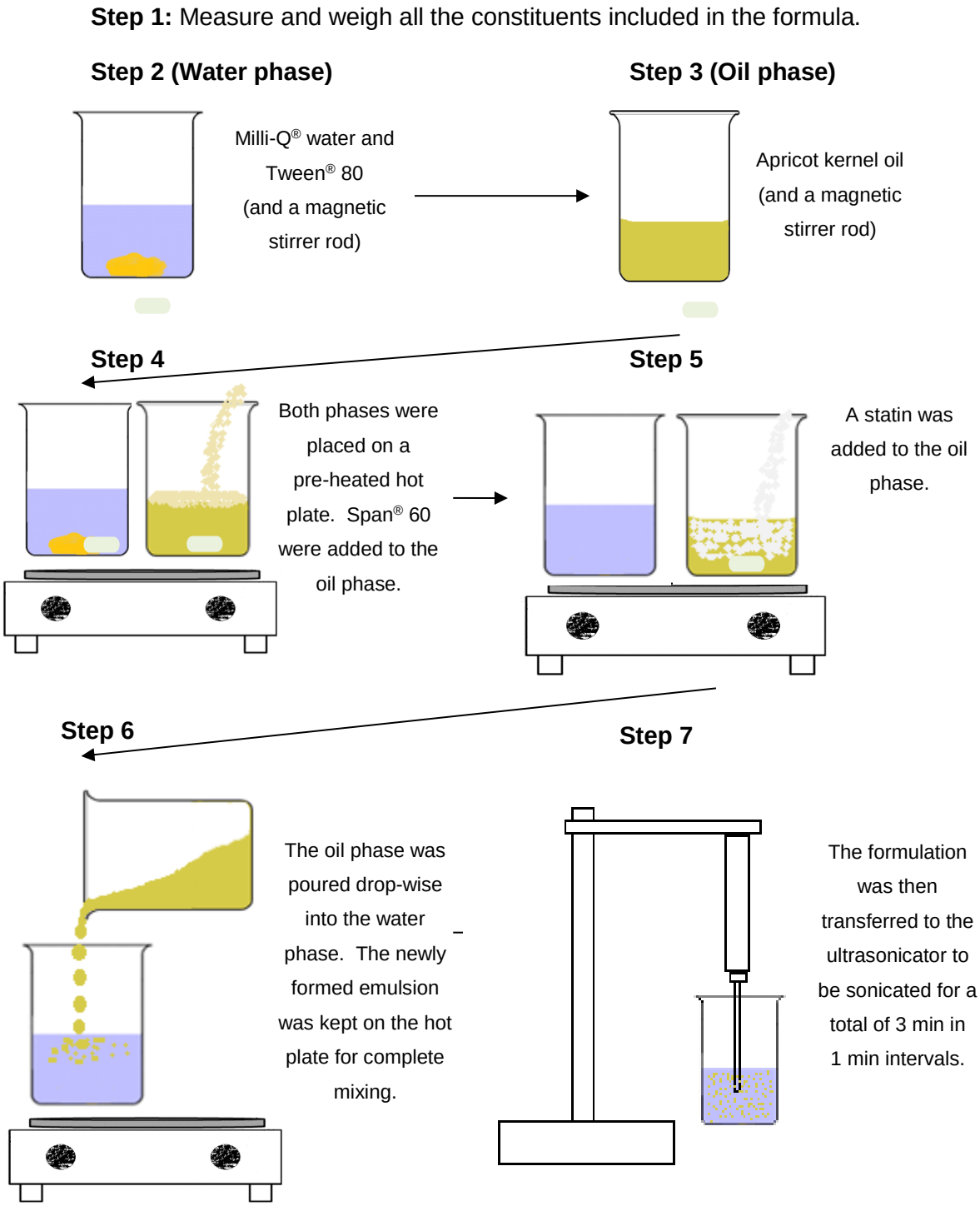


**Figure B.1:** Method followed to prepare nano-emulsions (for each individual statin)

## B.5 Methods used during the characterisation of the nano-emulsions

Various methods exist to analyse and characterise nano-emulsions (Nejadmansouria *et al.*, 2016:801), in this study the following characteristics were analysed on both the **NE1s** and **NE2s** (Kumar 2014:1; Nejadmansouria *et al.*, 2016:801-803).

- Visual inspection
- pH
- Surface potential measurement (zeta-potential)
- Droplet size and distribution
- Viscosity
- Morphological analysis (transmission electron microscopy)
- Entrapment efficiency (%EE)

### B.5.1 Visual inspection

Figure B.2 represents the dispersions of **NE1** and **NE2**, each containing a statin. There was no presence of sedimentation or flocculation in the formulations. The formulation of each statin presented as a whitish-milky appearance with the absence of visible oil droplets, thus it could be concluded that the oil droplets within in the water phase were effectively dispersed.

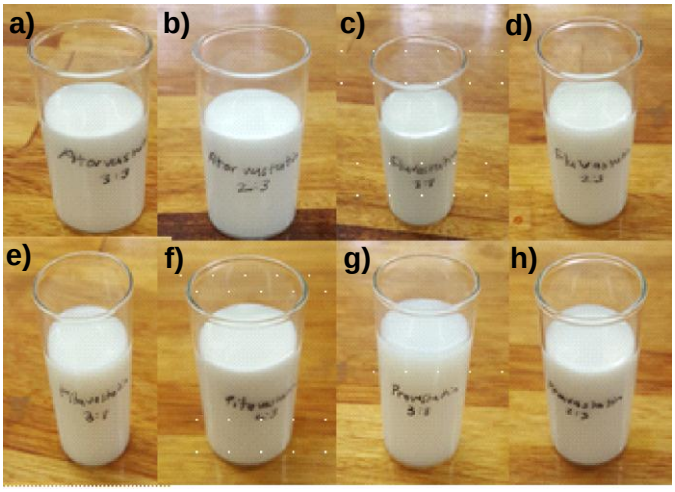


**Figure B.2:** Nano-emulsions (**NE1** and **NE2**) containing different statins individually: a) **NE1A**, b) **NE2A**, c) **NE1F**, d) **NE2F**, e) **NE1Pi**, f) **NE2Pi**, g) **NE1Pr** and h) **NE2Pr**

### B.5.2 pH

The pH measurement indicates a value determined by the quantity of hydrogen ions [H+] and hydroxide ions [$OH^-$] in the formulation and can be classified as acidic or basic accordingly (Hach Company, 2010:6). The reason for pH determination is to establish if the formulation will cause irritation when applied to human skin, which normally has a pH value of ± 5 (Ng & Lau, 2015:8; Williams, 2013:678). According to Barry (2002:512), the human skin can endure components with pH values of 3 – 9, which will serve as a guideline in this study.

The pH of the nano-emulsions was measured with a Mettler Toledo® pH meter (Mettler Toledo, CU), by inserting the Mettler Toledo® InLab® 410 electrode (Mettler Toledo, CU) into the nano-emulsion to provide the pH value.

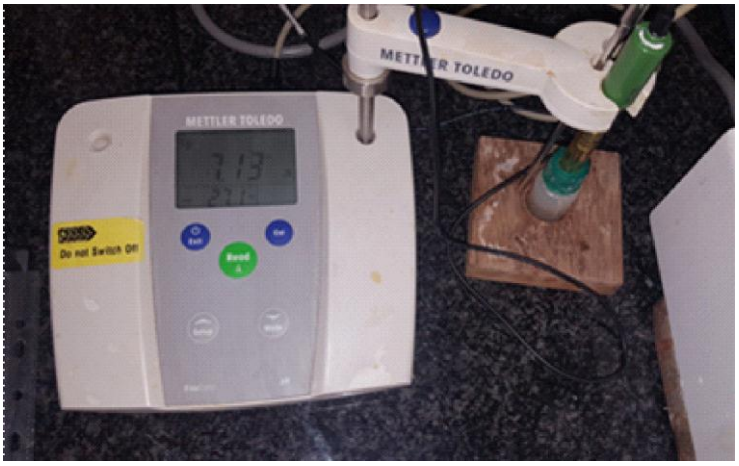


**Figure B.3:** Mettler Toledo® pH meter (Mettler Toledo, CU) utilised to measure the pH levels of the **NE1s** and **NE2s**

**Table B.3:** The measured pH values for the nano-emulsions (**NE1** and **NE2**) containing statins

| Formula | pH | | | |
|---|---|---|---|---|
| | 1 | 2 | 3 | Average |
| **NE1A** | 6.57 | 6.59 | 6.56 | 6.57 ± 0.012 |
| **NE2A** | 6.77 | 6.78 | 6.77 | 6.77 ± 0.005 |
| **NE1F** | 7.82 | 7.80 | 7.81 | 7.81 ± 0.008 |
| **NE2F** | 7.42 | 7.41 | 7.43 | 7.42 ± 0.008 |
| **NE1Pi** | 6.55 | 6.54 | 6.53 | 6.54 ± 0.008 |
| **NE2Pi** | 6.62 | 6.64 | 6.63 | 6.63 ± 0.008 |
| **NE1Pr** | 7.21 | 7.22 | 7.21 | 7.21 ± 0.004 |
| **NE2Pr** | 7.15 | 7.14 | 7.16 | 7.15 ± 0.008 |

Table B.4 indicates that the average pH for all the tested **NEs** varied between the values of 6 – 8. Since the human skin tolerates substances with pH values of 3 – 9 (Barry, 2002:512), it can be concluded that all the formulations' pH values were within these parameters and therefore should not act as an irritant towards the skin, when applied topically.

### B.5.3 Surface potential (zeta-potential)

One of the techniques to determine the dispersion stability of a nano-emulsion is to measure the zeta-potential, which will determine if the **NE** will endure environmental conditions when used (Asmawatia *et al.*, 2014: 247). Zeta-potential measures inter (surface charged)-activities, as well as long-lasting stability between elements present in the formulation through calculation of the electrophoretic motion of the dispersed oil particles (Kumar, 2014:5), thus the more stable a formulation, the higher the zeta-potential value will be, meaning that the **NE** is electrostatically stable, in turn reducing any risk of flocculation (Asmawatia *et al.*, 2014: 247).

The ideal zeta-potential varies from ± 20 mV and depends on the dispersant, as well as the chemistry of the surface area of the ingredients (Kumar, 2014:5). High zeta-potential values imply powerful repulsion forces between the elements within the formulation, this indicates higher stability than a zeta-potential value closer to zero, which improves the risk of flocculation and aggregation (unstable formulation) (Ribeiro *et al.*, 2015:2499). Influences that should also be considered when measuring zeta-potential are variations in pH, the type of salt the active ingredient represent and its concentration and the concentration of other constituents present in the formulation such as surfactants, gelling agents, etc. (Asmawatia, *et al.,* 2014: 247).

**Figure B.4:** Malvern Zetasizer Nano ZS (Malvern Instruments, Worcestershire, UK) utilised to measure the zeta-potential of **NE1s** and **NE2s**

The zeta-potential of the nano-emulsions was measured with a Malvern Zetasizer Nano ZS (Malvern Instruments, Worcestershire, UK). An extracted volume of each nano-emulsion was diluted separately with Milli-Q® water (1:100) and mixed thoroughly by rotating the flask while holding it. The solutions were then transferred, each in their own clear disposable zeta cell, using a syringe. Each sample's measurement was performed in triplicate.

**Table B.4:** Zeta-potential (mV) values of the nano-emulsions (**NE1s** and **NE2s**) containing statins

| Formula | Zeta-potential (mV) | | | |
|---|---|---|---|---|
| | 1 | 2 | 3 | Average |
| **NE1A** | -44.0 | -42.9 | -44.3 | -43.7 ± 0.6 |
| **NE2A** | -33.6 | -36.2 | -36.0 | -35.2 ± 1.3 |
| **NE1F** | -54.8 | -57.0 | -56.1 | -55.7 ± 1.2 |
| **NE2F** | -47.3 | -47.1 | -46.4 | -46.9 ± 0.4 |
| **NE1Pi** | -39.9 | -40.6 | -39.8 | -40.1 ± 0.4 |
| **NE2Pi** | -40.7 | -41.0 | -43.7 | -41.8 ± 1.2 |
| **NE1Pr** | -47.3 | -47.4 | -50.2 | -48.3 ± 1.3 |
| **NE2Pr** | -45.8 | -45.3 | -46.0 | -45.7 ± 0.3 |

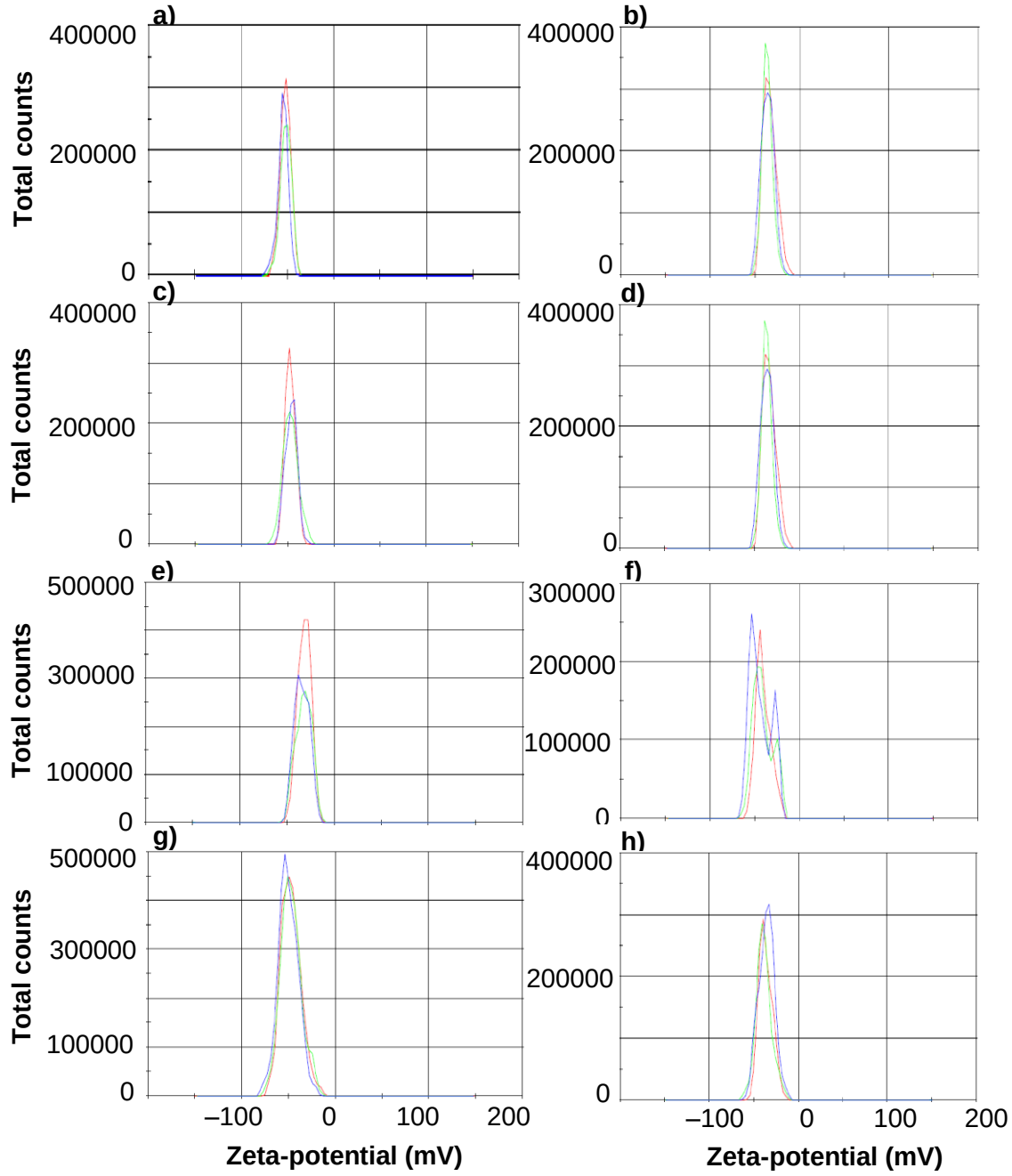


**Figure B.5:** The average zeta-potential (mV) of the nano-emulsions (**NE1s** and **NE2s**) containing statins: a) **NE1A**, b) **NE2A**, c) **NE1F**, d) **NE2F**, e) **NE1Pi**, f) **NE2Pi**, g) **NE1Pr** and h) **NE2Pr**

Table B.5 and Figure B.5 indicated the variations between the zeta-potential for **NE1** and **NE2**. The order of zeta-potential for the **NE1s** was **NE1F** > **NE1Pr** > **NE1A** > **NE1Pi** and for the **NE2s** was **NE2F** > **NE2Pr** > **NE2Pi** > **NE2A**. The zeta-potential of **NE1s** (**NE1F**, **NE1A** and **NE1Pr**) measured higher than **NE2s** (**NE2A**, **NE2F** and **NE2Pr**), indicating that **NE1s** were more stable nano-emulsions.

Since the ideal zeta-potential varies from ± 20 mV (Kumar, 2014:5), it can be concluded that the formulated **NEs** (**NE1** and **NE2**) for the involved statins' zeta-potential values were well within the required range for acceptable stability.

### B.5.4 Droplet size and distribution

One of the important physiochemical properties of a **NE** is the droplet size and distribution (Kumar, 2014:5). By measuring the droplet diameter through evaluation of the light scatterings, the size of the droplet as well as droplet distribution (polydispersity index (PdI)) can be determined (Malvern Instruments Limited, 2015:15). By determining the droplet size, stability can be evaluated (Solans *et al*., 2005:105); it should be noted that smaller droplet sizes improve emulsion's integral stability, as they lower the occurrence of sedimentation, creaming, flocculation and coagulation (Kumar, 2014:5; Solans *et al*., 2005:105). The required parameters for droplet sizes and PdI values of **NEs** are < 500 nm (Nalini *et al.,* 2017:1453) and < 0.5, respectively (Elmataeeshy *et al.,* 2018:24).

A Malvern Zetasizer Nano ZS (Malvern Instruments, Worcestershire, UK) was utilised in this study to determine the droplet size and distribution (see Figure B.4). This instrument operates by utilising photon correlation spectroscopy (PCS), which determines light fluctuations that occur between droplets in the **NE** as a result of Brownian motion (Gaur *et al*., 2014:40; Malvern Instruments Limited, 2015:15).

Dilutions of each **NE** were analysed separately by adding drops of the dispersion itself to a specific quantity of Milli-Q® water and mixed thoroughly by rotating the flask while holding it, identical to the method used in testing the zeta-potential. The solutions were then transferred, each in their own clear disposable zeta cell using a syringe. Each sample's measurement was performed in triplicate.

**Table B.5:** The average droplet size, as well as the PdI of **NE1** and **NE2**

| Formula | Average droplet size (nm) | Average PdI |
|---|---|---|
| **NE1A** | 137.403 ± 1.761 | 0.235 ± 0.004 |
| **NE2A** | 188.533 ± 10.995 | 0.249 ± 0.100 |
| **NE1F** | 165.400 ± 1.257 | 0.197 ± 0.008 |
| **NE2F** | 157.567 ± 2.414 | 0.254 ± 0.004 |
| **NE1Pi** | 130.733 ± 2.106 | 0.232 ± 0.013 |
| **NE2Pi** | 160.820 ± 0.432 | 0.157 ± 0.010 |
| **NE1Pr** | 114.233 ± 1.027 | 0.191 ± 0.009 |
| **NE2Pr** | 165.133 ± 1.401 | 0.200 ± 0.006 |

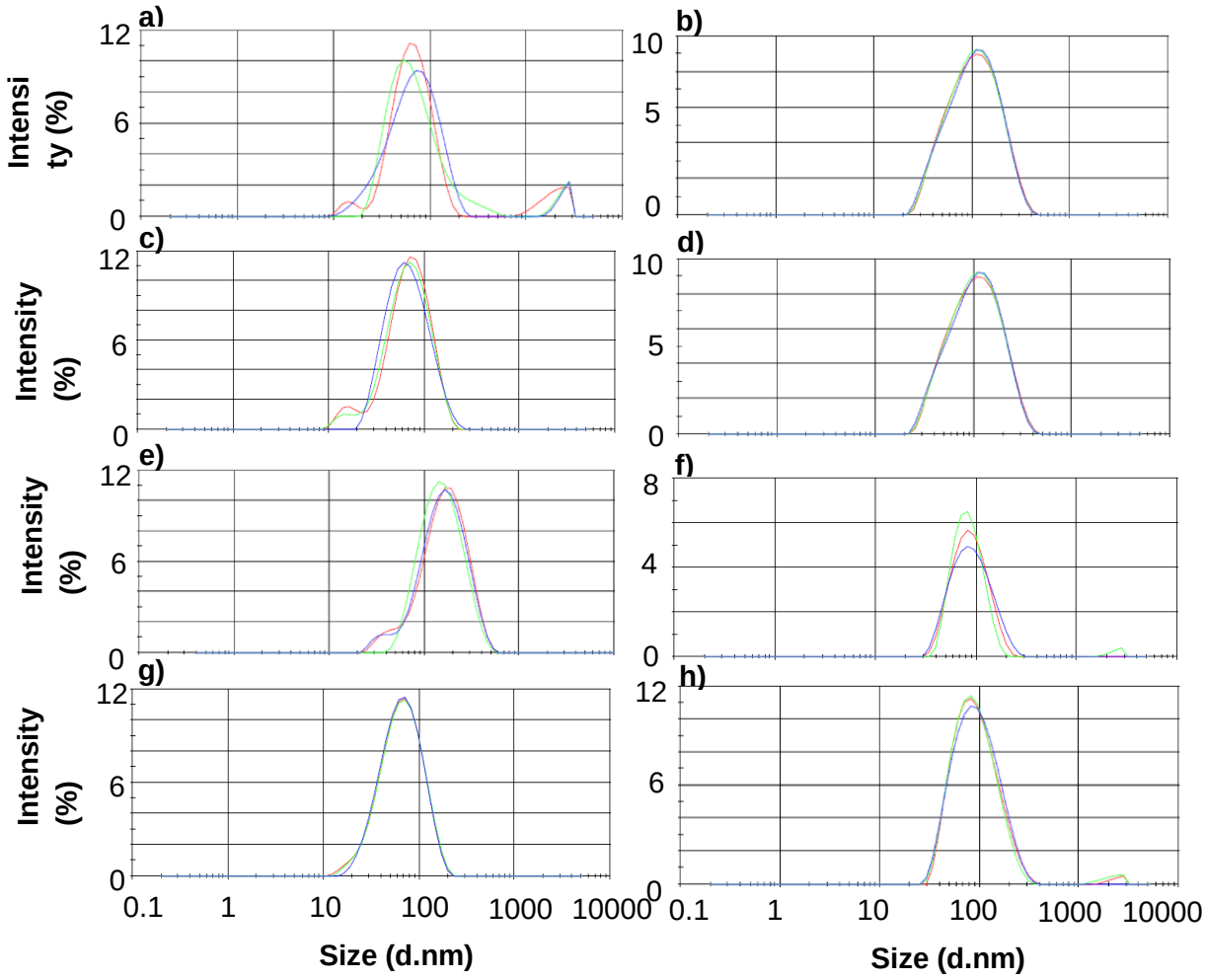


**Figure B.6:** Average droplet size (nm) of the nano-emulsions (**NE1s** and **NE2s**) containing statins: a) **NE1A**, b) **NE2A**, c) **NE1F**, d) **NE2F**, e) **NE1Pi**, f) **NE2Pi**, g) **NE1Pr** and h) **NE2Pr**

In Table B.6 and Figure B.6 the average droplet size (nm), and average PdI were measured for the **NE1s** and **NE2s** respectively. With the investigation of the average droplet size of the **NE1s**, it was discovered that **NE1F** had the average largest droplet size, followed by **NE1Pr**, **NE1Pi** and **NE1A**. **NE2s** displayed average droplet sizes in the order of **NE2A** > **NE2Pr** > **NE2Pi** > **NE2F**. When **NE1s** were compared to **NE2s**, the **NE2s** (**NE2A**, **NE2Pi** and **NE2Pr**) showed larger average droplet sizes than the **NE1s** (**NE1A**, **NE1Pi** and **NE1Pr**), with the exception of **NE1F**, which displayed larger than **NE2F**.

PdI values of the **NE1s** were compared and presented as **NE1A** > **NE1Pi** > **NE1F** > **NE1Pr**, while **NE2s** exhibited PdI values in the order of **NE2F** > **NE2A** > **NE2Pr** > **NE2Pi**. The comparison of **NE1s** to **NE2s** indicated that **NE2A**, **NE2F** and **NE2Pr** displayed larger PdI values than their respective **NE1s**, except for **NE1Pi**, which had a larger PdI value than **NE2Pi**.

All the nano-emulsions succeeded in abiding by the required parameters for droplet sizes (< 500 nm) (Nalini *et al.,* 2017:1453) and PdI (< 0.5) (Elmataeeshy *et al.,* 2018:24). Therefore, they reflect lower risks of sedimentation, creaming, flocculation and coagulation (Solans *et al*., 2005:105) (Kumar, 2014:5).

### B.5.5 Viscosity

The viscosity can be seen as a summary of the components (surfactants, oil and water) used in the formulation (Chime *et al*., 2014:97). A viscosity measurement can indicate the stability, as well as the API release of the formulation (Chime *et al*., 2014:97). In an o/w **NE**, the aqueous phase is the larger system in which the oil droplets are dispersed; therefore, low viscosity values are produced due to the water component (Chime *et al*., 2014:97). Conclusively, **NEs** are characterised as low viscosity dispersions (Shakeel *et al*., 2007:E6, Thakur *et al*., 2012:223).


**Figure B.7:** Brookfield Viscometer (DV2T LV Ultra-Middleboro, Massachusetts, USA), linked to a water bath (± 25 °C) was utilised to measure the viscosity of the **NE1** and **NE2**

To measure the viscosity of the **NE1** and **NE2**, a Brookfield Viscometer (DV2T LV Ultra-Middleboro, Massachusetts, USA) linked to a water bath (± 25 °C) was utilised. A cylindrical spindle (SC4-18) was found to be the most adequate to measure the viscosity of **NE1** and **NE2**. To reach the appropriate temperature (± 25 °C), **NE1** and **NE2** containing statins were placed into the water bath (± 25 °C) 1 h before the viscosity was measured. The spindle (SC4-18) was linked to the viscometer to hang down into the hollow of the sample adapter. A volume of the selected formula was poured into the hollow cylindrical sample compartment to which the sample compartment was then inserted (from the bottom) into the sample adapter attached to the viscometer, so that the spindle (SC4-18) could reach the formula. The spindle (SC4-18) was set to rotate at a speed of 200 rpm in order to determine the viscosity.

Viscosity was measured in centipoise (cP), at 10 second intervals for a time period of 50 seconds. Rheocalc T 1.2.19 software was used to analyse and calculate average viscosity values. This method was followed for each formula individually.

**Table B.6:** Viscosity (cP) and torque (%) readings of **NE1s** and **NE2s** (rotation speed at 200 rpm)

| **NE1A** | | | **NE2A** | |
|---|---|---|---|---|
| **Point** | **Viscosity (cP)** | **Torque (%)** | **Viscosity (cP)** | **Torque (%)** |
| 1 | 4.49 | 29.9 | 9.38 | 62.5 |
| 2 | 4.44 | 29.6 | 9.39 | 62.6 |
| 3 | 4.44 | 29.6 | 9.36 | 62.4 |
| 4 | 4.47 | 29.8 | 9.36 | 62.4 |
| 5 | 4.43 | 29.5 | 9.35 | 62.3 |
| **Averages** | **4.454 ± 0.02** | **29.68 ± 0.1** | **9.368 ± 0.01** | **62.44 ± 0.1** |
| **NE1F** | | | **NE2F** | |
| **Point** | **Viscosity (cP)** | **Torque (%)** | **Viscosity (cP)** | **Torque (%)** |
| 1 | 5.8 | 38.6 | 8.1 | 38.7 |
| 2 | 5.8 | 38.6 | 8.4 | 38.9 |
| 3 | 5.8 | 38.7 | 8.1 | 38.7 |
| 4 | 5.8 | 38.5 | 8.1 | 38.7 |
| 5 | 5.8 | 38.5 | 8.4 | 38.9 |
| **Averages** | **5.8 ± 0.01** | **38.6 ± 0.1** | **8.2 ± 0.1** | **38.8 ± 0.1** |
| **NE1Pi** | | | **NE2Pi** | |
| **Point** | **Viscosity (cP)** | **Torque (%)** | **Viscosity (cP)** | **Torque (%)** |
| 1 | 4.3 | 28.6 | 4.7 | 31.4 |
| 2 | 4.3 | 28.5 | 4.7 | 31.4 |
| 3 | 4.3 | 28.5 | 4.8 | 31.7 |
| 4 | 4.3 | 28.5 | 4.7 | 31.3 |
| 5 | 4.3 | 28.4 | 4.7 | 31.4 |
| **Averages** | **4.3 ± 0.01** | **28.5 ± 0.1** | **4.7 ± 0.02** | **31.4 ± 0.1** |
| **NE1Pr** | | | **NE2Pr** | |
| **Point** | **Viscosity (cP)** | **Torque (%)** | **Viscosity (cP)** | **Torque (%)** |
| 1 | 3.6 | 23.8 | 3.8 | 25.2 |
| 2 | 3.6 | 24.0 | 3.6 | 24.2 |
| 3 | 3.6 | 24.0 | 3.6 | 23.9 |
| 4 | 3.6 | 24.0 | 3.7 | 24.4 |
| 5 | 3.6 | 24.0 | 3.6 | 24.2 |
| **Averages** | **3.6 ± 0.01** | **23.9 ± 0.1** | **3.7 ± 0.1** | **24.4 ± 0.4** |

Water has a viscosity measure of 1 cP. Since this constant (1 cP) serves as an indication (V&P Scientific Inc., 2010), it was concluded from Table B.7 that all the formulated nano-emulsions were more viscous than water. The last-mentioned can be a result of Tween® 80, known to increase the viscosity of a formulation according to Kennedy and Kennedy (2007:E4). In addition, Span® 60 can also alter physical characteristics of formulations through reduced interfacial surface tension and enhanced viscosity (Zhao *et al.*, 2013:1837). Since the **NE2s** contained higher amounts of Span® 60, these formulas produced more viscous formulations than the **NE1** dispersions, which contained more Tween® 80.

### B.5.6 Transmission electron microscopy (TEM)

TEM has been used for over 50 years (Bogner *et al.,* 2007:391). TEM is an operative imaging method adapted to capture images at an extensively greater resolution (0.2 nm) compared to that of light microscopes (Egerton, 2005:13). TEM is frequently utilised in the morphological and structural research of nano-emulsions (Kalra, 2013:5).

TEM was performed to determine the structural form and droplet size of the **NE1s** and **NE2s** by capturing images of these prepared nano-emulsions by Dr A Jordaan at the Electron Microscopy Laboratory of the North-West University, Potchefstroom, with an Oxford INCA X-Sight EDS System utilising a FEI Tecnai G2 20S-Twin 200 kV high-resolution TEM (HRTEM) (Czech Republic, EU).

The **NEs** (**NE1** and **NE2**) prepared separately for each statin were diluted (1:100) with Milli-Q® water, of which only a small volume of this dilution was transferred, with a micropipette, to a microscopic copper grid (carbon-coated 300 mesh), and finally coloured with osmium tetroxide (Chime *et al*., 2014:96), to produce an effect of high-contrast quality to the captured images (Nomaki *et al.,* 2015:33). The osmium tetroxide has the ability (when dried for 10 – 15 min after colouring) to preserve the fatty acids present in the nano-emulsions, making it possible to capture quality images of oil droplets dispersed in the o/w **NE** (Nomaki *et al.,* 2015:33). After drying, the coloured copper grids were examined with the TEM and images were captured with a Gatan bottom mount camera and digital micrograph software.

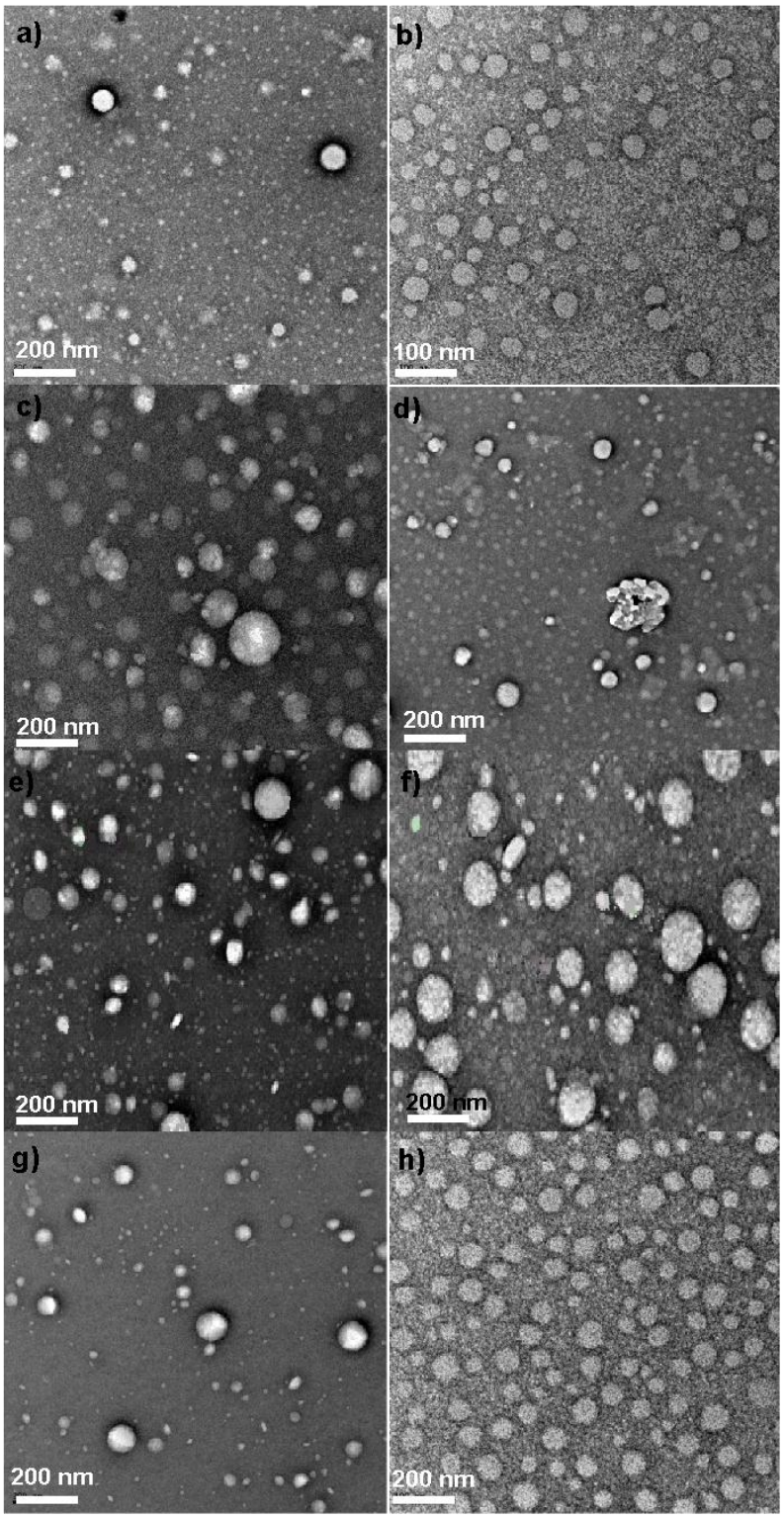


**Figure B.8:** TEM micrographs of the **NE1s** and **NE2** each containing a statin: a) **NE1A**, b) **NE2A**, c) **NE1F**, d) **NE2F**, e) **NE1Pi**, f) **NE2Pi**, g) **NE1Pr** and h) **NE2Pr**

In Figure B.8, the TEM micrographs for the **NE1s** and **NE2s** are displayed to indicate the morphology of the nano-emulsions.

The droplet sizes of **NE1A** ranged between 32.6 – 76.27 nm, compared to the droplet sizes of **NE2A,** which ranged between 12.27 – 51.19 nm, both formulations displayed spherical shaped dispersed droplets, although **NE1A** droplet distribution was wider than **NE2A**, with droplets almost touching each other, indicating poor stability and a greater possibility of coagulation. The droplet sizes of **NE1F** ranged between 23.11 – 112.48 nm in comparison with the droplet sizes of **NE2F,** which ranged between 29.38 – 90.14 nm, again both formulations displayed spherical shaped dispersed droplets, although **NE2F** displayed coagulation as indicated by the black square.

The droplet sizes of **NE1Pi** were in the range of 41.61 – 102.64 nm compared to the droplet sizes of **NE2Pi**, which ranged between 15.04 – 81.85 nm; both formulations presented with spherical shaped dispersed droplets, and were very similar to each other. The droplet sizes of **NE1Pr** ranged between 20.78 - 114.01 nm compared to the **NE2Pr**, which had droplet sizes alternating between 19.22 – 44.23 nm; both formulations displayed spherical shaped dispersed droplets, although **NE1Pr** droplet distribution was wider than **NE2Pr**, and the droplets were almost touching each other indicating poor stability and a lager risk for coagulation.

Nano-emulsions should have oil droplets (within the water phase) with a droplet size range below 500 nm (Nalini *et al.,* 2017:1453). It can be concluded that all the dispersions of **NE1** and **NE2** displayed nano-sized droplets in the required range.

### B.5.7 Entrapment efficacy

Entrapment efficiency (%EE) is defined as the ratio of entrapped drug to the ratio total drug. It is important to obtain a %EE higher than 50%, to reduce the possibility of bioactive outflow and to prevent flaws in the formulation (Divakaran, 2012:22). It has been suggested that **NE** containing lipophilic encapsulated APIs has the ability to produce a %EE of close to 100% (Loureiro *et al*., 2015:96).

To calculate the %EE, Equation B.1 (Kurakula *et al.*, 2012:37) was used, where *Ct* is the totalised quantity of API and *Cf* the quantity of unentrapped API:

$$\%EE = [(Ct - Cf)/Ct] \times 100 \qquad \textbf{Equation B.1}$$

A standard solution was prepared and injected with an HPLC (see Section A.3.1.1) to obtain a standard linearity curve for each statin.

Nano-emulsions (**NE1** and **NE2**) were formulated for each statin, then transferred to plastic test tubes and placed in an ultracentrifuge (Beckman Coulter, Optima™ L-100 XP), to rotate at 25 000 RPM for 50 min at 25 °C. The test tubes were then removed and 200 µl supernatant at was withdrawn and separately diluted in 5 ml THF. A volume of each dilution was transferred to vials and injected in an HPLC. Through data analysis and the use of Equation B.1, the %EE was determined.

**Figure B.9:** Ultracentrifuge (Beckman Coulter, Optima™ L-100 XP) utilised to rotate **NE1** and **NE2** for the extraction of supernatant

**Table B.7:** Entrapment efficacy (%EE) of the nano-emulsions (**NE1s** and **NE2s**) containing statins

| Formula | Entrapment efficacy (%EE) |
|---|---|
| **NE1A** | 98.98 |
| **NE2A** | 96.02 |
| **NE1F** | 90.77 |
| **NE2F** | 86.16 |
| **NE1Pi** | 91.82 |
| **NE2Pi** | 92.83 |
| **NE1Pr** | 90.98 |
| **NE2Pr** | 89.37 |

From Table B.8 the entrapment efficacy (%EE) of the **NE1s** was compared to the **NE2s**, where **NE1A** > **NE2A**, **NE1F** > **NE2F** and **NE1Pr** > **NE2Pr**; however, **NE1Pi** had a slightly lower entrapment efficacy than **NE2Pi**. The %EE for the **NE1s** were higher than the **NE2s**, therefore larger amounts of API can be transported to the intended area (Kurakula *et al*., 2012:37).

Statins were successful entrapped in the formulas, as the %EE was close to 100% (Loureiro *et al.,* 2015:96).

## B.6 Conclusion

Various methods were employed to analyse and characterise two nano-emulsion formulas (**NE1** and **NE2**) for each statin. The results of these methods were then compared to determine the optimised formula, which would be investigated further during this study. When visually inspected, there was no presence of sedimentation or flocculation in the formulas (**NE1** and **NE2**) for each statin. The pH values indicated that all the tested nano-emulsions varied between the parameters (3 – 9) (Barry, 2002:512) with values of 6 - 8, therefore, they should not act as an irritant towards the skin, when applied topically.

The involved statins' zeta-potential values were well within the required range for acceptable stability, although **NE1** for each statin prevailed when compared against **NE2**. Higher value zeta-potential implies higher stability (Honary & Zahir, 2013:265), therefore, **NE1** was the more stable formulation. All the formulated nano-emulsions succeeded in the required parameters for droplet sizes of < 500 nm (Nalini *et al.,* 2017:1453) and PdI values of < 0.5 (Elmataeeshy *et al.,* 2018:24), hence they reflect lower risks of sedimentation, creaming, flocculation and coagulation (Solans *et al*., 2005:105) (Kumar, 2014:5).

Considering viscosity, both Tween® 80 (Kennedy & Kennedy, 2007:E4) and Span® 60 are known to enhance viscosity (Zhao *et al.*, 2013:1837). Since **NE2** contained a higher amount of Span® 60, this formula produced more viscous formulations than the **NE1** formulas, which contained more Tween® 80, therefore, the amount of Span® 60 included in the formula had a larger effect on viscosity readings. Although the **NE2s** presented as more viscous, the **NE1s** formulas' viscosity results were in a similar range, but more favourable for comparison.

When observed under a TEM, dispersions of **NE1** and **NE2** displayed nano-sized droplets in the required range of < 500 nm. However, **NE2A** and **NE2Pr** indicated poor stability and a greater possibility of coagulation compared to **NE1s** as their droplets were narrowly distributed, and **NE2F** clearly displayed coagulation of droplets.

The %EE for the **NE1s** compared to **NE2s** of each statin was high and statins were effectively

entrapped in the formulas, as the %EE was close to 100% (Loureiro *et al.,* 2015:96). When the %EE of the **NE1s** were compared to **NE2s** of each statin, it was concluded that the **NE1s** prevailed for atorvastatin, fluvastatin and pravastatin, although, **NE1Pi** was slightly lower than **NE2Pi**.

From the aforementioned characteristics, it was apparent that the **NE1s** were more optimal overall and therefore chosen as the optimised formula. An optimised nano-emulsion formula should have the ability to deliver the APIs effectively (Gutiérrez *et al*., 2008:247). For the effective delivery, it is important to determine whether the APIs affect the characteristics of the optimised nano-emulsion formula. Therefore, in this appendix the optimised nano-emulsion (**NE1**) will be compared to the placebo (**NE1** without API), which will be further referred to as **PNE1**, in terms of visual inspection, pH, surface potential measurement (zeta-potential), droplet size and distribution, viscosity and morphological analysis (TEM) (Kumar 2014:1; Nejadmansouria *et al.*, 2016:801-803).

### B.7 Optimised o/w nano-emulsion method and formula with and without statins

An optimised o/w nano-emulsion formula containing the individual statins (**NE1**) and preparation method was analysed and determined.

**Table B.8:** Formula used to prepare the optimised **NEs** containing statins

| Phase | Constituent | Quantity | Concentration |
|---|---|---|---|
| | | NE1 | NE1 |
| Water phase | Milli-Q® water | 39.000 ml | 78.000% (w/v) |
| | Tween® 80 | 2.804 ml | 5.608% (w/v) |
| Oil phase | Apricot kernel oil | 4.350 ml | 8.700% (w/v) |
| | Span® 60 | 3 g | 6.000% (w/w) |
| | Statin | 1 g | 2.000% (w/w) |

The same formulation method as well as formula was used to prepare the placebo (**PNE1**) with the exception of excluding the API as seen in Table B.10.

**Table B.9:** Formula used to prepare **PNE1**

| Phase | Constituent | Quantity |
|---|---|---|
| | | **PNE1** |
| **Water phase** | Milli-Q® water | 40.000 ml |
| | Tween® 80 | 2.804 ml |
| **Oil phase** | Apricot kernel oil | 4.350 ml |
| | Span® 60 | 3 g |

## B.8 Methods used during the characterisation of the optimised o/w nano-emulsions

To determine if the APIs had any effects on the dispersions, **PNE1** was characterised and compared to the analysis of characteristics **NE1s** (**NE1A**, **NE1F**, **NE1Pi** and **NE1Pr**) by means of visual inspection, pH, droplet size and distribution, surface potential measurement (zeta-potential), viscosity and morphological analysis (TEM) (Nejadmansouria *et al.*, 2016:801-803).

### B.8.1 Visual inspection

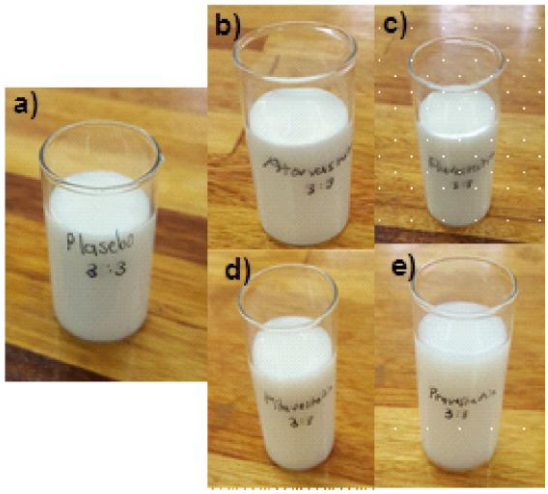


**Figure B.10:** Prepared nano-emulsions: a) **PNE1**, b) **NE1A**, c) **NE1F**, d) **NE1Pi** and e) **NE1Pr**

Figure B.10 represents the placebo (**PNE1**), as well as the optimised nano-emulsions (**NE1s**). Neither the **PNE1**, nor the **NE1s** presented with sedimentation or flocculation. All the dispersions (**PNE1** and **NE1s**) appeared white and milky, with no visible oil droplets, thus it could be concluded that without the statins included in the formula, oil droplets within in the water phase were still effectively dispersed.

### B.8.2 pH

Typically, the pH of the skin will measure at ± 5 (Ng & Lau, 2015:8; Williams, 2013:678); however, the skin can endure components with pH values of 3 – 9, which will serve as a guideline in this study, as mentioned in Section B.5.2.

The pH of the nano-emulsions were measured utilising a Mettler Toledo® pH meter (Mettler Toledo, CU), by inserting the Mettler Toledo® InLab® 410 electrode (Mettler Toledo, CU) (see Figure B.3) into the nano-emulsion to provide a value.

Table B.11 indicates the average pH measurements for **PNE1** compared to **NE1s**. **PNE1** as well as the **NE1s** (**NE1A**, **NE1F**, **NE1Pi** and **NE1Pr**) displayed average pH values in the range of 6 – 8, and the order was exhibited as **NE1F** > **NE1Pr** > **PNE1** > **NE1A** > **NE1Pi**.

It can be concluded that although the addition of the APIs did influence the pH of the formula when compared to the **PNE1**, the pH values of the affected formulations still ranged between the accepted pH values of 3 – 9 (Barry, 2002:512) and therefore should not act as an irritant or affect the integrity of the skin when applied.

**Table B.10:** The average pH for **PNE1** compared to the **NE1s**

| Formula | pH | | | |
|---|---|---|---|---|
| | 1 | 2 | 3 | Average |
| **PNE1** | 6.79 | 6.78 | 6.77 | 6.78 ± 0.008 |
| **NE1A** | 6.57 | 6.59 | 6.56 | 6.57 ± 0.012 |
| **NE1F** | 7.82 | 7.80 | 7.81 | 7.81 ± 0.008 |
| **NE1Pi** | 6.55 | 6.54 | 6.53 | 6.54 ± 0.008 |
| **NE1Pr** | 7.21 | 7.22 | 7.21 | 7.21 ± 0.004 |

### B.8.3 Surface potential (zeta-potential)

To determine the zeta-potential of the nano-emulsions, a Malvern Zetasizer Nano ZS (Malvern Instruments, Worcestershire, UK) (see Figure B.4) was used. An extracted volume of **PNE1** was diluted separately with Milli-Q® water (1:100), where after a similar method as described in Section B.5.3 was followed. The sample's measurement was performed in triplicate.

**Table B.11:** Average zeta-potential (mV) of **PNE1** compared to **NE1s** formulated with different statins

| Formula | Zeta-potential (mV) | | | |
|---|---|---|---|---|
| | **1** | **2** | **3** | **Average** |
| **PNE1** | -31.7 | -32.3 | -34.2 | -32.7 ± 1.1 |
| **NE1A** | -44 | -42.9 | -44.3 | -43.7 ± 0.6 |
| **NE1F** | -54.8 | -57.0 | -56.1 | -55.7 ± 1.2 |
| **NE1Pi** | -39.9 | -40.6 | -39.8 | -40.1 ± 0.4 |
| **NE1Pr** | -47.3 | -47.4 | -50.2 | -48.3 ± 1.3 |

Table B.12 and Figure B.11 indicated the variations between the zeta-potential for **PNE1** and the **NE1s**. The zeta-potential of **PNE1** measured lower than **NE1A**, **NE1F**, **NE1Pi** and **NE1Pr**; therefore, it can be concluded that the **NE1s** measured as more stable than the placebo nano-emulsion, although **PNE1**'s and **NE1s**' zeta-potential values were well within the required range (± 20 mV) (Kumar, 2014:5), suggesting that stability is acceptable.

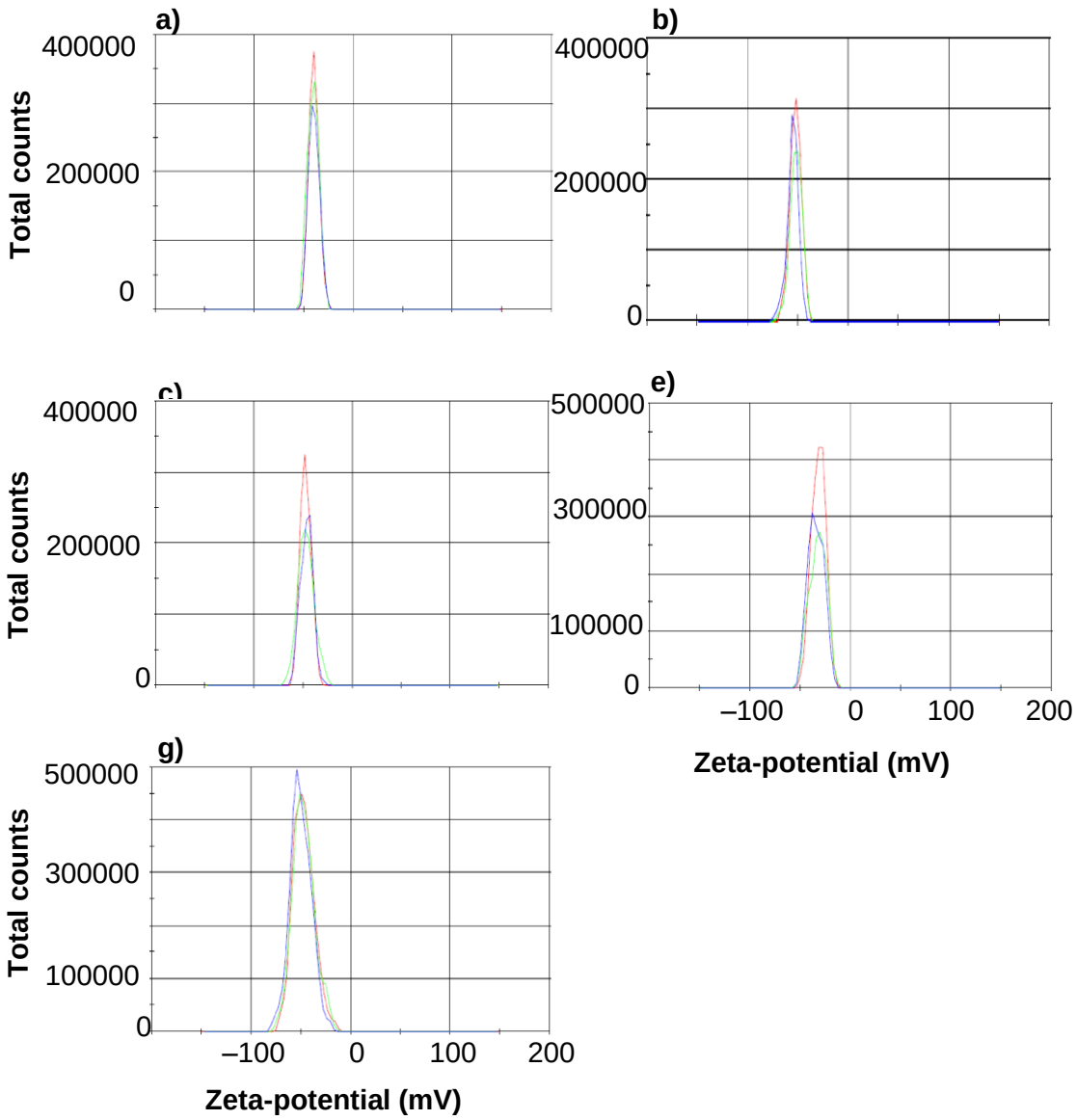


**Figure B11:** The average zeta-potential (mV) for the **PNE1** and **NE1s**: a) **PNE1**, b) **NE1A**, c) **NE1F**, d) **NE1Pi** and e) **NE1Pr**

### B.8.4 Droplet size and distribution

By measuring the droplet diameter, PdI as well as droplet size can be determined (Malvern Instruments Limited, 2015:15), therefore stability can be evaluated (Solans *et al*., 2005:105). Smaller droplet sizes improve the emulsion's integral stability and reduce the occurrence of sedimentation, creaming, flocculation and coagulation (Kumar, 2014:5; Solans *et al*., 2005:105).

A Malvern Zetasizer Nano ZS (Malvern Instruments, Worcestershire, UK) (see Figure B.4) was utilised to determine the droplet size and distribution, this instrument operates on utilising PCS, which determines light fluctuations that occur between droplets in the **NE** as a result of Brownian motion (Gaur *et al*., 2014:40; Malvern Instruments Limited, 2015:15).

A dilution of **PNE1** was analysed separately by adding drops of the formulation itself to a specific quantity of Milli-Q® water (1:100) and mixed thoroughly by rotating the flask while holding it, an identical to the method used in testing zeta-potential. The sample measurement was performed in triplicate.

**Table B.12:** The average droplet size as well as PdI for the **PNE1** and the **NE1s**

| NE | Average droplet size (nm) | Average polydispersity index (PdI) |
|---|---|---|
| **PNE1** | 198.0 ± 1.9 | 0.3 ± 0.0 |
| **NE1** | 137.4 ± 1.8 | 0.2 ± 0.0 |
| **NE1** | 165.4 ± 1.3 | 0.2 ± 0.0 |
| **NE1** | 130.7 ± 2.1 | 0.2 ± 0.0 |
| **NE1** | 114.2 ± 1.0 | 0.2 ± 0.0 |

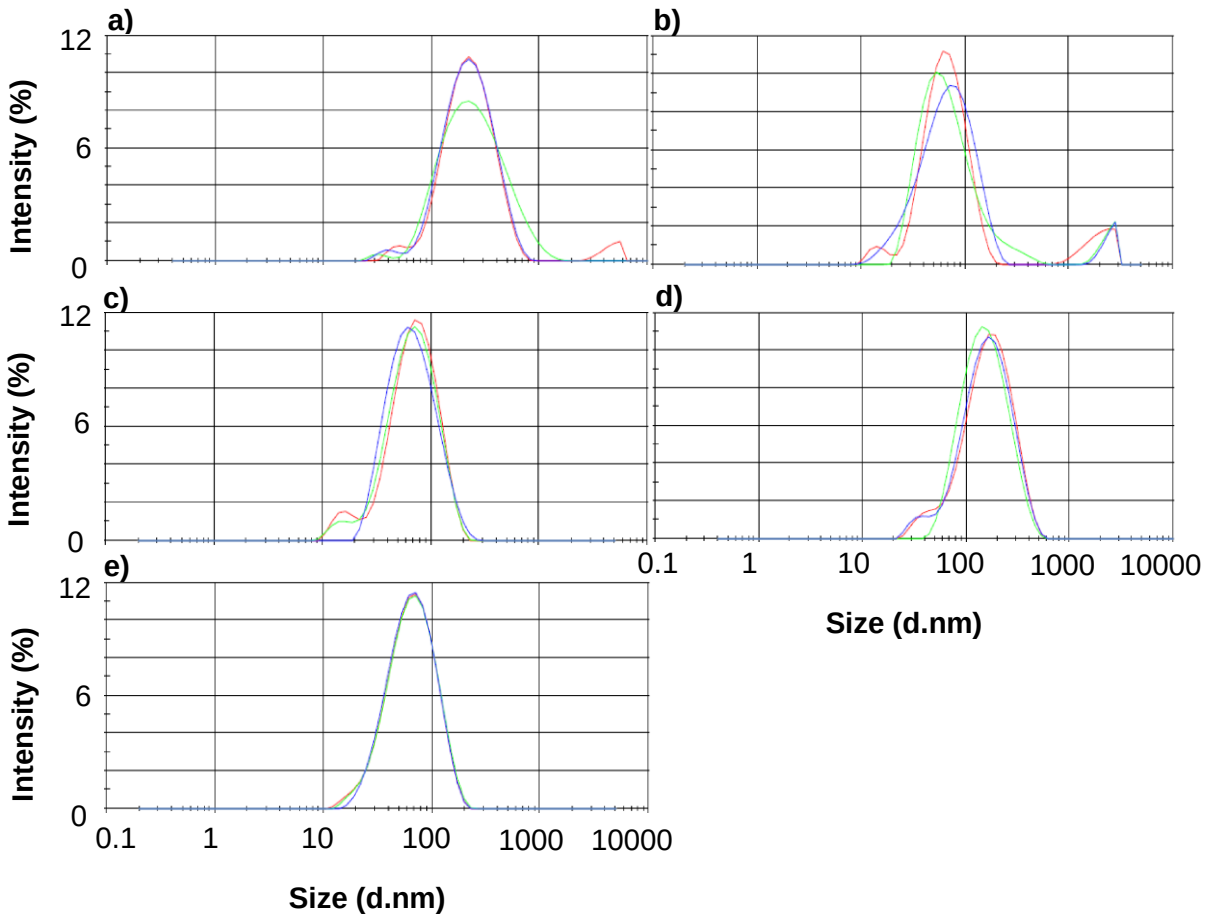


**Figure B.12:** The average droplet size (nm) of the **PNE1** and **NE1s**: a) **PNE1**, b) **NE1A**, c) **NE1F**, d) **NE1Pi** and e) **NE1Pr**

In Table B.13 and Figure B.12, the average droplet size (nm) and average PdI were measured for the **PNE1** and **NE1s**. **PNE1** had an average droplet size of 198 ± 1.925 nm and an average PdI of 0.256 ± 0.011. **PNE1** had a larger droplet size and a higher PdI value when compared to the **NE1s** (**NE1A**, **NE1F**, **NE1Pi** and **NE1Pr**).

**PNE1** as well as the formulated **NE1s,** which contained APIs (statins) ranging within the required parameters for droplet sizes (< 500 nm) (Nalini *et al.,* 2017:1453) as well as PdI values (< 0.5) (Elmataeeshy *et al.,* 2018:24). Therefore, they reflect low risks of sedimentation, creaming, flocculation and coagulation (Kumar, 2014:5; Solans *et al*., 2005:105).

### B.8.5 Viscosity

To measure the viscosity of the **PNE1**, a Brookfield Viscometer (DV2T LV Ultra; Middleboro, Massachusetts, USA) linked to a water bath (± 25 °C) (see Figure B.7) was utilised. A cylindrical spindle (SC4-18) was used to measure the viscosity of the **PNE1**. To reach the appropriate temperature (± 25 °C), the **PNE1** was placed into the water bath (± 25 °C) 1 h before the viscosity was measured. This method was identical to that of Section B 5.5 in order to compare the **PNE1** to the **NE1s**.

**Table B.13:** Viscosity readings of the **PNE1** compared to the **NE1s**

| Formula | Viscosity (cP) | Speed (rpm) | Torque (%) | Temp (°C) |
|---|---|---|---|---|
| **PNE1** | 4.166 ± 0.004 | 200 ± 0.000 | 27.76 ± 0.049 | 22.48 ± 0.075 |
| **NE1A** | 4.454 ± 0.022 | 200 ± 0.000 | 29.68 ± 0.147 | 22.06 ± 0.049 |
| **NE1F** | 5.79 ± 0.011 | 200 ± 0.000 | 38.58 ± 0.075 | 21.80 ± 0.120 |
| **NE1Pi** | 4.278 ± 0.010 | 200 ± 0.000 | 28.50 ± 0.063 | 22.98 ± 0.040 |
| **NE1Pr** | 3.594 ± 0.012 | 200 ± 0.000 | 23.96 ± 0.080 | 22.00 ± 0.126 |

The **PNE1** had viscosity value of 4.166 ± 0.004 cP compared to the **NE1s** (except for **NE1Pr**). **PNE1** displayed with a lower viscosity, which suggests that when the APIs were added to the formula, the viscosity value raised.

### B.8.6 Transmission electron microscopy

TEM was performed to determine the structural form and droplet size of the **PNE1** and compared to the **NE1** TEM images. TEM procedure was performed identical to the process followed in Section B.5.6, with an Oxford INCA X-Sight EDS System utilising a FEI Tecnai G2 20S-Twin 200 kV high-resolution transmission electron microscope (HRTEM) (Czech Republic, EU).

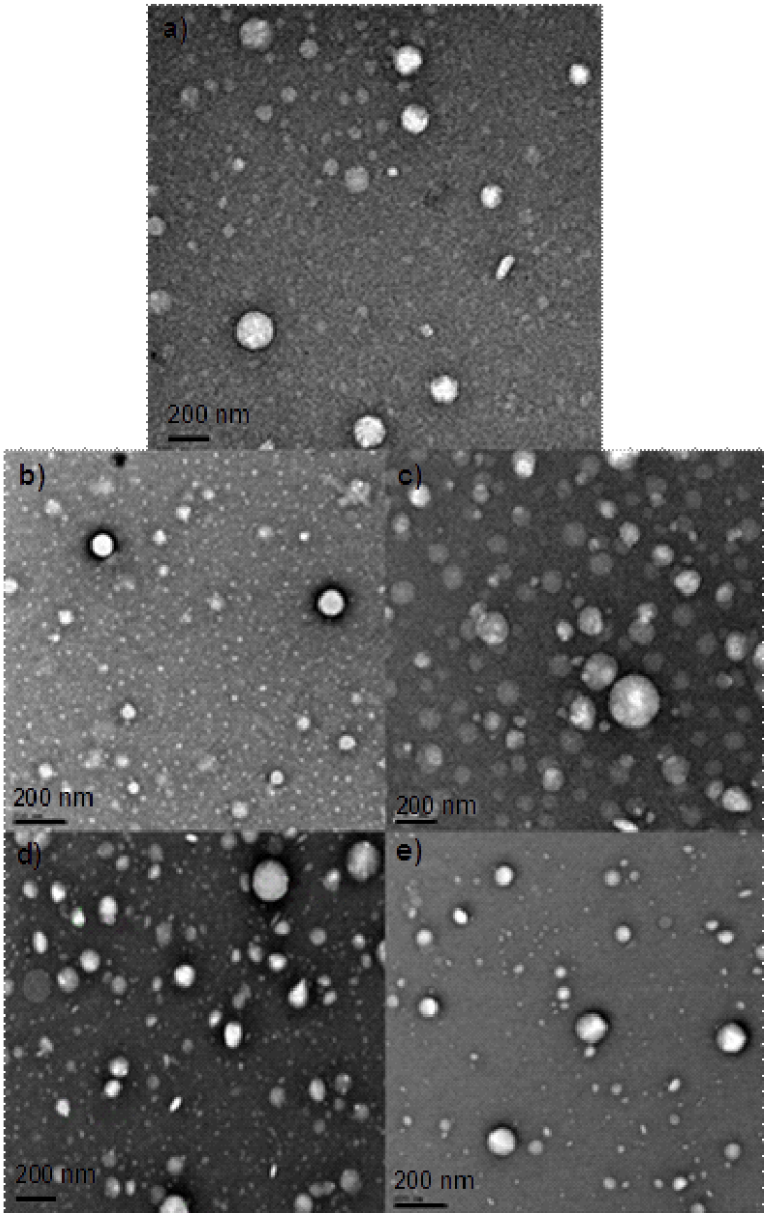


**Figure B.13:** TEM micrographs of **PNE1** compared to those of the **NE1s**: a) **NE1**, b) **NE1A**, c) **NE1F**, d) **NE1Pi** and e) **NE1Pr**

In Figure B.13, the TEM micrographs of the dispersions of the **PNE1** and **NE1s** indicate the morphology of the **PNE1** as well as **NE1s**. The droplet sizes of **PNE1** displayed as 34.17 – 93.53 nm. The droplet sizes of **NE1A** ranged between 32.6 – 76.27 nm, compared to **PNE1**; both dispersions displayed spherical shaped dispersed droplets, although **NE1A** displayed smaller droplet sizes. The droplet sizes of **NE1F** ranged between 23.11 – 112.48 nm compared to **PNE1**; both dispersions displayed spherical shaped dispersed droplets, although **NE1F** displayed larger droplet sizes, which were more narrowly distributed.

The droplet sizes of **NE1Pi** were in the range of 41.61 – 102.64 nm compared to those of **PNE1**; both dispersions presented with spherical shaped dispersed droplets, although **NE1Pi** displayed larger droplet sizes, which were also more narrowly distributed. The droplet sizes of **NE1Pr** ranged between 20.78 – 114.01 nm compared to **PNE1**, and both dispersions displayed spherical shaped dispersed droplets.

The oil droplets within the water phase of nano-emulsions should be below 500 nm (Nalini *et al.,* 2017:1453), hence it can be concluded that the **PNE1**, as well as the **NE1s** displayed nano-sized droplets in the required range; therefore, **NE1s** were adequately formulated.

### B.9 Conclusion

Various methods were utilised to analyse and characterise the **NE1s** and **NE2s**, each containing individual statins to determine an optimised **NE** formula (Section B.6.1 – B.6.6). In terms of visual inspection, pH, zeta-potential, droplet size and distribution, viscosity, TEM and %EE results, the **NE1s** were the favourable formula, thus chosen as the optimised **NE** formula.

The **PNE1** was formulated and characterised to determine if the APIs affected the formula of the **NE1s**. The following characteristics were determined and compared for the **PNE**1 with the optimised **NE1s**, namely visual inspection, pH, droplet size and distribution, surface potential measurement (zeta-potential), viscosity and morphological analysis (TEM) (Kumar 2014:1; Nejadmansouria *et al.*, 2016:801-803).

The **PNE1** and **NE1s** appeared white and milky, with no visible oil droplets when visually inspected, thus it could be concluded that both the dispersions, with or without the statins, were effectively dispersed.

It was found that the addition of the APIs did affect the pH levels of the formula when compared to the **PNE1**; however the pH levels still ranged between the accepted pH of values 3 – 9 (Barry, 2002:512) and therefore, should act as a non-irritant towards when applied to the skin.

Formulated nano-emulsions' (**PNE1** and **NE1**) zeta-potential values were well within the required range (± 20 mV) (Kumar, 2014:5), which suggested acceptable stability. However, the **NE1s** measured higher in stability than the **PNE1**.

The PdI values of the **PNE1**, as well as those of the **NE1s**, ranged within the required parameters of < 0.5 (Elmataeeshy *et al.,* 2018:24). This was an indication of low risks to sedimentation, creaming, flocculation and coagulation (Kumar, 2014:5; Solans *et al*., 2005:105). **PNE1,** as well as **NE1s** displayed nano-sized droplets in the required range (< 500 nm) (Nalini *et al.,* 2017:1453), therefore nano-emulsions were adequately sonicated and formulated.

**PNE1** displayed a lower viscosity, which implicates when APIs were added, the viscosity value raised.

The performed characterisation methods implicated that the **PNE1**, as well as the **NE1s** succeeded in the test requirements for optimal **NEs** and that there were no significant effects with the inclusion or exclusion of statins; however, the nano-emulsions are classified as low viscosity dispersions (Shakeel *et al*., 2007:E6, Thakur *et al*., 2012:223), which could propose challenges with application to the skin, as well as patient compliance. To improve on these predicaments and enhance the viscosity of the nano-emulsions, a thickening agent was included in the formula to produce nano-emulgel formulations. These formulations were characterised and discussed in Appendix C.

**References**


Asmawatia, B., Mustaphaa, W.A.W., Yusopa , S.M., Maskata, M.Y. & Shamsuddinc, A.F. 2014. Characteristics of cinnamaldehyde nanoemulsion prepared using APV-high pressure homogenizer and ultra turrax. *AIP conference proceedings*, 1614:244-250.

Abolmaali, S.S., Tamaddon, A.M., Farvadi, F.S., Daneshamuz, S. & Moghimi, H. 2011. Pharmaceutical nanoemulsions and their potential topical and transdermal applications. *Iranian journal of pharmaceutical sciences*, 7:139-150.

Alexander, A., Dwivedi, S., Ajazuddin, Giri, T.K., Saraf, S., Saraf, S. & Tripathi, D.K. 2012. Approaches for breaking the barrier of drug permeation through transdermal drug delivery. *Journal of controlled release*, 164:26-40.

Baibhav, J., Gurpreet, S., Rana, A.C., Seema, S. & Vikas, S. 2011. Emulgel: a comprehensive review on the recent advances in topical drug delivery. *International research journal of pharmacy*, 2:66-70.

Barry, B. 2002. Transdermal drug delivery. (*In* Aulton, M.E., ed. Pharmaceutics: the science of dosage form design. 2nd ed. London: Churchill Livingstone. p. 499-533).

Bogner, A., Jouneau, P.H., Thollet, G., Basset, D., Gauthier, C. 2007. A history of scanning electron microscopy developments: Towards ‘‘wet-stem’’ imaging. *Micron,* 38:390-401.

Chime, S.A., Kenechukwu, F.C. & Attama, A.A. 2014. Nanoemulsions: advances in formulation, characterization and application in drug delivery. (*In* Sezer, A.D., ed. Application of nanotechnology in drug delivery. p. 77-126). http://cdn.intechopen.com/pdfs-wm/47116.pdf Date of access: 20 Dec. 2017.

Cizinauskas, V., Elie, N., Brunelle, A., Briedies, V. 2017. Skin penetration enhancement by natural oils for dihydroquercetin delivery. *Molecules,* (22):1-16.

Debnath, S., Satayanarayana & Kumar, G.V. 2011. Nanoemulsion-a method to improve the solubility of lipophilic drugs. *Pharmanest: an international journal of advances in pharmaceutical sciences*, 2:72-83.

Divakaran, D. 2012. Preparation and characterization of nanoemulsions encapsulating polyphenol extracts. Karnal: Deemed University. (Thesis-M.Tech)

Egerton, R.F. 2005. Physical principles of electron microscopy: An introduction to TEM, SEM, and AEM. file:///C:/Users/22819509/Downloads/Physical_Principles_of_Electron_Microscopy__An_Introduction_to_TEM__SEM__and_AEM2.pdf Date of access: 28 Sept. 2018.

Eid, A.M., El-Enshasy, H.A., Aziz, R. & Elmarzugi, N.A. 2014. Preparation, characterization and anti-inflammatory activity of Swietenia macrophylla nanoemulgel. *Journal of nanomedicine and nanotechnology*, 5:1-10.

Elmataeeshy, M.E., Sokar, M.S., Bahey-El-Din, M.B. & Shaker, D.S. 2018. Enhanced transdermal permeability of terbinafine through novel nanoemulgel formulation. *Future journal of pharmaceutical sciences*, 4(1):18-28.

Fong, C. 2016. Statins in therapy: Understanding their hydrophilicity, lipophilicity, binding to 3-hydroxy-3-methylglutaryl-CoA reductase, ability to cross the blood brain barrier and metabolic stability based on electrostatic molecular orbital studies. *European journal of medicinal chemistry,* 85:661-674.

Gabera, M., Medhata, W., Hanya, M., Sahera, N., Fang, J., Elzoghby, A. 2017. Protein-lipid nanohybrids as emerging platforms for drug and gene delivery: Challenges and outcomes. *Journal of Controlled Release,* 254:75-91.

Gaur, S., Garg, A., Yadav, D., Beg, M. & Gaur, K. 2014. Nanoemulsion gel as novel oil based colloidal nanocarrier for topical delivery of bifonazole. *Indian research journal of pharmacy and science*, 1:36-54.

Gutiérrez, J.M., González, C., Maestro, A., Solè, I., Pey, C.M. & Nolla, J. 2008. Nano-emulsions: new applications and optimization of their preparation. *Current options in colloid and interface science*, 13:245-251.

Honary, S. & Zahir, F. 2013. Effect of zeta potential on the properties of nano-drug delivery systems-a review (Part 2). *Tropical journal of pharmaceutical research*, 12(2):265-273.

Hyma, P., Jahan, N., Raheemunissa, Sreelekha, G. & Babu, K. 2014. Emulgel: a review. *International journal of pharmaceutical archive*, 3:1-11.

Kaur, G., Bedi, P.M.S., Narang, J.K. 2017. Topical nanoemulgel: a novel pathway for investigating alopecia. *Journal of nanomedicine and nanotechnology,* 8:1-472. Kalra, A. 2013. Preparation and evaluation of oil-in-water self-nanoemulsifying systems with potential for pulmonary delivery. https://etd.ohiolink.edu/!etd.send_file?accession=mco1364764383&disposition=inline.pdf Date of access: 28 Sept. 2018.

Kaya, C., Kola, O., Ozer, M.S., Altan. 2008. Some characteristics and fatty acids composition of wild apricot (*Prunus pseudoarmeniaca* L.) kernel oil. *Asian journal of chemistry*, 20(4):2597-2602.

Kela, S.K. & Kaur, C.D. 2013. Pharmaceutical nanoemulsions an ardent carrier for drug delivery. *Indo American journal of pharmaceutical research*, 3:9202-9212.

Kennedy, R.A. & Kennedy, M.L. 2007. Effect of selected non-ionic surfactants on the flow behaviour of aqueous veegum suspensions. *American association of pharmaceutical scientists: PharmSciTech*, 8:E1-E6.

Koocheki, A., Kadkhodaee, R. 2011. Effect of alyssum homolocarpum seed gum, Tween 80 and NaCl on droplets characteristics, flow properties and physical stability of ultrasonically prepared corn oil-in-water emulsions. *Food hydrocolloids*, 25:1149-1157.

Kumar, S. 2014. Role of nano-emulsion in pharmaceutical sciences. *A review Asian journal of research in pharmaceutical sciences and biotechnology* 2(1):1-15.

Kumarn, G.P., Rajeshwarrao, P. & Padmavathi, T. 2011. India college of pharmacy, nonionic surfactant vesicular systems for effective drug delivery-an overview. *Acta pharmaceutica sinica B*, 1(4):208-219.

Kurakula, M., Srinivas, C., Kasturi, N. & Diwan, P.V. 2012. Formulation and evaluation of prednisolone proliposomal gel for effective topical pharmacotherapy. *International journal of pharmaceutical sciences and drug research,* 4:35-43.

Loureiro, A., Nogueira, E., Azoia, N.G., Sárria, M.P., Abreu, A.S., Shimanovich, U., Rollett, A., Härmark, J., Hebert, H., Guebitz, G., Bernardes, G.J.L., Preto, A., Gomes, A.C. & Cavaco-Paulo, A. 2015. Size controlled protein nanoemulsions for active targeting of folate receptor positive cells. Colloids and Surfaces B: Biointerfaces, 135:90-98.

Lu, W., Chiang, B., Haung, D. & Li, P. 2014. Skin permeation of D-limonene-based nanoemulsions as a transdermal carrier prepared by ultrasonic emulsification. *Ultrasonics sonochemistry*, 21:826-832.

Malvern Instruments Limited. 2015. A basic guide to particle characterization. http://www.cif.iastate.edu/sites/default/files/uploads/Other_Inst/Particle%20Size/Particle%20Ch aracterization%20Guide.pdf Date of access: 8 May 2018.

Mancini, G.B.J., Tashakkor, A.Y., Baker, S., Bergeron, J., Fitchett, D., Frohlich, J., Genest, J., Gupta, M., Hegele, R.A., Ng, D.S., Pearson, G.J., Pope, J. 2013. Diagnosis, prevention, and management of statin adverse effects and intolerance: Canadian working group consensus update. *Canadian journal of cardiology,* 29:1553-1568.

Marrow, D.I.J., McCarron, P.A., Woolfson, A.D. & Donnelly, R.F. 2007. Innovative strategies for enhancing topical and transdermal drug delivery. *The Open Drug Delivery Journal*, 1:36-59.

Naik, A., Kalia, Y.N. & Guy, R.H. 2000. Transdermal drug delivery: overcoming the skin's barrier function. *Pharmaceutical Science and Technology Today*, 3(9):318-326.

Nalini, T., Kumari, V.S. & Basha S.K. 2017. Novel nanosystems for herbal drug delivery. *World journal of pharmacy and pharmaceutical sciences*, 6(5):1447-1463.

Nejadmansouria, M., Hosseinia, S.M.H., Niakosaria, M., Yousefib, G.H. & Golmakani, M.T. 2016. Physicochemical properties and storage stability of ultrasound-mediated WPI-stabilized fish oil nanoemulsions. *Food hydrocolloids,* 61:801-811.

Hach Company. 2010. What is pH and how is it measured? : a technical handbook for industry. http://www.hach.com/asset-get.download.jsa?id=7639984488.pdf. Date of access: 20 May 2018.

Ng, K.W. & Lau, W.M. 2015. Skin deep: the basics of human skin structure and drug penetration. (*In* Dragicevic-Curic, N. & Maibach, H.I., eds. Percutaneous penetration enhancers: chemical methods in penetration enhancement: drug manipulation strategies and vehicle effects. Heidelberg: Springer. p. 3-12).

Nomaki, H., Toyofuku, T., Tsuchiya, M., Matsuzaki, T., Uematsu, K. & Tame, A. 2015. Three-dimensional observation of foraminiferal cytoplasmic morphology and internal structures using uranium-osmium staining and micro-X-ray computed tomography. *Marine micropaleontology*, 121:32-40.

Ochoa, A.A., Hernandez-Becerra, J.A., Cavazos-Garduno, A., Vernon-Carte, E.J., Garc, H.S. 2016. Preparation and characterization of curcumin nanoemulsions obtained by thin-film hydration emulsification and ultrasonication methods. http://www.scielo.org.mx/pdf/rmiq/v15n1/1665-2738-rmiq-15-01-00079.pdf. Date of access: 28 Sept. 2018.

Reddy, A.K., Debnath, S. & Babu, M.N. 2013. Nanoemulsions a novel approach for lipophilic drugs - a review. *Asian journal of pharmaceutical research*, 3:84-92.

Ribeiro, R.C.D., Gomes-Barreto, S.M.A., Ostrosky, E.A., Da Rocha-Filho, P.A., Veríssimo, L.M., Ferrari, M. 2015. Production and characterization of cosmetic nanoemulsions containing opuntia ficus-indica (l.) mill extract as moisturizing agent. *Molecules*, 20:2492-2509.

Setya, S., Talegaonkar, S. & Razdab, B.K. 2014. Nanoemulsions: formulation methods and stability aspects. *World journal of pharmacy and pharmaceutical sciences*: 3:2214-2228.

Silva, H.D., Cerqueira, M.A., Vicente, A.A. 2012. Nanoemulsions for food applications: development and characterization. *Food and bioprocess technology*, 5:854-867.

Shakeel, F., Baboota, S., Ahuja, A., Ali, J., Aqil, M. & Shafiq, S. 2007. Nanoemulsions as vehicles for transdermal delivery of aceclofenac. *American association of pharmaceutical scientists: PharmSciTech*, 8:E1-E9.

Solans, C., Izquierdo, P., Nolla, J., Azemar, N. & Garcia-Celma, M.J. 2005. Nano-emulsions. *Current Opinion in Colloid and Interface Science*, 10:102-110.

Smith, S.C., Blair, S.N., Bonow, R.O., Brass, L.M., Cerqueira, M.D., Dracup, C., Fuster, V., Gotto, A., Grundy, S.M., Miller, N.H., Jacobs, A., Jones, D., Krauss, R.M., Mosca, L., Ockene, I., Pasternak, R.C., Pearson, T., Pfeffer, M.A., Starke, R.D., Taubert, K.A. 2001. AHA/ACC Scientific Statement: AHA/ACC Guidelines for preventing heart attack and death in patients with atherosclerotic cardiovascular disease. *Journal of the American college of cardiology*, 38(5):1581-1583.

Tadros, T., Izquierdo, P., Esquena, J. & Solans, C. 2004. Formation and stability of nano-emulsions. *Advances in colloid and interface science*, 108(19):303-318.

Thakur, N., Garg, G., Sharma, P.K. & Kumar, N. 2012. Nanoemulsions: a review on various pharmaceutical application. *Global journal of pharmacology*, 6:222-225.

V&P Scientific, Inc. 2010. Viscosity tables. http://www.vp-scientific.com/Viscosity_Tables.htm Date of access: 5 May. 2018.

Williams, A.C. 2013. Topical and transdermal drug delivery. (*In* Aulton, M.E., ed. Aulton's pharmaceutics: the design and manufacture of medicines. 3rd ed. London: Churchill Livingstone. p. 675-697).

Zhang, D. 2009a. Polyoxyethylene sorbitan fatty acid esters. (*In* Rowe, R.C., Sheskey, P.J. & Quinn, M.E., eds. Handbook of pharmaceutical excipients. 6th ed. USA: Pharmaceutical Press. p. 549-553).

Zhang, D. 2009b. Sorbitan esters. (In Rowe, R.C., Sheskey, P.J. & Quinn, M.E., eds. Handbook of pharmaceutical excipients. 6th ed. USA: Pharmaceutical Press. p. 675-678).

Zhao, Q., Kuang, W., Long, Z., Fang, Liu, D., Yang, B., Zhao, M. 2013. Effect of sorbitan monostearate on the physical characteristics and whipping properties of whipped cream. *Food chemistry*, 141:1834-1840.

Hielscher Ultrasound technology. 1999. Ultrasonic Production of Stable Nanoemulsions. https://www.hielscher.com/ultrasonic-production-of-stable-nanoemulsions.htm Date of access: 28 Sept. 2018.

Zhao, Q., Kuang, W., Longa, Z., Fang, M., Liu, D., Yang, B., Zhao, M. 2013. Effect of sorbitan monostearate on the physical characteristics and whipping properties of whipped cream. *Food chemistry,* 141:1834-1840.

# APPENDIX C

FORMULATING AND CHARACTERISATION OF A NANO-EMULGEL COMPARED TO AN OPTIMISED O/W NANO-EMULSION BOTH CONTAINING STATINS IN COMBINATION WITH APRICOT KERNEL OIL

## C.1 Introduction

Optimal nano-emulsions (discussed in Appendix B) are isotropic systems, which consist of good stability and physiochemical characteristics (Chellapa, 2015:43). Nano-emulsions are excessively researched as an alternative drug delivery system to enhance the penetration of poorly soluble APIs, as this delivery system provides prolonged retention time at the area of interest, better transport through the skin and less adverse effects (Sutradhar, 2013:97). Research indicates that the bioavailability values of certain APIs are ± 3.5 times higher, when the transdermal route is followed compared with the oral route, due to the exclusion of metabolism through the liver (Chellapa, 2015:43).

To formulate stable nano-emulsions, surfactants such as Span® 60 (lipophilic) and Tween® 80 (hydrophilic) were included in the formula (Appendix B). These surfactants were also utilised to formulate the nano-emulgels in this study. Surfactants are surface acting agents, which are utilised to reduce tension between the oil and the water phases of the o/w nano-emulsion (Setya *et al*., 2014:2218), which leads to enhanced stability properties (Baibhav *et al*., 2011:68).

Nano-emulsions are very advantageous, however, they also have drawbacks such as low spreadability and poor viscosity (Chellapa, 2015:44). Another main hindrance when utilising the transdermal drug delivery route, is the stratum corneum with a thickness of 10 – 20 µm (Chellapa, 2015:43). Although this layer is not very thick, it serves as a barrier that consists of highly complicated structured protein-lipid matrix, therefore limiting transport through the skin (Chellapa, 2015:43).

To help overcome this barrier, and the fact that nano-emulsions have low spreadability and poor viscosity, combining a gelling agent in the formula to form a nano-emulgel, also known as a hydrogel-thickened nano-emulsion (HTN), can resolve these shortcomings (Chellapa, 2015:44). Nano-emulgels are known to display characteristics of nano-emulsions and gels combined (Kaur *et al*., 2017:1).

Nano-emulgels are classified among semi-solid dosage systems with a consistency somewhere between a liquid and a solid (Kaur *et al*., 2013:202). A semi-solid formulation

offers direct contact when applied on the skin and as a result, has a double function of assisting drug delivery, as well as acting as a carrier system (Gupta & Garg, 2002:144). A nano-emulgel can be defined as the creation of a nano-emulsion-based-hydrogel, by merging a nano-emulsion with a hydrogel medium, which is known to enhance skin permeability (Chellapa, 2015:44), as nano-emulgels consists of droplet sizes between 100 – 500 nm (Nalini *et al.,* 2017:1453) and present limited size distribution (Kumar, 2014:1).

An optimal nano-emulsion combined with a gelling agent to form a nano-emulgel (Chellapa, 2015:44; Eid *et al*., 2014:1) decreases interfacial and surface tension even more than nano-emulsions (Chellapa, 2015:45). Gelling agents also enhance formulation stability by preventing separation of particles (Mitsui, 1997:138). The addition of a gelling-agent causes swelling of the nano-emulsion, producing a formulation with a higher viscosity (Mahalingam *et al*., 2008:293; Mitsui, 1997:138) and increased permeation through the skin (Eid *et al*., 2014:1).

Formulations of nano-emulgels also increase patient compliance (Pund *et al*., 2015:152; Williams, 2013:687), as they are effortlessly applied and removed from the skin, compared to other topical formulations, for example creams and ointments (Chellapa, 2015:45).

The gelling-agent utilised in this study was Carbopol® Ultrez 20. Carbopol® Ultrez 20 is a whitish snow-like powder, with the advantageous ability to wet and dissolve rapidly (Lubrizol, 2018). This gelling-agent has many other properties, such as swelling, which results in a higher viscosity and in turn enhances the stability of the formulation as mentioned before. In addition to its unique stability over a wide pH range, which simplifies the formulation process, Carbopol® Ultrez 20 also assists compounds to dissolve when included in the formulation. When included in a formula, the whole formulation presents with a glowing rich appearance, which makes it favourable to use widely in gels, creams, lotions, shampoos, etc. (Lubrizol, 2018). Carbopol® Ultrez 20 has been utilised to higher the viscosity of nano-emulsions, as well as enhance permeability of formulations when applied topically (Chudasama, 2011:35).

Nano-emulgels also show enhanced adhesion characteristics when applied on the skin and furthermore, consist of an induced solubilisation capability, which results in a higher concentration gradient of API and in turn, a higher concentration of API can penetrate the skin (Chellapa, 2015:45).

In this chapter, the characteristics of the chosen optimised nano-emulsion (**NE1**), as discussed in Appendix B, will be compared to the characteristics of the nano-emulgel, which will further

be referred to as **NEG**. The codes for **NE1s** will remain as described in Appendix B and the following codes will be used to describe the **NEGs** that will be investigated:

- 2% atorvastatin in nano-emulgel (**NEGA**);
- 2% fluvastatin in nano-emulgel (**NEGF**);
- 2% pitavastatin in nano-emulgel (**NEGPi**),
- 2% pravastatin in nano-emulgel (**NEGPr**).

## C.2 Purpose of the formulation

Nano-emulsions are very promising and have many advantages, but one of the disadvantages are that they consist of a very low viscosity, which can lead to poor patient compliance (Pund *et al*., 2015:152) and reduced delivery of the API when applied on the skin (Ali *et al*., 2014:1128). Hence, the goal was to formulate a semi-solid, more specifically a nano-emulgel, to enhance the viscosity and possibly improve skin permeation.

### C.2.1 Formula and formulation method of the nano-emulgel

A nano-emulgel was formulated by utilising the optimised nano-emulsion formula (**NE1**) from Appendix B, combined with a gelling agent (Carbopol® Ultrez 20, Sigma & Aldrich, batch-0102052576).

**Table C.1:** Formula used to prepare nano-emulgel containing statins

| Phase | Constituent | Quantity |
|---|---|---|
| | | NEG |
| Water phase | Milli-Q® water | 39.000 ml |
| | Tween® 80 | 2.804 ml |
| | Carbopol® Ultrez 20 | 0.25 g |
| Oil phase | Apricot kernel oil | 4.350 ml |
| | Span® 60 | 3.00 g |
| | Statin | 2.00 g |

Table C.1 gives the formula to formulate **NEG**. A step-wise illustration of the process used during the manufacturing of the **NEG** is presented in Figure C.1.

**Step 1:** Measure and weigh all the constituents included in the formula.

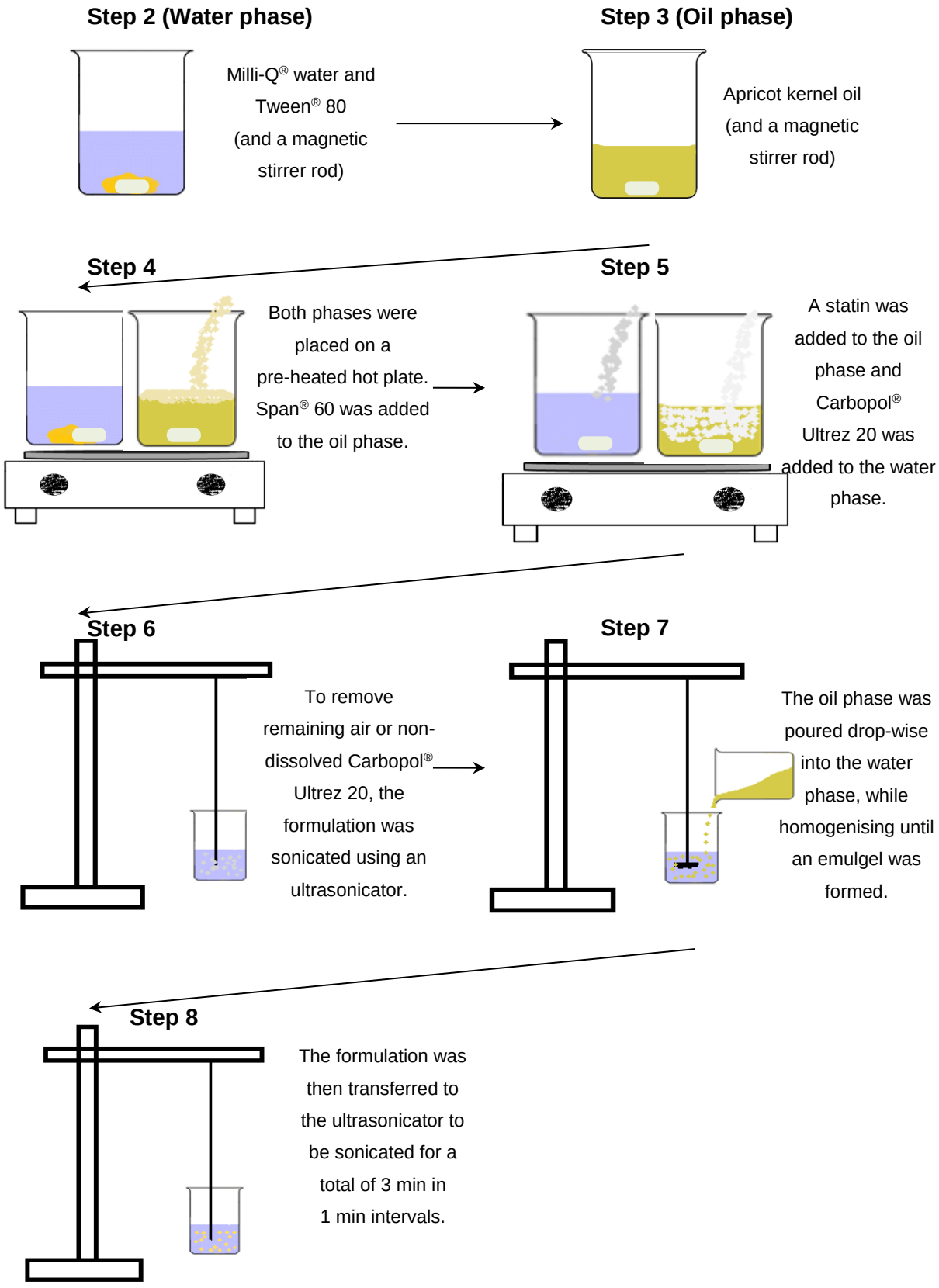


**Figure C.1:** Schematic representation of the method used to prepare the nano-emulgels

## C.3 Methods used during characterisation of a formulation

Characterisation of a formulation has great significance, as it offers data of whether the expected area (epidermal layer of the skin) will be theoretically reached. The following characterisation methods were performed (Nejadmansouria *et al.*, 2016:801-803; Kumar 2014:1) to analyse and characterise the **NEGs**, which were compared to **NE1s**:

- Visual inspection
- pH
- Surface potential measurement (zeta-potential)
- Droplet size and distribution
- Viscosity
- Light microscopy

### C.3.1 Visual inspection

In Figure C.2, the **NEGs** are compared to **NE1s** through visual inspection. The **NEGs**, which included Carbopol® Ultrez 20 as a thickening agent, presented with a shiny, smooth, white gel-like appearance. The **NEGs** also appeared to be higher in viscosity when compared to the **NE1s**, which presented with a whitish-milky appearance. Both the **NEGs** and the **NE1s** (separately containing the statins) showed absence of sedimentation, flocculation and visible oil droplets, therefore, the oil droplets within in the water phase were dispersed effectively.

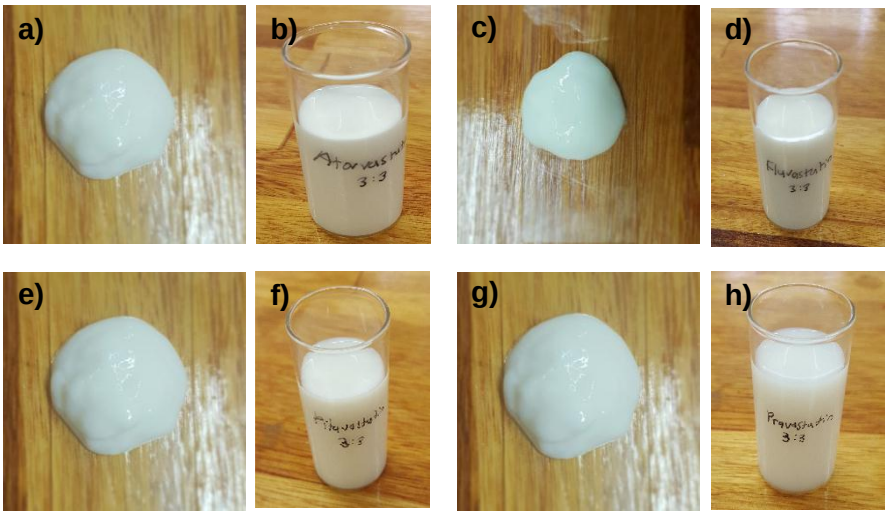


**Figure C.2:** Photographs taken of the different **NEGs** and **NE1s**: a) **NEGA**, b) **NE1A**, c) **NEGF**, d) **NE1F**, e) **NEGPi**, f) **NE1Pi**, g) **NEGPr** and h) **NE1Pr**

### C.3.2 pH

The pH is measured to establish whether the applied formulation will act as an irritant towards the human skin, which normally has a pH value of ± 5 (Ng & Lau, 2015:8; Williams, 2013:678). The human skin can endure components with pH values of 3 – 9 (Barry, 2002:512).

The pH of the **NEGs**, as well as the **NE1s** was measured with a Mettler Toledo® pH meter (Mettler Toledo, CU), by inserting the Mettler Toledo® InLab® 410 electrode (Mettler Toledo, CU) (see Figure B.3) into the nano-emulsion to provide the pH value.

**Table C.2:** The measured average pH of the **NEGs** and **NE1s**

| Formula | pH | | | |
|---|---|---|---|---|
| | 1 | 2 | 3 | Average |
| **NEGA** | 5.47 | 5.50 | 5.51 | 5.49 ± 0.017 |
| **NE1A** | 6.57 | 6.59 | 6.56 | 6.57 ± 0.012 |
| **NEGF** | 5.65 | 5.67 | 5.70 | 5.67 ± 0.021 |
| **NE1F** | 7.82 | 7.80 | 7.81 | 7.81 ± 0.008 |
| **NEGPi** | 4.80 | 5.00 | 4.90 | 4.90 ± 0.082 |
| **NE1Pi** | 6.55 | 6.54 | 6.53 | 6.54 ± 0.008 |
| **NEGPr** | 5.10 | 5.10 | 5.13 | 5.11 ± 0.014 |
| **NE1Pr** | 7.21 | 7.22 | 7.21 | 7.21 ± 0.004 |

Table C.2 indicates that the average pH levels of the **NEGs** varied between the values of 4 and 6, which was lower than the pH levels of **NE1s** (6 – 8). Carbopol® Ultrez 20 is an acidic polymer, which supports the decrease of the pH levels after being included in the formula (Lubrizol, 2009:2). To reach maximum viscosity, the Carbopol® Ultrez 20-containing formulation's pH level is ideally between 6 and 7, thus **NEGs'** pH levels for each statin had to be modified (neutralised) (Lubrizol, 2009:2) with sodium hydroxide (NaOH).

Since the human skin tolerates substances with pH values of 3 – 9 (Barry, 2002:512), it can be concluded that all the formulas' pH values were within these parameters and therefore should not act as an irritant towards the skin, when applied topically.

### C.3.3 Surface potential (zeta-potential)

Zeta-potential determines if the preparation will endure environmental conditions when used (Asmawatia *et al.*, 2014:247) through the measurement of inter (surface charged) activities, as well as long-lasting stability between elements present in the formulation through calculation of the electrophoretic motion of the dispersed oil particles (Kumar, 2014:5). Thus, the more stable a formulation, the higher the zeta-potential value will be, which in turn results in a reduced risk of flocculation (Asmawatia *et al.*, 2014:247) as it implies powerful repulsion forces between elements within the formulation (Huynh, 2012:87).

The ideal zeta-potential varies from ± 20 mv and depends on the dispersant, as well as the chemistry of the surface area of the ingredients (Kumar, 2014:5). Aspects that also affect zeta-potential measurements are pH variations, the type of salt of the active ingredient and its concentration and the concentration of other constituents present in the formulation, such as surfactants, gelling agents, etc. (Asmawatia *et al.,* 2014:247).

**Table C.3:** Average zeta-potential (mV) of the **NEGs**, as well as the **NE1s**

| Formula | Zeta-potential (mV) | | | |
|---|---|---|---|---|
| | 1 | 2 | 3 | Average |
| **NEGA** | -52.4 | -51.8 | -55.1 | -53.1 ± 1.4 |
| **NE1A** | -44.0 | -42.9 | -44.3 | -43.7 ± 0.6 |
| **NEGF** | -61.8 | -64.3 | -61.3 | -62.5 ± 1.3 |
| **NE1F** | -54.8 | -57.0 | -56.1 | -55.7 ± 1.2 |
| **NEGPi** | -48.3 | -49.9 | -48.6 | -48.9 ± 0.7 |
| **NE1Pi** | -39.9 | -40.6 | -39.8 | -40.1 ± 0.4 |
| **NEGPr** | -61.7 | -62.5 | -62.1 | -62.1 ± 0.3 |
| **NE1Pr** | -47.3 | -47.4 | -50.2 | -48.3 ± 1.3 |

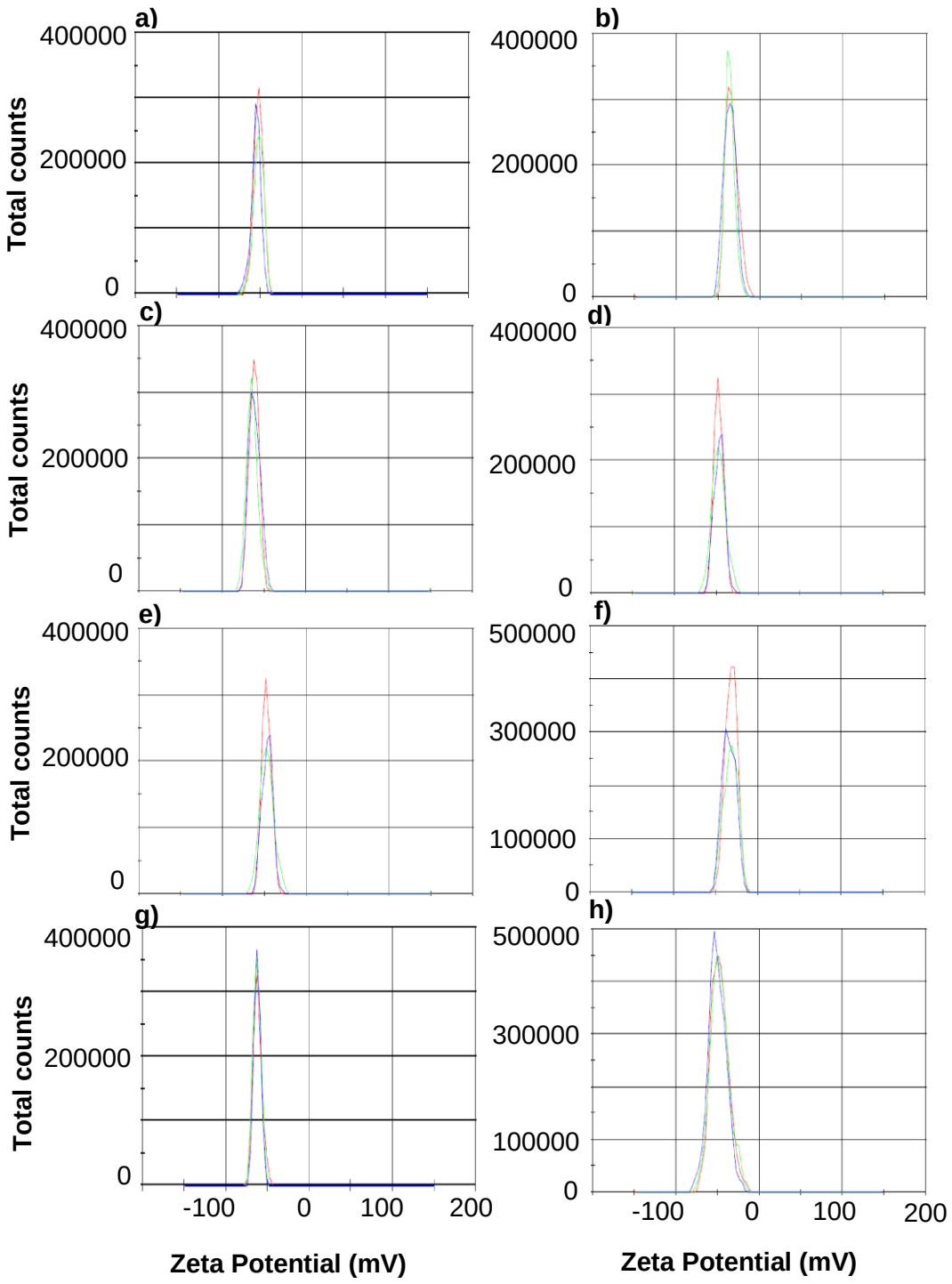


**Figure C.3:** Average zeta-potential (mV) of the different **NEGs** and **NE1s**: a) **NEGA**, b) **NE1A**, c) **NEGF**, d) **NE1F**, e) **NEGPi**, f) **NE1Pi**, g) **NEGPr** and h) **NE1Pr**

To determine the zeta-potential of the **NEGs**, a Malvern Zetasizer Nano ZS (Malvern Instruments, Worcestershire, UK) (see Figure B.4) was used. An extracted volume of each **NEG** was diluted separately with Milli-Q® water (1:100) and mixed thoroughly by rotating the flask while holding it. The solutions were then transferred, each in their own clear disposable zeta cell, using a syringe. Each sample's measurement was performed in triplicate.

The zeta-potential of the **NEGs** and the **NE1s** were compared and in all cases the **NEGs** (**NEGA**, **NEGF**, **NEGPi** and **NEGPr**) presented with higher zeta-potential values than the respective **NE1** (**NE1A**, **NE1F**, **NE1Pi** and **NE1Pr**), indicating that the **NEGs** are more stable than their respective **NE1**. Since the ideal zeta-potential values were higher than ± 20 mV (Kumar, 2014:5), it can be concluded that the formulas (**NEGs** and **NE1s**) were well within the required range for acceptable stability, where the **NEGs** had the highest zeta-potential values of all the formulas.

### C.3.4 Droplet size and distribution

The stability can be evaluated by determining the droplet size (Solans *et al*., 2005:105). It should be noted that smaller droplet sizes enhance the integral stability as they lower the occurrence of sedimentation, creaming, flocculation and coagulation (Kumar, 2014:5; Solans *et al*., 2005:105). The required parameters for droplet sizes and PdI values of nano-emulsions are < 500 nm (Nalini *et al.,* 2017:1453) and < 0.5, respectively (Elmataeeshy *et al.,* 2018:24).

A Malvern Zetasizer Nano ZS (Malvern Instruments, Worcestershire, UK) (see Figure B.4) was utilised in this study to determine the droplet size and distribution of **NEGs**. This instrument operates on utilising photon correlation spectroscopy (PCS), which determines light fluctuations that occur between droplets in the nano-emulsion due to Brownian motion (Gaur *et al*., 2014:40; Malvern Instruments Limited, 2015:15).

Dilutions of each formulation were analysed separately by adding drops of the formula itself to a specific quantity of Milli-Q® water and mixing it thoroughly by rotating the flask while holding it, (identical to the method used in testing zeta-potential). The solutions were then transferred, each in their own clear disposable zeta cell using a syringe. Each sample's measurement was performed in triplicate.

**Table C.4:** The average droplet size and the average PdI values of the **NEGs** and **NE1s**

| Formula | Average droplet size (nm) | Average PdI |
|---|---|---|
| **NEGA** | 212.867 ± 1.266 | 0.209 ± 0.001 |
| **NE1A** | 137.403 ± 1.761 | 0.235 ± 0.004 |
| **NEGF** | 201.733 ± 1.360 | 0.244 ± 0.003 |
| **NE1F** | 165.400 ± 1.257 | 0.197 ± 0.008 |
| **NEGPi** | 256.034 ± 1.042 | 0.244 ± 0.011 |
| **NE1Pi** | 130.733 ± 2.106 | 0.232 ± 0.013 |
| **NEGPr** | 267.532 ± 1.982 | 0.334 ± 0.034 |
| **NE1Pr** | 114.233 ± 1.027 | 0.191 ± 0.009 |

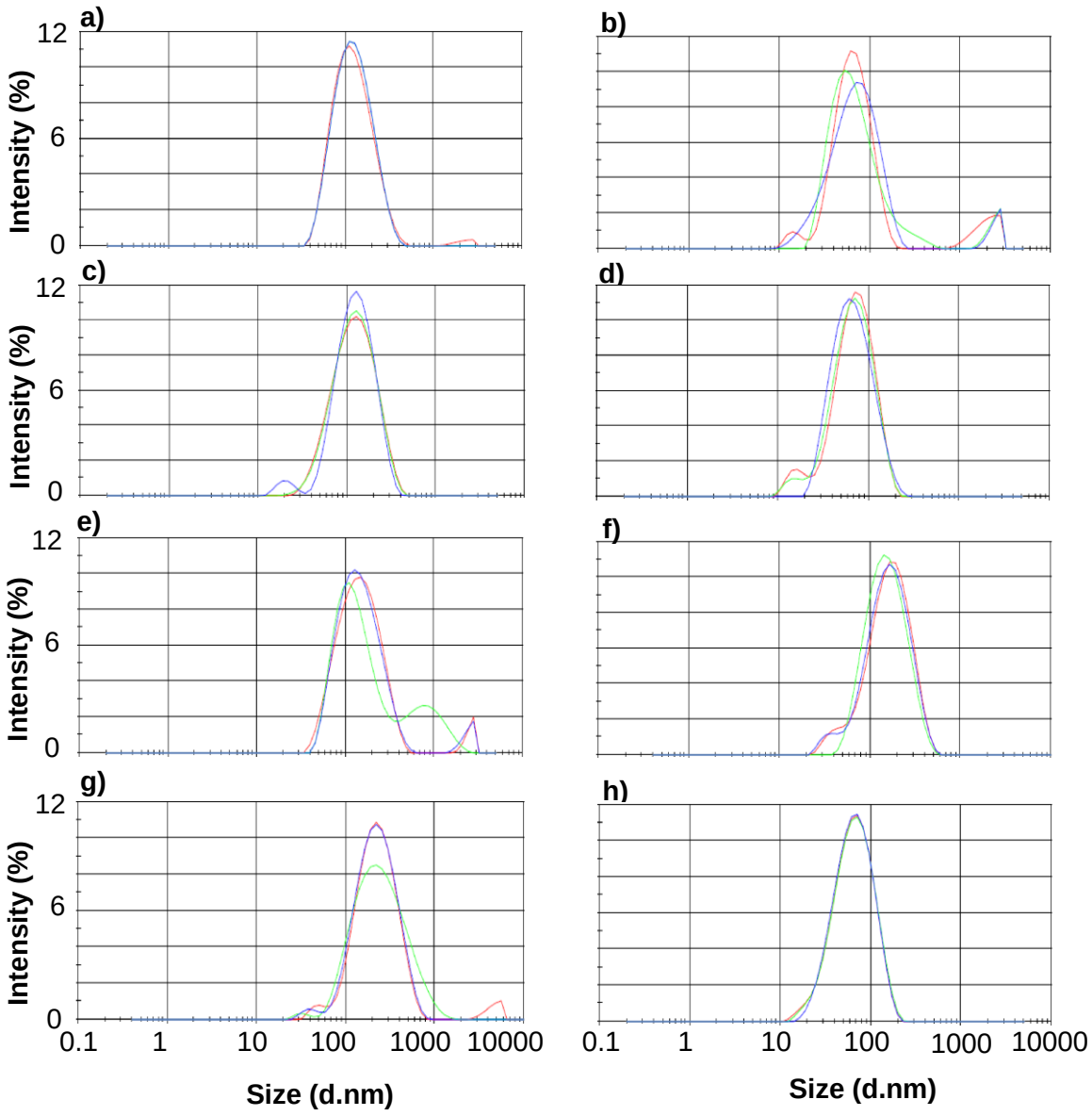


**Figure C.4:** Average droplet size (nm) of the different **NEGs** and **NE1s**: a) **NEGA**, b) **NE1A**, c) **NEGF**, d) **NE1F**, e) **NEGPi**, f) **NE1Pi**, g) **NEGPr** and h) **NE1Pr**

In Table C.4, the average droplet size (nm) and average PdI for the **NEGs** and **NE1s** were presented. After comparing the average droplet sizes of the **NEGs** and the **NE1s**, it is observed that the average droplet sizes of the **NEGs** were larger than the droplet sizes of the **NE1s**. Thus, by the addition of Carbapol® to **NE1s** to produce **NEGs**, enhanced droplet sizes were obtained, which can be due to increased formation of cross-links in **NEGs** (Eid *et al*., 2014:5).

When the average PdI of the **NEGs** were compared to the average PdI of the **NE1s**, it was detected that the **NEGs** had insignificantly higher PdI values than their respective **NE1s**, except for **NEGA**, which presented with a slightly smaller PdI value than and **NE1A**, which agrees with literature that Carbapol® containing **NEGs** does not have significant PDI value variations compared to **NEs** (Eid *et al*., 2014:5).

### C.3.5 Viscosity

Viscosity is the resistance that a substance offers to the motion of flowing (Brookfield engineering; 2017). In an o/w nano-emulsion, the aqueous phase is the larger system in which the oil droplets are dispersed, therefore low viscosity values are produced due to the water component (Chime *et al*., 2014:97). Nano-emulsions are characterised as low viscosity dispersions (Shakeel *et al*., 2007:E6), hence by adding a gelling-agent to the formula of the nano-emulsion, to produce a nano-emulgel (Chellapa, 2015:44), the gelling-agent has the tendency to swell, which enhances the water phase's viscosity (Chellapa, 2015:45), producing a formulation with a higher viscosity (Mahalingam *et al*., 2008:293; Mitsui, 1997:138).

To measure the viscosity of the different **NEGs**, a Brookfield Viscometer DV2T LV Ultra (Middleboro, Massachusetts, USA) (see Figure B.6), linked to a water bath (± 25 °C), was utilised. A T-bar spindle (T-C spindles were utilised except for pravastatin, where a T-D spindle was used) was found to be the most adequate to measure the viscosity of the **NEGs**, where a cylindrical spindle (SC4-18) was utilised for measuring the viscosity of **NE1s**. To reach the appropriate temperature (± 25 °C), the **NEGs** were placed into the water bath (± 25 °C) 1 h before the viscosity was measured. The T-bar spindle was linked to the viscometer and the sample adapter was detached from the viscometer, so that the T-bar spindle could hang directly into the container with the formula. To measure the viscosity, the T-bar spindle was set to rotate at a speed of 20 – 30 rpm. Viscosity readings were measured in centipoise (cP), at 20 sec intervals for a period of 2 min. Rheocalc T 1.2.19 software was used to collect multipoint data to analyse and calculate average viscosity values. This method was followed for each formula individually.

**Table C.5:** Viscosity readings of the **NE1s** and the **NEGs**

| NE Averages | Viscosity (cP) | Speed (RPM) | Torque (%) | Temp (°C) |
|---|---|---|---|---|
| **NEGA** | 2937.67 ± 23.89 | 30.00 ± 0.00 | 94.80 ± 0.77 | 25.81 ± 0.03 |
| **NE1A** | 4.45 ± 0.02 | 200.00 ± 0.00 | 29.68 ± 0.15 | 22.06 ± 0.05 |
| **NEGF** | 5935.67 ± 30.76 | 30.00 ± 0.00 | 94.80 ± 0.41 | 25.80 ± 0.00 |
| **NE1F** | 5.79 ± 0.01 | 200.00 ± 0.00 | 38.58 ± 0.08 | 21.80 ± 0.12 |
| **NEGPi** | 3612.50 ± 43.97 | 20.00 ± 0.00 | 77.60 ± 1.75 | 25.90 ± 0.00 |
| **NE1Pi** | 4.28 ± 0.01 | 200.00 ± 0.00 | 28.50 ± 0.06 | 22.98 ± 0.04 |
| **NEGPr** | 1911 ± 5.57 | 30.00 ± 0.00 | 61.15 ± 0.17 | 25.72 ± 0.04 |
| **NE1Pr** | 3.59 ± 0.01 | 200.00 ± 0.00 | 23.96 ± 0.08 | 22.00 ± 0.13 |

Table C.5 indicates the viscosity readings (cP) of the different **NEGs** and **NE1s** for each statin. The **NEGs** had a significantly larger viscosity reading than the **NE1s**, which agrees with literature that combining an optimal nano-emulgel with a gelling agent enhances the water phase's viscosity, as it reduces interfacial and surface tension even more than nano-emulsions (Chellapa, 2015:45). Since the **NEGs** pH levels were modified (neutralised) (Lubrizol, 2009:2) with sodium hydroxide (NaOH) to a level of 6 – 7, the viscosity drastically increased, which could be visually observed. The speed (rpm) to which the spindles were rotating in the **NEGs** were also slower than the speed of the **NE1s,** and different types of spindles were used due to the viscosity differences. The torque (%) of the **NEGs** were also substantially higher, which indicates that the extent to which resistance was offered from the **NEGs** against the spindle were more than those of the **NE1s**.

### C.3.6 Light microscopy

Morphological analysis such as TEM could not be performed as **NEGs** have high viscosity, which can be harmful to the TEM equipment, thus light microscopy was performed instead. Light microscopy, also known as optical microscopy (OM), is an absolute method to establish the size, droplet distribution and shape of particles during characterisation and stability studies (Particle sciences, 2010:1), as well as the aggregation occurrence in a formulation, e.g. semi-solid dosage forms (Silva *et al*., 2012:862). The sizes and shapes of the entrapped particles are of great importance, as they determine the behaviour of formulation (Particle sciences, 2010:1). A light microscope uses light and an organisation of lenses to enlarge samples to a visible size (Carllson, 2007:5).

Light microscopy was performed on the **NEGs** by transferring a drop of each **NEG** separately on a microscope slide, these slides were then covered with a glass cover slip and inspected under a Nikon Eclipse 50i microscope (at 50 x magnification), which is linked to a Nikon DSFi1

camera (Nikon, Japan Linkam THMS600). To capture the micrographs of the **NEG** droplets, NIS-Elements D 4.00.01 software was utilised. Microscopy was used to investigate the morphology, more so the droplet size, of the semi-solid dosage forms.

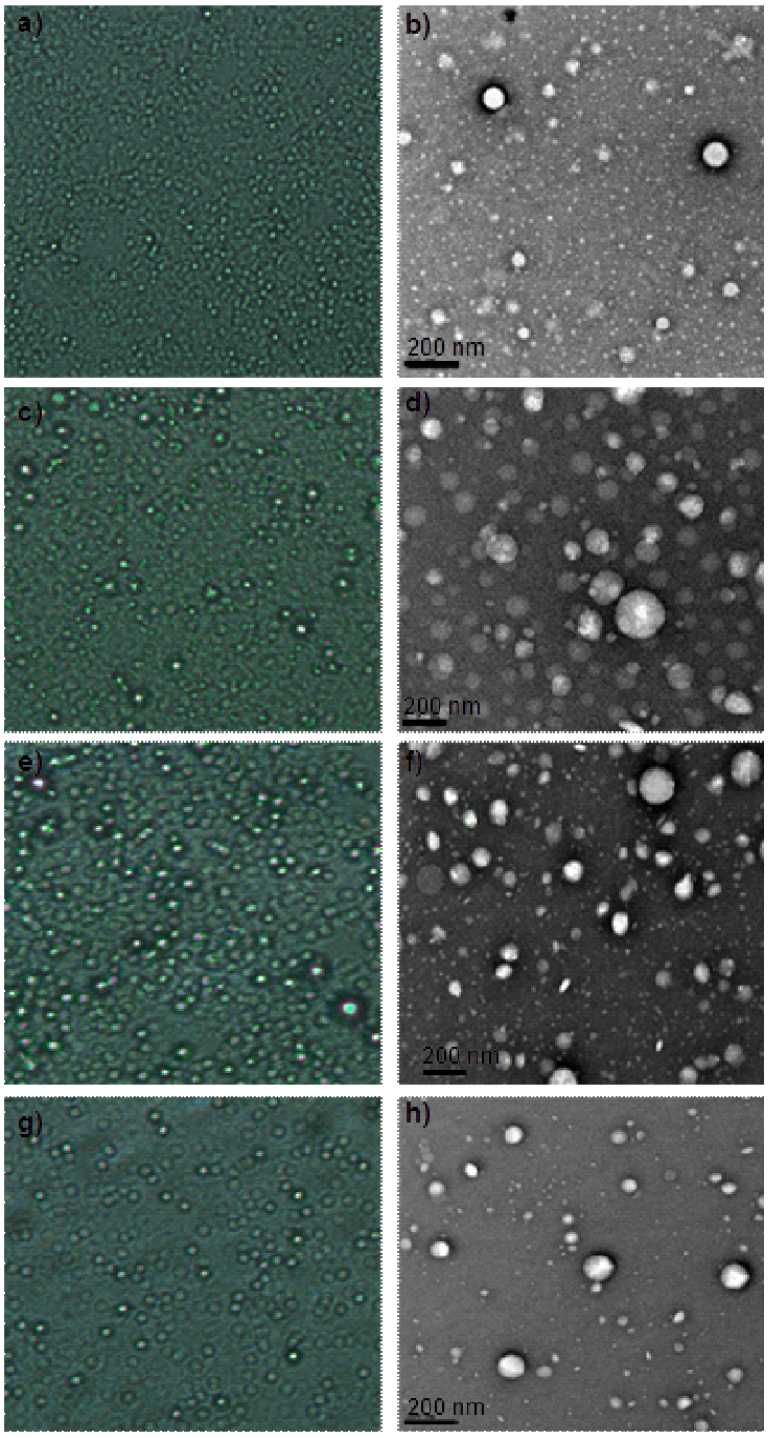


**Figure C.5:** Light microscopy micrographs of the **NEGs** compared to TEM micrographs of the **NE1s**: a) **NEGA**, b) **NE1A**, c) **NEGF**, d) **NE1F**, e) **NEGPi**, f) **NE1Pi**, g) **NEGPr** and h) **NE1Pr** (Light microscopy micrographs of the **NEGs** and TEM micrographs are not o the same scale, as magnification differs)

### C.3.7 Conclusion

Characterisation methods were performed (Kumar 2014:1; Nejadmansouria *et al.*, 2016:801-803) to analyse and characterise the **NEGs**, which were compared to optimised **NE1s** (characterised in Appendix B). In conclusion, the addition a gelling agent to the **NE1s** to form the **NEGs**, initiated swelling of the formulation and as a result thickened, producing a white gel-like formulation with a higher viscosity (Mahalingam *et al*., 2008:293; Mitsui, 1997:138), which should enhance skin permeability (Chellapa, 2015:44; Eid *et al*., 2014:1) and improve stability by the prevention of particle separation in the formulation (Mitsui, 1997:138). This phenomenon was clear when visually inspected and tested with the viscometer.

The pH for the **NEGs** tested well below that of the **NE1s**, as they contained Carbopol® Ultrez 20, which has the tendency to reduce a formulation's pH, since it is an acidic polymer (Lubrizol, 2009:2). To reach maximum viscosity, the Carbopol® Ultrez 20-containing formulation's pH level was neutralised (6 – 7), (Lubrizol, 2009:2) with NaOH, therefore, the NEGs should not irritate the skin since the human skin tolerates substances with pH values of 3 – 9 (Barry, 2002:512).

Surface potential measurement (zeta-potential) of the formulas (**NE1s** and **NEGs**) were well within the required range (± 20 mV) (Kumar, 2014:5), although zeta-potential values for the **NEGs** tested well above **NE1s**, which is an indicator of higher stability (the higher the zeta-potential, the lower the risk of flocculation) (Asmawatia *et al.*, 2014: 247) and improved skin permeability (Chellapa, 2015:44, Eid *et al*., 2014:1).

**NEG** and **NE1s** both consist of nano-scale droplet sizes < 500 nm (Abolmaali *et al*., 2011:140; Nalini *et al.,* 2017:1453). However, **NEGs** in general were more stable than the **NE1s**, as the oil droplets, which encapsulate the lipophilic APIs, were more effectively dispersed in the gel-structure. Subsequently, efficacies of APIs with a limited half-life are extended, since this structure regulates the release of the APIs (Chellapa, 2015:45).

From these findings, it can be concluded that the **NEGs** were more stable and should enable better skin permeability than **NE1s**. Further testing to determine skin permeability of the **NEGs** and **NE1s** via diffusion studies will be investigated in Appendix D.

**References**


Abolmaali, S.S., Tamaddon, A.M., Farvadi, F.S., Daneshamuz, S. & Moghimi, H. 2011. Pharmaceutical nanoemulsions and their potential topical and transdermal applications. *Iranian journal of pharmaceutical sciences*, 7:139-150.

Ali, M.S., Alam, M.S., Alam, N. & Siddiqui, M.R. 2014. Preparation, characterization and stability of dutasteride loaded nanoemulsion for treatment of benign prostatic hypertrophy. *Iranian journal of pharmaceutical research*, 13:1125-1140.

Asmawatia, B., Mustaphaa, W.A.W., Yusopa , S.M., Maskata, M.Y. & Shamsuddinc, A.F. 2014. Characteristics of cinnamaldehyde nanoemulsion prepared using APV-high pressure homogenizer and ultra turrax. *AIP conference proceedings*, 1614:244-250.

Baibhav, J., Gurpreet, S., Rana, A.C., Seema, S. & Vikas, S. 2011. Emulgel: a comprehensive review on the recent advances in topical drug delivery. *International research journal of pharmacy*, 2:66-70.

Barry, B. 2002. Transdermal drug delivery. (*In* Aulton, M.E., ed. Pharmaceutics: the science of dosage form design. 2nd ed. London: Churchill Livingstone. p. 499-533.

Basera, K., Bhatt, G., Kothiyal, P. & Gupta, P. 2015. Nanoemulgel: a novel formulation approach for topical delivery of hydrophobic drugs. *World journal of pharmacy and pharmaceutical sciences*, 4:1871-1886.

Brookfield engineering. 2017. Brookfield Ametek. https://www.brookfieldengineering.com/learning-center/learn-about-viscosity/what-is-viscosity Date of access: 12 Sept. 2018.

Carllson, K. 2007. Light microscopy: Physics of biomedical microscopy. https://www.kth.se/social/files/542d1251f276544bf2492088/Compendium Light.Microscopy.pdf. Date of access: 3 Oct 2018.

Chellapa, P., Mohamed, A.T., Keleb, E.I., Elmahgoubi, A., Eid, A.M., Issa, Y.S. & Elmarzugi, N.A. 2015. Nanoemulsion and nanoemulgel as a topical formulation. *IOSR journal of pharmacy*, 5(10):43-47.

Chime, S.A., Kenechukwu, F.C. & Attama, A.A. 2014. Nanoemulsions: advances in formulation, characterization and application in drug delivery. (*In* Sezer, A.D., ed. Application of nanotechnology in drug delivery. p. 77–126). http://cdn.intechopen.com/pdfs–wm/47116.pdf Date of access: 20 Dec. 2017.

Chudasama, A., Patel, V., Nivsarkar, M., Vasu, K. & Shishoo, C. 2011. Investigation of microemulsion system for transdermal delivery of itraconazole. *Journal of advanced pharmaceutical technology & research*, 2(1):30-38.

Eid, A.M., El-Enshasy, H.A., Aziz, R. & Elmarzugi, N.A. 2014. Preparation, characterization and anti-inflammatory activity of Swietenia macrophylla nanoemulgel. *Journal of nanomedicine and nanotechnology*, 5:1-10.

Elmataeeshy, M.E., Sokar, M.S., Bahey-El-Din, M.B. & Shaker, D.S. 2018. Enhanced transdermal permeability of terbinafine through novel nanoemulgel formulation. *Future journal of pharmaceutical sciences*, 4(1):18-28.

Gaur, S., Garg, A., Yadav, D., Beg, M. & Gaur, K. 2014. Nanoemulsion gel as novel oil based colloidal nanocarrier for topical delivery of bifonazole. *Indian research journal of pharmacy and science*, 1:36-54.

Gupta, P. & Garg, S. 2002. Recent advances in semisolid dosage forms for dermatological application. *Pharmaceutical technology*, 144-162.

Huynh, P.T. 2012. Solvent-free beta-carotene nanoparticles for food fortification. The State University of New Jersey: New Jersey. (Dissertation - PhD).

Kaur, G., Bedi, P.M.S., Narang, J.K. 2017. Topical Nanoemulgel: A Novel Pathway for Investigating Alopecia. *Journal of nanomedicine and nanotechnology,* 8:1-472.

Kaur, P., Kaur, L. & Khan, M.U. 2013. Topical formulations and hydro-gel: an overview. *International journal of advances in pharmacy, biology and chemistry*, 2:201-2060.

Kumar, S. 2014. Role of nano-emulsion in pharmaceutical sciences. *A review Asian journal of research in pharmaceutical sciences and biotechnology* 2(1):1-15.

Lai, F., Sinico, C., Valenti, D., Manca, M.L. & Fadda, A.M. 2008. Nanoemulsions as vehicle for topical 8-methoxypsoralen delivery. *Journal of biomedical nanotechnology*, 4:1-5.

Lubrizol. 2018. Carbapol® Ultrez 20 polymer. http://www.lubrizol.com Date of access: 27 Aug 2018.

Lubrizol. 2009. Viscosity of carbopol® polymers in aqueous systems. http://www.lubrizol.com>lubrizol>Techicaldatasheet Date of access: 27 Aug 2018.

Mahalingam, R., Li, X. & Jasti, B.R. 2008. Semisolid dosages: ointments, creams and gels. (*In* Gad, S.C., ed. Pharmaceutical manufacturing handbook: production and processes. New Jersey: John Wiley & Sons. p. 267-309).

Malvern Instruments Limited. 2015. A basic guide to particle characterization. http://www.cif.iastate.edu/sites/default/files/uploads/other_inst/particle%20size/particle%20characterization%20guide.pdf Date of access: 8 May 2018.

Mitsui, T. 1997. Polymers. (*In* Mitsui, T., ed. New cosmetic science. Netherlands: Elsevier. p. 138-140).

Nalini, T., Kumari, V.S. & Basha S.K. 2017. Novel nanosystems for herbal drug delivery. *World journal of pharmacy and pharmaceutical sciences*, 6(5):1447-1463.

Nejadmansouria, M., Hosseinia, S.M.H., Niakosaria, M., Yousefib, G.H. & Golmakani, M.T. 2016. Physicochemical properties and storage stability of ultrasound-mediated WPI-stabilized fish oil nanoemulsions. *Food hydrocolloids,* 61:801-811.

Ng, K.W. & Lau, W.M. 2015. Skin deep: the basics of human skin structure and drug penetration. (*In* Dragicevic-Curic, N. & Maibach, H.I., eds. Percutaneous penetration enhancers: chemical methods in penetration enhancement: drug manipulation strategies and vehicle effects. Heidelberg: Springer. p. 3-12).

Particle sciences. 2010. Particle size determination in semisolid formulations. https://particlescieces.com>docs.pdf. Date of access: 3 Oct. 2018.

Pund, S., Pawar, S., Gangurde, S. & Divate, D. 2015. Transcutaneous delivery of leflunomide nanoemulgel: mechanistic investigation into physicomecanical characteristics, in vitro anti-psoriatic and anti-melonoma activity. *International journal of pharmaceutics*, 487:148-156.

Setya, S., Talegaonkar, S. & Razdab, B.K. 2014. Nanoemulsions: formulation methods and stability aspects. *World journal of pharmacy and pharmaceutical sciences*: 3:2214-2228.

Shakeel, F., Baboota, S., Ahuja, A., Ali, J., Aqil, M. & Shafiq, S. 2007. Nanoemulsions as vehicles for transdermal delivery of aceclofenac. *American association of pharmaceutical scientists: PharmSciTech*, 8:E1–E9.

Silva, H.D., Cerqueira, M.A., Vicente, A.A. 2012. Nanoemulsions for food applications: development and characterization. *Food and Bioprocess Technology*, 5:854-867.

Solans, C., Izquierdo, P., Nolla, J., Azemar, N. & Garcia-Celma, M.J. 2005. Nano-emulsions. *Current opinion in colloid and interface science*, 10:102-110.

Sutradhar, K.B. & Amin, L. 2013. Nanoemulsion: increasing possibilities drug delivery. *European journal of nanomedicine*, 5(2):97-110.

# APPENDIX D

DIFFUSION STUDIES OF O/W NANO-EMULSIONS AND NANO-EMULGELS CONTAINING STATINS AND APRICOT KERNEL OIL

## D.1 Introduction

The human skin, classified as the largest organ of the human body (2 $m^2$), is divided into three layers namely the epidermis, the dermis and the hypodermis (Ali *et al*., 2015:104; Bouwstra & Ponec, 2006:2081; Foldvari, 2000:417; Menon, 2002:S3-S4; Ng & Lau, 2015:4; Williams, 2013:677-678). Among other essential functions, these layers co-operatively protect the body against exterior agents and assist with the regulation of oxygen and moisture interchange with the surrounding environment (Ali *et al*., 2015:104).

The skin's outmost layer is identified as the stratum corneum (10 – 15 µm in thickness), which forms part of the non-viable epidermis. This outmost layer consists of protein (keratin), water (resists rupturing and offers suppleness) and lipid components such as cholesterol, ceramides and long chain saturated fatty acids (Ali *et al*., 2015:104; El Maghraby *et al.,* 2008:2004; Jepps *et al*., 2013:154; Venus *et al.,* 2011:471; Williams, 2013:677). Known as the least penetrable layer, the stratum corneum is the barrier (Ali *et al*., 2015:104; Kute & Saudagar, 2013:368; Williams, 2013:677) that regulates API passage through the skin (Williams, 2003:10; Williams, 2013:677) when formulations are applied topically. As a result of this barrier, the efficiency to which an API is absorbed and delivered across the skin (transdermal drug delivery) relies highly on the delivery system (Weiss, 2011:471).

A transdermal drug delivery system is designed to release the API to travel through the skin (stratum corneum, epidermis and dermis) and into the blood stream at a regulated continuous rate to achieve systemic therapeutic effects without accumulation of the API within skin layers (Ali *et al*., 2015:103). Nano-emulsions were chosen as an appropriate transdermal delivery system, since they are appropriate pharmaceutical formulations for dermal and transdermal delivery of APIs (Chime *et al*., 2014:95-98). Nano-emulsions promote skin penetration and transport of poor soluble APIs through prolonged exposure at the target area (Sutradhar, 2013:97). Nano-emulsions (**NE1s**) were modified to produce nano-emulgels (**NEGs**) by including a gelling agent, which are known to further improve skin permeability and also patient compliance, as they consist of better stability and enhanced viscosity (Mahalingam *et al.,* 2008:293; Mitsui, 1997:138) to be easily applied on the skin (Chellapa, 2015:45).

To determine if the APIs (statins) were released from the (**NE1s**) and (**NEGs**) formulas, membrane release studies were performed. Skin diffusion studies and tape stripping were finally executed to establish whether the formulas succeeded in transdermal and/or topical delivery.

## D.2 Methods

### D.2.1 HPLC analysis of statin samples

An HPLC analytical method was developed by and successfully validated (described in Appendix A). This method was utilised to detect the quantity of statins present in the injected samples gathered from Franz cell release and diffusion studies together with tape stripping. Samples collected were analysed with an HPLC system (Dionex UltiMate 3000 dual system with ternary gradient pumps, column ovens autosampler and diode array detectors). Samples extracted from the receptor phase during diffusion studies were filtered with 0.45 µm nylon membrane filters (Agela Technologies, Newark, DE) prior to HPLC analysis, as it contained biological material.

Chromatograms were evaluated with Chromeleon 7.2, and for processing of data, analysis software (Thermo Fisher Scientific Inc., Waltham, MA) was utilised. A Restek Ultra C18, 250 x 4.6 mm, 5 µm (Restek, Bellefonte, PA) column was used during analysis, and the laboratorial temperature was controlled (25 °C). The ideal developed HPLC method to detect the statins present in the receptor compartment, as well as the skin layers was with a flow rate of 1.0 ml/min, a 10 µl injection volume, detection wavelength (UV) of 240 nm and a run time of 15 min with PBS (pH 7.4) as a solvent. The retention times (min) of the statins were ± 8.53 min (atorvastatin), ± 8.95 min (fluvastatin), ± 4.84 min (pitavastatin) and ± 5.84 min (pravastatin). The mobile phase consisted of ACN/Milli-Q® water with 0.1% orthophosphoric acid, which starts at 30% acetonitrile and increase linearly to 70% after 4 min, which is then held at 70% for 10 min and thereafter it re-equilibrates at start conditions.

### D.2.2 Solubility of statins

#### D.2.2.1 Solubility in PBS (pH 7.4)

The solubility of statins was determined by utilising PBS (pH 7.4; pH of blood) (OECD, 2011:29). A volume of 10 ml PBS (pH 7.4) was poured into separate test tubes after which the PBS (pH 7.4) was saturated separately with the four statins (atorvastatin, fluvastatin, pitavastatin and pravastatin) until precipitation was present. This step was performed in triplicate. The test tubes were shaken and placed in a preheated water bath for 24 h at 32 °C

(temperature on top of the skin) and repeatedly observed to ensure that saturation was maintained. The solutions in the test tubes were then removed from the water bath and centrifuged for 15 min where after an amount of PBS (containing dissolved statin) from each test tube was extracted and filtered through a 0.45 µm nylon membrane filters into HPLC vials for analysis (triplicate).

A standard solution was formulated by dissolving 5 mg of each statin (separately) in 100 ml methanol, a volume of 1 ml of each standard was transferred to HPLC vials and injected at several injection volumes (2.5, 5.0, 7.5 and 10.0 µ to produce a linear regression line used during analysis of the sample.

#### D.2.2.2 Solubility in *n*-octanol

The method to determine *n*-octanol solubility is similar to that of the PBS (pH 7.4) solubility, with the exception of diluting 1 ml of the extracted *n*-octanol (containing dissolved statin) after centrifugation with methanol to a volume of 25 ml. A volume of these dilutions were separately transferred to HPLC vials for analysis (triplicate). A standard solution (identical to that of the PBS (pH 7.4) solubility) was also prepared and inserted into the HPLC for injection to obtain a linear regression line.

### D.2.3 Octanol buffer distribution coefficient (log D) of statins

Literature on log D values for statins are limited and differ significantly; therefore, the log D values for each statin had to be determined. Consequently, PBS (pH 7.4) and *n*-octanol solubility tests were performed on statins (Sections D.2.2.1 and D.2.2.2) prior to the log D determination. Log D was determined to establish the solubility of statins in co-saturated *n*-octanol and PBS (pH 7.4), to reach a conclusion of the phase in which statins would be more soluble (hydrophilic or lipophilic).

The technique used to determine the log D value of compounds is known as the shake flask method. This method has shown valuable results for the determination of compound lipophilicity (Wenlock, *et al*., 2001:348). To determine log D, equal volumes of PBS (pH 7.4) and *n*-octanol was mixed and equilibrated in a separating funnel over a time period of 24 h to accomplish co-saturation of the two phases. *n*-Octanol has a lower density than the PBS (pH 7.4); therefore, forms the top layer in the funnel and PBS (pH 7.4) the bottom. After 24 h, the bottom layer (pre-saturated PBS at pH 7.4) was removed from the funnel by turning the tap connected to the bottom of the funnel (note that the lid of the funnel should be removed to prevent the occurrence of a vacuum), where after the pre-saturated *n*-octanol phase was removed.

A volume of 20 ml pre-saturated *n*-octanol was poured into four separate volumetric flasks, to which ± 40 mg of each statin was transferred to separately. The pre-saturated *n*-octanol/statin flasks were mixed thoroughly, where after a volume of 3 ml pre-saturated *n*-octanol/statin was withdrawn from each volumetric flask and placed in separate test tubes. This was performed in triplicate to produce three test tubes per statin. An equal amount (3 ml) of pre-saturated PBS (pH 7.4) was then added to each test tube (*n*-octanol/statin) individually. To ensure adequate mixing, the test tubes were placed into a shaker water bath at 32 °C for 8 h. Test tubes were removed and a volume of 1 ml octanol phase of each test tube, represented by the top layer, was transferred to separate 10 ml volumetric flasks with a micropipette and made up to volume with methanol. The volumetric flasks were mixed adequately, where after a volume of each volumetric flask was transferred to separately marked HPLC vials. A volume of the bottom phase (pre-saturated PBS (pH 7.4)) of each tube was directly transferred to separately marked HPLC vials. The vials were analysed by averages of HPLC to determine the concentration of statins present in each phase.

A standard solution was also prepared for each statin and analysed by averages of HPLC to obtain a standard linear regression curve (see Section A.3.1).

### D.2.4 Franz cell method

The *in vitro* Franz cell diffusion method has become one of the most significant methods for investigating transdermal drug administration. The use of *in vitro* Franz cells assesses skin permeability and provides vital information regarding relations between the skin, API and the formulation. This method is favourably as it assists with the development, dose assessment and quality evaluation of formulations (Cabral *et al*., 2014:1). The Franz cell method was followed to determine the release and diffusion of the statins from the **NE1s** and **NEGs**.

*In vitro* studies ought to be near to an exact simulation of an *in vivo* environment (Modi & Shah, 2015:1). Since temperature affects the diffusion rate, it is one of the main variables that should be carefully observed (Shahzad *et al*., 2015:2). To imitate the *in vivo* environment, the water bath in which the prepared Franz cells are placed, should be preheated and monitored at 37 °C (skin temperature) (Williams, 2013:685).

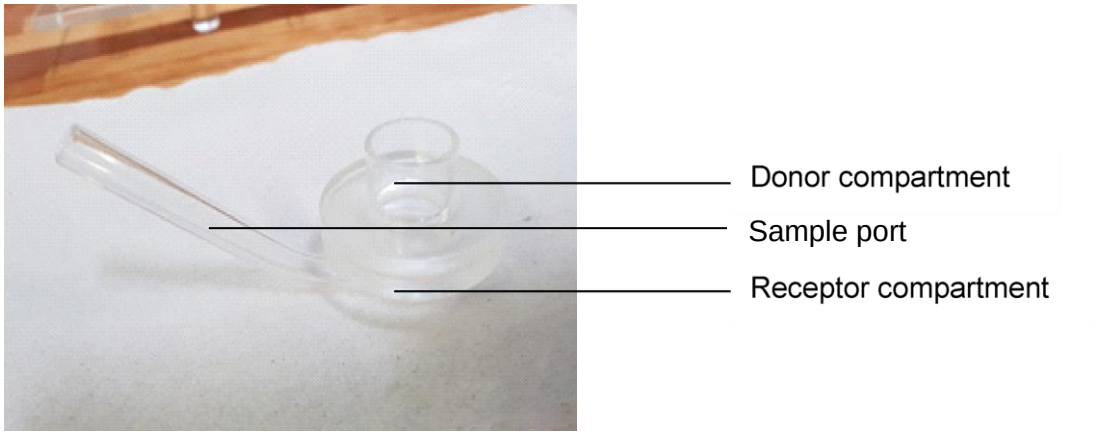


**Figure D.1:** The compartments of a Franz diffusion cell

Franz cells consist of two compartments namely the donor and the receptor compartments (Figure D.1). The donor compartment's function is to hold the formulation (imitates formulation applied on the human stratum corneum). This compartment fits on top of the receptor compartment, which contains the PBS (imitates blood phase underneath skin) (Williams, 2013:683). In between these two phases a membrane or skin sample is placed to complete the imitation (Williams, 2013:683).

### D.2.4.1 Donor phase preparation

Nano-emulsions (**NE1A**, **NE1F**, **NE1Pi** and **NE1Pr**) and nano-emulgels (**NEGA**, **NEGF**, **NEGPi** and **NEGPr**) were utilised as the donor phases during the Franz diffusion cell studies. Placebo formulas (**PNE1** and **PNEG**) were included to serve as a control.

### D.2.4.2 Preparation of PBS (pH 7.4) as receptor phase of the Franz cells

PBS (pH 7.4) was utilised as the receptor phase in diffusion studies, as it is non-toxic to body fluids and cells, and has a pH level similar to that of human blood (OECD, 2011:29). To formulate PBS, 3.0250 g sodium hydroxide (NaOH) was dissolved in 800 ml Milli-Q® water while stirring on a magnetic stirrer. A mass of 13.6497 g potassium dihydrogen orthophosphate ($KH_2PO_4$) was dissolved in 500 ml of Milli-Q® water separately while stirring on a magnetic stirrer. When both solutions were completely dissolved, the NaOH solution was poured into the $KH_2PO_4$ solution, while stirring on a magnetic stirrer. A volume of 700 ml of Milli-Q® water added to the solution to produce a 2 000 ml solution. A Mettler Toledo® pH meter (Mettler Toledo, CU), kitted with a Mettler Toledo® InLab® 410 electrode (Mettler Toledo, CU) was utilised to measure the pH of the newly prepared PBS. The pH was adapted with NaOH to a reading of 7.4.

### D.2.4.3 Membrane release studies

Membrane release studies were performed to investigate if **NE1s** and **NEGs** were able to release statins from within the formula to the receptor phase, under *in vitro* conditions. In membrane release studies a membrane is located between the donor and receptor compartment. The PBS (pH 7.4) and the formulas were placed in preheated Grant® water baths (Grant Instruments, UK), at temperatures of 37 °C and 32 °C, respectively, 1 h prior to the release studies. An additional water bath was preheated at 37 °C (for the prepared Franz cells).


**Figure D.2:** Grant® water bath (Grant Instruments, UK)

The following step was to prepare the Franz cells. Dow Corning® high vacuum grease was carefully smeared on the bottom of the donor compartments and on the top of the receptor compartments, where the two compartments are to be attached. A small magnetic stirrer was placed into each receptor compartment, where after polyvinylidene fluoride (PVDF) (Pall® Life Sciences, Michigan, USA) membranes (25 mm in diameter and a pore size of 0.45 µm) were gently placed on top of this compartment. The receptor compartments were kept in an upright position throughout the experiment. The vacuum greased donor compartments were then fitted on the vacuum greased receptor compartments and the rims of these cells were sealed with vacuum grease. To prevent leakage and ensure these compartments stay intact and secure, horseshoe clamps were fastened over them. Each Franz cell's receptor compartment was filled with 2 ml PBS at pH 7.4 (37 °C), followed by visual inspection to ensure the absence of air bubbles. Each donor compartment was filled with 1 ml of **NE1s** or **NEGs** (32 °C), and enclosed with Parafilm® as well as a plastic lid to secure the formulation. The PBS (pH 7.4) was returned to the water bath (37 °C) and the Franz cells, in their filled order, were placed in

the preheated water bath (37 °C) equipped with a Variomag® magnetic stirring plate (Variomag, USA).


**Figure D.3:** a) Dow Corning® high vacuum grease, b) horseshoe clamp, c) Parafilm®, d) prepared Franz diffusion cell and e) filled Franz diffusion cells placed in the water bath (37 °C) on a Variomag® magnetic stirring plate (Variomag, USA)

The receptor phases were extracted individually via the sampling port in the same order as filled, and receptor compartments were refilled with PBS at pH 7.4 (37 °C). The extraction and refilling of the receptor compartments were performed in 1 h intervals for 6 h. Every hour's extracted content was transferred to separate HPLC vials for analysis.

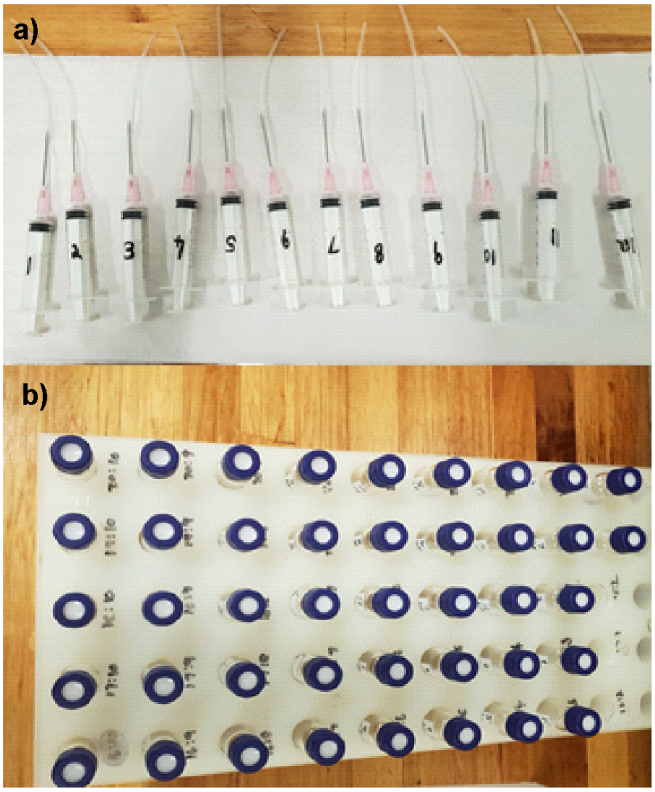


**Figure D.4:** a) Modified syringes for extraction of receptor phase and b) filled marked vials ready for HPLC analysis

A standard solution was prepared prior to each study, by dissolving 20 mg of the involved statin in 100 ml methanol. A volume of 5 ml was then extracted from the standard solution and then diluted with methanol to a volume of 50 ml. A volume of 5 ml was then extracted from the aforementioned dilution and further diluted with methanol to a volume of 50 ml. Volumes of the standard solution, as well as each dilution was withdrawn and transferred to HPLC vials. HPLC injections were performed in duplicate, with injection volumes of 2.5, 5.0, 7.5 and 10.0 µl to obtain a linear regression line for analysis.

### D.2.4.4 *In vitro* skin diffusion studies

#### D.2.4.4.1 Skin collection and ethical aspects

The skin utilised for diffusion studies was Caucasian female skin, attained after post-abdominoplasty surgery. Ethical approval was acquired from the Health Research Ethics Committee of the North-West University (NWU-00111-17-A1-01) for experimental use of human skin (biological material) to perform *in vitro* transdermal drug delivery studies. Signed informed consent forms were obtained from surgeons, as well as donor patients. The collected skin was transported in a cooler and transferred to the freezer (- 20 °C).

#### D.2.4.4.2 Preparation of skin for *in vitro* diffusion studies

The obtained skin was defrosted and spread out on a paper towel, with the skin side (stratum corneum) facing upwards. To remove the skin (with a thickness of roughly 400 µm) a dermatome™ (Zimmer TDS, United Kingdom) was used. To dermatome skin effectively, the dermatome was angled (30 – 45 °) on the skin and moved with constant pressure. The dermatomed skin was spread out on Whatman® filter paper, wrapped with aluminium foil and returned to the freezer (- 20 °C). Prior to skin diffusion studies, dermatomed skin was visually inspected for inadequacies and cut into circles (similar size to Franz cells diffusion area).

#### D.2.4.4.3 *In vitro* skin diffusion studies

Skin diffusion studies can establish the correlation between skin diffusion, the delivery system and the API of the formulation (Ng *et al*., 2010:210). Therefore, this method enables the determination of drug delivery through the skin. For *in vitro* skin diffusion studies, a similar technique was performed as for the membrane release studies (Section D.2.4.3), with the exception that instead of PVDF membranes, single cut circles of dermatomed skin was placed between the donor and the receptor compartments (stratum corneum fronted upwards). The receptor phases were extracted individually after a time period of 12 h, via the sampling port in the same order as filled, and transferred into separately marked HPLC vials. These vials were then placed into the HPLC for testing. A standard solution was also prepared as for membrane release studies. Once HPLC analysis was completed, chromatograms were evaluated and integrated.

#### D.2.4.4.4 Tape stripping

Tape stripping is a valuable procedure to determine if the formulated APIs succeed to the targeted area efficiently, as it assesses if topical delivery of the formulation or API was achieved. After the receptor phases were extracted during *in vitro* skin diffusion studies, the horseshoe clamps on each Franz cell were loosened and the donor compartments were separated from the receptor compartments. Adequate sized Parafilm® was attached to a wooden board and circles of dermatomed skin were removed from receptor compartments and pinned to the Parafilm®. Surplus formulation was dabbed off with paper towel, after which suitable proportioned adhesive tape (3M Scotch® Magic™ Tape) strips were used to detach the SCE. The SCE layer of each of the circles of dermatomed skin was removed with sixteen different tape strips, disposing of the first strip of every tape stripping cycle. The fifteen remaining strips containing the SCE were placed in a single polytop with 5 ml of methanol. The residual skin (ED) was removed from the Parafilm®, cut into pieces and placed into a

separate polytop containing 5 ml methanol. Each Franz cell thus included two polytops one containing the tape strips and the other the pieces of skin. These polytops were stored in the fridge (± 4 °C) for a time period of ± 8 h. Finally, each polytop's content was extracted and filtered (0.45 µm nylon membrane filters) into HPLC vials for analysis.

### D.2.5 Data analysis

The average %released (%) together with the average and median flux (µg/cm$^2$.h) of the selected statins in the **NE1s** and **NEGs** were calculated during membrane release studies. These experiments provided data on whether the statins were released from the formulas and at which rate.

The average %diffused (%), average and median amount per area (µg/cm$^2$) together with the average concentrations (µg/ml) of the selected statins in the **NE1s** and **NEGs** were calculated. The average and median concentrations (µg/ml) of the selected statins in the **NE1s** and **NEGs** were calculated that permeated in the SCE and ED, respectively.

### D.2.6 Statistical data analysis

Statistical analysis was performed on the data of the membrane release studies, as well as the skin diffusion studies with statistical methods such as ANOVA (analysis of variance between the means of more than two groups) and t-tests (to compare the means of two groups). The aforementioned are parametric statistical methods utilised to test a specified hypothesis namely the null hypothesis ($H_0$), usually a hypothesis of indifference. Results of these tests are revealed and analysed with p-values (Consonni, 2017:328).

P-values (calculated probabilities) are commonly used to summarise and conclude data. In simplified terms this value states the likelihood (probability) of the difference in means between groups, to be similar or more significant (extreme) than its experimental value, when the $H_0$ (here no differences in means) of the study is considered as true, utilising a particular statistical model (Consonni, 2017:328). In general, p-values less than 0.05 (chosen significance) reflect a statistical significant result. Thus if the p-value is < 0.05, the $H_0$ is rejected and the alternative hypothesis (opposite of $H_0$) is accepted as true, as acceptable evidence supports the alternative hypothesis and vice versa.

The $H_0$ of this study is stated as no mutual differences between the actual means of the test samples, and the alterative hypothesis, at least one of the test sample's actual mean will differ from these of the other samples.

Statistical data reflecting skewed distributions can be logarithmically transformed in advance to produce distributions near to the normal (Hamada, 2018:16). After an ANOVA was performed and to test for a significant group effect ($p < 0.05$), Tukey's honestly significant difference (HSD) post-hoc test was utilised. This test compares the means of all possible combinations of groups and ranks them categorically (a, b, c, etc.) according to their homogeneity (Hamada, 2018:16). For example, groups ranked in a single category are seen as homogenous as their means show little statistical differences.

### D.3 Results and discussions

#### D.3.1 Solubility

The results of the *n*-octanol and PBS solubility of statins were determined and are tabulated in Table D.1.

**Table D.1:** The average amount of statins (mg/ml) soluble in *n*-octanol and PBS (pH 7.4)

| Statin | Octanol (mg/ml) | PBS (mg/ml) |
|---|---|---|
| Atorvastatin | 9.673 ± 1.246 | 0.596 ± 0.024 |
| Fluvastatin | 11.028 ± 0.603 | 0.529 ± 0.088 |
| Pitavastatin | 37.665 ± 0.498 | 0.452 ± 0.038 |
| Pravastatin | 4.750 ± 0.133 | 0.882 ± 0.003 |

According to literature, atorvastatin has an aqueous solubility of 0.190 mg/ml (PBS at pH 6.8) (Rodde *et al.,* 2014:3) and fluvastatin 0.2 mg/ml (PBS at pH 7.2) (Cayman chemical, 2010:2). In this study, atorvastatin and fluvastatin displayed higher solubility results. However, pitavastatin's (0.5 mg/ml in PBS at pH 7.2) (Cayman chemical, 2014) and pravastatin's (10 mg/ml in PBS at pH 7.2) (Cayman chemical, 2015:4) solubility were higher compared to pitavastatin's and pravastatin's solubility in this study. The differences in solubility values between the experimental and those obtained from the literature can be ascribed to pH differences of PBS (literature pH 6.8 – 7.2 and this study pH 7.4), as well as temperature variations during experiments, which also affects solubility (Lynch *et al.,* 2001:1549). As the required aqueous solubility of an API to effectively penetrate the skin is > 1 mg/ml (Naik *et al.,* 2000:319) atorvastatin, fluvastatin and pitavastatin, which are lipophilic might experience difficulties. However, pravastatin being the nearest to 1 mg/ml could produce a different result.

The results of *n*-octanol solubility indicated that pitavastatin was the most soluble in *n*-octanol, followed by fluvastatin, atorvastatin and pravastatin.

From solubility results, the appropriate amount of statins (mg/ml) required to be added to both pre-saturated phases (PBS and *n*-octanol) during log D determination, could be calculated.

### D.3.2 Octanol buffer distribution coefficient of statins

The log D was determined as the relation of the statin concentration present in the *n*-octanol phase to the statin concentration present in the PBS (buffer phase). The log D of each statin was determined with Equation D.1.

$$Log\ D\ =\ Log\left(\frac{concentration\ statin-octanol}{concentration\ statin\ PBS}\right) \qquad \textbf{Equation D.1}$$

**Table D.2:** Determined log D values of the statins

| Statin | Log D |
|---|---|
| Atorvastatin | 1.238 ± 0.001 |
| Fluvastatin | 1.358 ± 0.003 |
| Pitavastatin | 1.034 ± 0.030 |
| Pravastatin | -0.394 ± 0.005 |

Atorvastatin, fluvastatin and pitavastatin had log D values between 1 and 3, indicating that these statins had log D values within the ideal log D range, which might improve drug delivery (Subedi *et al.,* 2010:339; Williams, 2003:36). Conversely, pravastatin revealed a log D value below 1, therefore incompliant to ideal physiochemical properties regarding log D. This indicates that pravastatin is more hydrophilic than lipophilic (Fong, 2016:6), even though literature indicates that pravastatin is a type 1 statin, which are more lipophilic in nature.

### D.3.3 Membrane release studies

Membrane release studies were performed on each of the statin's **NE1** and **NEG** formula. The results of membrane release studies are tabulated in Table D.3 for all eight formulations. The cumulative amount per area (µg/cm$^2$) of the statin released from each **NE1** and **NEG** formula, performed in 1 h intervals for 6 consecutive hours are presented by the membrane drug release graphs (Figures D.5 to D.21).

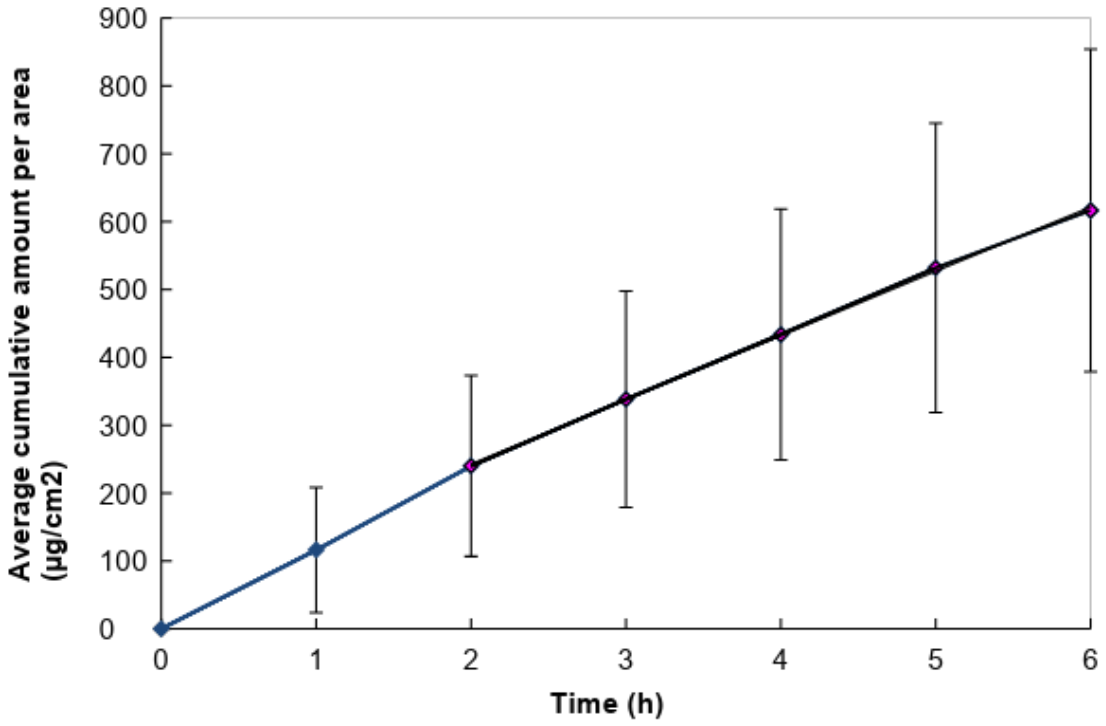


**Figure D.5:** Average cumulative amount per area (µg/cm$^2$) of **NE1A** that was released through the membranes to indicate the average flux between 2 – 6 h (n = 10)

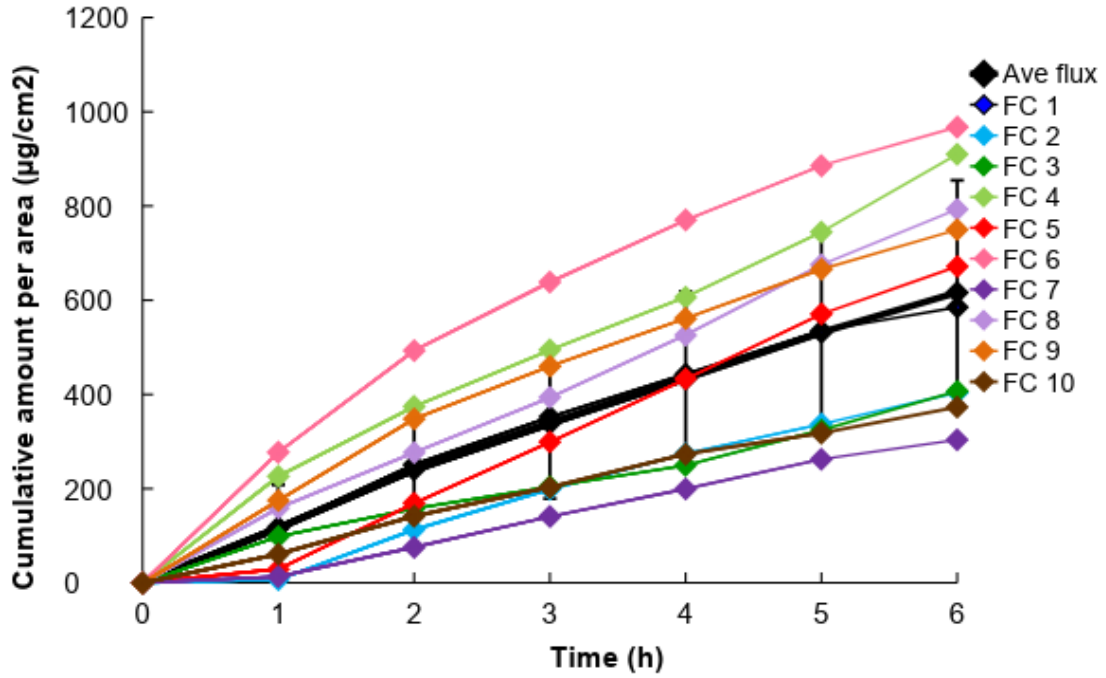


**Figure D.6:** Cumulative amount per area (µg/cm$^2$) of **NE1A** that was released through the membranes of each individual Franz cell over 6 h (n = 10)

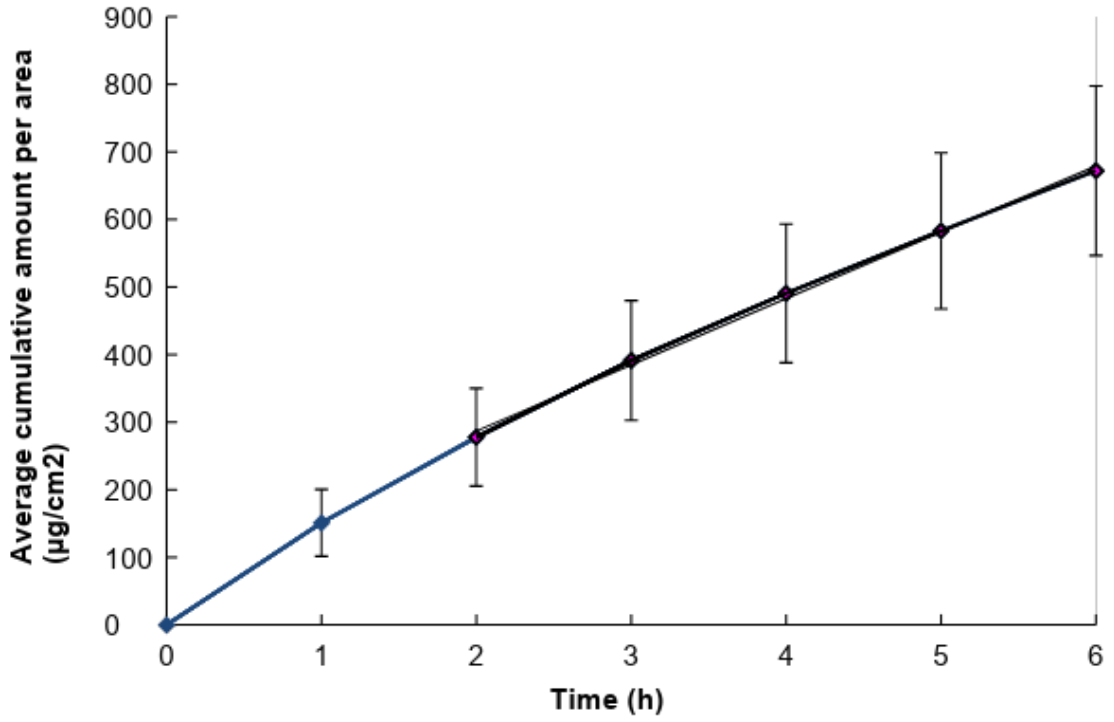


**Figure D.7:** Average cumulative amount per area (µg/cm$^2$) of **NEGA** that was released through the membranes to indicate the average flux between 2 – 6 h (n = 10)

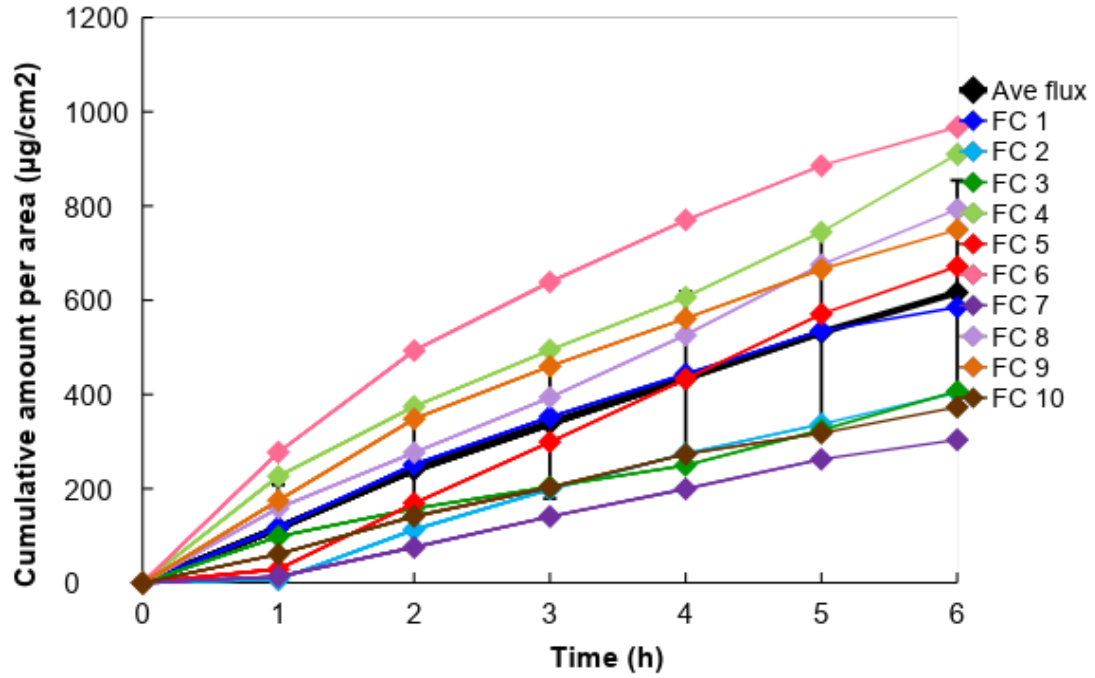


**Figure D.8:** Cumulative amount per area (µg/cm$^2$) of **NEGA** that was released through the membranes of each individual Franz cell over 6 h (n =10)

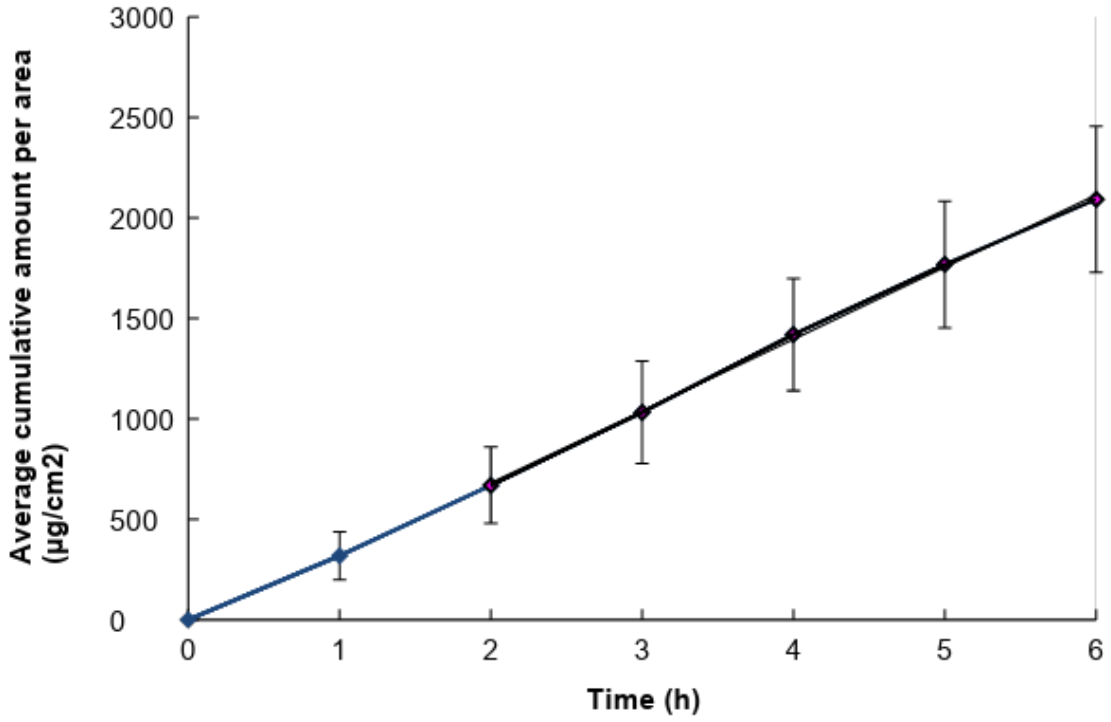


**Figure D.9:** Average cumulative amount per area (µg/cm$^2$) of **NE1F** that was released through the membranes to indicate the average flux between 2 – 6 h (n = 11)

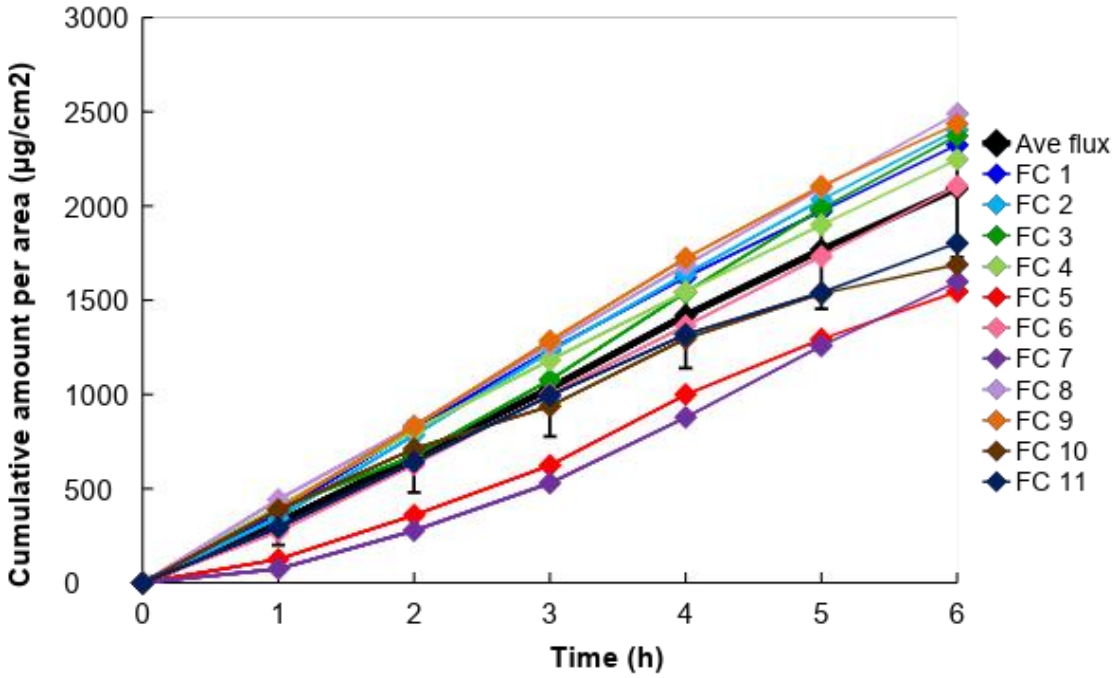


**Figure D.10:** Cumulative amount per area (µg/cm$^2$) of **NE1F** that was released through the membranes each individual Franz cell over 6 h (n = 11)

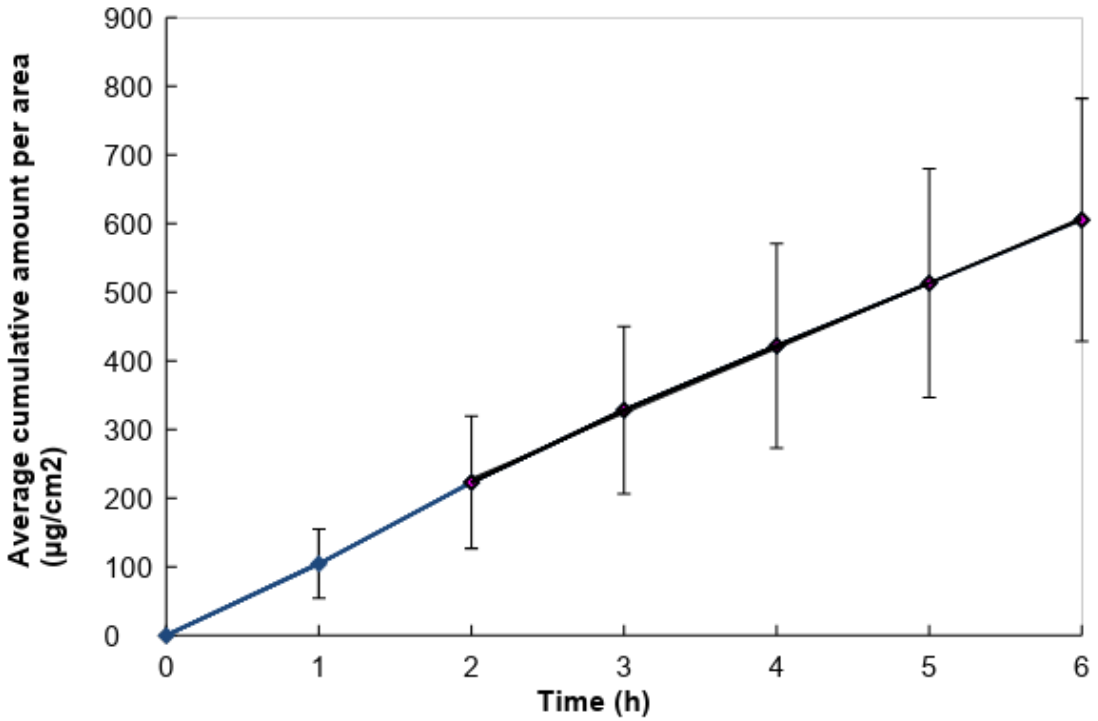


**Figure D.11:** Average cumulative amount per area (µg/cm$^2$) of **NEGF** that was released through the membranes to indicate the average flux between 2 – 6 h (n = 10)

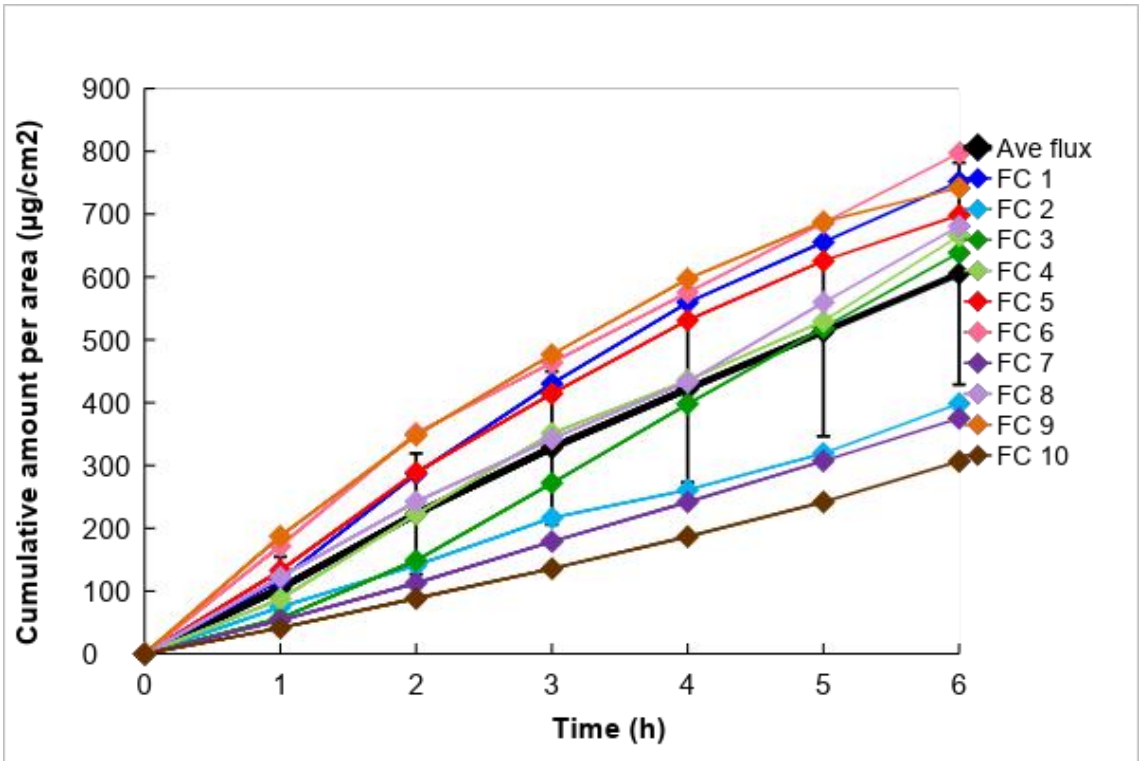


**Figure D.12:** Cumulative amount per area (µg/cm$^2$) of **NEGF** that was released through the membranes of each individual Franz cell over 6 h (n = 10)

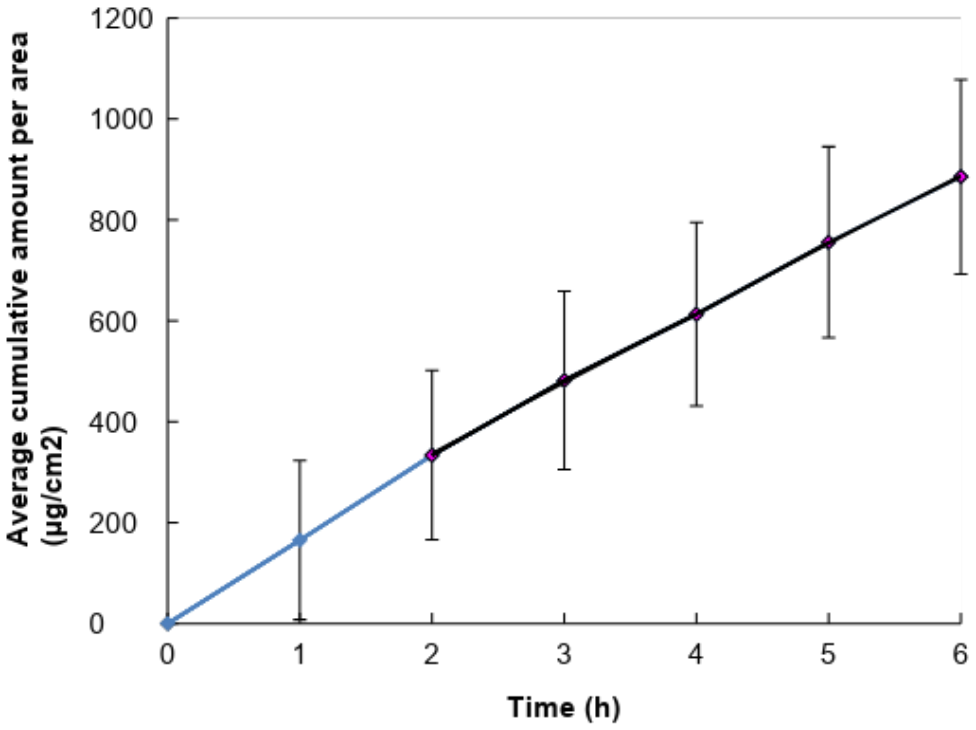


**Figure D.13:** Average cumulative amount per area (µg/cm$^2$) of **NE1Pi** that was released through the membranes to indicate the average flux between 2 – 6 h (n = 9)

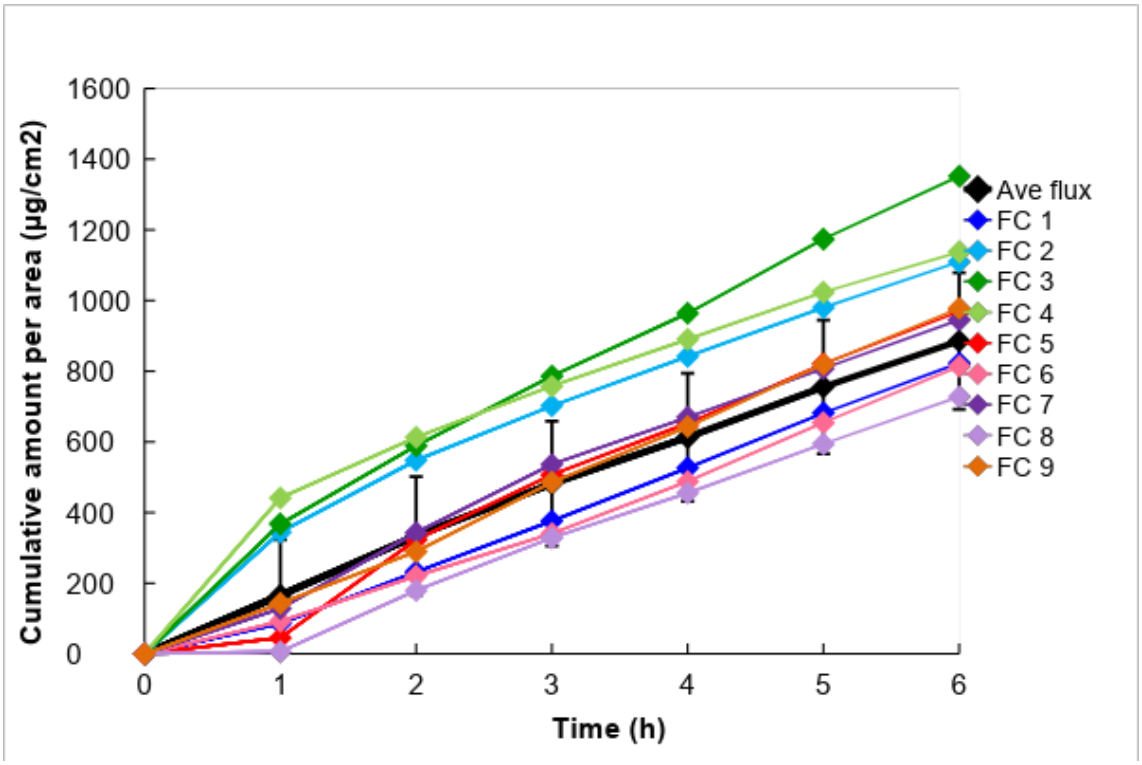


**Figure D.14:** Cumulative amount per area (µg/cm$^2$) of **NE1Pi** that was released through the membranes of each individual Franz cell over 6 h (n = 9)

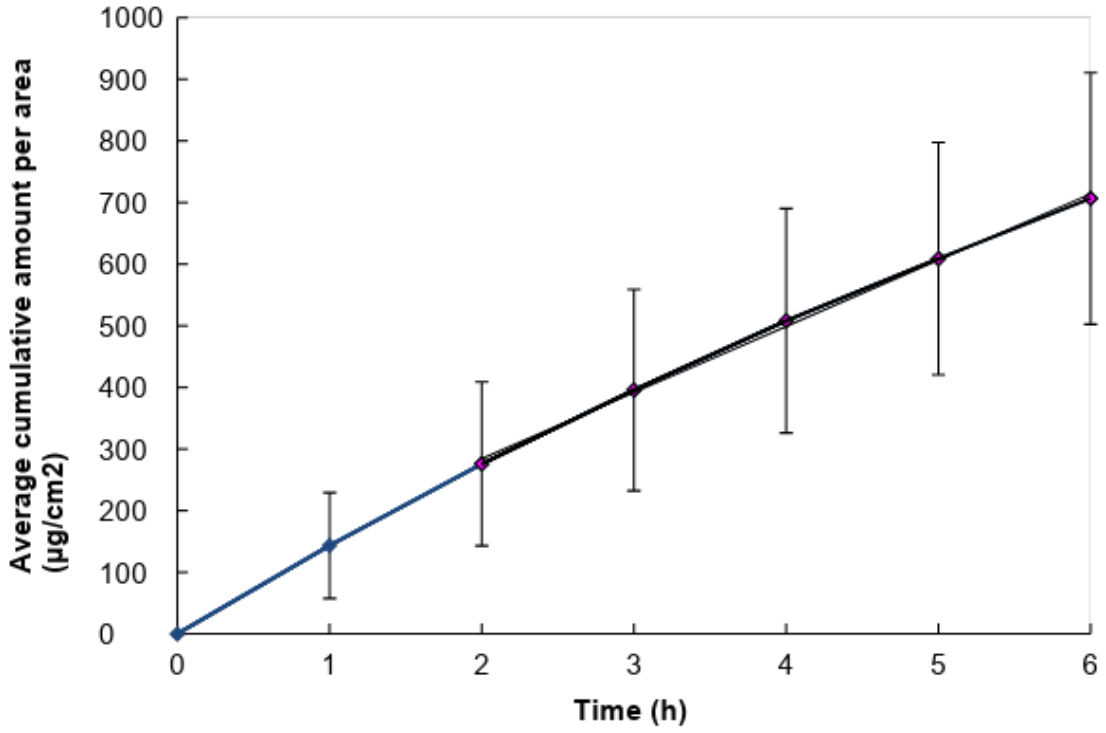


**Figure D.15:** Average cumulative amount per area (µg/cm$^2$) of **NEGPi** that was released through the membranes to indicate the average flux between 2 – 6 h (n = 11)

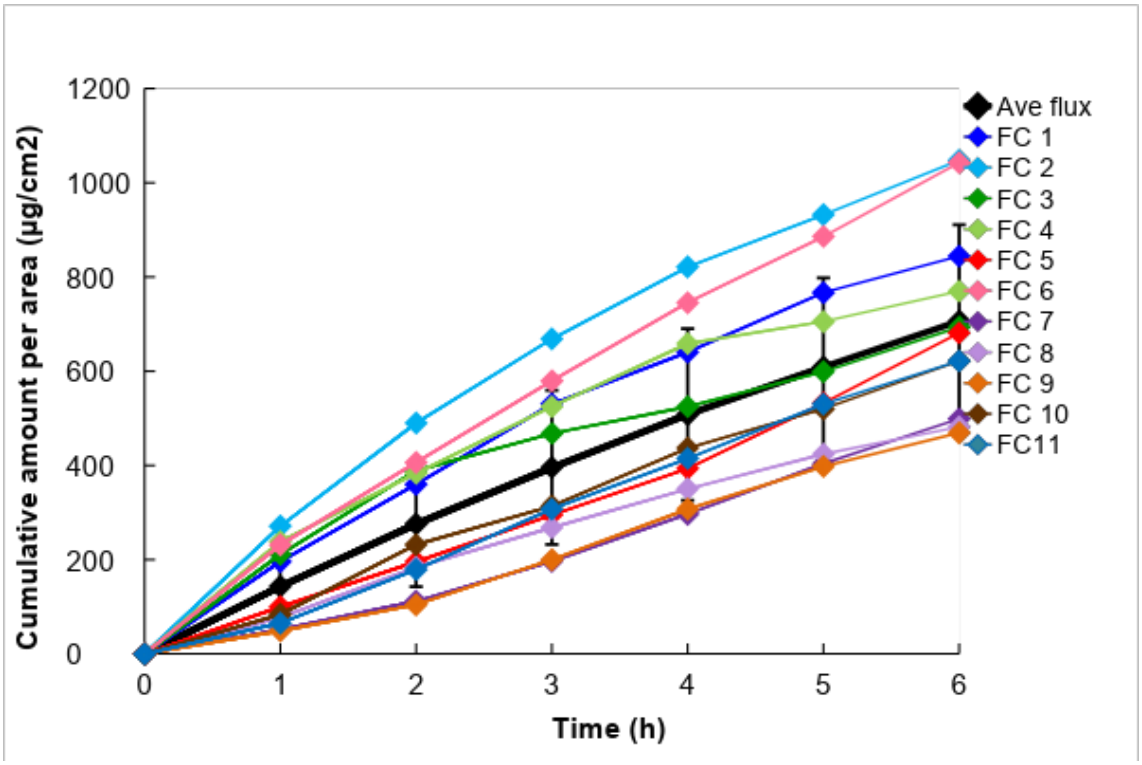


**Figure D.16:** Cumulative amount per area (µg/cm$^2$) of **NEGPi** that was released through the membranes of each individual Franz cell over 6 h (n = 11)

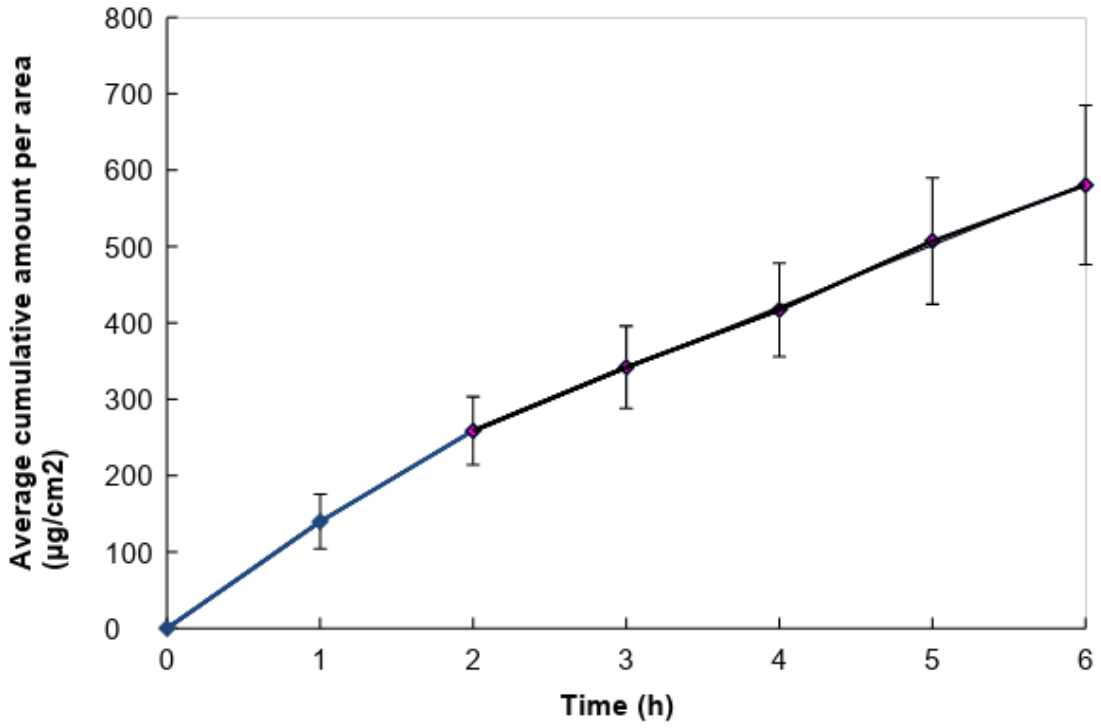


**Figure D.17:** Average cumulative amount per area (µg/cm$^2$) of **NE1Pr** that was released through the membranes to indicate the average flux between 2 – 6 h (n = 8)

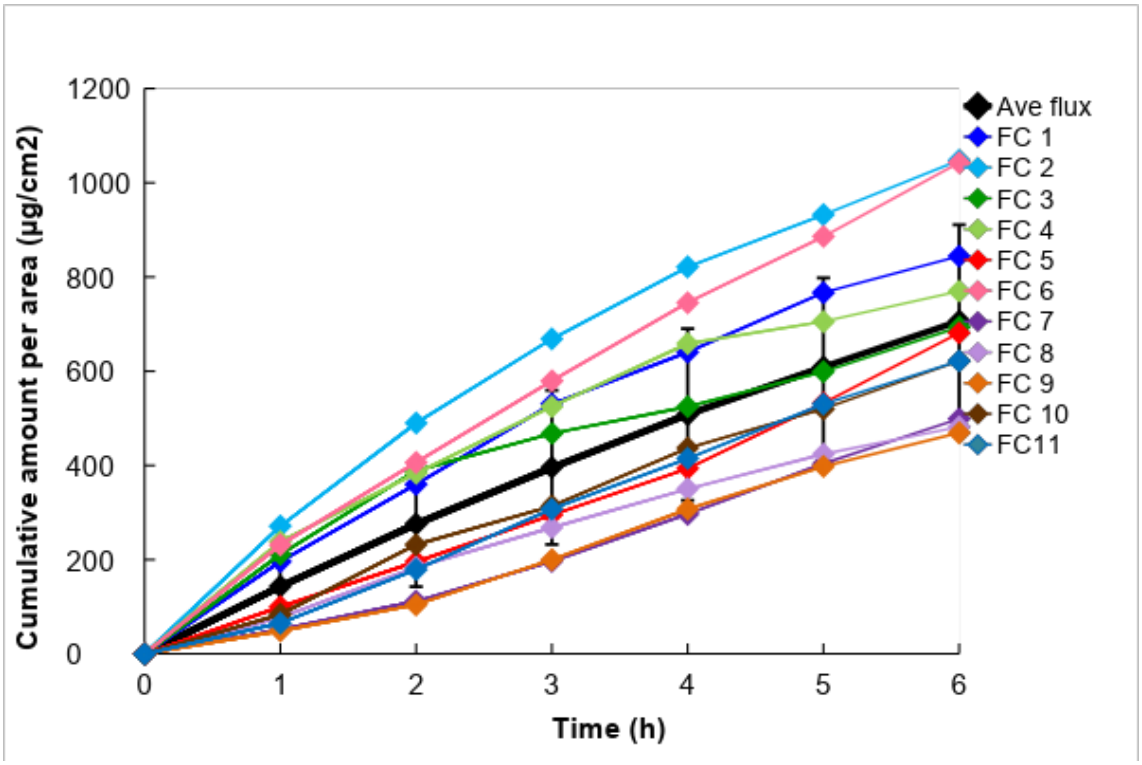


**Figure D.18:** Cumulative amount per area (µg/cm$^2$) of **NE1Pr** that was released through the membranes of each individual Franz cell over 6 h (n = 8)

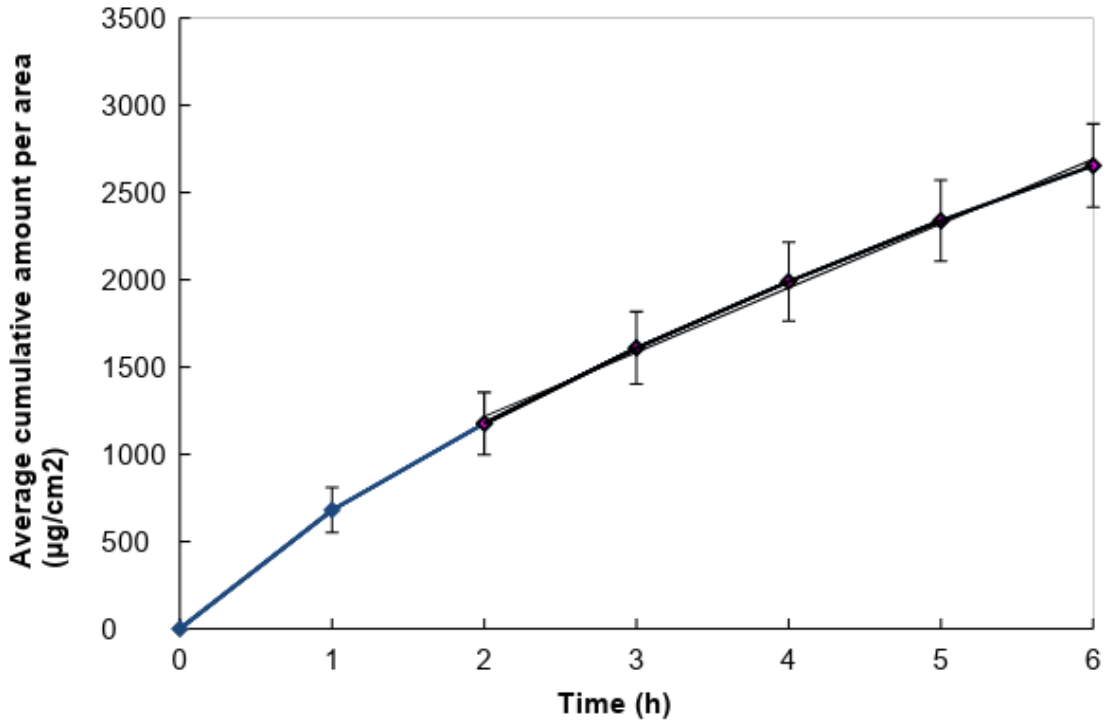


**Figure D.19:** Average cumulative amount per area (µg/cm$^2$) of **NEGPr** that was released through the membranes to indicate the average flux between 2 – 6 h (n = 11)

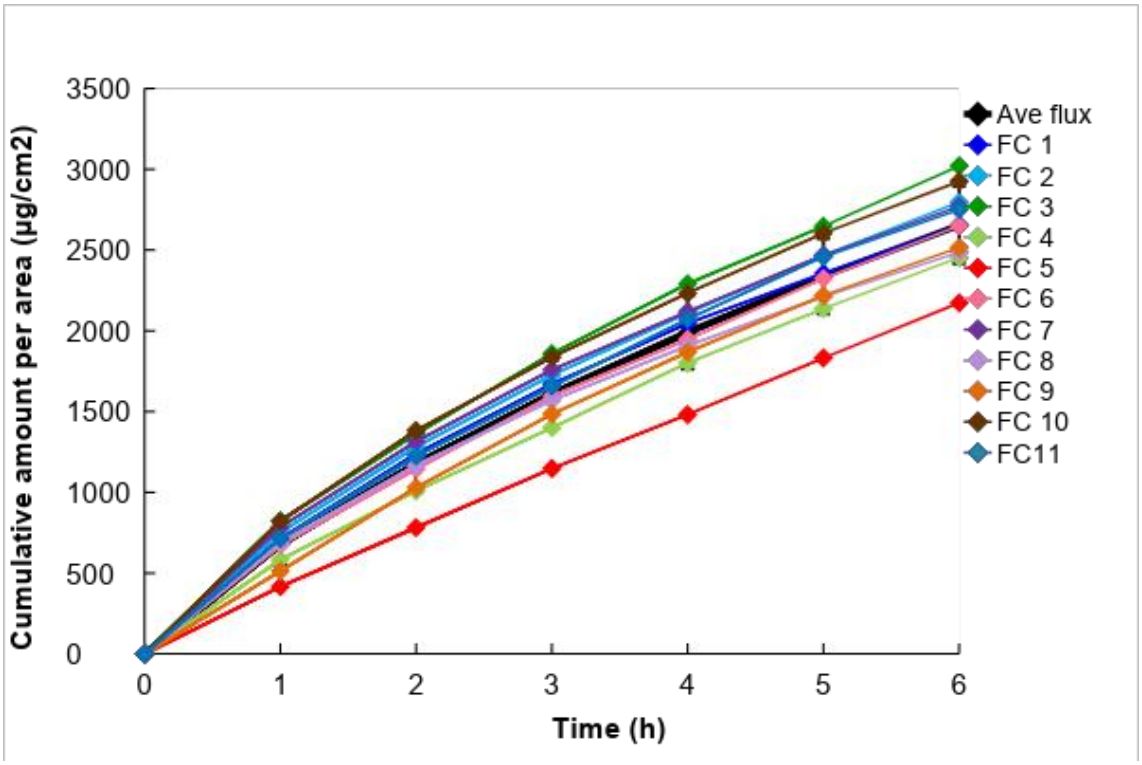


**Figure D.20:** Cumulative amount per area (µg/cm$^2$) of **NEGPr** that was released through the membranes of each individual Franz cells over 6 h (n = 11)

**Table D.3:** The average %released, the average and median flux (µg/cm$^2$.h) for each formula obtained after a 6 h membrane release study

| Preparation | Quantity of Franz cell (n) | Average %released | Average flux (µg/cm$^2$.h) | Median flux (µg/cm$^2$.h) |
|---|---|---|---|---|
| **NE1A** | 10 | 1.658 ± 0.639 | 94.636 ± 31.423 | 102.9833 |
| **NEGA** | 10 | 1.807 ± 0.337 | 98.024 ± 15.509 | 101.1957 |
| **NE1F** | 11 | 5.626 ± 0.976 | 365.192 ± 54.130 | 367.1524 |
| **NEGF** | 10 | 1.628 ± 0.475 | 94.972 ± 24.801 | 111.5819 |
| **NE1Pi** | 9 | 2.646 ± 0.518 | 153.018 ± 18.916 | 150.3878 |
| **NEGPi** | 11 | 1.900 ± 0.549 | 107.475 ± 25.509 | 107.3441 |
| **NE1Pr** | 8 | 1.561 ± 0.281 | 80.883 ± 18.379 | 93.3947 |
| **NEGPr** | 11 | 7.137 ± 0.642 | 368.542 ± 22.241 | 393.3500 |

The flux values (µg/cm$^2$.h) of the **NE1s** and **NEGs** for each statin during the membrane release studies over six consecutive hours were utilised to determine median flux values of each formula.

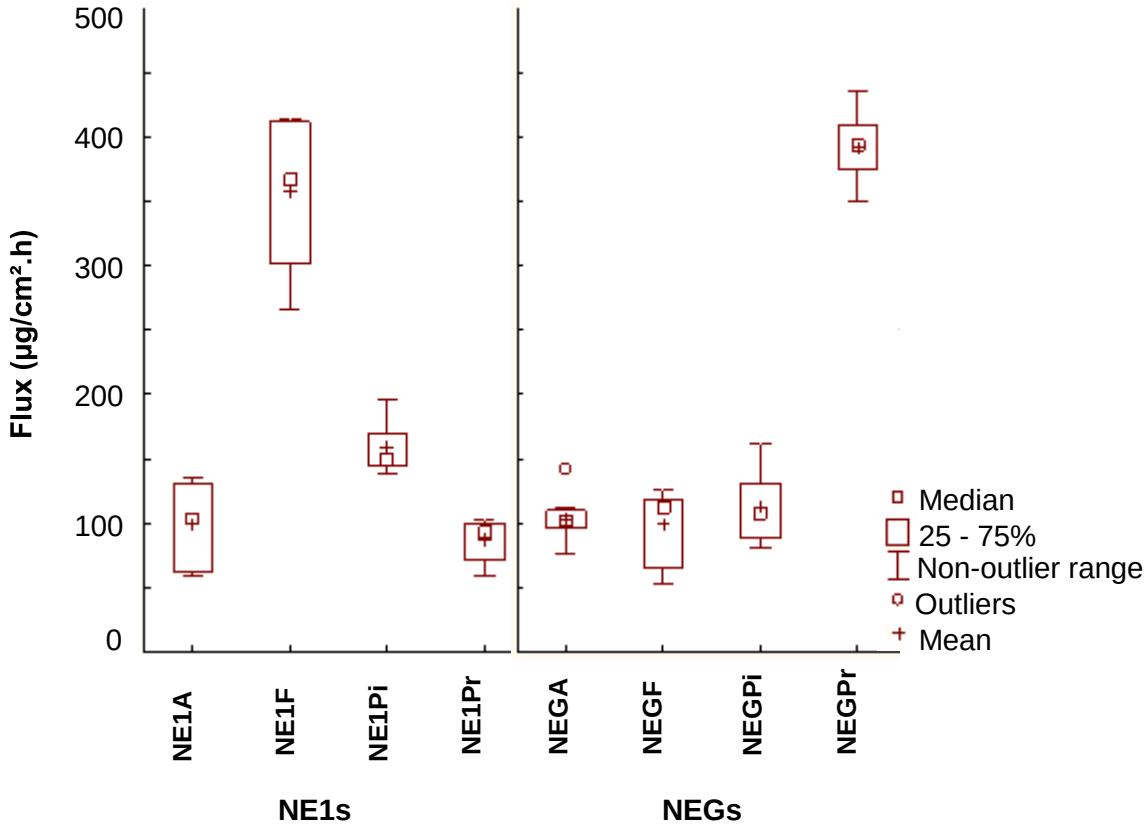


**Figure D.21:** Box-plots of the flux values (µg/cm$^2$.h) of **NE1s** and **NEG** formulas for each statin during the membrane release studies over 6 h

From Table D.3, median flux values present more accurately than the mean (average) flux values, as outliers/extremes affects the average values; hence, medians remain unaffected (Dawson & Trapp, 2004). Consequently, only median flux values will be discussed.

The average %released and the average flux of the **NE1s** and **NEGs**, during the membrane release study, were also analysed. **NE1F** had the highest median flux, followed by **NE1Pi**, **NE1A** and lastly, **NE1Pr**. The median flux values for the **NEGs** were inspected and revealed that the **NEGPr** had the highest median flux value, followed by **NEGF**, **NEGPi** and lastly, **NEGA**. Median flux values for the **NE1s** were higher for **NE1A**, **NE1F** and **NE1Pi**, when compared to its **NEGs**-counterpart. **NEGPr** was the only **NEG** to show a higher median flux value than its **NE1**-counterpart. This can be ascribed to Carbopol® Ultrez 20 being included in the **NE1** formula, this created a hydrophilic environment through which water soluble APIs can diffuse rapidly. In addition, this gelling agent further advanced dissolution of the hydrophilic APIs, resulting in the leakage of API from within the formula and in turn increasing the flux (Dhawan *et al.,* 2014:74).

### D.3.4 *In vitro* skin diffusion studies

Two skin diffusion studies were performed on each of the statins' **NE1** and **NEG**. The results of *in vitro* skin diffusion studies for all eight formulations are presented in Table D.6.

**Table D.4:** The average percentage, average amount and median concentration of statins that diffused through skin from each formula (**NE1** and **NEG**) during the *in vitro* skin diffusion studies after 12 h (n = quantity of Franz diffusion cells)

| Formula | n | Average %diffused (%) | Average concentration diffused (µg/ml) | Average amount per area diffused (µg/cm$^2$) | Median amount per area diffused (µg/cm$^2$) |
|---|---|---|---|---|---|
| **NE1A** | 6 | 0.0002 ± 0.00 | 0.033 ± 0.024 | 0.061 ± 0.047 | 0.0530 |
| **NEGA** | 6 | 0.0003 ± 0.00 | 0.067 ± 0.057 | 0.125 ± 0.108 | 0.0735 |
| **NE1F** | 8 | 0.0004 ± 0.00 | 0.081 ± 0.030 | 0.151 ± 0.072 | 0.1250 |
| **NEGF** | 7 | 0.007 ± 0.01 | 1.383 ± 1.127 | 2.572 ± 2.095 | 2.8070 |
| **NE1Pi** | 6 | 0.001 ± 0.00 | 0.287 ± 0.172 | 0.534 ± 0.335 | 0.3865 |
| **NEGPi** | 6 | 0.002 ± 0.00 | 0.419 ± 0.346 | 0.778 ± 0.657 | 0.7220 |
| **NE1Pr** | 6 | 0.001 ± 0.00 | 0.177 ± 0.134 | 0.329 ± 0.259 | 0.2845 |
| **NEGPr** | 7 | 0.002 ± 0.00 | 0.492 ± 0.316 | 0.916 ± 0.587 | 1.1350 |

The amount per area (µg/cm$^2$) of statins that diffused through the skin of each Franz cell (FC) from the **NE1s** and **NEGs** formulas during *in vitro* skin diffusion studies after 12 h are presented in Figures D.22 to D.29.

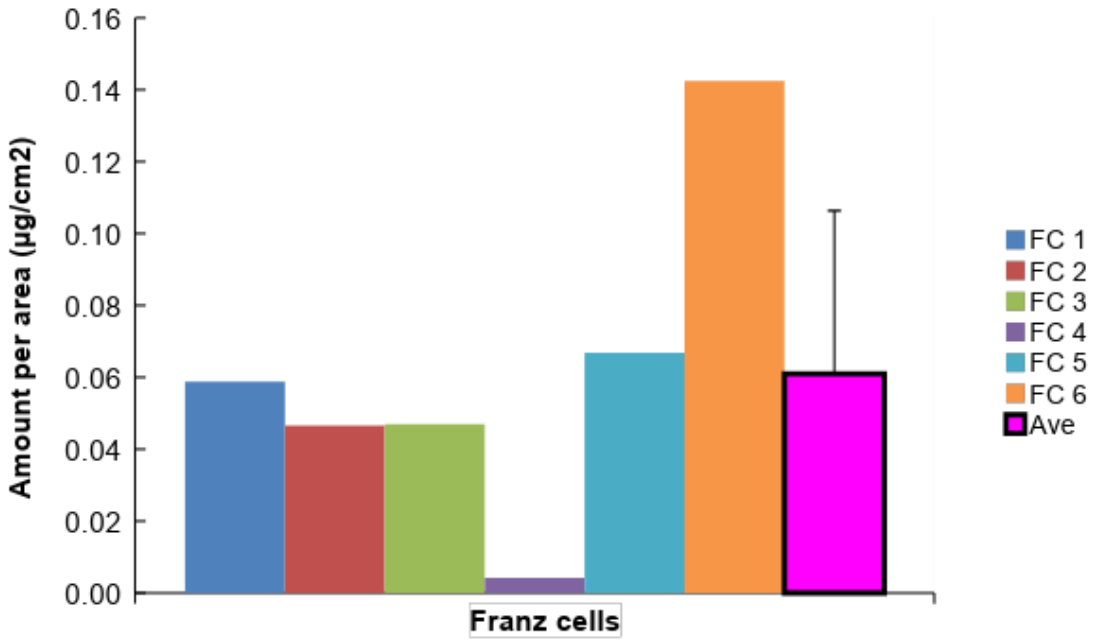


**Figure D.22:** The amount per area of **NE1A** that diffused through skin after a 12 h diffusion study (n = 6)

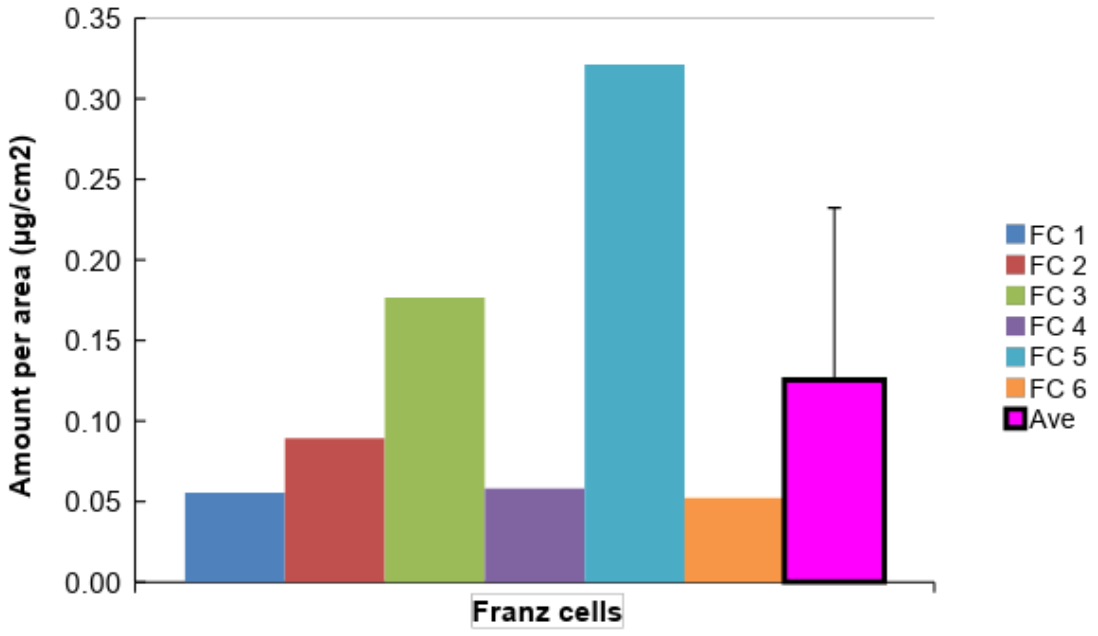


**Figure D.23:** The amount per area of **NEGA** that diffused through skin after a 12 h diffusion study (n = 6)

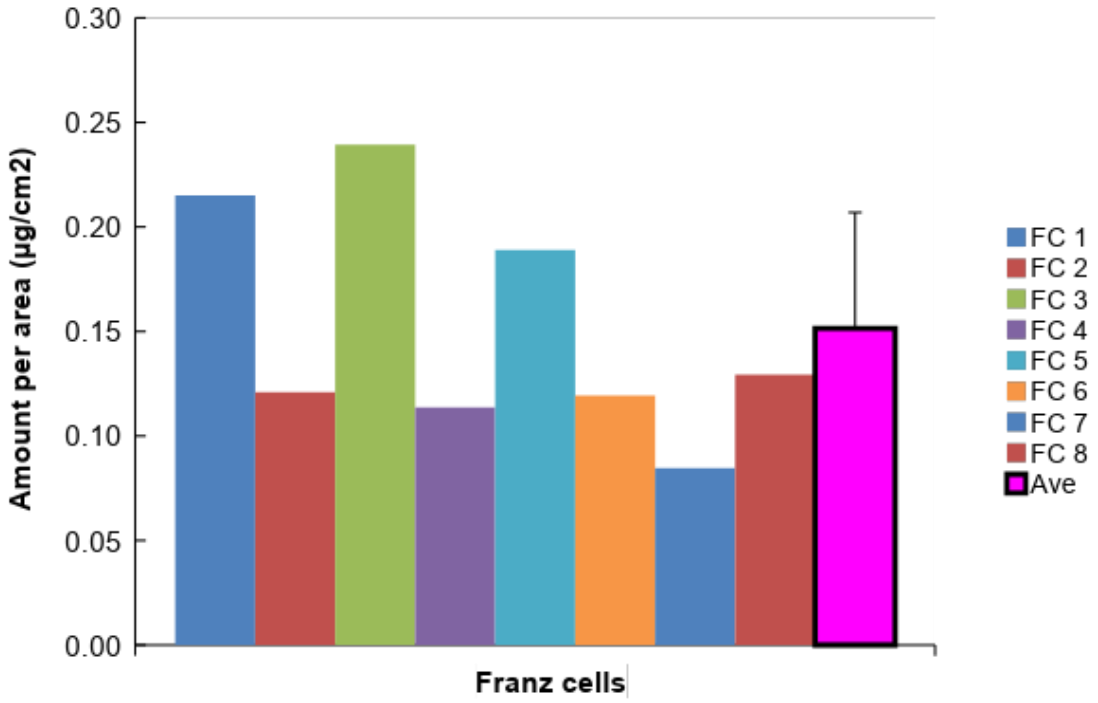


**Figure D.24:** The amount per area of **NE1F** that diffused through skin after a 12 h diffusion study (n = 8)

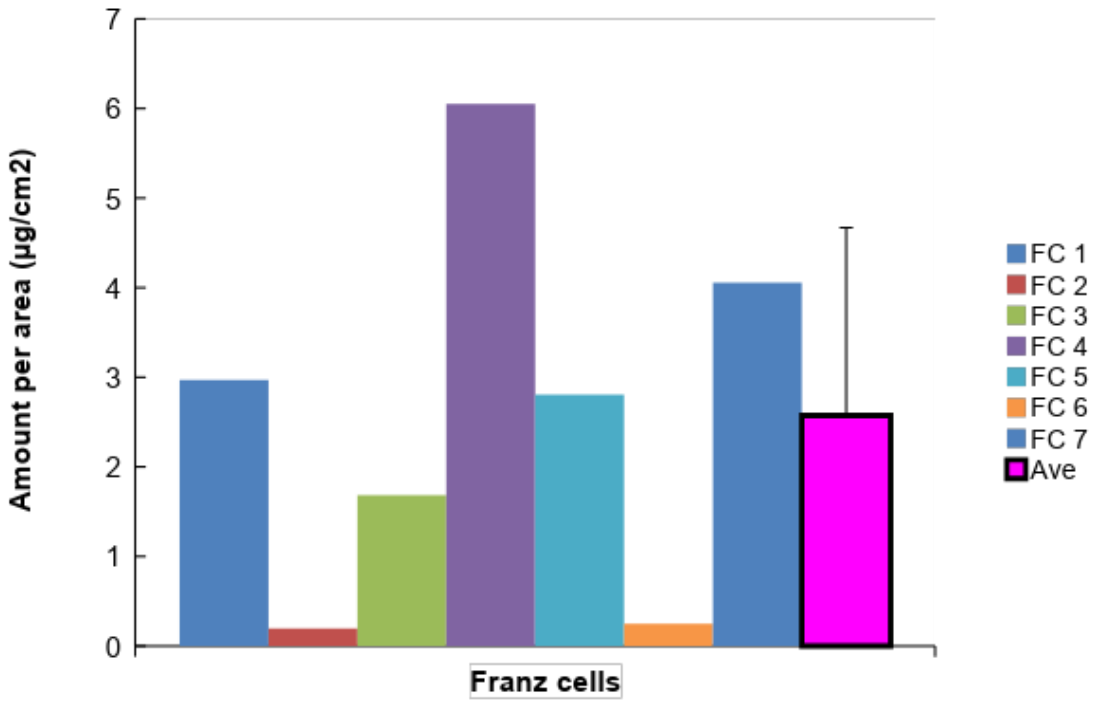


**Figure D.25:** The amount per area of **NEGF** that diffused through skin after a 12 h diffusion study (n = 7)

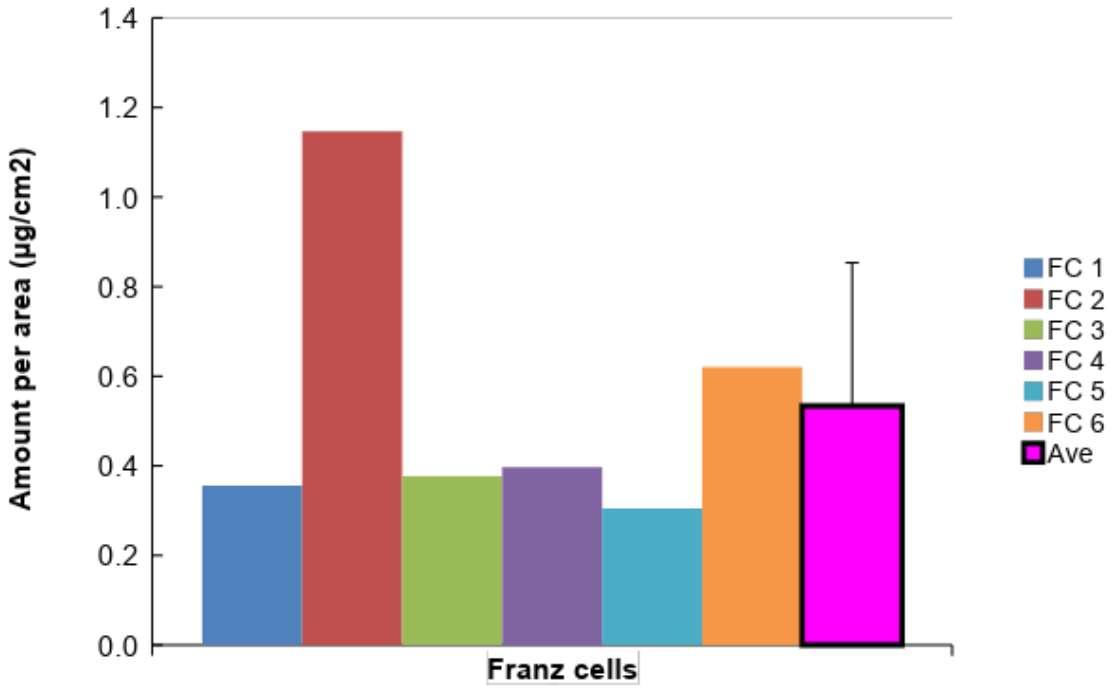


**Figure D.26:** The amount per area of **NE1Pi** that diffused through skin after a 12 h diffusion study (n = 6)

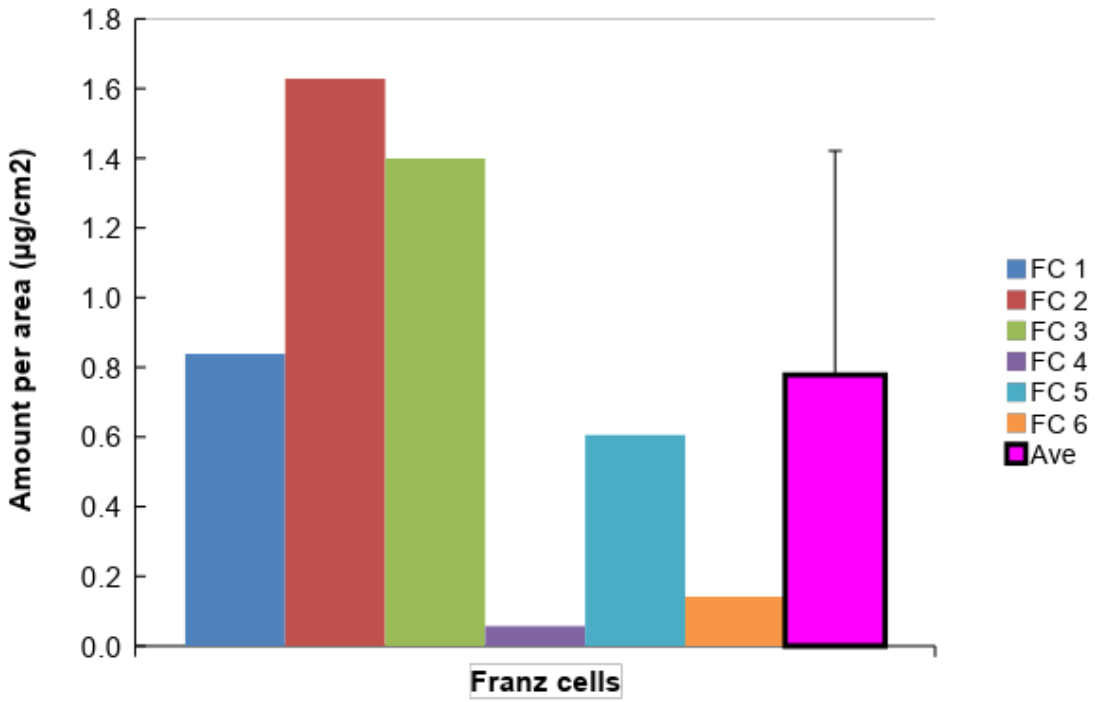


**Figure D.27:** The amount per area of **NEGPi** that diffused through skin after a 12 h diffusion study (n = 6)

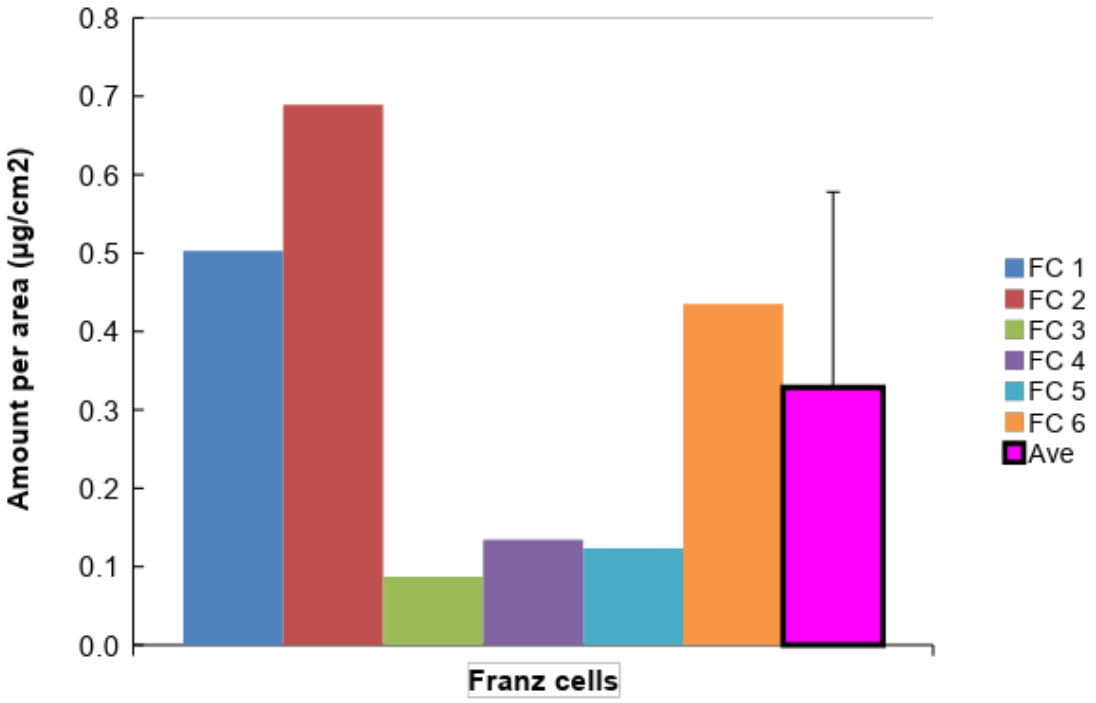


**Figure D.28:** The amount per area of **NE1Pr** that diffused through skin after a 12 h diffusion study (n = 6)

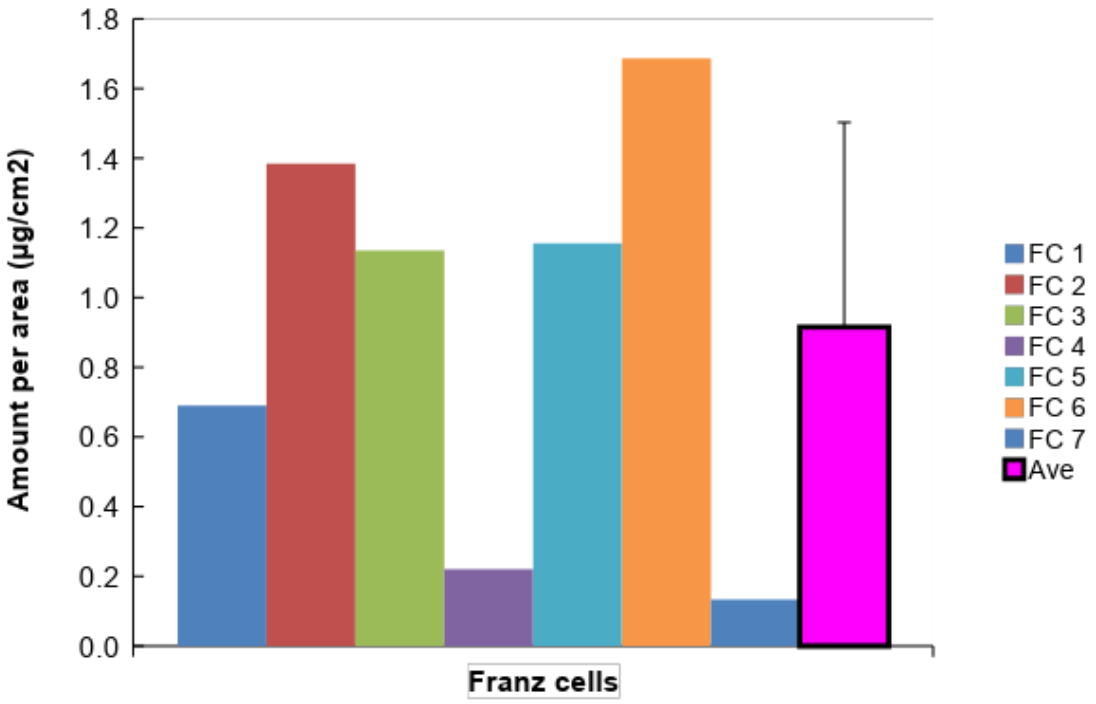


**Figure D.29:** The amount per area of **NEGPr** that diffused through skin after a 12 h diffusion study (n = 7)

The median amount per area diffused presented with more accurate values than the average amount per area diffused, as outliers (extremes) do not affect the medians, but in fact do influence average values (Dawson & Trapp, 2004) (Figure D.30), thus only median amount per area diffused will be discussed.

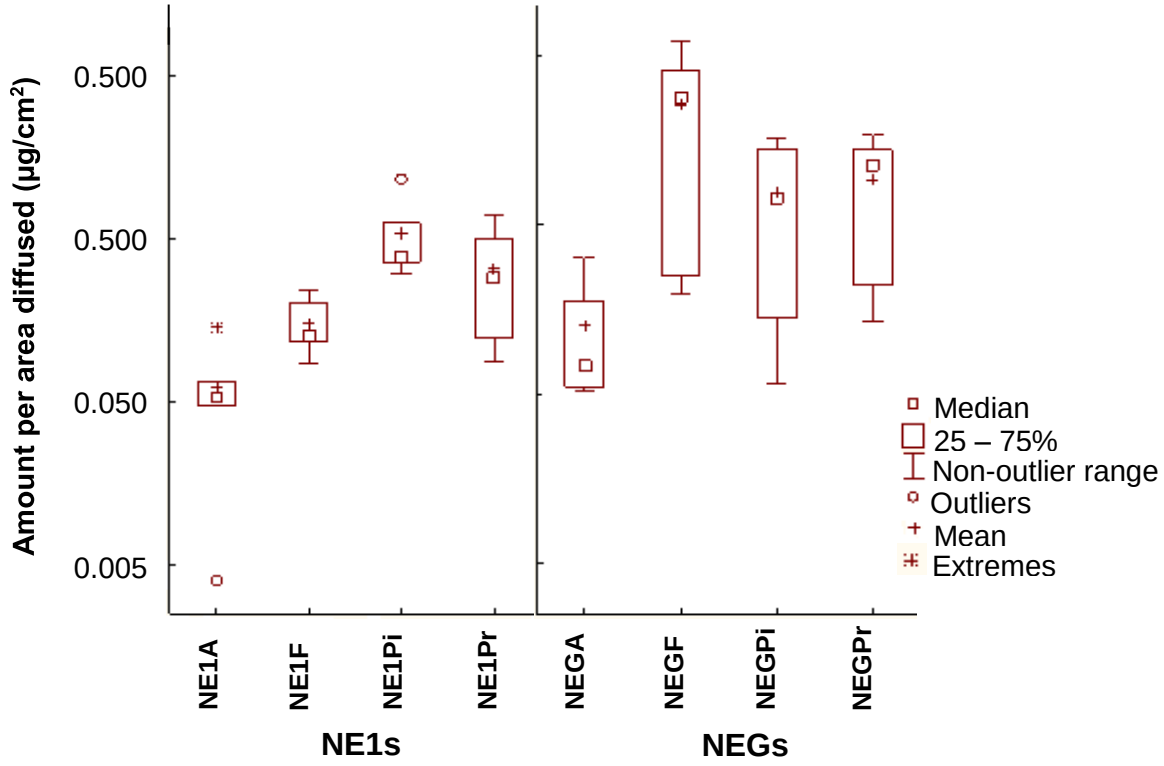


**Figure D.30:** Box-plot presenting the average and median amount per area diffused (µg/cm$^2$) of the **NE1s** and **NEGs** for each statin that diffused through the skin after 12 h

The concentration present in the receptor phase (average concentration diffused (µg/ml) through the skin) of the statins in the **NE1s** and **NEGs** were higher than the LOD and LOQ values (Table A.40 in Appendix A), with the exception of **NE1A** and could therefore be quantified and analysed.

From Table D.4, the median amount per area diffused (µg/cm$^2$) through skin was investigated. It was found that the **NE1** with the highest median amount per area diffused through skin was the **NE1Pi**, followed by **NE1Pr**, **NE1F** and lastly, **NE1A**. The **NEG** with the highest median amount per area diffused was **NEGF**, followed by **NEGPr**, **NEGPi** and lastly, **NEGA**.

The **NE1** of each statin was compared with its **NEG**-counterpart to evaluate the median amount per area diffused through skin. The **NEGs** (**NEGA**, **NEGF**, **NEGPi** and **NEGPr**) prevailed with higher median amounts per area diffused than their **NE1**-counterparts (**NE1A**, **NE1F**, **NE1Pi** and **NE1Pr**). By the inclusion of Carbopol® Ultrez 20 in the **NE1** formula, diffusion through the skin can either be reduced (e.g. aceclofenac), increased (e.g.

amphotericin) or remain unaltered (e.g. diclofenac diethylamine). However, in this study an increase in transdermal diffusion data was observed for **NEGs** (Nastiti *et al.,* 2017:11).

Pitavastatin (**NE1Pi**) was the statin which prevailed with the highest median amount per area diffused through skin for the **NE1s**. **NE1A** and **NEGA** presented with the lowest median amount per area diffused through skin. Hence, when **NE1s** were modified to the **NEGs**, fluvastatin (**NEGF**) dominated all the tested formulas.

According to literature, the plasma concentrations after oral administration of statins are 0.0009 µg/ml atorvastatin (DeGorter *et al.,* 2013:403), 1.7300 µg/ml fluvastatin (Routes, 2004:48), 0.3000 µg/ml pitavastatin (Therapeutic goods administration, 2013:38) and 0.0641 µg/ml pravastatin (Clarke *et al.,* 2011:1947). Compared to transdermal delivery of statins obtained in this study, **NE1A** (0.033 ± 0.024 µg/ml) and **NEGA** (0.067 ± 0.057 µg/ml) had substantially higher concentrations.

For fluvastatin, **NE1F** (0.081 ± 0.030 µg/ml) and **NEGF** (1.383 ± 1.127 µg/ml) showed lower concentrations to reach circulation than that of the oral administration. Concentrations for **NE1Pi** (0.287 ± 0.172 µg/ml) was slightly lower than that of oral administered pitavastatin, hence **NEGPi** (0.419 ± 0.346 µg/ml) concentration was 1.4 times higher than the oral administered pitavastatin. **NE1Pr** (0.177 ± 0.134 µg/ml) and **NEGPr** (0.492 ± 0.316 µg/ml), both displayed significantly higher concentrations compared to the oral route of administration.

### D.3.5 Tape stripping

Tape stripping was performed after completing the *in vitro* skin diffusion study of the **NE1s** and **NEGs** containing a selected statin, to determine the average and median concentration of statins present in the SCE ad ED after 12 h.

**Table D.5:** The average and median concentration (µg/ml) of the statins present in the SCE and ED from each formula (**NE** and **NEG**) during tape stripping (n = quantity of Franz diffusion cells)

| Formula | n | Average concentration in the SCE (µg/ml) | Median concentration in the SCE (µg/ml) | Average concentration in the ED (µg/ml) | Median concentration in the ED (µg/ml) |
|---|---|---|---|---|---|
| **NE1A** | 6 | 7.275 ± 2.584 | 7.0865 | 46.026 ± 58.593 | 24.5545 |
| **NEGA** | 6 | 0.935 ± 0.607 | 0.7189 | 4.350 ± 2.079 | 3.8193 |
| **NE1F** | 8 | 0.374 ± 0.124 | 0.4148 | 3.078 ± 2.147 | 2.6555 |
| **NEGF** | 7 | 0.482 ± 0.469 | 0.3871 | 1.391 ± 0.948 | 1.0510 |
| **NE1Pi** | 6 | 2.446 ± 1.728 | 1.6720 | 16.612 ± 18.581 | 6.4808 |
| **NEGPi** | 6 | 1.475 ± 1.243 | 1.2155 | 8.804 ± 1.942 | 9.7714 |
| **NE1Pr** | 6 | 1.355 ± 0.941 | 1.0540 | 4.350 ± 2.079 | 2.4706 |
| **NEGPr** | 7 | 1.475 ± 0.610 | 1.5076 | 2.589 ± 1.887 | 1.8380 |

The concentration (µg/ml) of the statins that was delivered topically (SCE and ED) from the **NE1s** and **NEGs** are presented in Figures D.31 to D.46.

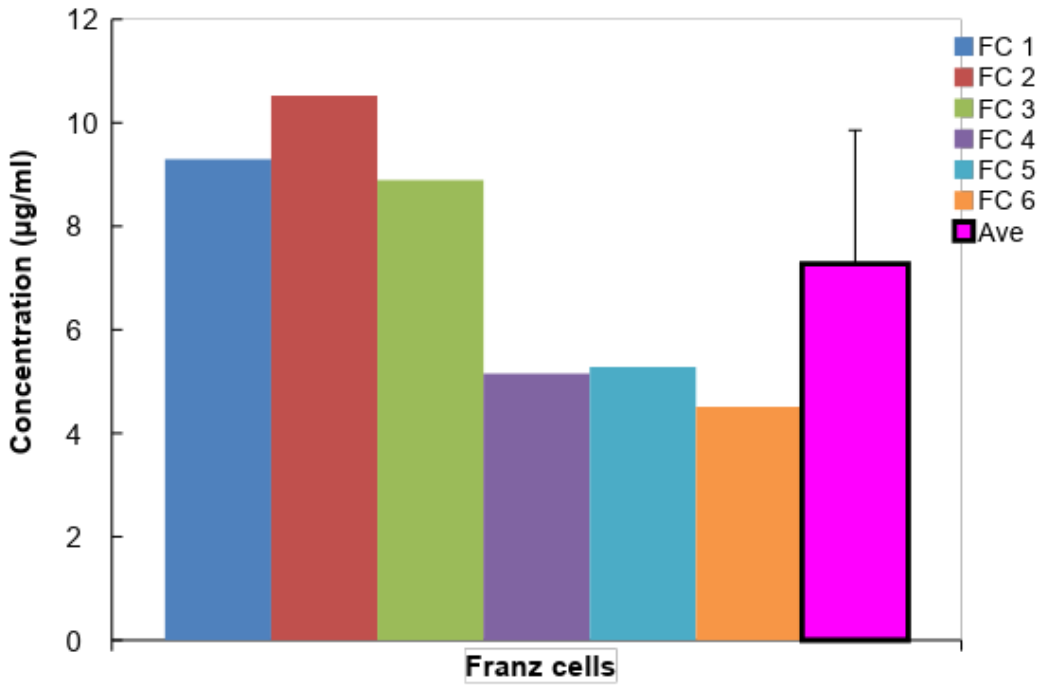


**Figure D.31:** The concentration (µg/ml) of **NE1A** present in the SCE after 12 h

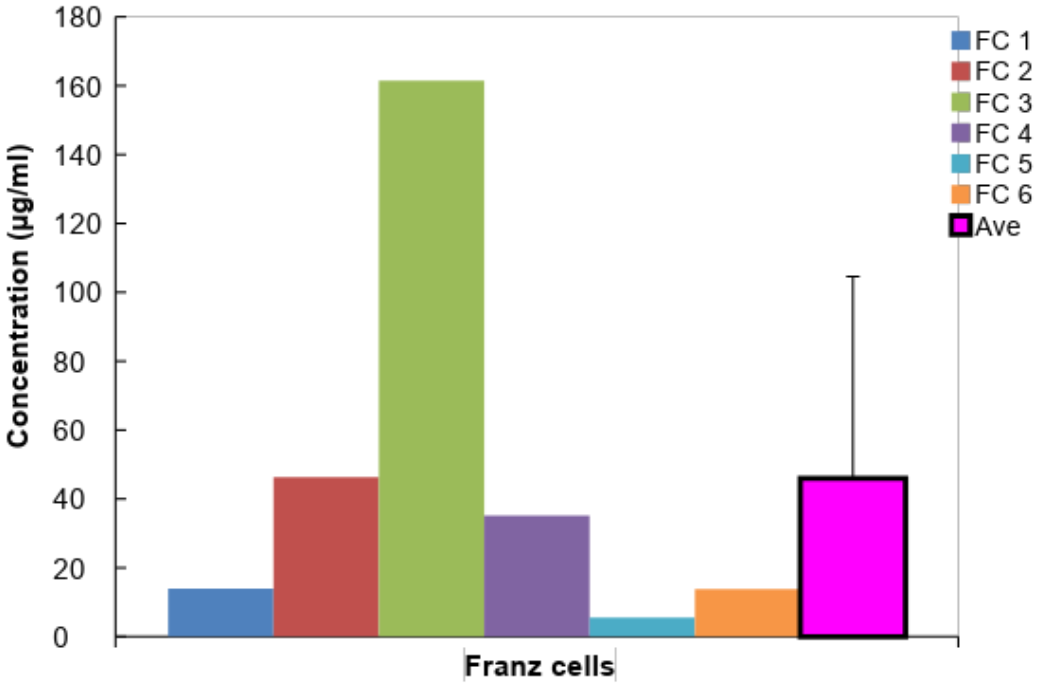


**Figure D.32:** The concentration (µg/ml) of **NE1A** present in the ED after 12 h

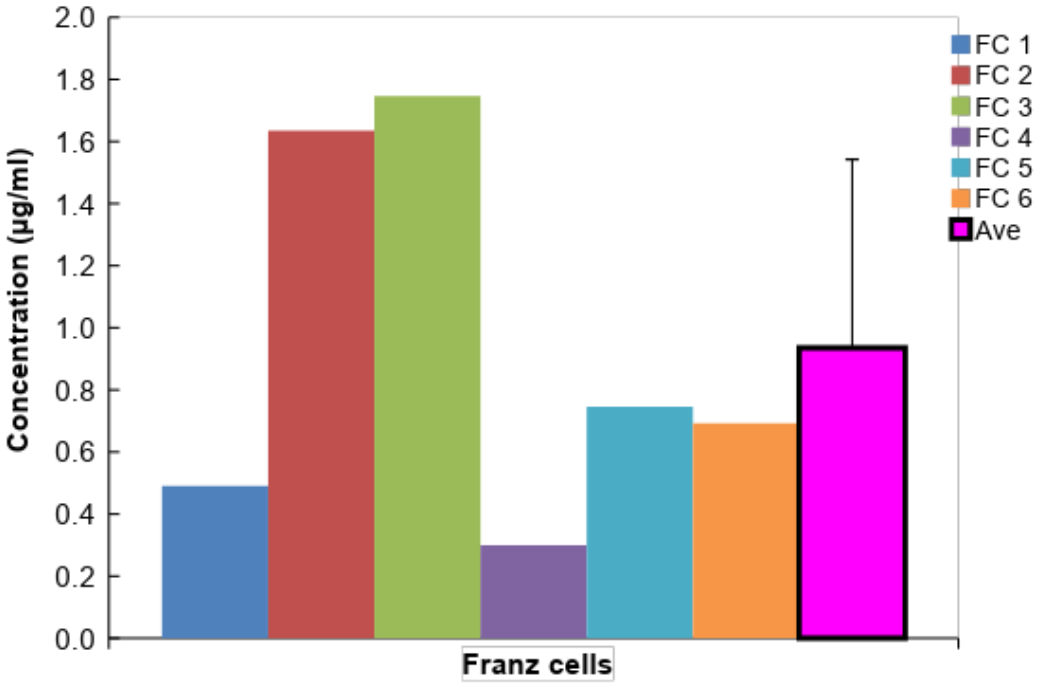


**Figure D.33:** The concentration (µg/ml) of **NEGA** present in the SCE after 12 h

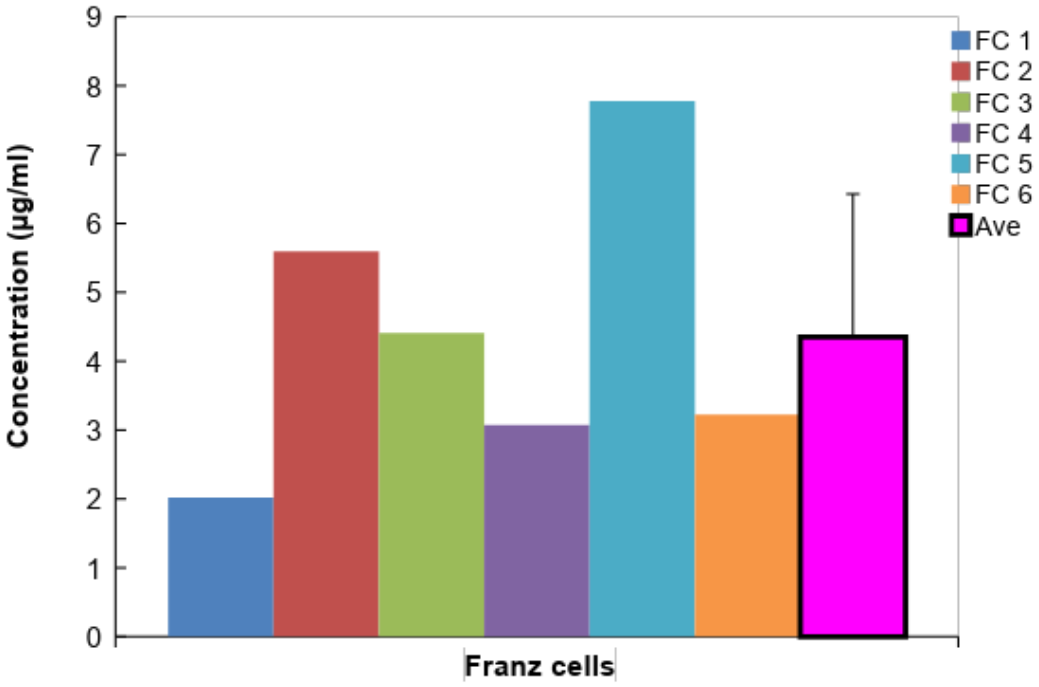


**Figure D.34:** The concentration (µg/ml) of **NEGA** present in the ED after 12 h

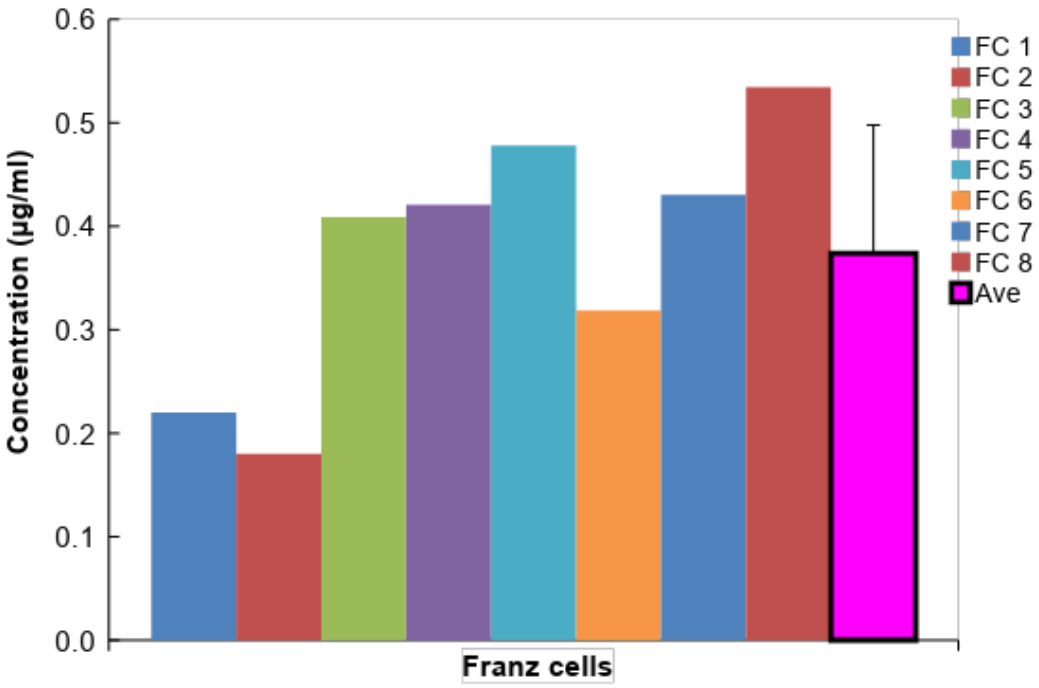


**Figure D.35:** The concentration (µg/ml) of **NE1F** present in the SCE after 12 h

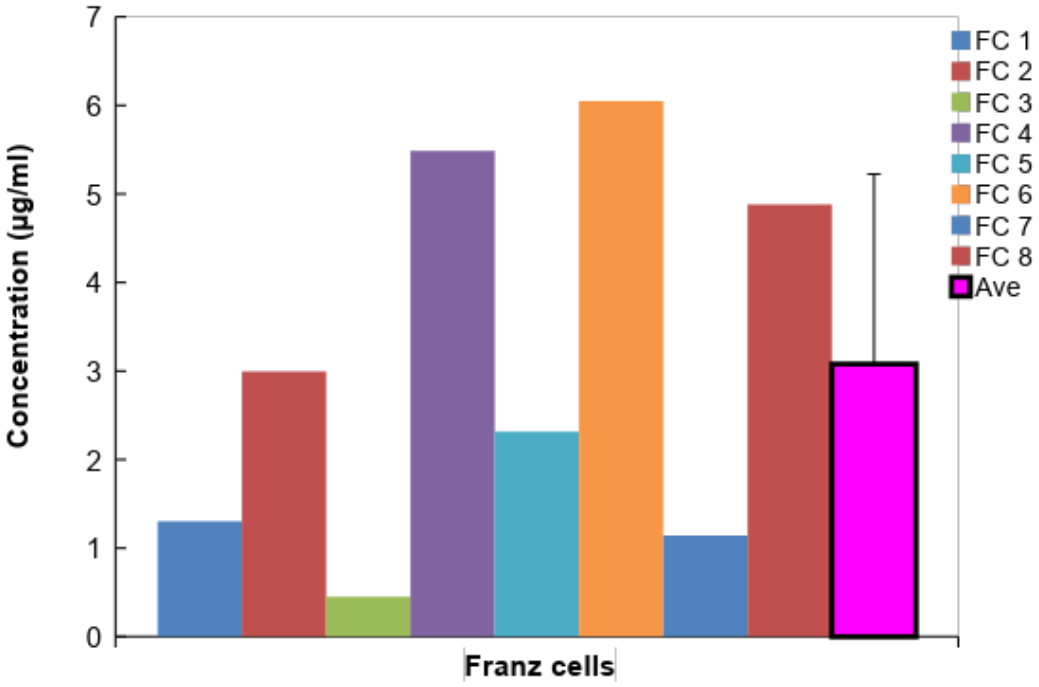


**Figure D.36:** The concentration (µg/ml) of **NE1F** present in the ED after 12 h

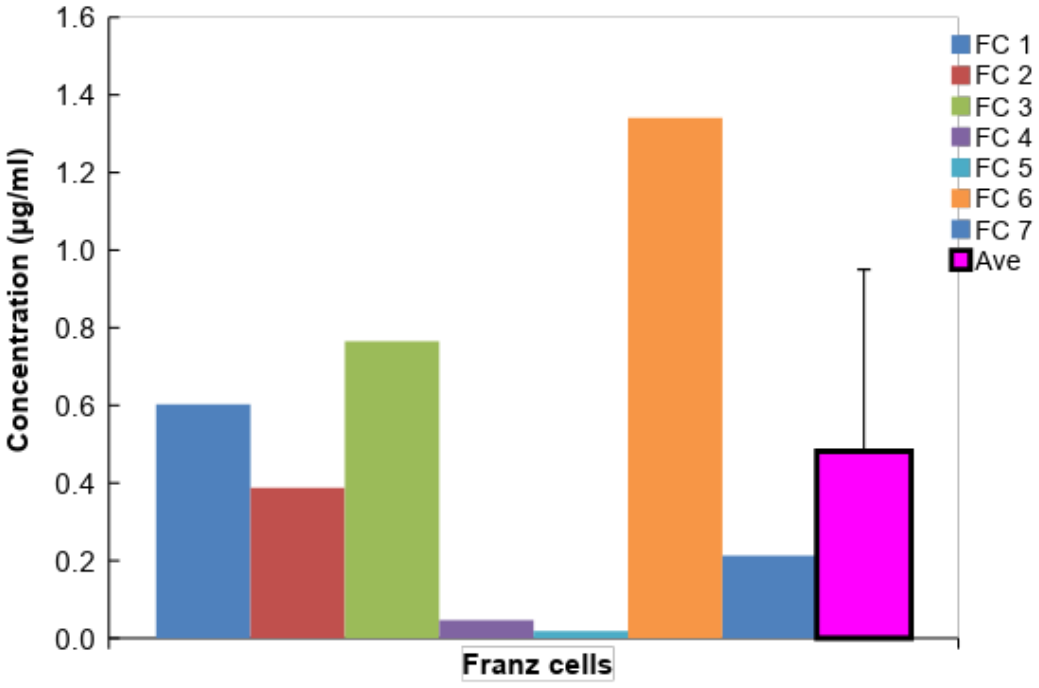


**Figure D.37:** The concentration (µg/ml) of **NEGF** present in the SCE after 12 h

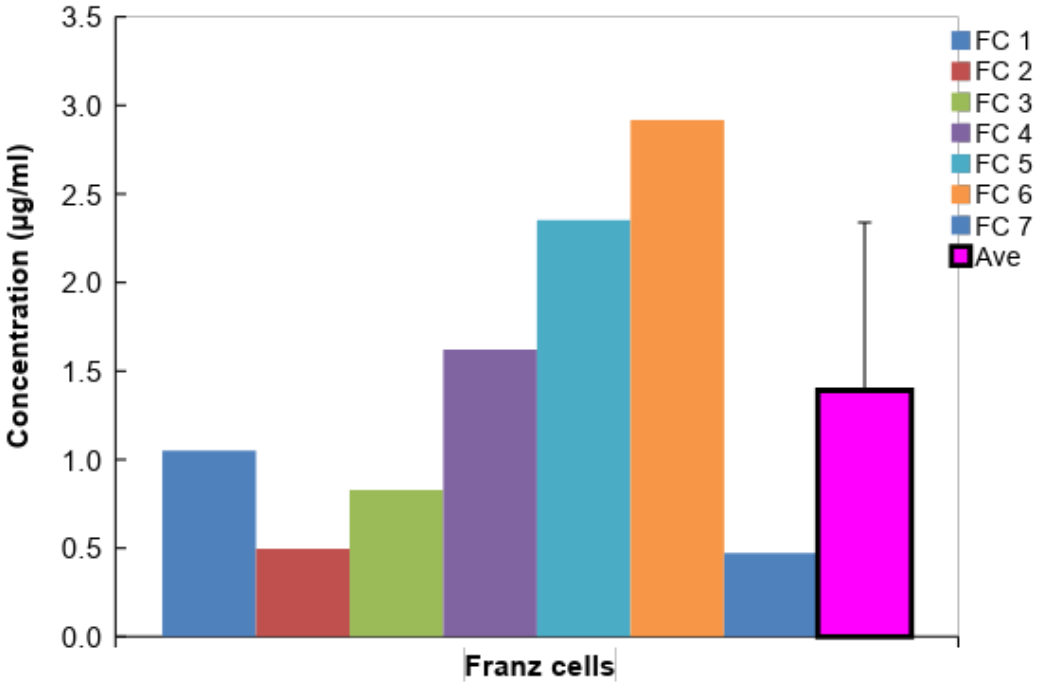


**Figure D.38:** The concentration (µg/ml) of **NEGF** present in the ED after 12 h

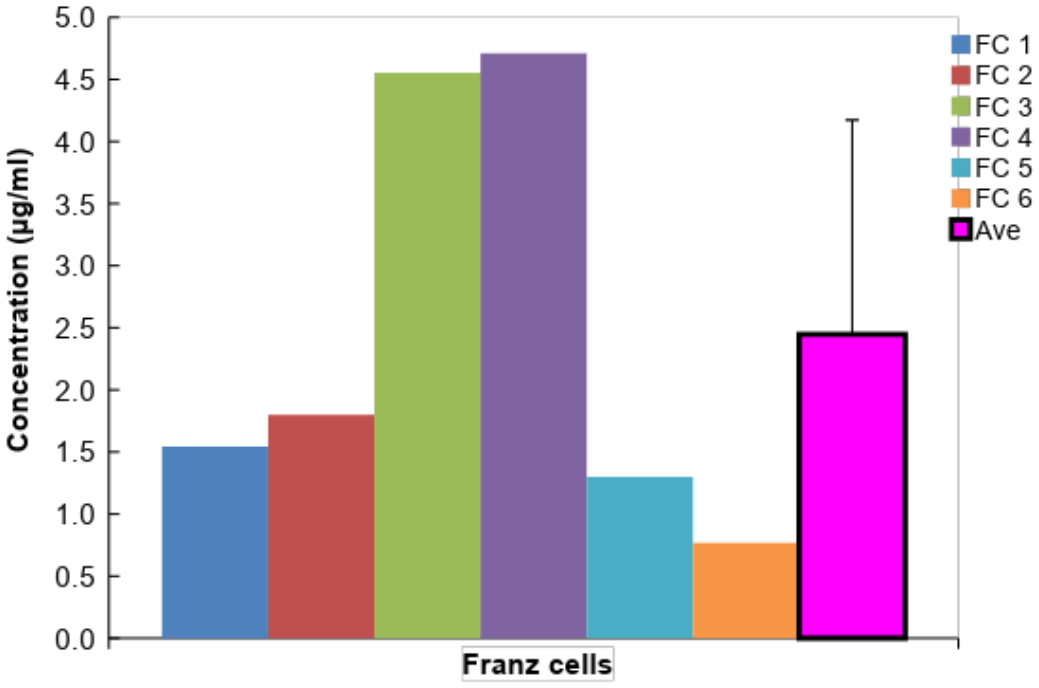


**Figure D.39:** The concentration (µg/ml) of **NE1Pi** present in the SCE after 12 h

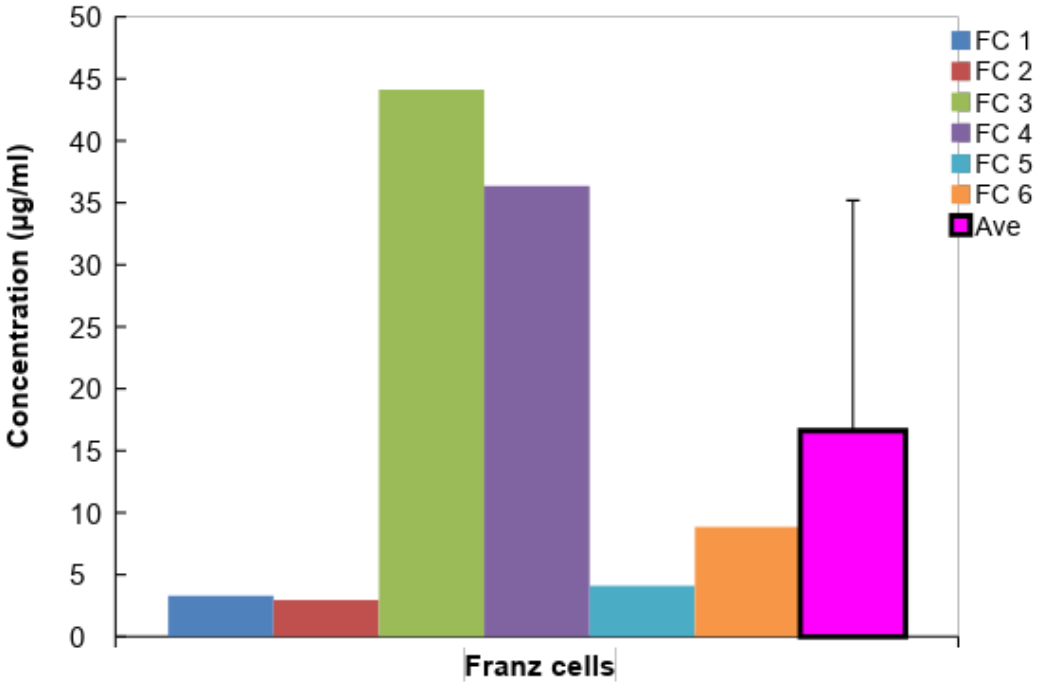


**Figure D.40:** The concentration (µg/ml) of **NE1Pi** present in the ED after 12 h

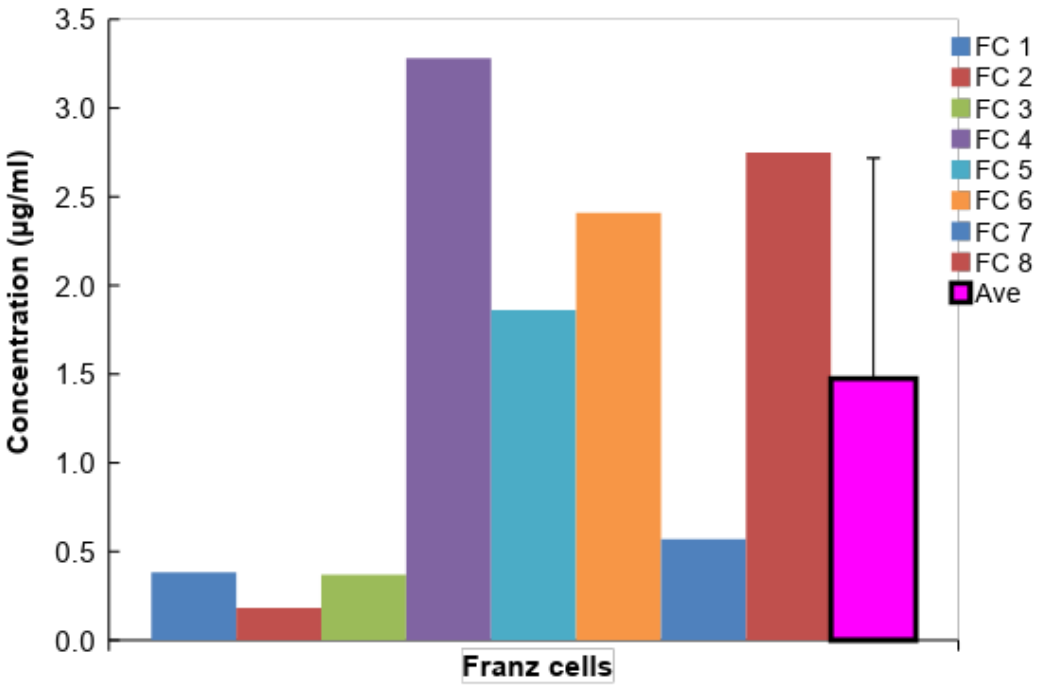


**Figure D.41:** The concentration (µg/ml) of **NEGPi** present in the SCE after 12 h

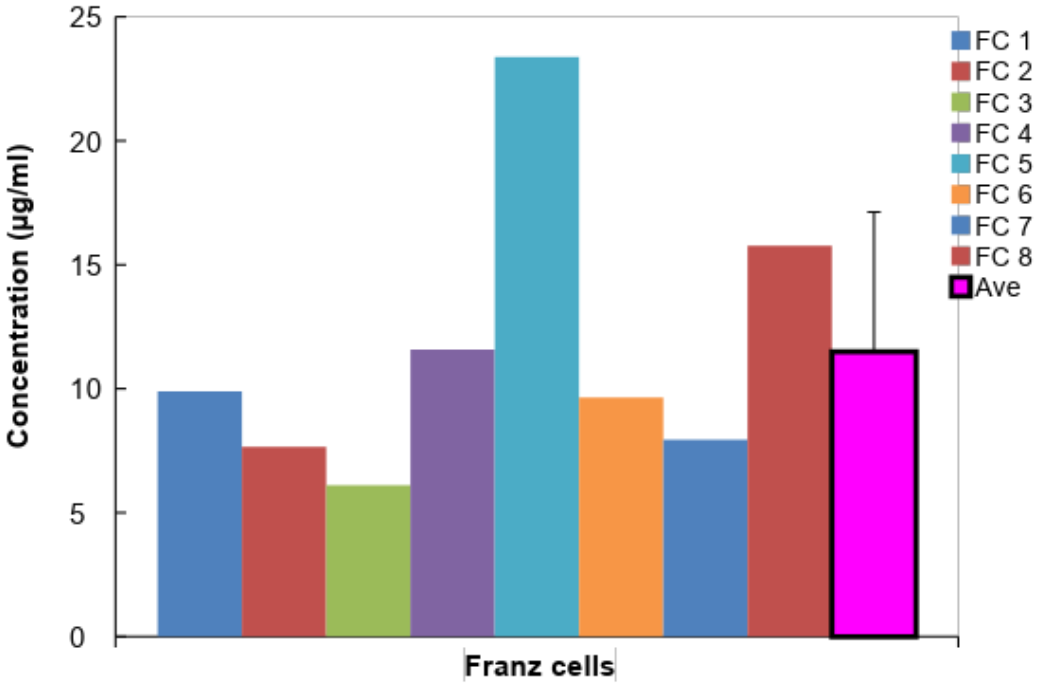


**Figure D.42:** The concentration (µg/ml) of **NEGPi** present in the ED after 12 h

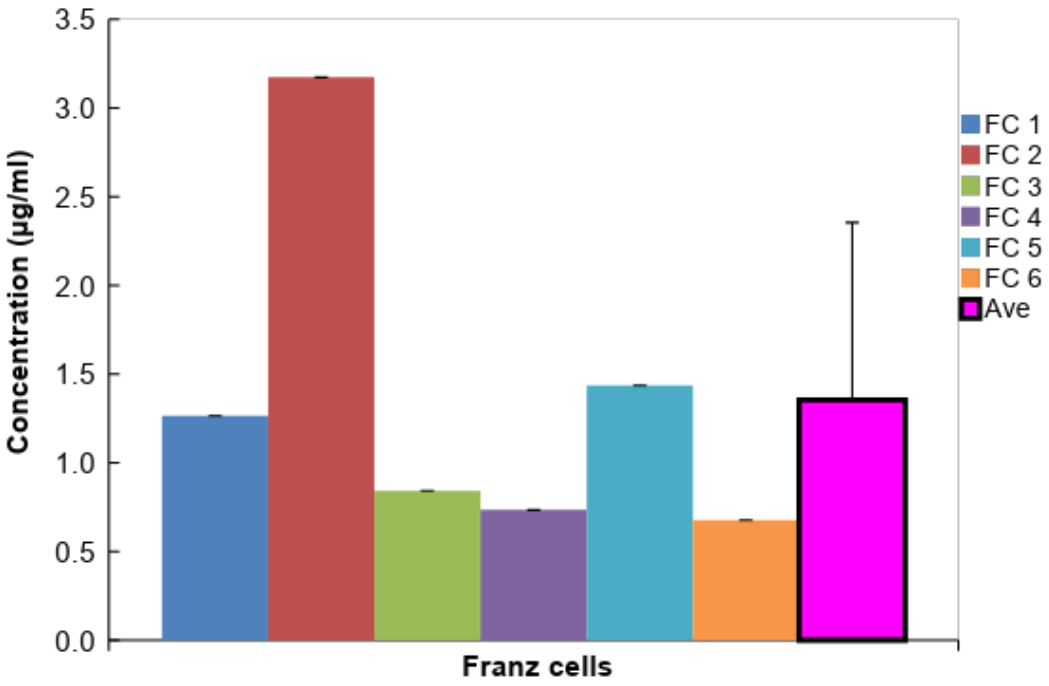


**Figure D.43:** The concentration (µg/ml) of **NE1Pr** present in the SCE after 12 h

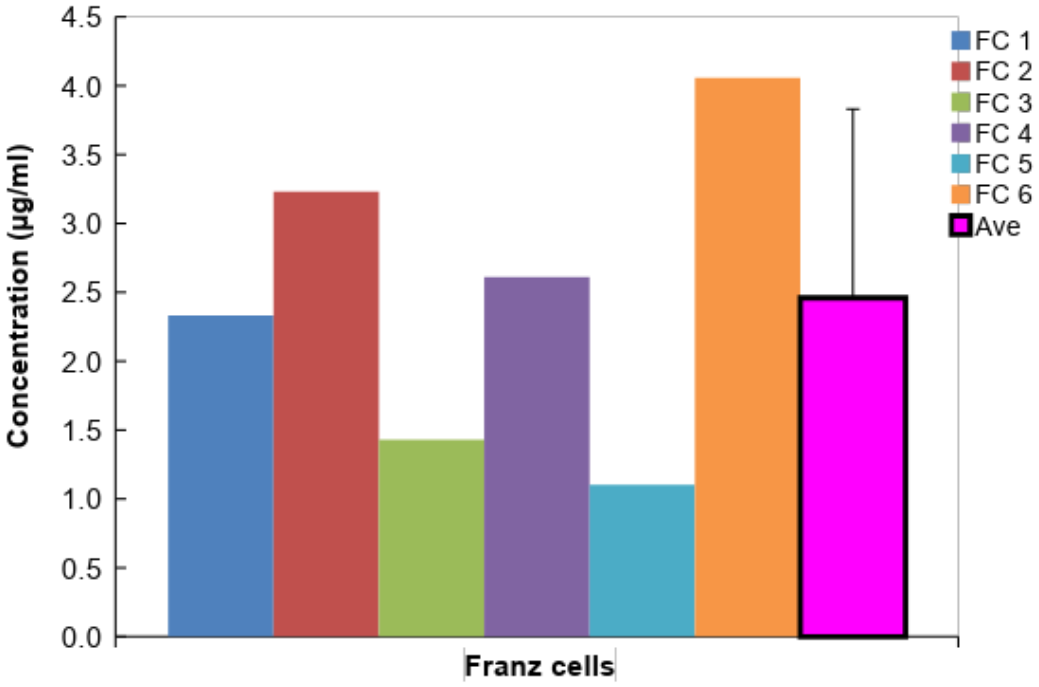


**Figure D.44:** The concentration (µg/ml) of **NE1Pr** present in the ED after 12 h

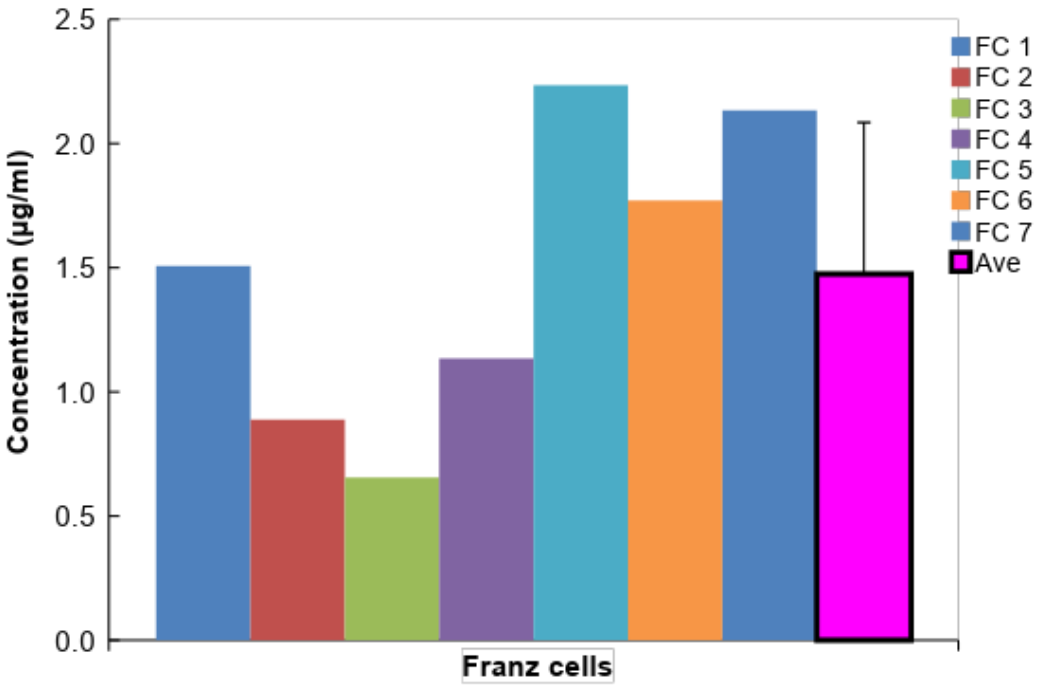


**Figure D.45:** The concentration (µg/ml) of **NEGPr** present in the SCE after 12 h

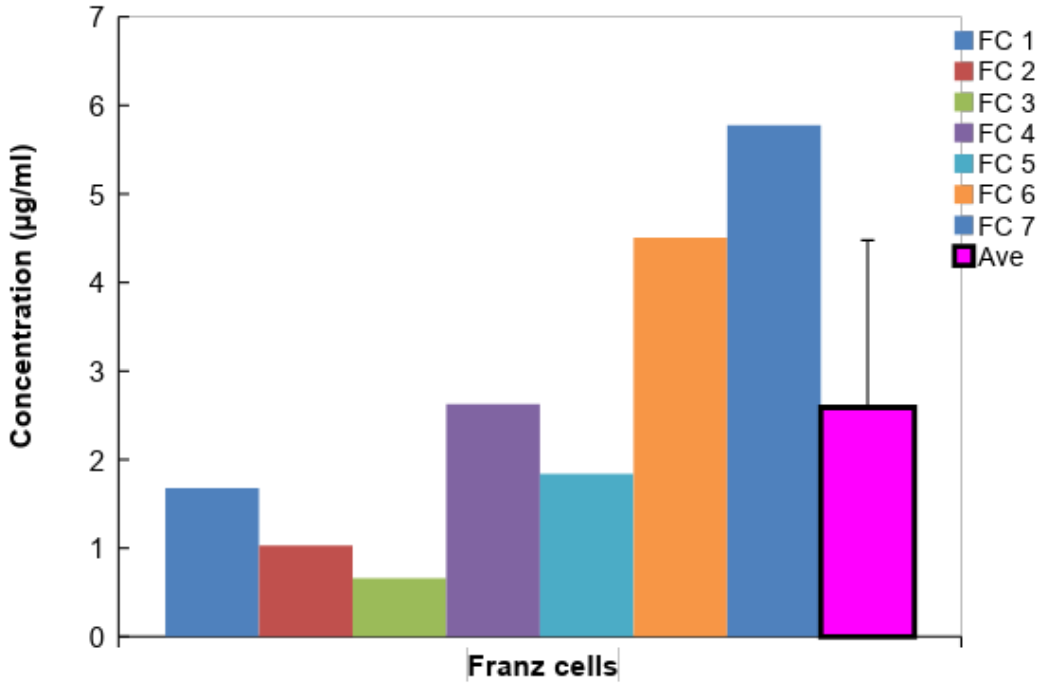


**Figure D.46:** The concentration (µg/ml) of **NEGPr** present in the ED after 12 h

Since median values are known to present more accurate values than the average values (Dawson & Trapp, 2004) (Figure D.47), only the median concentration values of the statin present in the SCE ad ED will be discussed.

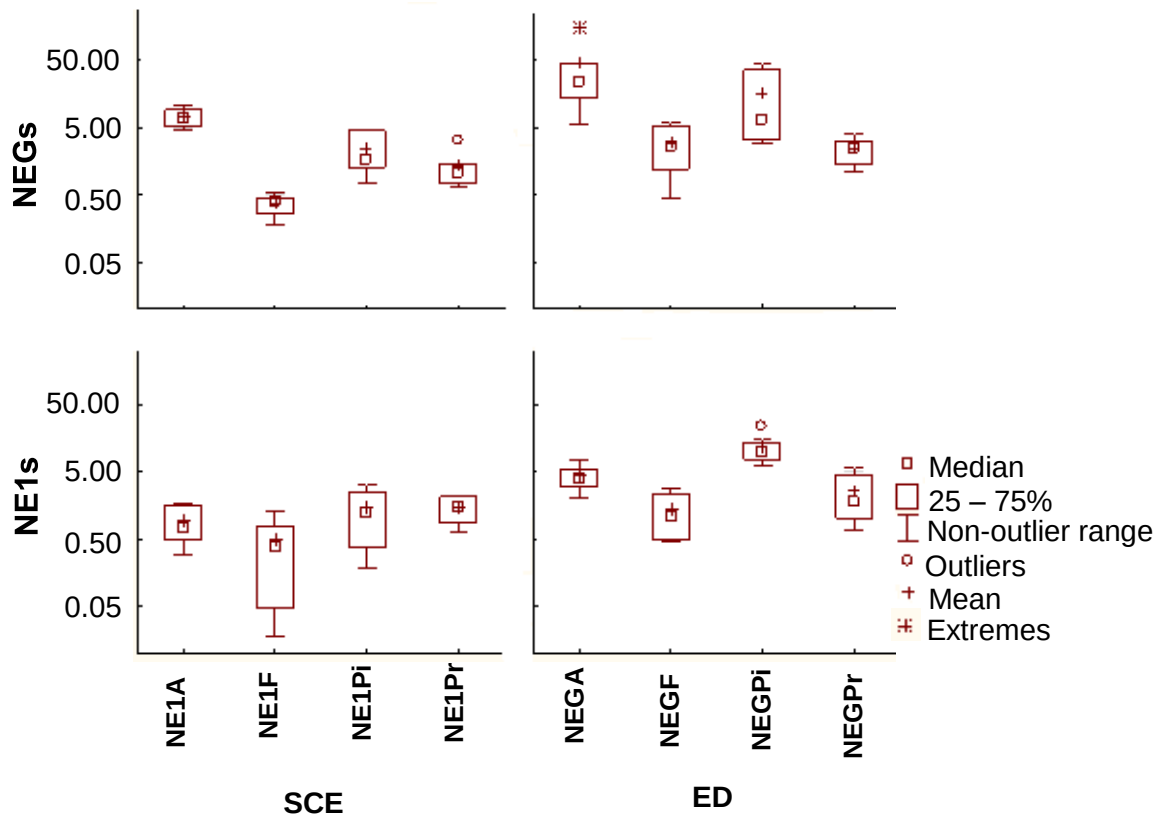


**Figure D.47:** Average concentration (µg/ml) of the **NE1s** as well as the **NEGs** for each statin present in the SCE and ED

The median concentrations of the different statins present in the SCE for the **NE1s** indicated that **NE1A** was substantially higher compared to **NE1Pi**, followed by **NE1Pr** and lastly, **NE1F**. The median concentration in the SCE of the **NEGs** was the highest for **NEGPr**, followed by **NEGPi**, **NEGA** and lastly, **NEGF**.

When the **NE1** of each statin was compared to its **NEG**-counterpart, it was found that the median concentration in the SCE was higher for **NE1A** compared to **NEGA**, **NE1Pi** compared to **NEGPi** and **NE1F** compared to **NEGF**. Pravastatin (**NEGPr**) was the only statin of which its **NEG** formula was higher than its **NE1**-counterpart (**NE1Pr**). From characterisation results (Appendix C), **NE1s** comprise of droplet sizes below that of **NEG** formulations, which may increase permeation into the stratum corneum, and may accumulate in that region (Arora, 2014:11).

When the median concentration statin present in the ED for the **NE1s** were investigated, it was found that **NE1A** had the highest median concentration, followed by **NE1Pi**, **NE1F** and lastly, **NE1Pr**. With inspection of the **NEGs**, **NEGPi** displayed the highest median concentration in the ED, followed by **NEGA**, **NEGPr** and lastly, **NEGF**.

When the **NE1** of each statin was compared to its **NEG**-counterpart, it was found that **NE1A**, **NE1F** and **NE1Pr** had higher median concentration in the ED than its **NEG**-counterparts (**NEGA**, **NEGF** and **NEGPr**). The exception was **NEGPi** which revealed a higher median concentration than its **NE1**-counterpart (**NE1Pi**).

Atorvastatin (**NE1A**) was the statin with the highest concentration present in the SCE and the ED for **NE1s**, while pravastatin (**NEGPr**) and pitavastatin (**NEGPi**) was the highest for the **NEGs** in the SCE and the ED, respectively. Fluvastatin had the lowest median concentration from both the **NE1s** (**NE1F**) and **NEGs** (**NEGF**) in the SCE, but it only had the lowest median concentration from the **NEGs** (**NEGF**) in the ED.

### D.3.6 Statistical analysis

#### D.3.6.1 Statistical analysis of membrane release studies

Statistical analysis was performed on membrane release studies by means of ANOVA, t-tests and Tukey's HSD post-hoc tests.

A two-way ANOVA was performed on **NE1s** and **NEGs**. The interaction between the type of formula (**NE1/NEG**) and the statin revealed a p-value of $< 0.001$. Therefore, a statistical significant interaction was observed. As a result, a one-way ANOVA was performed for each of the nano-emulsions and nano-emulgels to compare the statins.

**Table D.6:** The p-values of the one-way ANOVAs that were performed on the statin for the different **NE1s** and **NEGs** formulas

| Study | Comparison | p-value |
|---|---|---|
| **Membrane release** | Statin for **NE1** | $< 0.001$ |
| | Statin for. **NEG** | $< 0.001$ |

Table D.6, indicates that when the means (averages) of the **NE1s** were compared and the means of the **NEGs** were compared, differences between the actual means of the statins of the test samples were both significant ($p < 0.001$, which is smaller than $< 0.05$). Confirming that both displayed significant effects. Tukey's HSD post-hoc tests were performed for each type of formula to pairwise compare the means of the statins.

**Table D.7:** Tukey's HSD post-hoc tests of the statins in the different **NE1s** and **NEGs** (separately) according to the homogenous groups (in terms of means)

| Combination | Statin order |
|---|---|
| **NE1** | **NE1Pr**[a] |
| | **NE1A**[a] |
| | **NE1Pi**[b] |
| | **NE1F**[c] |
| **NEG** | **NEGF**[a] |
| | **NEGA**[a] |
| | **NEGPi**[a] |
| | **NEGPr**[b] |

Homogenous groups (a, b, c) respectively for each combination

### D.3.6.2 Statistical analysis of the *in vitro* skin diffusion studies

Statistical analysis was performed on the *in vitro* skin diffusion studies' data by means of ANOVA, t-tests and Tukey's HSD post-hoc test. The results were categorised as the statin that diffused through the skin and the statin that was present in skin layers (SCE-ED). In this section, statistical data reflected biased distribution, thus logarithmic transformation was performed in advance to produce near to normal distribution.

#### D.3.6.2.1 Statistical analysis of the statin that diffused through the skin from the NE1s and NEGs

A two-way ANOVA was performed on the **NE1s** and **NEGs** containing the statins that diffused through the skin. An interaction between the type of formula (**NE1/NEG**) and the statin occurred and revealed a p-value of 0.025. Therefore, a statistical significant interaction was observed. Consequently, a one-way ANOVA was performed for each of the **NE1s** and the **NEGs** to compare the statins.

**Table D.8:** The p-values of the one-way ANOVA performed on both the **NE1s** and **NEG** that diffused through the skin

| Study | Comparison | p-value |
|---|---|---|
| **Diffused through skin** | Statin for **NE1** | < 0.001 |
| | Statin for **NEG** | 0.003 |

Table D.8 indicates that the log-cumulative concentrations of the statins in the **NE1s** were compared; the same was done for the statins in the **NEGs**. Here p-values were below 0.05 (< 0.001 and 0.003, respectively), thus indicative of statistical significant variances.

**Table D.9:** Tukey's HSD post-hoc test of the **NE1s** and **NEG** formulas that diffused through the skin, grouped according to their homogenous relationships (respectively) with the cumulative concentrations as a variable

| Comparison | Statin order |
|---|---|
| **NE1** | **NE1A**[b] |
| | **NE1F**[ab] |
| | **NE1Pr**[a] |
| | **NE1Pi**[a] |
| **NEG** | **NEGA**[b] |
| | **NEGPi**[ab] |
| | **NEGPr**[a] |
| | **NEGF**[a] |

Homogenous groups (a, b) respectively for each comparison

Table D.9 suggests that **NE1F**, **NE1Pr** and **NE1Pi** had homogenous relationships; however, **NE1A** was in a separate group, which indicated similar properties of **NE1F**. A similar pattern was observed for the **NEGs**; hence, **NEGPi** was the formula that related to both **NEGPr** and **NEGF**, and **NEGA** as a separate group.

#### D.3.6.2.2 Statistical analysis of the statins present in the skin layers (SCE and ED)

Statistical analysis was performed to determine the ANOVA of statins present in skin layers.

**Table D.10:** The p-values of the ANOVA for the effects of the statin, type of formula (**NE1s** and **NEGs**) and the skin layers (ED or SCE)

| Study | Level of interaction | Interaction | p-value |
|---|---|---|---|
| **Skin layers (SCE-ED)** | Two-way | Statin*Skin layers | 0.013 |
| | Two-way | Statin*Type of formula | < 0.001 |
| | Two-way | Skin layers*Type of formula | 0.619 |
| | Three-way | Statin*Skin layers*Type of formula | 0.497 |

* interaction between statin and skin layers, etc.

Table D.10 displays the interactions between the statins and the skin layers (SCE-ED), and the statins and the type of formula, which were 0.013 and < 0.001, respectively, indicating

statistical significant interactions. Hence, p-values of the remaining two-way interaction and the three-way interaction were above 0.05 (0.619 and 0.497, respectively), also indicative of statistical insignificant interactions.

Since some significant interactions occurred in Table D.10, one-way ANOVAs to compare statins were performed on each of the combinations of the skin layer and the type of formula, followed by t-tests to compare SCE with ED for each formula containing a statin.

**Table D.11:** The p-values of the one-way ANOVA performed on the statin to compare the type of formula (**NE1s** and **NEGs**) with the skin layer (SCE and ED)

| Study | Combination | p-value |
|---|---|---|
| **Statin** | SCE and **NE1** | < 0.001 |
| | ED and **NE1** | < 0.001 |
| | SCE and **NEG** | 0.030 |
| | ED and **NEG** | < 0.001 |

Table D.11 suggests that the p-values of each compared group (SCE vs. **NE1**, ED vs. **NE1**, SCE vs. **NEG** and ED vs. **NEG**) were below 0.05 (< 0.001, < 0.001, 0.030 and < 0.001, respectively). This is an indication that statistical significant variations were observed for each comparison.

Since ANOVA compares groups, it can determine if interactions were detected. To obtain more specific data of interactions, t-tests were performed.

**Table D.12:** T-tests for comparisons of the skin layers presented in combinations of the statin and the type of formula

| Study | T-test | Combinations | p-value |
|---|---|---|---|
| **Skin layers (SCE-ED)** | 1 | **NE1A** | 0.041 |
| | 2 | **NEGA** | < 0.001 |
| | 3 | **NE1F** | < 0.001 |
| | 4 | **NEGF** | 0.011 |
| | 5 | **NE1Pi** | 0.028 |
| | 6 | **NEGPi** | < 0.001 |
| | 7 | **NE1Pr** | 0.060 |
| | 8 | **NEGPr** | 0.259 |

Table D.12 indicates that the p-values for t-tests 1 – 6 (specified statin formulated in a specified formula type present in the layers of the skin) were below 0.05, indicating that statistical significant variations occurred. However, t-test 8 (**NEGPr** present in the layers of the skin) presented with a p-value of 0.259, indicative of a statistical insignificant variation, while t-test 7 was almost significant (p = 0.06).

Tukey's HSD post-hoc tests were then performed to indicate homogenous relationships between specified statins formulated in a specified type formula compared to the layer of the skin the statin presented in.

**Table D.13:** Tukey's HSD post-hoc of the different formulas (**NE1** and **NEG**) containing statins in combination with the layer of the skin (SCE and ED) the statin presented in

| Combinations | Statin order | Combinations | Statin order |
|---|---|---|---|
| **SCE and NE1** | **NE1F**$^{b}$ | **SCE and NEG** | **NEGF**$^{a}$ |
| | **NE1Pr**$^{a}$ | | **NEGA**$^{ab}$ |
| | **NE1Pi**$^{a}$ | | **NEGPi**$^{ab}$ |
| | **NE1A**$^{c}$ | | **NEGPr**$^{b}$ |
| **ED and NE1** | **NE1Pr**$^{a}$ | **ED and NEG** | **NEGF**$^{a}$ |
| | **NE1F**$^{a}$ | | **NEGPr**$^{ab}$ |
| | **NE1Pi**$^{ab}$ | | **NEGA**$^{bc}$ |
| | **NE1A**$^{b}$ | | **NEGPi**$^{c}$ |

Homogenous groups (a, b, c) respectively for each combination

Table D.13 indicates that the pravastatin and pitavastatin formed a homogenous group in each of the combinations, excluding for the ED and **NEG** combination. It was noticed that the atorvastatin and fluvastatin was only partly homogenous in the SCE and **NEG** combination and therefore non-relatable in the other three combinations.

## D.4 Conclusion

The median flux values for the **NE1s** and **NEGs** during the membrane release study indicated that **NE1F** and **NEGPr**, respectively had the highest median flux values for the **NE1s** and **NEGs**. This correlates with the characterisation results regarding viscosity where **NEGPr** had the lowest viscosity which entails faster release. Median flux values for the **NE1s** were higher for **NE1A**, **NE1F** and **NE1Pi**, compared to its respective **NEGs** (**NEGA**, **NEGF** and **NEGPi**). This may be as a result of the higher viscosity of the **NEG** formulations due to their gel-like structure (Arora *et al*., 2014:11; Begur *et al*., 2015:78), thus a slower, more regulated release is expected. **NEGPr** was the only **NEG** with a higher median flux value than its **NE1**-counterpart (**NE1Pr**). The aforementioned can be due to o/w nano-emulsions favouring lipophilic APIs (Chaudhary *et al*., 2018:178); therefore, pravastatin being more hydrophilic than other statins can explain its lowered median flux. However, this occurrence was overcome when **NE1Pr** was modified to a nano-emulgel seeing that **NEGPr** prevailed with the highest median flux.

Plasma concentrations of the statins after oral administration (found in the literature) were used as a guideline to compare to the average concentrations of the statins after transdermal delivery (obtained in this study). It was observed that all the formulas delivered higher concentrations of the statins in the receptor phase than the plasma concentrations after oral administration, except for **NE1F, NEGF** and **NE1Pi** (only slightly lower).

The median amount per area that diffused through the skin was investigated and indicated that the order from highest to lowest median amount per area diffused for **NE1s** was **NE1Pi** > **NE1Pr** > **NE1F** > **NE1A**. During the investigation of the **NEGs**, it was found that **NEGF** displayed the highest median amount per area diffused, followed by **NEGPr** > **NEGPi** > **NEGA**. The **NE1** of each statin was compared with its **NEG**-counterpart to evaluate the median amount per area diffused through skin and it was found that the **NEGs** prevailed with higher median values than their **NE1**-counterparts. The fact that all of the **NEGs** prevailed in the median amount per area diffused, can be a result of **NEGs** producing better spreadability when applied (Chellapa, 2015:44) and are more stable, as they prevent separation of particles in the formulation (Mitsui, 1997:138) since oil droplets, which encapsulates the lipophilic APIs, are dispersed more effectively in the gel-like formulation (Chellapa, 2015:45). Since skin

diffusion studies were performed over a period of 12 h, the stability of formulas could play a role. **NEGs** also comprise of enhanced adhesion characteristics when applied to the skin, and consist of better solubilisation capability, which result in a higher concentration gradient of API and in turn a higher concentration of API can penetrate (Chellapa, 2015:45).

The **NE1s** displayed median concentration in the SCE in the order of **NE1A** > **NE1Pi** > **NE1Pr** > **NE1F**. When the median concentrations in the ED were investigated, it is observed that the **NE1s** displayed median concentration in the order of **NE1A** > **NE1Pi** > **NE1F** > **NE1Pr**. The large concentration of atorvastatin present in the SCE and ED can be attributed to its high molecular weight, atorvastatin (1155.34 g/mol) (Al-Adl *et al.,* 2017:1), as it is larger than 500 Da its penetration through the skin is restricted (Jia *et al.,* 2017:2). Thus, **NE1A** accumulated in the skin layers rather than diffused through.

**NEGs** presented with an order of **NEGPr** > **NEGPi** > **NEGA** > **NEGF**. **NE1s** (**NE1A**, **NE1Pi** and **NE1F**) had higher median concentrations in the SCE compared to its **NEG**-counterparts, with the exception of **NEGPr**. The **NEGs'** order of median concentrations were displayed as **NEGPi** > **NEGA** > **NEGPr** > **NEGF**. The **NE1s** (**NE1A**, **NE1F** and **NE1Pr**) exhibited higher median concentrations in the ED than their **NEG**-counterparts, except for **NEGPi** which had a higher median concentration than **NE1Pi**.

The median amount per area that diffused through the skin was investigated and indicated that atorvastatin had the lowest concentrations diffused through the skin for the **NE1s** (**NE1A**), as well as the **NEGs** (**NEGA**). The large concentration of atorvastatin present in the SCE and ED of **NE1A** might be attributed to its high molecular weight (1155.34 g/mol) preventing penetration through the skin (Jia *et al.,* 2017:2). **NEGA** presented with low concentrations of atorvastatin in the SCE, as well as the receptor phase, but in the ED it was delivered moderately (**NEGA** was delivered fourth best of all the formulas in the ED). The aforementioned might indicate that **NEGA** was trapped in this layer or preferred to stay in the ED, which then (other than the large molecular weight) could have contributed to the lower concentration of atorvastatin in the receptor phase.

The concentration of fluvastatin (**NEGF**) that diffused was the highest in the receptor phase, but also the lowest in the SCE and ED when compared to all the formulas (**NE1s** and **NEGs**). This might imply that the **NEG** formula was ideal (ideally formulated) for the delivery of fluvastatin transdermally, as high concentrations in the receptor phase and low concentrations in the SCE and ED suggest optimal targeting. **NE1F** concentrations were low in the SCE, as well as in the receptor phase and even though it ranked third of all the **NE1s** and fifth for all

the formulas in the ED, it supports the statement, that by including a gelling agent to the **NE1s**, it may have contributed to the targeted delivery of **NEGF**.

Pravastatin (**NEGPr**) showed the second highest concentration of statin present in the receptor phase and the second lowest concentration in the ED among **NE1s** and **NEG** formulations. The concentration pravastatin (**NEGPr**) present in the SCE prevailed among **NEG** formulations (ranked first of all the **NEGs**), and placed third highest of all the tested formulas. It can be suggested that the release of **NEGPr** from the SCE was delayed; hence the **NEG** increased the release of pravastatin from the ED to the receptor phase indicating high transdermal delivery. **NE1Pr** presented with low to average concentrations in the SCE, ED and the receptor phase. Therefore, it can be concluded that the **NEG** definitely had an influence on the transdermal delivery of pravastatin.

The concentration **NEGPi** that diffused through the skin was the third highest of all the formulas. **NEGPi** compared to the **NEGs** presented with the second highest concentration in the SCE and obtained the fourth highest concentration compared to all the formulas. **NEGPi** presented with the highest concentration in the ED among the **NEGs** and had the second highest concentration when compared to all the formulas in the ED. It can be suggested that **NEGPi** permeated rapidly to the ED from the SCE, consequently delivering high concentrations to the receptor phase. **NE1Pi** persisted with the highest concentrations delivered to the receptor phase when compared to **NE1s** and the fourth highest concentrations in the receptor phase when compared to all the formulas. **NE1Pi** presented with the second highest concentrations in the SCE among all the formulas. **NE1Pi** also presented with the second highest delivery among the **NE1s** in the ED and the third highest concentration among all the formulas. Thus, it can be suggested that by adapting the formula of **NEGPi**, the transdermal delivery of pitavastatin may be increased and even targeting might be achieved.

It is however evident, when inspecting the transdermal and topical data, that the **NE1s** (in general) had improved the delivery of the statins topically (SCE and ED) when compared to its **NEG**-counterparts, whereas **NEGs** improved the delivery of the statins transdermally (receptor phase); this might also be the reason why the **NE1s** had higher concentrations topically than the **NEGs**, since the **NEGs** improved penetration through the skin, into the systemic circulation. Hence, the occurrence of **NEGs** displaying with lower median concentrations in the SCE can be ascribed to the addition of a gelling-agent (Carbopol® Ultrez 20). This agent causes swelling of the **NE1s** and produce formulations with higher viscosity (Mahalingam *et al.,* 2008:293; Mitsui, 1997:138) which in turn increases API permeation through the skin (Eid *et al.,* 2014:1).

The following conclusions were reached:

- An alternative administration route does exist for administration of statins, as the **NE1s** as well as the **NEGs** succeeded in delivering the statins transdermally, confirming that the goal of the study was achieved.
- **NEGs** are the favourable transport system to deliver statins through the skin into the systemic circulation, as concentrations in the receptor phase was generally higher than that of the **NE1s**.
- **NEGs** in comparison with the oral administered plasma concentrations of the different statins, delivered higher concentrations transdermally than the orally administered plasma concentrations (except for **NEGF**).
- **NE1s** succeed in delivering statins transdermally (less than the **NEGs**); however, only **NE1Pr** and **NE1A** had higher concentrations in the receptor phase when compared to the orally administered plasma concentrations of the different statins; although, **NE1Pi** was only slightly lower.

**References**


Ali, S., Shabbir, M., Shahid, N. 2015. The structure of skin and transdermal drug delivery system. *Research journal of pharmacy and technology*, 8(2):103-109.

Arora, R., Aggarwal, G., Harikumar, S.L., Kaur, K. 2014. Nanoemulsion based hydrogel for enhanced transdermal delivery of ketoprofen. *Advanced in pharmaceutics*, 1-12.

Therapeutic goods administration. 2013 Australian public assessment report for pitavastatin. https://www.tga.gov.au/sites/default/files/auspar-pitavastatin-130902.docx. Date of access: 18 Nov. 2018.

Begur, M., Pai, V.K., Gowda, D.V., Srivastava, A., Raghundan, H.V., Shinde, C.G., Manusri N. 2015. Enhanced permeability of Cyclosporine from a transdermally applied nanoemulgel. Der pharmacia sinica, 6(2):69-79.

Bouwstra, J.A. & Ponec, M. 2006. The skin barrier in healthy and diseased state. *Biochimica et biophysica acta (BBA)-Biomembranes*, 1758:2080-2095.

Cabral, M.E.S., Ramos, A. N., Cabrera, C.A., Valdez, J.C., Gonzalez, S.N. 2014. Equipment and method for in vitro release measurements on topical dosage forms. *Pharmaceutical development and technology*, 1-7.

Cayman chemical. 2010. Fluvastatin (sodium salt) (Material safety data sheet). https://s3-us-west-2.amazonaws.com/drugbank/msds/DB01095.pdf?1374296087. Date of access: 18 Oct 2018.

Cayman chemical. 2014. Pitavastatin calcium salt (Product information 15414) https://www.caymanchem.com/pdfs/15414.pdf Date of access: 18 Oct 2018.

Cayman chemical. 2015. Pravastatin (sodium salt) (Material safety data sheet). https://www.caymanchem.com/msdss/10010343m.pdf Date of access: 18 Oct 2018.

Chaudhary, S., Verma, N.K., Panda, P., Singh, A.P., Alam, G. 2018. Nanoemulsion based drug delivery. *European journal of pharmaceutical and medical research*, 5(6):178-191.

Chellapa, P., Mohamed, A.T., Keleb, E.I., Elmahgoubi, A., Eid, A.M., Issa, Y.S. & Elmarzugi, N.A. 2015. Nanoemulsion and nanoemulgel as a topical formulation. *IOSR journal of pharmacy*, 5(10): 43-47.

Chime, S.A., Kenechukwu, F.C. & Attama, A.A. 2014. Nanoemulsions: advances in formulation, characterization and application in drug delivery. (*In* Sezer, A.D., ed. Application of nanotechnology in drug delivery. p. 77-126). -http://cdn.intechopen.com/pdfs-wm/47116.pdf Date of access: 20 Dec. 2017.

Clarke, E.G.C., Moffat, A.C., Osselton, M.D. & Widdop, B. 2011. Clarke`s analysis of drugs and poisons in pharmaceuticals, body fluids and postmortem material. 4th ed. Pharmaceutical Press. p. 1947.

Chinembiri, T. N., Gerber, M., Du Plessis, L., Du Preez, J., Du Plessis, J. 2015. Topical delivery of 5-fluorouracil from Pheroid™ formulations and the *in vitro* efficacy against human melanoma. *Journal of American association of pharmaceutical scientists*, 6:61390-1399.

Consonni, D., Bertazzi, P.A. 2017. Health significance and statistical uncertainty: The value of P-value. *Medicina del lavaro,* 108(5): 327-331.

Dawson, B. & Trapp, R.G. 2004. Basic & clinical biostatistics. 4th ed. New York: McGraw-Hill. 438 p.

DeGorter, M.K., Tirona, R.G., Schwarz, U.I., Choi, Y., Dresser, G.K., Suskin, N., Myers, K., Zou, G.Y., Iwuchukwu, O., Wei, W., Wilke, R.A., Hegele, R.A., Kim, R.B. 2013. Clinical and pharmacogenetic predictors of circulating atorvastatin and rosuvastatin concentrations in routine clinical care. *Circulation cardiovascular genetics,* 6:400-408.

El Maghraby, G.M., Barry, B.W. & Williams, A.C. 2008. Liposomes and skin: from drug delivery to model membranes. *European journal of pharmaceutical sciences*, 34:203-222.

Encyclopaedia Britannica. 2016. Partition coefficient. http://global.britannica.com/science/partition-coefficient. Date of access: 6 Sept 2018.

Foldvari, M. 2000. Non-invasive administration of drugs through the skin: challenges in delivery system design. *Pharmaceutical sciences and technology today*, 3:417-425.

Hamada, C. 2018. Statistical analysis for toxicity studies. *Journal of toxicology and pathology*, 31:15-22.

Hörmann, K. & Zimmer, A. 2016. Drug delivery and drug targeting with parenteral lipid nanoemulsions-a review. Journal of Controlled Release, 223:85-98.

Jepps, O.W., Dancik, Y., Anissimov, Y.G. & Roberts, M.S. 2013. Modelling the human skin barrier-towards a better understanding of dermal absorption. *Advanced drug delivery reviews*, 65:152-168.

Kute, S.B. & Saudagar, R.B. 2013. Emulsified gel: a novel approach for delivery of hydrophobic drugs: an overview. *Journal of advanced pharmacy education and research,* 3:368-376.

Lynch, J.C., Myers, K.F., Brannon, J.M. & Delfino, J.J. 2001. Effects of ph and temperature on the aqueous solubility and dissolution rate of 2,4,6-trinitrotoluene (tnt), hexahydro-1,3,5-trinitro-1,3,5-triazine (rdx), and octahydro-1,3,5,7-tetranitro-1,3,5,7-tetrazocine (HMX). *Journal of chemical and engineering data*, 46:1549-1555.

Mahalingam, R., Li, X. & Jasti, B.R. 2008. Semisolid dosages: ointments, creams and gels. (*In* Gad, S.C., ed. Pharmaceutical manufacturing handbook: production and processes. New Jersey: John Wiley & Sons. p. 267-309).

Menon, G.K. 2002. New insights into skin structure: scratching the surface. *Advanced drug delivery reviews*, 54:S3-S17.

Modi, P.B. & Shah, N.J. 2015. Optimization of an in vitro release test for topical formulations containing eberconazole nitrate and mometasonefuroate. *Der Pharma Chemica*, 7:1-9.

Mitsui, T. 1997. Polymers. (*In* Mitsui, T., ed. New cosmetic science. Netherlands: Elsevier. p. 138-140).

Ng, K.W. & Lau, W.M. 2015. Skin deep: the basics of human skin structure and drug penetration. (*In* Dragicevic-Curic, N. & Maibach, H.I., eds. Percutaneous penetration enhancers: chemical methods in penetration enhancement: drug manipulation strategies and vehicle effects. Heidelberg: Springer. p. 3-12).

OECD (Organisation for economic co-operation and development). 2011. Guidance notes on dermal absorption: series on testing and assessment, No. 156. http://www.oecd.org/chemicalsafety/testing/48532204.pdf Date of access: 6 Sep. 2018.

Rodde, M.S., Divase, G.T., Devkar, T.B., Tekade, A.R. 2014. Solubility and bioavailability enhancement of poorly aqueous soluble atorvastatin: *in vitro*, *ex vivo*, and *in vivo* studies. *BioMed research international*, 1-11.

Routes, A.E. 2004. Drug absorption, distribution and elimination; pharmacokinetics. http://www.columbia.edu/itc/gsas/g9600/2004/GrazianoReadings/Drugabs.pdf. Date of access: 18 Nov. 2018.

Shahzad, Y., Louw, R., Gerber, M. & Du Plessis, J. 2015. Breaching the skin barrier through temperature modulations. *Journal of controlled release*, 202: 1-13.

Subedi, R.K., Oh, S.Y., Chun, M. & Choi, H. 2010. Recent advantages in transdermal drug delivery. *Archives of pharmacal research*, 33:339-351.

Sutradhar, K.B. & Amin, L. 2013. Nanoemulsion: increasing possibilities drug delivery. *European journal of nanomedicine*, 5(2):97-110.

Weiss, S.C. 2011. Conventional topical delivery systems. Dermatologic therapy, 24: 471-474.

Wenlock, M.C., Potter, T., Barton, P., Austin,R.P. 2011. A method for measuring the lipophilicity of compounds in mixtures. *Journal of biomolecular screening,* 16(3):348-355.

Wiechers, J.W. 2008. Skin delivery: what it is and why we need it. (*In* Wiechers, J.W., ed. Science and applications of skin delivery systems. Carol Stream, IL: Allured Publishing Corporation. p. 1-21).

Williams, A.C. 2003. Structure and function of human skin. (*In* Williams, A.C., ed. Transdermal and topical drug delivery: from theory to clinical practice. London: pharmaceutical press. p. 1-26).

Williams, A.C. 2013. Topical and transdermal drug delivery. (*In* Aulton, M.E., ed. Aulton's pharmaceutics: the design and manufacture of medicines. 3rd ed. London: Churchill Livingstone. p. 675-697).

Venus, M., Waterman, J. & McNab, I. 2011. *Basic physiology of the skin. Surgery* (Oxford), 29:471-474.

Yourick, J.J., Jung, C.T. & Bronaugh, R.L. 2008. In vitro and in vivo percutaneous absorption of retinol from cosmetic formulations: significance of the skin reservoir and prediction of systemic absorption. Toxicology and Applied Pharmacology, 231:117-121.

# APPENDIX E

CYTOTOXICITY STUDIES OF O/W NANO–EMULSIONS

## E.1 Introduction

By definition, cytotoxicity is the measurement to which a certain agent disturbs cellular connectivity, causes drastic changes in cell morphology, presents harmful (inhibition) to cell dividing/growth or produces complete cell destruction (Niles *et al*., 2008:655). Cytotoxicity studies portray a large influence in the process of cosmetic or pharmaceutical product development and consequently, only minor to zero toxicity is required (McGaw *et al*., 2014:181). Cytotoxicity studies are purely an estimate of possible toxic occurrences for *in vivo* models as they are carried out on *in vitro* models (Fotakis & Timbrell, 2005:171), and since *in vitro* studies exclude pharmacokinetic processes (absorption, distribution, metabolism and excretion) (Yoon *et al*., 2012:634) the two models are not to be directly compared (Yoon *et al*., 2012:634).

Cytotoxicity studies are valuable preliminary measurements to establish possible toxicity of a specified constituent (McGaw *et al*., 2014:181). These studies determine growth, viability and/or proliferation of a cell (ATCC, 2011:1; Li *et al*., 2015:617) on the principle of measuring the damaging effects on cells such as membrane disturbance and/or disruption of organelle (mitochondrial or lysosomal, etc.) viability and integrity (Fröhlich, 2013:977).

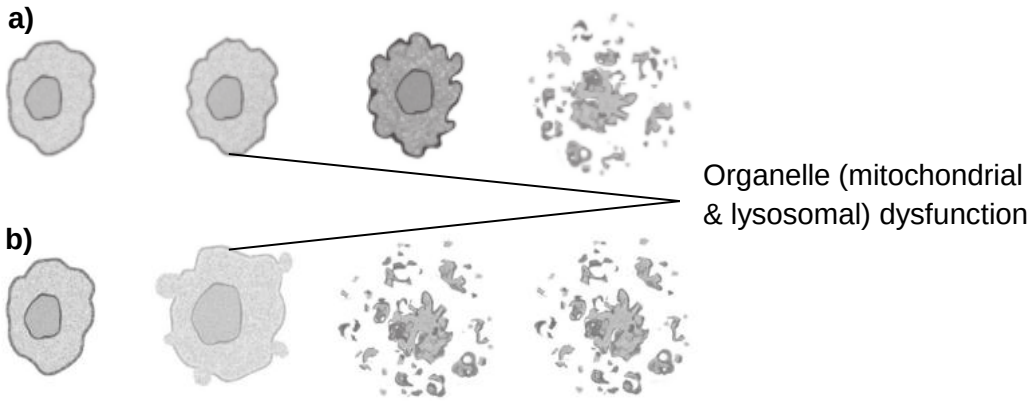


**Figure E.1:** Simplified representation of cytotoxic effects on cells: a) normal cell death (apoptosis) and b) cytotoxic cell death (necrosis) (Niles *et al*., 2008:657).

Cell fatality can be organised in correspondence with the morphological aspects of the destructive course, which, amongst others, are the course of apoptosis and necrosis (Galluzzi *et al.,* 2007:1237).

Figure E.1.a represents cell death by means of apoptosis, which is characterised by cytoplasmic and chromatin reduction, nucleic destruction, cell membrane deformation and small alterations of organelles (Galluzzi *et al.,* 2007:1239). Necrosis, conversely, is identified with enlargement of cytoplasmic material and damaged organelles (mitochondrial/lysosomal dysfunction), membrane partition and mild chromatin reduction (Galluzzi *et al.,* 2007:1237).

In this study, the possible cytotoxicity of compounds was determined with methylthiazol tetrazolium (MTT) and neutral red (NR). MTT is based on the concept of the dehydrogenase enzymes of live mitochondria present in viable cells that transform soluble MTT into insoluble purple formazan, which will remain in the viable cells, as it is unable to overcome the membranes. This will be indicative of necrosis (cytotoxicity) (see Figure E.1), as dead cells will not incorporate purple formazan as they lack live mitochondria (Fotakis & Timbrell, 2006:172). NR is based on the fact live cells absorb the red dye through active transport into the lysosomes, which will not occur in dead cells as live lysosomes are non-existent here. MTT and NR are recognised as trustworthy techniques to determine cell proliferation (ATCC, 1; Repetto *et al*., 1993:503).

Cytotoxicity experiments comprised of testing the dispersions (**NE1** and **PNE1**) for each individual statin in different concentrations. Pure statin solutions and excipients such as apricot kernel oil, Tween® 80 and Span® 60 were also tested. The testing of these compounds was performed on the pre-malignant human immortalised keratinocytes (HaCaT), since the human skin consists mainly of keratinocytes (López-García *et al.,* 2014:44).

The objective of this study was to uncover whether HaCaT cell lines were impaired or damaged by the following samples dosed in different concentrations:

- Statin solutions
- Nano-emulsions (**NE1s**)
- Placebo nano-emulsions (**PNE1**)
- Tween® 80, Span® 60 and Span® 60-apricot kernel oil combination

Results of these MTT and NR-assays were utilised to determine cell viability (Stoddart, 2011:1). The inhibition of HaCaT cells dosed with specified concentrations of the compounds listed above was also calculated, as the concentration to which these compounds inhibited 50% of the cell growth ($IC_{50}$) (Roesler *et al.,* 2010:814).

## E.2 Preparation for cell toxicity studies

*In vitro* toxicity experiments and all processes before and during the cytotoxic studies (cell cultivation, feeding, seeding, and cell line treatment) were performed by Dr W Pheiffer under aseptic conditions in the Laboratory for Applied Molecular Biology (LAMB), in the Mammalian Cell Culture Laboratory at the North-West University (NWU), Potchefstroom Campus (RSA).

### E.2.1 Materials

The materials used during the cytotoxicity experiments with MTT and NR are presented in Table E.1.

**Table E.1:** Materials utilised during the *in vitro* cytotoxicity studies

| Product | Supplier | Batch number |
|---|---|---|
| Dulbecco's Modified Eagle's Medium (DMEM) with high glucose, 4.0 mM L-glutamine, sodium pyruvate | HyClone™ | AC11223315 |
| L-glutamine | Lonza™ | 5MB180 |
| Penicillin/Streptomycin (Pen/Strep) | Sigma-Aldrich® | SLBG0033v |
| Trypan blue solution (0.4%) | Sigma-Aldrich® | RNBC9030 |
| MTT (methylthiazol tetrazolium) | Sigma-Aldrich® | MKBX6716V |
| Phosphate buffered saline (1x) | HyClone™ | AB212873 |
| Trypsin-Versene® (EDTA) | Sigma-Aldrich® | – |
| Foetal bovine serum (FBS) | Gibco™ | 4209352K |
| Dimethyl sulfoxide (DMSO) | Sigma-Aldrich® | SHBH2447V |
| Neutral Red Solution (0.33%) | Sigma-Aldrich® | RNBF9155 |
| Neutral Red Fixative | Sigma-Aldrich® | SLBT9587 |
| Neutral Red Solubilisation Solution | Sigma-Aldrich® | SLBT8171 |

### E.2.2 Cell line selection

The appropriate cell line selection is important, therefore a selection criteria needs to be considered, including the cell species type, characteristics, normal/transformed cell lines, growth conditions, etc. (Gibco®, 2016:18). In order to fulfil the objectives of this study, a naturally preserved human keratinocyte line, namely the HaCaT, was chosen, as keratinocytes are the main cell types present in the human skin (López-García *et al.,* 2014:44). Given that the formulation will be applied on human skin, the HaCaT cell lines are appropriate

and the most suitable, since these cells have proliferative epidermal characteristics (López-García *et al*., 2014:44).

### E.2.3 Seeding of cells

The work surface in the laminar flow hood, as well as all the items to be placed within, were properly sterilised with ethanol (70%). Growth media (high-glucose DMEM) and phosphate buffered saline were preheated (37 °C) prior to use.

Growth media was removed with a pipette from the incubated cell flask; drops on the outside rim were removed with a soaked 70% ethanol paper towel. The flask containing the cells was rinsed twice with 10 ml preheated phosphate buffer saline solution drops on the outside rim and it was removed similarly as mentioned before. Cells were then detached from the bottom of the well plates by utilising Trypsin-Versene®. A volume of 3 ml Trypsin-Versene® was added to the flask, the lid was closed and equal distribution of Trypsin-Versene® in the flask was ensured before placing it into the $CO_2$ incubator. The flask was incubated at 37 °C for 3 – 5 min, examining the detachment of the cells after every 2 min by lightly shaking the flask. When the best part of the cells was detached, the cells were pipetted with a serological pipette. A volume of 6 ml preheated growth medium was added to the flask and removed gently with a pipette. The cell suspension was then transferred to a 50 ml tube for the determination of the number of cells.

### E.2.4 Haemocytometer and cell counting

The number of cells was determined using Trypan blue, which is a staining method used for counting viable cells. The concept of this method is based on live cells not absorbing the dye, hence the dead cells will stain (Sigma, 2018).

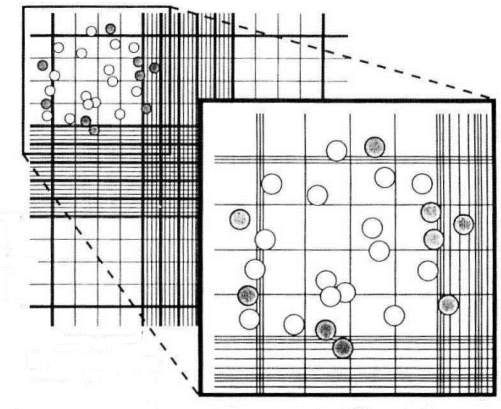

**Figure E.2:** Cell counting by means of a haemocytometer under a microscope (Provost & Wallert, 2015:1).

A cover slide was located in the centre of the haemocytometer. A microcentrifuge tube was used to combine 25 µl Trypan blue (0.4%) and 15 µl phosphate buffer saline. The cell suspension was continuously mixed and a volume of 10 µl of this suspension was extracted. The 10 µl cell suspension was mixed with the Trypan blue mixture and incubated at room temperature for 3 min. The counting mixture was pipetted thoroughly and a volume of 10 µl of this suspension was extracted and placed slowly at the verge of the cover slip, so that the suspension is drawn into the chamber by capillary action, this was repeated with the other side of the counting chamber. The haemocytometer was then viewed under a microscope to complete cell counting.

Each side of the counting chamber is divided into nine large squares with a total surface area of 9 $mm^2$. Live cells (clear, round) in the centre square, as well as each corner square were counted, therefore, five squares per side of the counting chamber; both sides were determined. The total number of live cells counted in the 10 squares were added together and divided by 2 to determine the average of the two sides and then divided by 5 to determine the average per square, the answer was then multiplied with the dilution factor ($5 \times 10^4$) to determine the quantity of live cells (per ml) of cell suspension ($C_1$). The cell concentration was then multiplied with the total volume of cell suspension, to determine the total number of cells existing in the suspension. The following equation was utilised to determine the number of live cells.

$C_1V_1 = C_2V_2$ **Equation E.1**

Where:

$C_1$ = live cells (per ml) of cell suspension

$V_1$ = calculated volume of the cell suspension

$V_2$ = total volume of cell suspension per well

The diluted cell suspension was mixed continuously with a Pasteur pipette, while filling each well of the 96-well plates with the required volume of cell suspension (± 15 000 cells per well). The 96-well plates were then inserted into the $CO_2$ incubator (5% $CO_2$, 95% humidity) and maintained by exchanging fresh growth medium (preheated 37 °C) every day until ready for performing the experiment. Three 96-well plates were utilised in this study.

### E.2.5 Preparation of treatments

Statin solutions were prepared by dissolving 400 mg of each statin (separately) in methanol adding up to a 100 ml in a volumetric flask. A volume of 0.3 ml of each solution was combined with 9.7 ml DMEM. Cells were not exposed to methanol concentrations higher than 5% (v/v) during toxicity studies. The treatments tested were prepared as follows:

- **NE1s** and the **PNE1** (see Appendix B) were prepared for dosing by combining a volume (0.2 ml) of each with 9.8 ml DMEM.
- Span® 60 and Tween® 80 were separately dissolved in methanol to produce an 8% solution; a volume of 0.12 ml of each solution was added to 7.88 ml DMEM.
- Span® 60-apricot kernel oil was prepared by adding 0.012 g Span® 60 to 17.48 µl (0.16%) apricot kernel oil, where after this combination was added to 9.9705 ml DMEM.

### E.2.6 Concentration of treatments to be dosed on separate 96-well plates

Statin solutions (Table E.2), **NE1s**, **PNE1** (Table E.3) and excipients (Tween® 80, Span® 60 and Span® 60-oil combination) (see Table E.4) were dosed in different concentrations. Since no wells were available on the 96-well plate used for **NE1**, **PNE1** were dosed on the 96-well plate used for the excipients, however they were dosed in concentrations similar to **NE1s**. The 96-well plates were dosed according to the following representation:

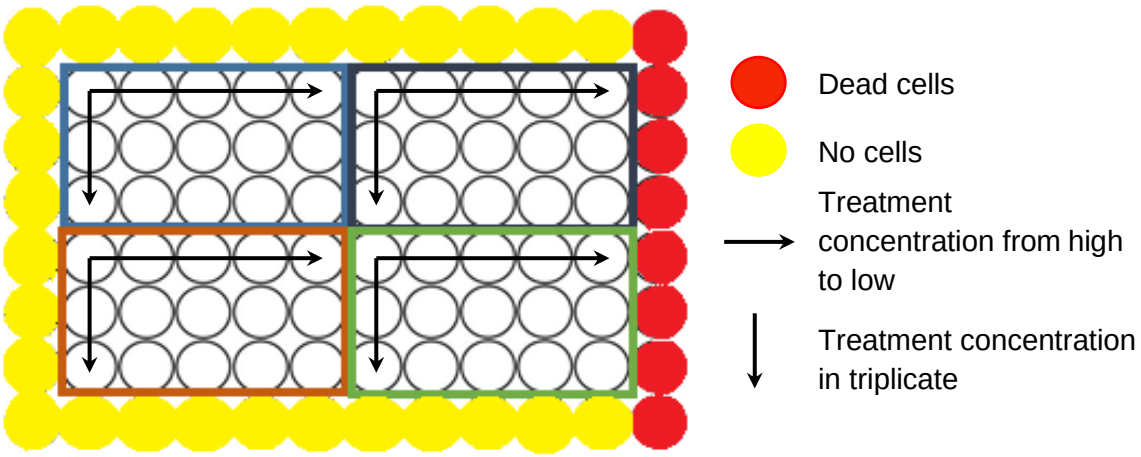


**Figure E.3:** Representation of 96-well plates to be treated

Five different concentrations were used to treat HaCaT cells, as indicated with the horizontal arrow, and this was performed in triplicate as indicated with the vertical arrow (Figure E.3).

Different concentrations were dosed to determine if the treatment was harmful towards the HaCaT cells, and if so, which approximate concentration.

**Table E.2:** Statin solutions dosed in different concentrations for MTT as well as NR

| Concentration of treatment mg/ml | Concentration (%) | Stock solution (µl) | Media (µl) | Total (µl) |
|---|---|---|---|---|
| 0.0075 | 0.00075 | 200.0 | 0.0 | 200 |
| 0.0150 | 0.00150 | 100.0 | 100.0 | 200 |
| 0.0300 | 0.00300 | 50.0 | 150.0 | 200 |
| 0.0600 | 0.00600 | 25.0 | 175.0 | 200 |
| 0.1200 | 0.01200 | 12.5 | 187.5 | 200 |

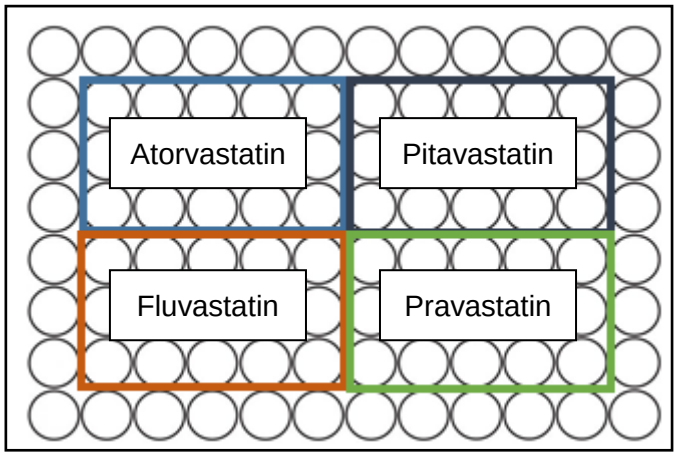


**Figure E.4:** Illustrative 96-well plate indicating statins dosed in different concentrations for MTT as well as NR

**Table E.3:** **NE1s** and **PNE1** dosed in different concentrations for MTT as well as NR

| Concentration of treatment (mg/ml) | Concentration (%) | Stock solution (µl) | Media (µl) | Total (µl) |
|---|---|---|---|---|
| 0.025 | 0.0025 | 12.5 | 187.5 | 200 |
| 0.050 | 0.0050 | 25.0 | 175.0 | 200 |
| 0.100 | 0.0100 | 50.0 | 150.0 | 200 |
| 0.200 | 0.0200 | 100.0 | 100.0 | 200 |
| 0.400 | 0.0400 | 200.0 | 0.0 | 200 |

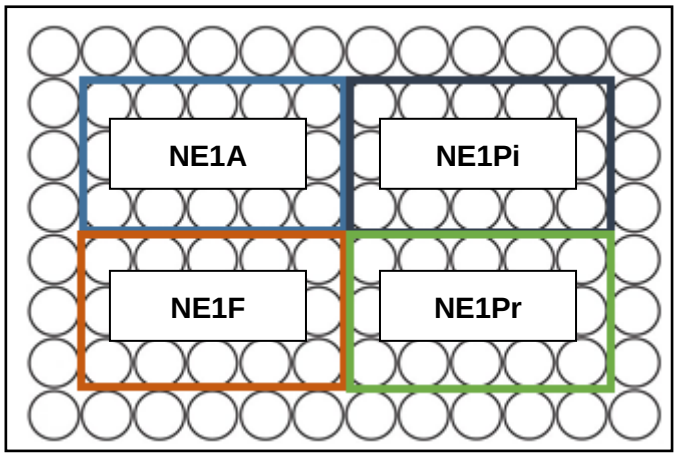


**Figure E.5:** Illustrative 96-well plate indicating **NE1s** dosed in different concentrations for MTT as well as NR

**Table E.4:** Tween® 80, Span® 60 and Span® 60-oil combination dosed in different concentrations for MTT as well as NR

| Concentration of treatment (mg/ml) | Concentration (%) | Stock solution (µl) | Media (µl) | Total (µl) |
|---|---|---|---|---|
| 0.075 | 0.0075 | 12.5 | 187.5 | 200 |
| 0.150 | 0.0150 | 25.0 | 175.0 | 200 |
| 0.300 | 0.0300 | 50.0 | 150.0 | 200 |
| 0.600 | 0.0600 | 100.0 | 100.0 | 200 |
| 1.200 | 0.1200 | 200.0 | 0.0 | 200 |

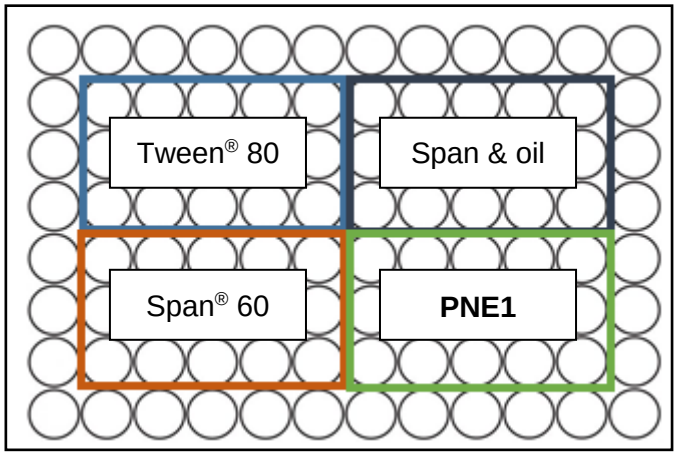


**Figure E.6:** Illustrative 96-well plate indicating the excipients together with **PNE1** dosed in different concentrations for MTT as well as NR

Although the **PNE1** was located on the same 96-well plate as the excipients, it was treated with the same concentrations as the **NE1s**, which contained both statins and excipients.

### E.3 *In vitro* toxicity testing

*In vitro* cytotoxicity experiments were performed on HaCaT cells to determine possible change in the cell viability. Cytotoxicity was established by performing an MTT as well as an NR-assay.

#### E.3.1 Methylthiazol tetrazolium (MTT)

MTT-assays determine cell viability, through the formation of insoluble, purple formazan. The concept of this assay is the fact that the live cells' mitochondria have dehydrogenase enzymes, which convert soluble MTT into insoluble purple formazan; this purple formazan remains in the viable cells, as it is unable to overcome the membranes. Damaged cells will not incorporate purple formazan (Fotakis & Timbrell, 2006:172).

##### E.3.1.1 MTT-assay

An adequate amount of MTT solution was prepared and used on the same day of the assay. MTT was dissolved in assay media in a 50 ml centrifuge tube, covered with foil, as it is light sensitive, and stored at room temperature. The medicated 96-well plates were removed from the incubator and the cells were visually inspected under a microscope. The growth medium from control wells (outer side) was extracted and cells were executed with 200 µl of 100% methanol for a period of ± 5 min.

The growth medium was removed from wells, and cells were gently rinsed by pipetting 150 µl of phosphate buffer saline into the wells. Phosphate buffer saline was then removed from wells and a volume 100 µl MTT-solution was pipetted into each well, including control wells (outer side) which do not contain cells. The 96-well plates containing MTT-solution were incubated for 2 h in the $CO_2$ incubator under standard growing conditions. After which the 96-well plates were removed from the incubator and the cells were visually inspected under a microscope to detect formazan crystals. Yellow MTT-solution was extracted from the 96-well plates and a volume of 200 µl DMSO was added to each well, including control wells (outer side), for 15 – 30 min to dissolve the blue formazan crystals. Lastly, absorbance was measured at 560 nm with a background of 630 nm with a SpectraMax® Paradigm® Multi-Mode Microplate reader (Molecular Devices, California, USA) analysed with SoftMax® Pro 6.2.1 Software.

$$\%live/viable\ cells = \frac{(Sample_{560-630}) - (Blank_{560-630})}{(Negative\ control_{560-630}) - (Blank_{560-630})}$$ **Equation E.2**

### E.3.1.2 MTT-assay results and discussion on treated HaCaT cells

The cytotoxic effect of a specific treatment can be classified according to the percentage of cell viability (López-García *et al*., 2014:44) as follows:

- non-cytotoxic: > 80%
- weak cytotoxicity: 80 – 60%
- moderate cytotoxicity: 60 – 40%
- strong cytotoxicity: < 40%

The MTT %cell viability of the HaCaT cell line, were measured with a SpectraMax® Paradigm® Multi-Mode Microplate reader after 12 h of treatment with statin solutions (Table E.2), **NE1** and **PNE1** (Table E.3), and excipients (Table E.4). The MTT %cell viability of the HaCaT cell line after 12 h of treatment was measured and will be discussed in Sections E.3.1.2.1 to E.3.2.1.4.

#### E.3.1.2.1 Cell viability of the statin solutions during MTT-assay on treated HaCaT cells

Statin solutions were dosed in different concentrations during the MTT-assay and displayed the following cell viability (%) results as seen in Table E.5 and Figures E.7 and E.8.

**Table E.5:** The cell viability (%) of the statin solutions dosed in different concentrations during the MTT-assay

| Concentration of treatment (mg/ml) | Cell viability (%) | | | |
|---|---|---|---|---|
| | Atorvastatin (blue) | Fluvastatin (yellow) | Pitavastatin (green) | Pravastatin (pink) |
| 0.0075 | 85.091 | 89.344 | 91.489 | 108.511 |
| 0.0150 | 86.180 | 84.858 | 92.340 | 103.887 |
| 0.0300 | 84.442 | 87.295 | 95.513 | 108.096 |
| 0.0600 | 76.379 | 73.960 | 83.903 | 103.020 |
| 0.1200 | 51.909 | 50.153 | 61.450 | 88.630 |

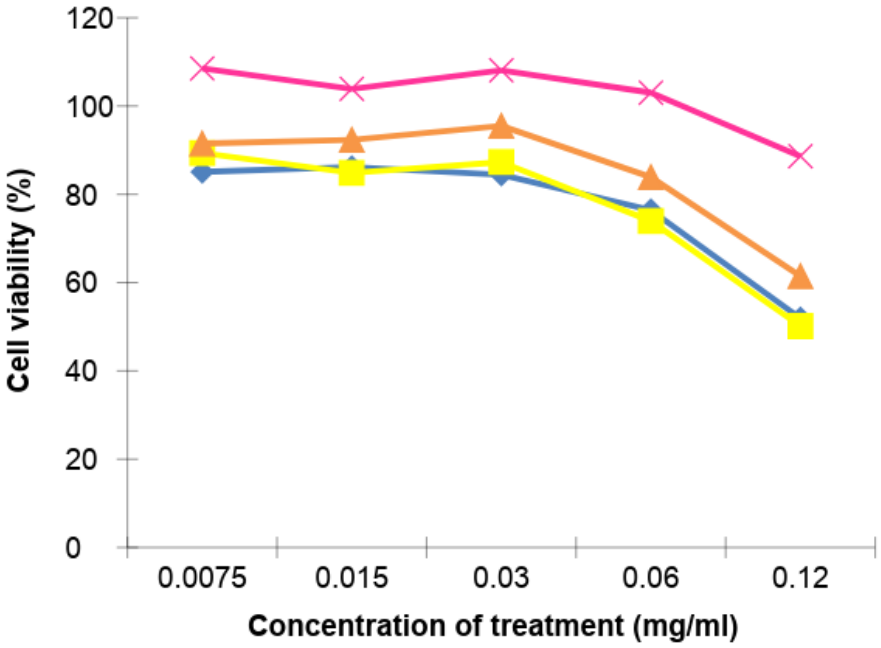


**Figure E.7:** The cytotoxic effects of the statin solutions dosed in different concentrations during the MTT-assay

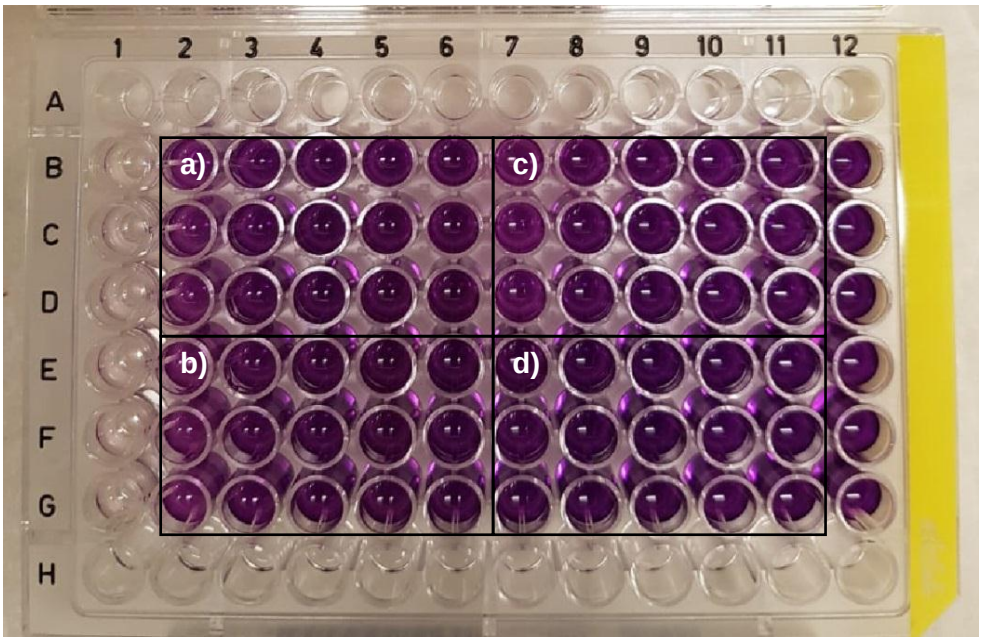


**Figure E.8:** Image of a 96-well plate containing cells treated with the statin solutions dosed in different concentrations during the MTT-assay: a) atorvastatin, b) fluvastatin, c) pitavastatin and d) pravastatin

From Table E.5 and Figure E.7, the cell viability (%) of the statin solutions dosed in different concentrations was compared to the parameters of cell viability (López–García *et al*., 2014:44) when treated with MTT and the following was observed:

- Atorvastatin (blue) at concentrations of 0.0075 – 0.0300 mg/ml had a non-cytotoxic effect on the cells, as the cell viability was greater than 80%, but when the concentrations were higher (0.0600 – 0.1200 mg/ml), the cytotoxic effect was weak/moderate, as the cell viability was between 50 – 80%.
- Fluvastatin (yellow) at concentrations of 0.0075 – 0.03 mg/ml were non-cytotoxic (> 80%), although, when concentrations were increased (0.0600 – 0.1200 mg/ml), the cytotoxic effect was weak/moderate, as the cell viability ranged between 50 and 80%.
- Pitavastatin (green) at concentrations of 0.0075 – 0.0600 mg/ml posed as non-cytotoxic (> 80%), however, when the concentrations were higher (0.1200 mg/ml), the cytotoxic effect was weak, as the cell viability was > 60% (61.450%).
- Pravastatin (pink) at concentrations of 0.0075 – 0.1200 mg/ml was non-cytotoxic (> 80%) throughout the experiment.

Figures E.7 and E.8 show the correlations between cell viability results per concentration and visual inspection as purple formazan remained in the viable cells. Formazan was unable to overcome the membranes (Fotakis & Timbrell, 2006:172), which indicated weak toxicity.

#### E.3.1.2.2 Cell viability of the NE1s and PNE1 during MTT-assay on treated HaCaT cells

**NE1s** and **PNE1** were dosed in different concentrations during the MTT-assay and displayed the following cell viability (%) results as seen in Table E.6 and Figures E.9, E.10 and E.12.d.

**Table E.6:** The cell viability (%) of the **NE1s** and the **PNE1** dosed in different concentrations during the MTT-assay

| Concentration of treatment (mg/ml) | NE1A (blue) | NE1F (yellow) | NE1Pi (green) | NE1Pr (pink) | PNE1 (red) |
|---|---|---|---|---|---|
| 0.025 | 97.532 | 95.186 | 97.360 | 102.635 | 94.467 |
| 0.050 | 66.586 | 78.499 | 83.956 | 96.780 | 90.589 |
| 0.100 | 25.680 | 37.570 | 40.692 | 66.733 | 87.105 |
| 0.200 | 14.652 | 16.348 | 16.590 | 40.603 | 74.607 |
| 0.400 | 2.071 | 0.234 | 0.962 | 17.834 | 9.455 |

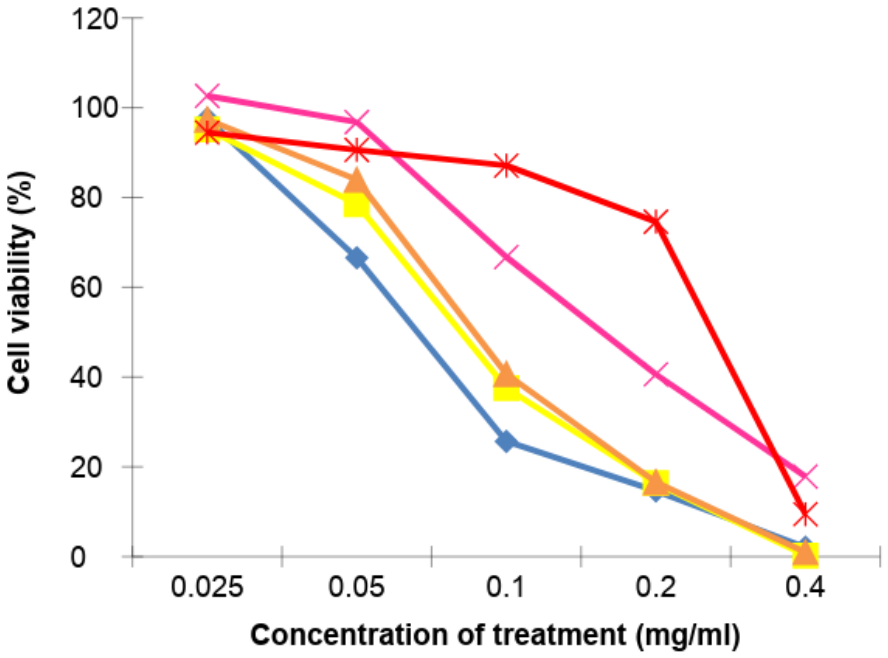


**Figure E.9:** The cytotoxic effects of the **NE1s** and the **PNE1** dosed in different concentrations during the MTT-assay

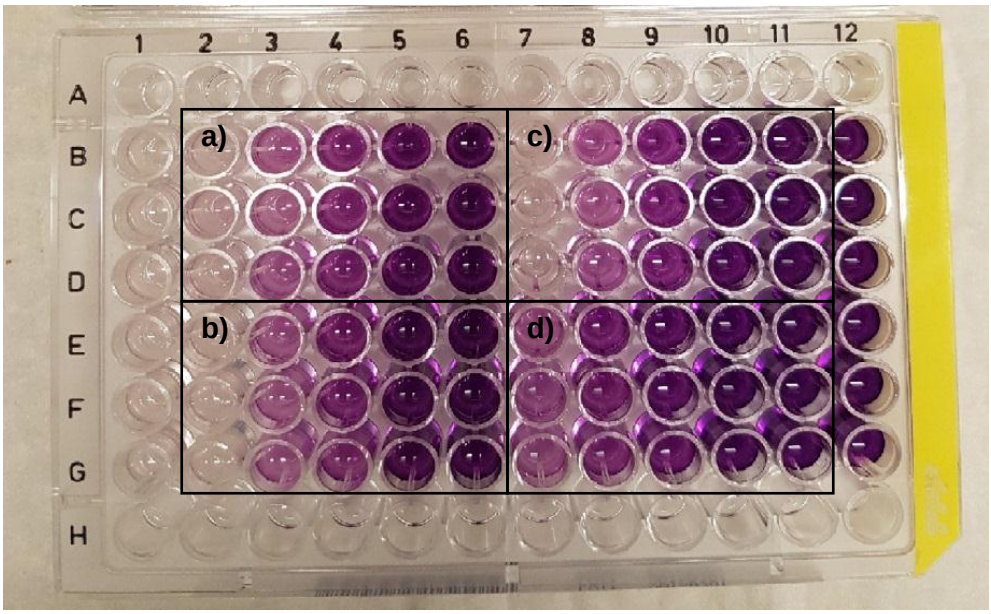


**Figure E.10:** Image of a 96-well plate containing cells treated with different concentrations of the **NE1s** during the MTT-assay: a) **NE1A**, b) **NE1F**, c) **NE1Pi** and d) **NE1Pr**

From Table E.6 and Figure E.9, the cell viability (%) of the **NE1s** and the **PNE1** dosed in different concentrations was compared to the parameters of cell viability (López–García *et al*., 2014:44) when treated with MTT and the following was detected:

- **NE1A** (blue) at a concentration of 0.025 mg/ml had a non-cytotoxic effect on the cells, as the cell viability was greater than 80%; hence, when the concentration was elevated to 0.050 mg/ml, the cytotoxic effect was weak (66.586%). The cytotoxicity was strong (< 40%) at concentrations of 0.100 – 0.400 mg/ml, as the cell viability ranged between 2.071 – 2.680%.
- **NE1F** (yellow) at a concentration of 0.025 mg/ml was non-cytotoxic (> 80%), however, when the concentration was increased to 0.050 mg/ml, the cytotoxic effect was weak (78.499%). At concentrations of 0.100 – 0.400 mg/ml, the cytotoxic effect was strong, since the cell viability was below 40% (0.234 – 37.570%).
- **NE1Pi** (green) at concentrations of 0.025 – 0.050 mg/ml were non-cytotoxic (> 80%), but when the concentration was higher (0.100 mg/ml), the cytotoxic effect was moderate. It became strong cytotoxic to cells at concentrations of 0.200 – 0.400 mg/ml due to the cell viability being < 40% (0.962 – 16.590%).

- **NE1Pr** (pink) at concentrations of 0.025 – 0.050 mg/ml were non-cytotoxic (> 80%), although, during higher concentrations (0.100 – 0.200 mg/ml) the cytotoxic effect posed as moderate and at a concentration of 0.400 mg/ml, the cytotoxic effect on the cell viability was strong, as it was below 40% (17.834%).
- **PNE1** (red) at concentrations of 0.025 – 0.100 mg/ml posed as non-cytotoxic, as the cell viability was greater than 80%, while the concentration at 0.200 mg/ml had a moderate cytotoxic effect. At the concentrations of 0.400 mg/ml, it had a strong cytotoxic effect (< 40%) on the cell viability (9.455%).

Figure E.10 indicated that when visually inspected, **NE1A**, **NE1F**, **NE1Pi** and **NE1Pr** had cytotoxic effects on the cells at the strongest concentrations, as damaged cells did not incorporate purple formazan. Hence, viable cells treated with lower concentrations remained purple. From Figure E.12.d, the **PNE1** was visually inspected and when the cells were treated with high concentrations, toxicity was indicated. As a result, these cells appeared light purple compared to the cells treated with lower concentrations.

#### E.3.1.2.3 Cell viability of the excipients during MTT-assay on treated HaCaT cells

Tween® 80, Span® 60 and Span® 60-oil were dosed in different concentrations during the MTT-assay and displayed the cell viability (%) results as illustrated in Table E.7 and Figures E.11 and E.12.a-c.

**Table E.7:** The cell viability (%) of the excipients dosed in different concentrations during the MTT-assay

| Concentration of treatment (mg/ml) | Tween® 80 (blue) | Span® 60 (yellow) | Span® 60-apricot kernel oil (green) |
|---|---|---|---|
| 0.075 | 93.157 | 95.886 | 105.533 |
| 0.150 | 88.290 | 87.338 | 101.956 |
| 0.300 | 78.378 | 78.184 | 100.163 |
| 0.600 | 68.431 | 60.184 | 94.025 |
| 1.200 | 20.283 | 25.792 | 84.199 |

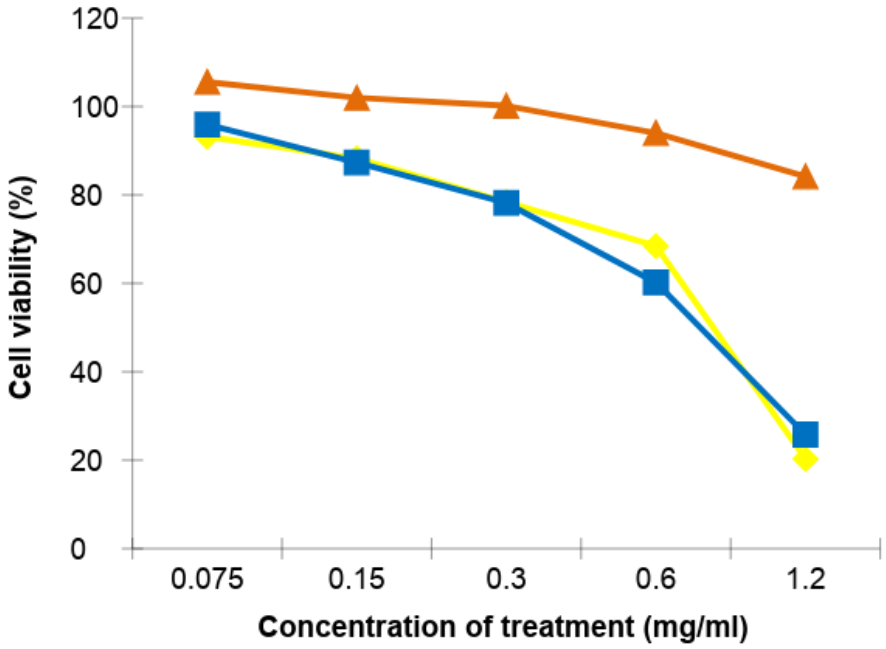


**Figure E.11:** The cytotoxic effects of the excipients dosed in different concentrations during the MTT-assay

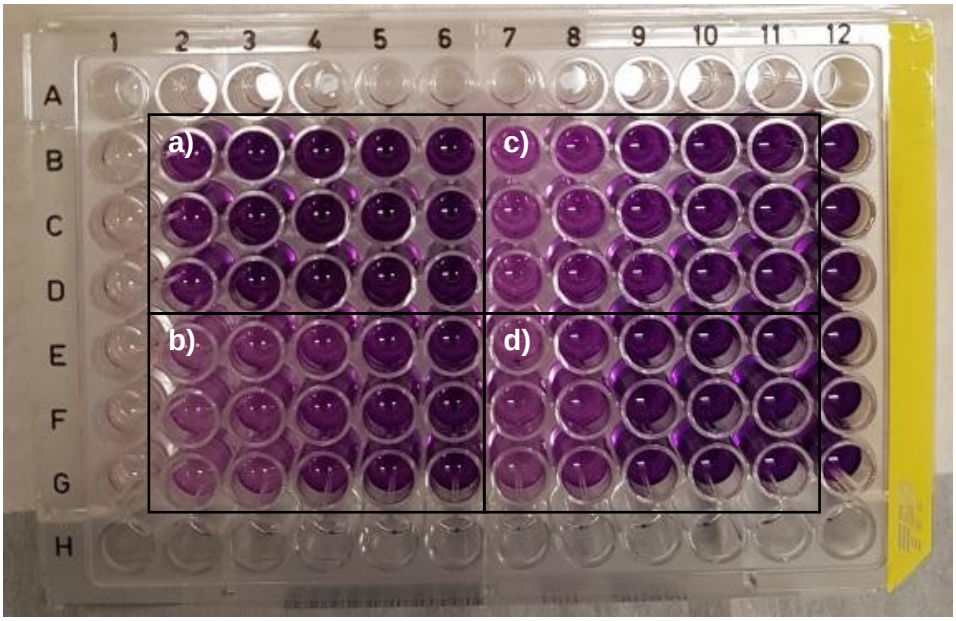


**Figure E.12:** Image of a 96-well plate containing cells treated with different concentrations of the excipients during the MTT-assay: a) Tween® 80, b) Span® 60, c) Span® 60-oil and d) **PNE1** (discussed in Section E.3.1.2.2)

From Table E.7 and Figure E.11, the cell viability (%) of excipients dosed in different concentrations was compared to the parameters of cell viability (López-García *et al*., 2014:44) when treated with MTT and the following was noticed:

- Tween® 80 (blue) and Span® 60 (yellow) had non-cytotoxic effects on cells at concentrations of 0.075 – 0.150 mg/ml, since the cell viability was greater than 80%; however, when the concentration was elevated to 0.300 – 0.600 mg/ml, the cytotoxic effects were weak (60 – 80%). Strong cytotoxic effects (< 40%) on the cells were detected at a concentration of 1.200 mg/ml (20.283 and 25.792 %, respectively).
- Span® 60-apricot kernel oil (green) at concentrations of 0.075 – 1.200 mg/ml reduced the cell viability as concentrations raised, but stayed non-cytotoxic (> 80%) throughout the experiment (84.199 – 105.533%).

Figure E.12.a-c indicated that Tween® 80, Span® 60 and Span® 60-apricot kernel oil treatments had effects on the viability of cells at the strongest concentrations, as the purple shading became lighter as concentrations enhanced.

#### E.3.1.2.4 $IC_{50}$ values during the MTT-assay

The $IC_{50}$ values of statin solutions, **NE1s**, **PNE1** and excipients (Tween® 80, Span® 60 and Span® 60-apricot kernel oil) during MTT-assays were calculated by firstly subtracting the concentration viable cells after treatment (calculated from Equation E.2) from 100 (initial concentration live cells). This calculation was applied to each treatment concentration. A linear line graph was plotted, where *y* was set as 50 (50% inhibition), *m* represented the slope, *c* the intercept to calculate *x* the $IC_{50}$ value (Kumar & Sandhya, 2014:1606).

$$y = mx + c \qquad \textbf{Equation E.3}$$

**Table E.8:** Calculated $IC_{50}$ values of statin solutions, **NE1s**, **PNE1** and the excipients from the MTT-assay results

| Solutions | Compounds | $IC_{50}$ values (µg/ml) |
|---|---|---|
| **Statin solutions** | Atorvastatin | 0.1334 |
| | Fluvastatin | 0.1244 |
| | Pitavastatin | 0.1682 |
| | Pravastatin | 0.3638 |
| **Statin dispersions (NE1) and placebo dispersion (PNE1)** | **NE1A** | 0.1144 |
| | **NE1F** | 0.1362 |
| | **NE1Pi** | 0.1465 |
| | **NE1Pr** | 0.2211 |
| | **PNE1** | 0.7485 |
| **Excipients alone** | Tween® 80 | 0.7767 |
| | Span® 60 | 0.7864 |
| | Span® 60-oil | 3.0591 |

From Table E.8, $IC_{50}$ values (µg/ml) for statin solutions indicated that fluvastatin inhibited HaCaT cells at a lower concentration (0.1244 µg/ml), thus presented as the most toxic to the cells, followed by atorvastatin (0.1334 µg/ml) and pitavastatin (0.1682 µg/ml) and lastly, pravastatin (0.3638 µg/ml) with the lowest toxicity and highest $IC_{50}$ value.

Comparisons of the **NE1s** and the **PNE1** indicated that the **PNE1** (0.7485 µg/ml) showed the lowest toxicity as it presented with the highest $IC_{50}$ value. The **NE1sA** (0.1144 µg/ml) displayed the lowest $IC_{50}$ value, followed by **NE1F** (0.1362 µg/ml), **NE1Pi** (0.1465 µg/ml) and lastly, the **NE1Pr** (0.2211 µg/ml), which presented with the highest $IC_{50}$ value among the statins and thus, the lowest toxicity. The order of $IC_{50}$ values of statins formulated in the **NE1s** differed from the statin solutions, therefore Tween® 80, Span® 60 and Span® 60-apricot kernel oil could have played a role.

Excipients' $IC_{50}$ results indicated that Tween® 80 (0.7767 µg/ml) and Span® 60 (0.7864 µg/ml) had similar $IC_{50}$ values. The Span® 60-apricot kernel oil presented as the least toxic, with the highest $IC_{50}$ value among the excipients (3.0591 µg/ml).

### E.3.2 Neutral red (NR)

NR-assays determine the viable, live cells through the uptake of neutral red dye past exposure to treatments. This system is uncomplicated, precise and outcomes are reproducible. The concept of this assay is the fact that the viable, live cells absorb the dye through active transport into the lysosomes; this occurrence will not appear in dead cells, therefore they will

not incorporate any red dye. Conclusively, the amount of red dye included in the cells specifies level of cytotoxicity produced by the added samples during the experiment.

### E.3.2.1 NR-assay

The medicated 96-well plates were removed from the incubator and the cells were visually inspected under a microscope. The growth medium from control wells (outer side) was extracted and cells were executed with 200 µl of 100% MeOH for a period of ± 5 min. The growth medium was then removed from wells and neutral red solution (0.33%) was added into the wells including control wells (outer side). The 96-well plates were incubated for 2 h in the $CO_2$ incubator under standard growing conditions; they were then removed from the incubator and the cells were swiftly rinsed with neutral red assay fixative. The fixative was extracted and a volume of Neutral Red Assay Solubilisation Solution (equivalent to the initial volume of culture medium) was added to each well to solubilise the incorporated dye. The 96-well plates were then placed on a gyratory shaker at room temperature for 10 min to ensure proper mixing. Finally, absorbance was measured at 560 nm with a background of 630 nm with a SpectraMax® Paradigm® Multi-Mode Microplate reader (Molecular Devices, California, USA) analysed with SoftMax® Pro 6.2.1 Software.

### E.3.2.2 NR-assay results and discussion on treated HaCaT cells

The cytotoxic effect of the treatments was classified according to the percentage of cell viability parameters (see section E.3.1.2). To determine NR %cell viability of the HaCaT cell line, a SpectraMax® Paradigm® Multi-Mode Microplate reader was utilised.

#### E.3.2.2.1 Cell viability of the statin solutions during NR-assay on treated HaCaT cells

Statin solutions were dosed in different concentrations during the NR-assay and displayed the following cell viability (%) results as seen in Table E.9 and Figures E.13 and E.14.

**Table E.9:** The cell viability (%) of the statin solutions dosed in different concentrations during the NR-assay

| Concentration of treatment (mg/ml) | Atorvastatin (blue) | Fluvastatin (yellow) | Pitavastatin (green) | Pravastatin (pink) |
|---|---|---|---|---|
| 0.0075 | 105.222 | 93.955 | 98.259 | 101.741 |
| 0.0150 | 100.992 | 88.097 | 87.292 | 113.794 |
| 0.0300 | 91.821 | 88.321 | 91.522 | 101.366 |
| 0.0600 | 87.966 | 76.867 | 87.685 | 118.604 |
| 0.1200 | 64.477 | 63.073 | 78.308 | 107.486 |

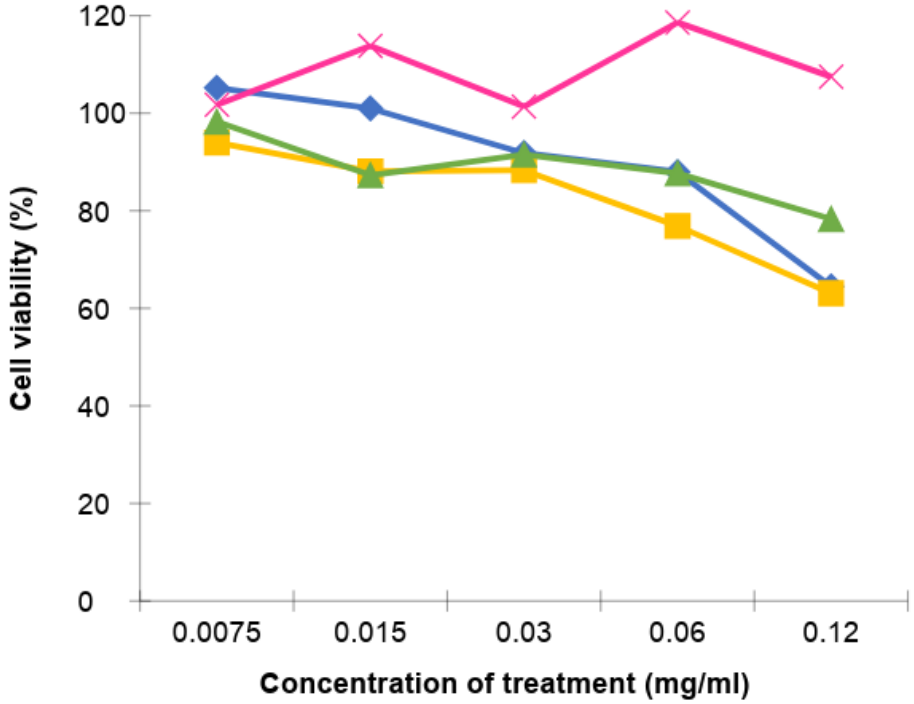


**Figure E.13:** The cytotoxic effects of the statin solutions dosed in different concentrations during the NR-assay

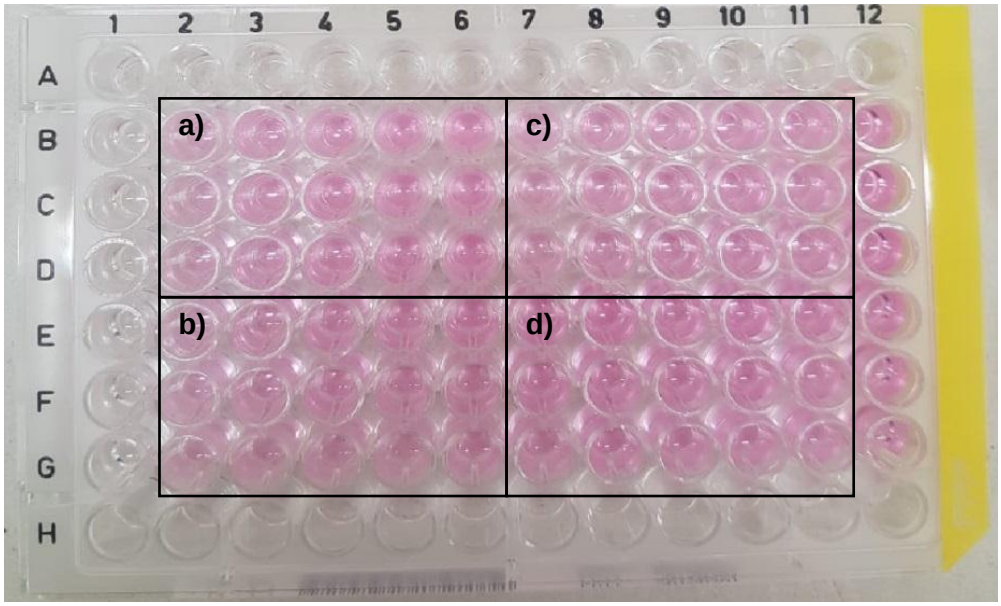


**Figure E.14:** Image of a 96-well plate containing cells treated with the statin solutions dosed in different concentrations during the NR-assay: a) atorvastatin, b) fluvastatin, c) pitavastatin and d) pravastatin

From Table E9 and Figure E.13, the cell viability (%) of the statin solutions dosed in different concentrations was compared to the parameters of cell viability (López-García *et al*., 2014:44) when treated with NR and the following was detected:

- Atorvastatin (blue) at concentrations of 0.0075 – 0.0600 mg/ml had a non-cytotoxic effect on the cells, as the cell viability was greater than 80%; although, when the concentration was higher (0.1200 mg/ml), the cytotoxic effect was weak, as the cell viability was 64.477%.
- Fluvastatin (yellow) at concentrations of 0.0075 – 0.0300 mg/ml were non-cytotoxic (> 80%); hence, when the concentrations were increased to 0.0600 – 0.1200 mg/ml, the cytotoxic effect was weak, since the cell viability ranged between 60 and 80%.
- Pitavastatin (green) at concentrations of 0.0075 – 0.0600 mg/ml were non-cytotoxic (> 80%); however, when concentrations were higher (0.1200 mg/ml), the cytotoxic effect was weak, as cell viability was > 60% (78.308%).
- Pravastatin (pink) at concentrations of 0.0075 – 0.1200 mg/ml remained non-cytotoxic (> 80%) throughout the experiment.

Figures E.13 and E.14 showed correlations between toxicity results and visual inspection, as neutral red dye was absorbed by the viable cells overall, which indicated weak toxicity.

#### E.3.2.2.2 Cell viability of the NE1s and PNE1 during NR-assay on treated HaCaT cells

**NE1s** and **PNE1** were dosed in different concentrations during the NR-assay and displayed the following cell viability (%) results as seen in Table E.10 and Figures E.15, E.16 and E.18.d.

**Table E.10:** The cell viability (%) of the **NE1s** and the **PNE1** dosed in different concentrations during the NR-assay

| Concentration of treatment (mg/ml) | NE1A (blue) | NE1F (yellow) | NE1Pi (green) | NE1Pr (pink) | PNE1 (red) |
|---|---|---|---|---|---|
| 0.025 | 103.768 | 101.862 | 93.633 | 106.367 | 107.417 |
| 0.050 | 77.066 | 77.564 | 93.070 | 107.580 | 109.836 |
| 0.100 | 57.661 | 73.644 | 60.693 | 79.903 | 102.152 |
| 0.200 | 49.453 | 54.954 | 47.439 | 39.664 | 117.597 |
| 0.400 | 22.599 | 2.371 | 17.380 | 17.639 | 112.878 |

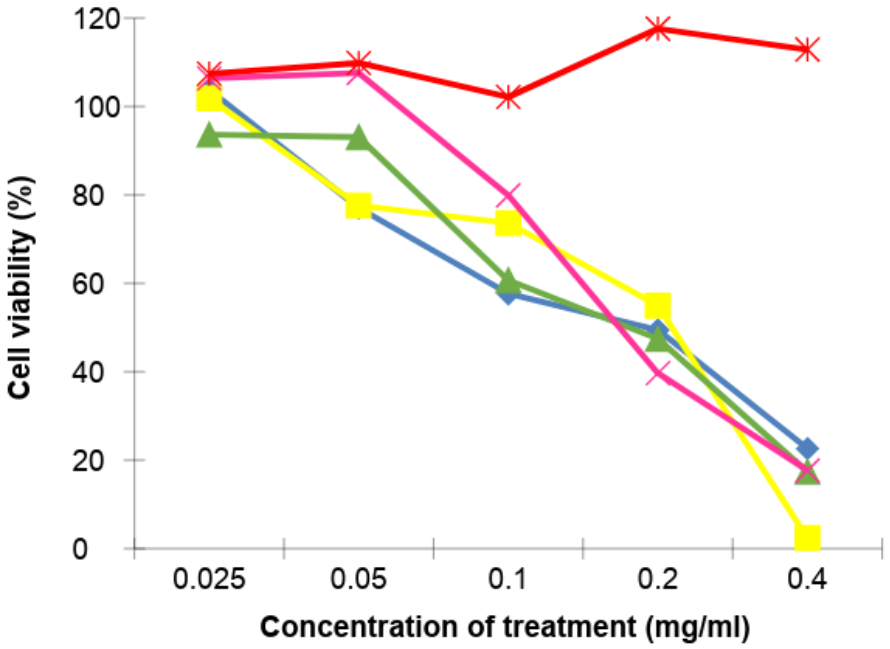


**Figure E.15:** The cytotoxic effects of the **NE1s** and the **PNE1** dosed in different concentrations during the NR-assay

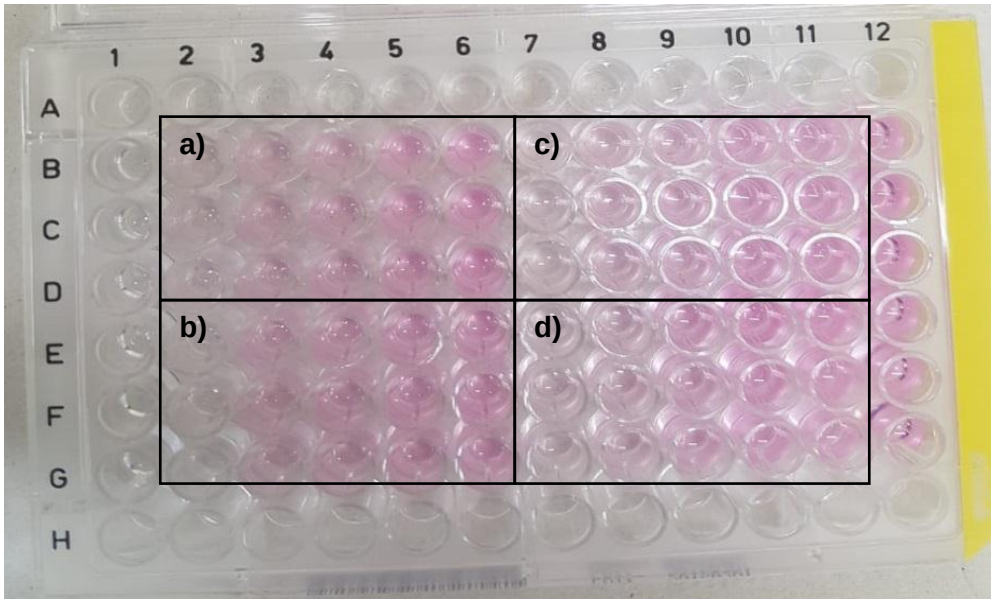


**Figure E.16:** Image of a 96-well plate containing cells treated with different concentrations of the **NE1s** during the NR-assay: a) **NE1A**, b) **NE1F**, c) **NE1Pi** and d) **NE1Pr**

From Table E.10 and Figure E.15, the cell viability (%) of the **NE1s** and the **PNE1** dosed in different concentrations was compared to the parameters of cell viability (López-García *et al*., 2014:44) when treated with NR and the following was noticed:

- **NE1A** (blue) at a concentration of 0.025 mg/ml, the cell viability was greater than 80% and therefore had a non-cytotoxic effect on the cells; but when the concentration was elevated to 0.050 mg/ml, the cytotoxic effect was weak (77.066%) and became moderate when the concentrations were at 0.100 – 0.200 mg/ml, since the cell viability ranged between 49.453 and 57.661% (40 – 60%). At a concentration of 0.400 mg/ml, atorvastatin formulations had strong cytotoxicity (22.599%), as the cell viability was below 40%.
- **NE1F** (yellow) at a concentration of 0.025 mg/ml was non-cytotoxic (>80%); although, when the concentration was increased to 0.050 – 0.100 mg/ml, the cytotoxic effect was weak (77.564 – 73.644). At a concentration of 0.200 and 0.400 mg/ml, the cytotoxic effect was moderate (54.954%) and strong (2.371%) on the cell viability, respectively.
- **NE1Pi** (green) at concentrations of 0.025 – 0.050 mg/ml posed as non-cytotoxic (> 80%), when the concentration was increased at 0.100 mg/ml, the cytotoxic effect was weak, but became moderate at a concentration of 0.200 mg/ml, as the cell viability was 40 – 60% (47.439). At a concentration of 0.400 mg/ml, **NE1Pi** had a strong cytotoxic effect on the cell viability, as it was below 40% (17.380%).
- **NE1Pr** (pink) at concentrations of 0.025 – 0.050 mg/ml remained non-cytotoxic (> 80%); hence, during a higher concentration (0.100 mg/ml), the cytotoxic effect was weak (79.903%), as it ranged between 60 and 80% and at the concentrations of 0.200 – 0.400 mg/ml, the cytotoxic effect on the cell viability was strong, since it was below 40% (39.664 to 17.639%).
- **PNE1** (red) at concentrations of 0.025 – 0.400 mg/ml stayed non-cytotoxic as the cell viability was greater than 80% throughout the experiment.

Figure E.15 indicated that when visually inspected, **NE1A**, **NE1F**, **NE1Pi** and **NE1Pr** had cytotoxic effects on the cells at the strongest concentrations, as damaged cells did not incorporate neutral red dye; viable cells treated with lower concentrations remained pink due to neutral red dye being absorbed by the viable cells. From Figure E.17.d, the **PNE1** was inspected visually and cells appeared to have incorporated neutral red dye.

#### E.3.2.2.3 Cell viability of the excipients during NR-assay on treated HaCaT cells

Tween® 80, Span® 60 and Span® 60-oil were dosed in different concentrations during NR-assay and displayed the following cell viability (%) results as seen in Table E.11 and Figures E.17 and E.18.a-c.

**Table E.11:** The cell viability (%) of the excipients dosed in different concentrations during the NR-assay

| Concentration of treatment (mg/ml) | Tween® 80 (blue) | Span® 60 (yellow) | Span® 60-oil (green) |
|---|---|---|---|
| 0.075 | 83.040 | 95.105 | 92.583 |
| 0.150 | 94.221 | 107.066 | 87.070 |
| 0.300 | 93.532 | 96.483 | 87.915 |
| 0.600 | 73.354 | 92.284 | 90.737 |
| 1.200 | 67.269 | 65.995 | 75.915 |

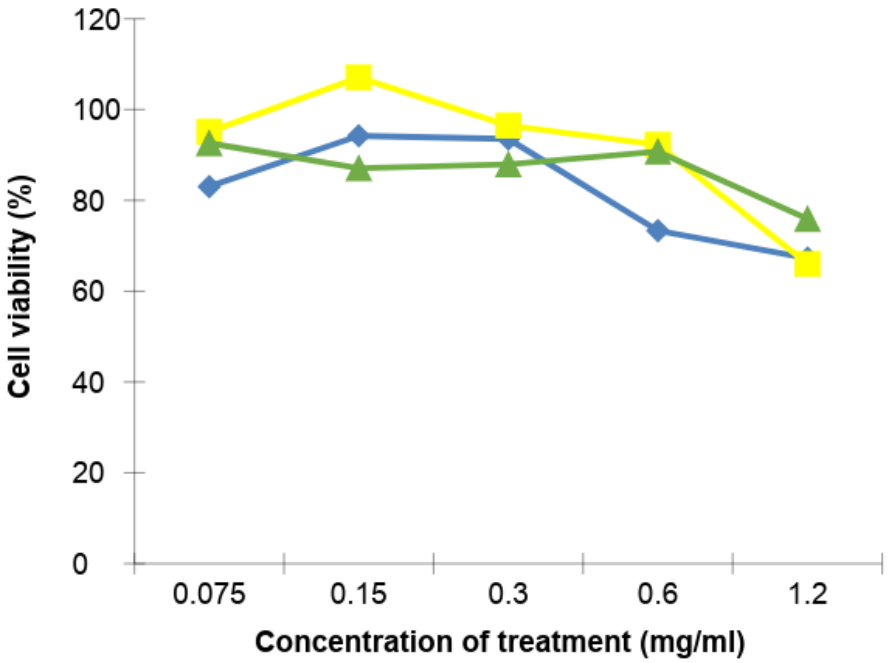


**Figure E.17:** The cytotoxic effects of the excipients dosed in different concentrations during the NR-assay

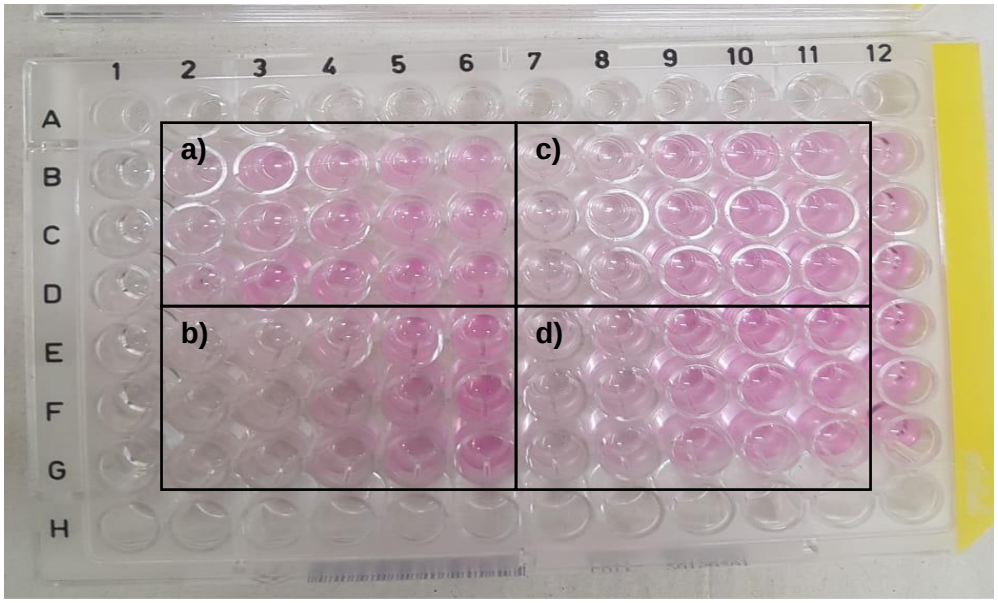


**Figure E.18:** Image of a 96-well plate containing cells treated with different concentrations of the excipients during the NR-assay: a) Tween® 80, b) Span® 60, c) Span® 60-oil and d) **PNE1** (discussed in Section E.3.2.2.2)

From Table E.11 and Figure E.17, the cell viability (%) of the excipients dosed in different concentrations were compared to the parameters of cell viability (López–García *et al*., 2014:44) when treated with NR and the following was observed:

- Tween® 80 (blue) and Span® 60 (yellow) had non-cytotoxic effects on cells at concentrations of 0.075 – 0.300 mg/ml, as the cell viability was greater than 80%. When the concentration was elevated to 0.600 mg/ml, the cytotoxic effects of Span® 60 was still non-cytotoxic (92.284%), but the cell viability of Tween® 80 became weak (73.354%). At a concentration of 1.200 mg/ml, the cell viability ranged between 60 – 80%, therefore, both Tween® 80 and Span® 60 (67.269 and 65.995%, respectively) had weak cytotoxic effects.
- Span® 60-apricot kernel oil (green) at concentrations of 0.075 – 0.600 mg/ml maintained a non-cytotoxic effect (> 80%) throughout the experiment, but as the concentration raised to 1.200 mg/ml, the cytotoxic effect of Span® 60-apricot kernel oil combination was weak (75.915%), as it ranged between 60 and 80%.

Figure E.18.a-c indicated that Tween® 80, Span® 60 and Span® 60-apricot kernel oil treatments had weak effects on the viability of cells at the strongest concentrations. This was because the damaged cells were not incorporated with neutral red dye to the same ability as the viable cells, treated with lower concentrations, which remained pink as neutral red dye was absorbed.

#### E.3.2.2.4 $IC_{50}$ values during the NR-assay

During the determination of $IC_{50}$ values for the NR-assays, the calculation method utilised in the MTT-assays (see Section E.3.1.2.4) was applied.

**Table E.12:** Calculated $IC_{50}$ values of statin solutions, **NE1s**, **PNE1** and the excipients from the NR-assay results

| Solutions | Compounds | $IC_{50}$ values (µg/ml) |
|---|---|---|
| **Statin solutions** | Atorvastatin | 0.1633 |
| | Fluvastatin | 0.1672 |
| | Pitavastatin | 0.3269 |
| | Pravastatin | 1.7275 |
| **Statin dispersions (NE1) and placebo dispersion (PNE1)** | **NE1A** | 0.2213 |
| | **NE1F** | 0.2052 |
| | **NE1Pi** | 0.2163 |
| | **NE1Pr** | 0.2354 |
| | **PNE1** | 8.6707 |
| **Excipients alone** | Tween® 80 | 1.9536 |
| | Span® 60 | 1.8091 |
| | Span® 60-oil | 3.5509 |

From Table E.12, $IC_{50}$ values (µg/ml) for statin solutions indicated that atorvastatin (0.1633 µg/ml) and fluvastatin (0.1672 µg/ml) inhibited HaCaT cells at a lower concentration, thus presented as the most toxic to the cells compared to pitavastatin (0.3269 µg/ml) and pravastatin (1.7275 µg/ml), which had the lowest toxicity and highest $IC_{50}$ value.

Investigation of the **NE1s** and the **PNE1** indicated that the **PNE1** (8.6707 µg/ml) showed the lowest toxicity, since it presented with the highest $IC_{50}$ value. For the **NE1s**, **NE1F** (0.2052 µg/ml) was the most inhibitory towards cells and displayed the lowest $IC_{50}$ value compared to and **NE1Pi** (0.2163 µg/ml), **NE1A** (0.2213 µg/ml) and **NE1Pr** (0.2354 µg/ml). Excipient and concentration doses could have played a role, due to the order of which the statins' $IC_{50}$ values varied from statin solutions'.

The results of excipients' $IC_{50}$ values displayed that Span® 60 (1.8091 µg/ml) and Tween® 80 (1.9536 µg/ml) had similar $IC_{50}$ values. Whereas, Span® 60-apricot kernel oil displayed as least toxic with the highest $IC_{50}$ value among the excipients (3.5509 µg/ml).

## E.4 Conclusion

The MTT- and NR-assays together with the $IC_{50}$ values offered data as to whether the statin solutions, **NE1s**, **PNE1** and excipients had cytotoxic effects on human epidermal cells. As mentioned before, all the treatments were performed in different concentrations, to determine the cytotoxic effects at specific concentrations.

The MTT results for statin solutions showed that purple formazan remained in the viable cells, as it was unable to overcome the membranes, which indicated weak toxicity. The $IC_{50}$ values for MTT results of statin solutions indicated that fluvastatin presented as the most toxic to the cells compared to atorvastatin, pitavastatin and pravastatin. NR-assay results for statin solutions showed that neutral red dye was absorbed by the viable cells overall, which indicated weak toxicity. NR-assay results for $IC_{50}$ values of statin solutions indicated that atorvastatin and fluvastatin presented more toxic to the cells compared to pitavastatin and pravastatin.

The **NE1s**, as well as **PNE1**, indicated cytotoxic effects on the cells during MTT-assays at high treatment concentrations; the **PNE1** showed the lowest toxicity $IC_{50}$ value. The **NE1A** displayed the lowest $IC_{50}$ value compared to **NE1F**, **NE1Pi** and **NE1Pr**, which again presented with the highest $IC_{50}$ value among the statins. The NR-assay results for the **NE1s**, as well as the **PNE1**, were cytotoxic on the cells at high concentrations; the **PNE1** however showed the lowest toxicity $IC_{50}$ value. The **NE1F** was the most toxic towards cells with the lowest $IC_{50}$ value compared to and **NE1Pi**, **NE1A** and **NE1Pr**.

The MTT- and NR-assay results for excipients alone indicated that Tween® 80, Span® 60 and Span® 60-apricot kernel oil treatments affected cell viability at high concentrations. Span® 60 and Tween® 80 had similar $IC_{50}$ values compared to Span® 60-apricot kernel oil, which displayed as least toxic with the highest $IC_{50}$ value among the excipients.

The MTT- and NR-assays were greatly affected by lipophilic formulations (Stockert *et al*., 2012:786), therefore, lipophilic statins, dispersions (**NE1** and **PNE1**) and lipophilic excipients could interfere with data and counter accurate results, especially in higher concentrations. MTT- and NR-assays were still utilised as a relative detection of cytotoxic effects of treatments on human epidermal cells, as they are the main cytotoxicity assays used to determine cell viability. Hence, to determine cell viability more accurately, additional examination, especially *in vivo* investigation should be performed.

**References**

ATCC see American Type Culture Collection

American type culture collection. 2011. MTT cell proliferation assay. https://www.atcc.org/~/media/DA5285A1F52C414E864C966FD78C9A79.ashx Date of access: 3 Sept. 2018.

Fotakis, G. & Timbrell, J.A. 2006. In vitro cytotoxicity assays: comparison of LDH, neutral red, MTT and protein assay in hepatoma cell lines following exposure to cadmium chloride. *Toxicology letters*, 160:171 – 177.

Fröhlich, E. 2013. Cellular targets and mechanisms in the cytotoxic action of nonbiodegradable engineered nanoparticles. *Current drug metabolism,* 14(9):976–988.

Galluzzi, L., Maiuri, M.C. Vitale, I., Zischka, H., Castedo, M., Zitvogel, L., Kroemer, G. 2007. Cell death modalities: classification and pathophysiological implications. *Cell death and differentiation*, 14:1237–1266.

Gibco®. 2016. Cell culture basics. http://www.vanderbilt.edu/viibre/CellCultureBasicsEU.pdf Date of access: 3 Sept. 2018.

Kumar, G.V.S., Sandhya, G.V. 2014. Preliminary phytochemical screening, total phenol content and in vitro antioxidant activity of *Caralluma Umbellata Haw*. *Journal of global trends in pharmaceutical sciences,* 5(2):1603 – 1611.

Li, W., Zhou, J., & Xu, Y.I. 2015. Study of the in vitro cytotoxicity testing of medical devices (review). *Biomedical reports*, 3:617 – 620.

López–García, J., Lehocký, M., Humpolíček, P. & Sáha, P. 2014. HaCaT keratinocytes response on antimicrobial atelocollagen substrates: extent of cytotoxicity, cell viability and proliferation. *Journal of functional biomaterials*, 5:43 – 57.

McGaw, L.J., Elgorashi, E.E., Eloff, J.N. 2014. Cytotoxicity of African medicinal plants against normal animal and human cells. *Toxicological survey of african medicinal plants*, Pages 181 – 233.

Niles, A.L., Moravec, R.A., Riss, T.L. 2008. Update on *in vitro* cytotoxicity assays for drug development. *Expert opinion on drug discovery*, 3(6) 655 – 669.

Niles, A.L., Moravec, R.A. & Riss, T.L. 2009. In vitro viability and cytotoxicity testing and same– well multi–parametric combinations for high throughput screening. *Current chemical genomics*, 3:33 – 41.

Provost & Wallert. 2015. Hemocytometer cell counting protocol. http://www.ruf.rice.edu/~bioslabs/methods/microscopy/cellcounting.html.pdf. Date of access: 29 Oct 2018.

Riss, T.L., Moravec, R.A., Niles, A.L., Benink, H.A., Worzella, T.J. & Minor, L. 2013. Assay guidance manual: cell viability assays. http://europepmc.org/books/NBK144065;jsessionid=nsYziiJZlQeP5FICGHoq.7. Date of access: 3 Sept. 2018.

Repetto, G., Sanz, P. 1993. Neutral red uptake, cellular growth and lysosomal function: in vitro effects of 24 metals. *Alternative to laboratory animals*, 21:501 – 507.

Repetto, G., Del Peso, A., Zurita, J.L. 2008. Neutral red uptake assay for the estimation of cell viability/cytotoxicity. *Nature protocols*, 3:1125 – 1131.

Roesler, R., Lorencini, M., Pastore, G. 2010. Brazilian cerrado antioxidants sources: cytotoxicity and phototoxicity *i vitro. Ciencia e tecnologia de alimentos,* 30(3):814 – 821.

Sigma. Trypten blue. https://www.researchgate.net/.../Sigma+trypan+blue+cell+counting.pdf. Date of access: 29 Oct 2018.

Stockert, J.C., Blázquez–Castro, A., Cañete, M., Horobin, R.W. & Villanueva, Á. 2012. MTT assay for cell viability: intracellular localization of the formazan product is in lipid droplets. *Acta histochemica*, 114:785 – 796.

Stoddart, M.J. Mammalian cell viability. http://file.zuma.ac.ir/ebook/023-Mammalian%20Cell%20viability%20-%20Methods%20and%20Protocols%20(Methods%20in%20Molecular%20Biology)-Martin%20 J.%20Sto.pdf. Date of access: 12 Oct 2018.

Yoon, M., Campbell, J.L., Andersen, M.E. & Clewell, H.J. 2012. Quantitative *in vitro* to *in vivo* extrapolation of cell–based toxicity assay results. *Critical Reviews in Toxicology*, 42:633 – 652.

# Appendix F

AUTHOR GUIDELINES: DIE PHARMAZIE

## F.1 Aim

The journal Die Pharmazie publishes reviews, experimental studies, letters to the editor, as well as book reviews.

The following fields of pharmacy are covered:

- Pharmaceutical and medicinal chemistry,
- pharmaceutical analysis and drug control,
- pharmaceutical technology, biopharmacy (biopharmaceutics, pharmacokinetics, biotransformation),
- experimental and clinical pharmacology,
- pharmaceutical biology (pharmacognosy), and
- history of pharmacy.

## F.2 Articles are published in English (preferred) or German and are classified as:

### F.2.1 Reviews

A summarizing presentation encompassing the current state of our knowledge, and providing comprehensive interpretation with citation of the literature.

### F.2.2 Original articles

Publications from all fields mentioned above.

### F.2.3 Short communications

Brief publications about the fields mentioned above (see Preparation of manuscripts)

### F.2.4 Book reviews

## F.3 Conditions

1. For submitted manuscripts, it is the responsibility of the author(s) to demonstrate novelty or a new approach taken in his research. The references should reflect the most recent relevant articles, and the discussion should compare the author's findings

with the results of former investigations. For an experimental work, the data have to be determined and classified in a suitable way, problems must be formulated in view of the data, hypotheses should be suggested an/or the author should give possible explanations for any inconsistencies.

If possible, the author(s) should perform mathematical or statistical calculations, fit the curves appropriate, and carry out the experiments under controlled conditions. Studies involving animals or human volunteers must include details of ethical approval.

2. Authors are requested to submit all manuscripts online.

Paper copy submissions are no longer acceptable.

Articles are considered for publication depending on their value and pharmaceutical relevance and with the understanding that they have not been published previously and are submitted exclusively to the journal Die Pharmazie.

3. All manuscripts are subject to experts review. Additional corrections may be done by the editors.
4. A PDF-file of the article is delivered free of charge after the paper has been published in the journal. Please not that, by copyright reasons, this is for personal use of the authors only and must not be made available, e.g. by posting on a freely accessible website.
5. Publication charges: Publication fees for publication in DiePharmazie are 250 € per manuscript (excl.VAT), regardless of type and lenght. Authors will receive an invoice right after acceptance of their paper which will not be published before the fee has been paid.
6. Delivery of a PDF-file of the article is included in the publication fee. Please note that, by copyright reasons, this is for personal use of the authors only and must not be made available, e.g. by posting on a freely accessible website.
7. The quotation of registered names, trade names, trademarks, etc. in this journal does not imply, even in the absence of a specific statement, that such names are exempt from the relevant laws and regulations and therefore free for general use.

### F.4 Preparation of manuscripts

In order to achieve uniform presentation and to avoid unnecessary delays because of further inquiries, all authors are requested to observe the following guidelines:

1. Below the title, the surname(s) of the author(s) with initials should be given without academic and professional degrees. The full address of the author for correspondence should appear below author names. Details on the institution where the work was done are requested and should be given above the title.
2. Each manuscript should start with an abstract, containing the most essential results of the study. Extensive review papers and articles for continuous education should be preceded by an outline of topics.

Papers should be subdivided into chapters and subchapters according to the decimal system (e.g. 2.1.3.).

3. To achieve clarity and brevity of the presentation, original contributions should be subdivided after the abstract (see 2.) as follows:

    3.1 Introduction: This should indicate the question under investigation which is generally based on a brief interpretation of the literature considering the current state of knowledge in the subfield and explaining the necessary theoretical foundations.

    3.2 Investigations and results or synthesis of compounds: Methods should only be described generally (see "Experimental"), referring to previous or analogous studies. The presentation of results should be precise, with necessary formulas (numbered in sequence with Arabic numerals), diagrams, tables and figures added separately (together with the legend) to the manuscripts. Numerical values of results should generally be presented either in tables or curves (please mark statistical limits).

    3.3 Discussion (unless covered by 2. as Investigations, results and discussion): It should not repeat results already given, but should state the conclusions drawn from the results or provide a theoretical debate and comparison with literature citations.

    3.4 Experimental: This part describes briefly the detailed experimental conditions. Unless directions taken from literature have been modified, it suffices to refer to the original source. In the case of well known inorganic or organic compounds chemical formulae or common abbreviations may be used (e.g. NaCI, H2SO4, CH3OH, C6H6: Ac, Eth, Me, Phe, DMSO) under "Experimental". In other parts of the paper this is not desirable.

Results of elemental analyses can be omitted if it is stated that all the results were in an acceptable error range.

4. Short communications are published as rapidly as possible. The length of a manuscript is limited to 100 lines (including short summary; subdivisions are not required; the "Experimental" - if there is one - should be marked), up to 15 citations of literature and a maximum of 2 supplementary materials (schemes, figures, tables) are allowed.
5. Only the surnames of authors are given in the text. When there are more than two authors, only the name of the first one is used, followed by *et al*.
6. References in the text have to be cited by author and year, if there are three or more authors, use et al. (Miller 1997; Miller and Smith 2000; Miller et al. 2001). If the year is the same for several references identify these with a, b, c etc (Smith 1998a; Smith 1998b etc.) both in the text and in the reference list. At the end of the paper, references are listed in alphabetical order under the first authors surname. If there are several references to items with the same first author, arrange these chronologically regardless the alphabetical order of the co-authors ("alphabetic-chronological" order).

Journal names should be abbreviated according to "Index Medicus" (Medline) or "Chemical Abstracts Service Source Index".

### F.5 Quotations have to follow the following style:

#### F.5.1 Journal articles:

Lee J (2002) Formulation development of epidermal growth factor. Pharmazie 57: 787 – 790.

Lee EB, Shin KH, Woo WS (1984) Pharmacological study on piperine. Arch Pharm Res 7: 127 - 132.

If each issue of a journal has its own pagination the issue number should be indicated in brackets after the volume number.

#### F.5.2 Books/Book chapters

Krishan K, Andersen ME (1994) Physiologically based pharmacokinetic modeling in toxicology. In: Hayes W (ed.) Principles and methods of toxicology, 3rd ed., New York, p. 149 – 187

Only if each issue of a journal has its own pagination the issue number should be indicated in brackets after the volume number.

7. For the identification of pharmaceutical substances, the International Nonproprietary Names (INN) proposed or recommended by the WHO should be used. Registered Trade Marks (usually indicated with R; in an article this sign should only be used when it is first mentioned or used in the summary), trivial names and chemical nomenclature can be added.
8. Nomenclature and spelling should conform to the directions given by IUPAC and IUB.
9. Units of measurement are determined by the directions of the International Units System SI as symbols; M instead of mol/l or mol * l-1 is allowed
10. Botanical names (species, genus) should be marked in italics.
11. The following abbreviations should be used consequently (except in the title and all subtitles). All other abbreviations have to be explained in the manuscript at first usage, if aforementioned directions are not applicable. Abs. = absolute: anh. = anhydrous; b.p.; b.r. = boiling point, -range; calcd. = calculated; CC = column chromatography; conc. = concentrated; dec. = decomposition, eq. = equation; Fig. = figure; GC = gas chromatography, - chromatogram, HPLC = high performance liquid chromatography, -chromatogram; i.m. = intramuscular; i.p. = intraperitoneal; IR = infrared; i.v. = intravenous; m.p.; m.r. = melting point, -range; MS = mass spectometry, mass spectrum; NMR = nuclear magnetic resonance spectrum; PC = paper chromatography, - chromatogram, % = per cent, percentage, p.o. = peroral; s.c. = subcutaneous; TLC = thin layer chromatography, - chromatogram; UV = ultraviolet.
12. Footnotes must be numbered consecutively and are to be added separately to the manuscript. They are printed following the "Experimental".
13. Dedications (e.g., on the occasion of the 60th or higher birthday) should be inserted between author(s) and summary.
14. Additions to legends of table should be marked by *,**,*** or a,b,c,d etc.
15. Figures have to be of sufficient quality for reproduction process. Even after size reduction the figures' key has to be easy to read. Manuscripts containing figures of insufficient quality cannot be accepted.

# Appendix G

THE INTERNATIONAL JOURNAL OF PHARMACEUTICS: GUIDE FOR AUTHORS

## G.1 Introduction

The International Journal of Pharmaceutics publishes innovative papers, reviews, mini-reviews, rapid communications and notes dealing with physical, chemical, biological, microbiological and engineering studies related to the conception, design, production, characterisation and evaluation of drug delivery systems in vitro and in vivo. "Drug" is defined as any therapeutic or diagnostic entity, including oligonucleotides, gene constructs and radiopharmaceuticals.

Areas of particular interest include: pharmaceutical nanotechnology; physical pharmacy; polymer chemistry and physical chemistry as applied to pharmaceutics; excipient function and characterisation; biopharmaceutics; absorption mechanisms; membrane function and transport; novel routes and modes of delivery; responsive delivery systems, feedback and control mechanisms including biosensors; applications of cell and molecular biology to drug delivery; prodrug design; bioadhesion (carrier-ligand interactions); and biotechnology (protein and peptide formulation and delivery).

Note: For details on pharmaceutical nanotechnology, see Editorials in 279/1-2 281/1, and 288/1.

## G.2 Types of paper

### G.2.1 Full Length Manuscripts

### G.2.2 Reviews and Mini-Reviews

Suggestions for review articles will be considered by the Review-Editor. "Mini-reviews" of a topic are especially welcome.

## G.3 Ethics in publishing

Please see our information pages on Ethics in publishing and Ethical guidelines for journal publication.

## G.4 Studies in humans and animals

If the work involves the use of human subjects, the author should ensure that the work described has been carried out in accordance with The Code of Ethics of the World Medical Association (Declaration of Helsinki) for experiments involving humans. The manuscript should be in line with the Recommendations for the Conduct, Reporting, Editing and Publication of Scholarly Work in Medical Journals and aim for the inclusion of representative human populations (sex, age and ethnicity) as per those recommendations. The terms sex and gender should be used correctly.

Authors should include a statement in the manuscript that informed consent was obtained for experimentation with human subjects. The privacy rights of human subjects must always be observed.

All animal experiments should comply with the ARRIVE guidelines and should be carried out in accordance with the U.K. Animals (Scientific Procedures) Act, 1986 and associated guidelines, EU Directive 2010/63/EU for animal experiments, or the National Institutes of Health guide for the care and use of Laboratory animals (NIH Publications No. 8023, revised 1978) and the authors should clearly indicate in the manuscript that such guidelines have been followed. The sex of animals must be indicated, and where appropriate, the influence (or association) of sex on the results of the study.

Examples of potential conflicts of interest include employment, consultancies, stock ownership, honoraria, paid expert testimony, patent applications/registrations, and grants or other funding.

## G.5 Declaration of interest

All authors must disclose any financial and personal relationships with other people or organizations that could inappropriately influence (bias) their work. Examples of potential competing interests include employment, consultancies, stock ownership, honoraria, paid expert testimony, patent applications/registrations, and grants or other funding. Authors must disclose any interests in two places: 1. A summary declaration of interest statement in the title page file (if double-blind) or the manuscript file (if single-blind). If there are no interests to declare then please state this: 'Declarations of interest: none'. This summary statement will be ultimately published if the article is accepted. 2. Detailed disclosures as part of a separate Declaration of Interest form, which forms part of the journal's official records. It is important for potential interests to be declared in both places and that the information matches. More information.

### G.6 Submission declaration and verification

Submission of an article implies that the work described has not been published previously (except in the form of an abstract, a published lecture or academic thesis, see 'Multiple, redundant or concurrent publication' for more information), that it is not under consideration for publication elsewhere, that its publication is approved by all authors and tacitly or explicitly by the responsible authorities where the work was carried out, and that, if accepted, it will not be published elsewhere in the same form, in English or in any other language, including electronically without the written consent of the copyright-holder. To verify originality, your article may be checked by the originality detection service Crossref Similarity Check.

### G.7 Preprints

Please note that preprints can be shared anywhere at any time, in line with Elsevier's sharing policy. Sharing your preprints e.g. on a preprint server will not count as prior publication (see 'Multiple, redundant or concurrent publication' for more information).

### G.8 Use of inclusive language

Inclusive language acknowledges diversity, conveys respect to all people, is sensitive to differences, and promotes equal opportunities. Articles should make no assumptions about the beliefs or commitments of any reader, should contain nothing which might imply that one individual is superior to another on the grounds of race, sex, culture or any other characteristic, and should use inclusive language throughout. Authors should ensure that writing is free from bias, for instance by using 'he or she', 'his/her' instead of 'he' or 'his', and by making use of job titles that are free of stereotyping (e.g. 'chairperson' instead of 'chairman' and 'flight attendant' instead of 'stewardess').

### G.9 Author contributions

For transparency, we encourage authors to submit an author statement file outlining their individual contributions to the paper using the relevant CRediT roles: Conceptualization; Data curation; Formal analysis; Funding acquisition; Investigation; Methodology; Project administration; Resources; Software; Supervision; Validation; Visualization; Roles/Writing - original draft; Writing - review & editing. Authorship statements should be formatted with the names of authors first and CRediT role(s) following. More details and an example

### G.10 Authorship

All authors should have made substantial contributions to all of the following: (1) the conception and design of the study, or acquisition of data, or analysis and interpretation of data, (2) drafting the article or revising it critically for important intellectual content, (3) final approval of the version to be submitted.

### G.11 Changes to authorship

Authors are expected to consider carefully the list and order of authors before submitting their manuscript and provide the definitive list of authors at the time of the original submission. Any addition, deletion or rearrangement of author names in the authorship list should be made only before the manuscript has been accepted and only if approved by the journal Editor. To request such a change, the Editor must receive the following from the corresponding author: (a) the reason for the change in author list and (b) written confirmation (e-mail, letter) from all authors that they agree with the addition, removal or rearrangement. In the case of addition or removal of authors, this includes confirmation from the author being added or removed.

Only in exceptional circumstances will the Editor consider the addition, deletion or rearrangement of authors after the manuscript has been accepted. While the Editor considers the request, publication of the manuscript will be suspended. If the manuscript has already been published in an online issue, any requests approved by the Editor will result in a corrigendum.

### G.12 Article transfer service

This journal is part of our Article Transfer Service. This means that if the Editor feels your article is more suitable in one of our other participating journals, then you may be asked to consider transferring the article to one of those. If you agree, your article will be transferred automatically on your behalf with no need to reformat. Please note that your article will be reviewed again by the new journal. More information.

### G.13 Copyright

Upon acceptance of an article, authors will be asked to complete a 'Journal Publishing Agreement' (see more information on this). An e-mail will be sent to the corresponding author confirming receipt of the manuscript together with a 'Journal Publishing Agreement' form or a link to the online version of this agreement.

Subscribers may reproduce tables of contents or prepare lists of articles including abstracts for internal circulation within their institutions. Permission of the Publisher is required for resale or distribution outside the institution and for all other derivative works, including compilations and translations. If excerpts from other copyrighted works are included, the author(s) must obtain written permission from the copyright owners and credit the source(s) in the article. Elsevier has preprinted forms for use by authors in these cases.

For gold open access articles: Upon acceptance of an article, authors will be asked to complete an 'Exclusive License Agreement' (more information). Permitted third party reuse of gold open access articles is determined by the author's choice of user license.

### G.14 Author rights

As an author you (or your employer or institution) have certain rights to reuse your work. More information.

Elsevier supports responsible sharing

Find out how you can share your research published in Elsevier journals.

### G.15 Role of the funding source

You are requested to identify who provided financial support for the conduct of the research and/or preparation of the article and to briefly describe the role of the sponsor(s), if any, in study design; in the collection, analysis and interpretation of data; in the writing of the report; and in the decision to submit the article for publication. If the funding source(s) had no such involvement then this should be stated.

### G.16 Funding body agreements and policies

Elsevier has established a number of agreements with funding bodies which allow authors to comply with their funder's open access policies. Some funding bodies will reimburse the author for the gold open access publication fee. Details of existing agreements are available online.

## G.17 Open access

This journal offers authors a choice in publishing their research:

**Subscription**

- Articles are made available to subscribers as well as developing countries and patient groups through our universal access programs.
- No open access publication fee payable by authors.
- The Author is entitled to post the accepted manuscript in their institution's repository and make this public after an embargo period (known as green Open Access). The published journal article cannot be shared publicly, for example on ResearchGate or Academia.edu, to ensure the sustainability of peer-reviewed research in journal publications. The embargo period for this journal can be found below.

**Gold open access**

- Articles are freely available to both subscribers and the wider public with permitted reuse.
- A gold open access publication fee is payable by authors or on their behalf, e.g. by their research funder or institution.

Regardless of how you choose to publish your article, the journal will apply the same peer review criteria and acceptance standards. For gold open access articles, permitted third party (re)use is defined by the following Creative Commons user licenses:

**Creative Commons Attribution (CC BY)**

Lets others distribute and copy the article, create extracts, abstracts, and other revised versions, adaptations or derivative works of or from an article (such as a translation), include in a collective work (such as an anthology), text or data mine the article, even for commercial purposes, as long as they credit the author(s), do not represent the author as endorsing their adaptation of the article, and do not modify the article in such a way as to damage the author's honor or reputation.

**Creative Commons Attribution-NonCommercial-NoDerivs (CC BY-NC-ND)**

For non-commercial purposes, lets others distribute and copy the article, and to include in a collective work (such as an anthology), as long as they credit the author(s) and provided they do not alter or modify the article.

The gold open access publication fee for this journal is USD 3700, excluding taxes. Learn more about Elsevier's pricing policy: https://www.elsevier.com/openaccesspricing.

**Green open access**

Authors can share their research in a variety of different ways and Elsevier has a number of green open access options available. We recommend authors see our green open access page for further information. Authors can also self-archive their manuscripts immediately and enable public access from their institution's repository after an embargo period. This is the version that has been accepted for publication and which typically includes author-incorporated changes suggested during submission, peer review and in editor-author communications. Embargo period: For subscription articles, an appropriate amount of time is needed for journals to deliver value to subscribing customers before an article becomes freely available to the public. This is the embargo period and it begins from the date the article is formally published online in its final and fully citable form. Find out more.

This journal has an embargo period of 12 months.

### G.18 Elsevier Researcher Academy

Researcher Academy is a free e-learning platform designed to support early and mid-career researchers throughout their research journey. The "Learn" environment at Researcher Academy offers several interactive modules, webinars, downloadable guides and resources to guide you through the process of writing for research and going through peer review. Feel free to use these free resources to improve your submission and navigate the publication process with ease.

### G.19 Language (usage and editing services)

Please write your text in good English (American or British usage is accepted, but not a mixture of these). Authors who feel their English language manuscript may require editing to eliminate possible grammatical or spelling errors and to conform to correct scientific English may wish to use the English Language Editing service available from Elsevier's WebShop.

## G.20 Submission

Our online submission system guides you stepwise through the process of entering your article details and uploading your files. The system converts your article files to a single PDF file used in the peer-review process. Editable files (e.g., Word, LaTeX) are required to typeset your article for final publication. All correspondence, including notification of the Editor's decision and requests for revision, is sent by e-mail.

Authors must state in a covering letter when submitting papers for publication the novelty embodied in their work or in the approach taken in their research. Routine bioequivalence studies are unlikely to find favour. No paper will be published which does not disclose fully the nature of the formulation used or details of materials which are key to the performance of a product, drug or excipient. Work which is predictable in outcome, for example the inclusion of another drug in a cyclodextrin to yield enhanced dissolution, will not be published unless it provides new insight into fundamental principles.

Note:

The choice of general classifications such as "drug delivery" or "formulation" are rarely helpful when not used together with a more specific classification.

## G.21 Referees

Please submit, with the manuscript, the names, addresses and e-mail addresses of at least four potential reviewers. Good suggestions lead to faster processing of your paper. Please note:

Reviewers who do not have an institutional e-mail address will only be considered if their affiliations are given and can be verified.

Please ensure that the e-mail addresses are current.

International reviewers who have recently published in the appropriate field should be nominated, and their areas of expertise must be stated clearly.

Note that the editor retains the sole right to decide whether or not the suggested reviewers are contacted.

To aid the editorial process when suggested reviewers are not chosen or decline to review, ensure that the classifications chosen as the field of your paper are as detailed as possible. It is not sufficient to state "drug delivery" or "nanotechnology" etc.

### G.22 Use of word processing software

It is important that the file be saved in the native format of the word processor used. The text should be in single-column format. Keep the layout of the text as simple as possible. Most formatting codes will be removed and replaced on processing the article. In particular, do not use the word processor's options to justify text or to hyphenate words. However, do use bold face, italics, subscripts, superscripts etc. When preparing tables, if you are using a table grid, use only one grid for each individual table and not a grid for each row. If no grid is used, use tabs, not spaces, to align columns. The electronic text should be prepared in a way very similar to that of conventional manuscripts (see also the Guide to Publishing with Elsevier). Note that source files of figures, tables and text graphics will be required whether or not you embed your figures in the text. See also the section on Electronic artwork.

To avoid unnecessary errors you are strongly advised to use the 'spell-check' and 'grammar-check' functions of your word processor.

### G.23 Article structure

#### G.23.1 Subdivision - numbered sections

Divide your article into clearly defined and numbered sections. Subsections should be numbered 1.1 (then 1.1.1, 1.1.2), 1.2, etc. (the abstract is not included in section numbering). Use this numbering also for internal cross-referencing: do not just refer to 'the text'. Any subsection may be given a brief heading. Each heading should appear on its own separate line.

#### G.23.2 Introduction

State the objectives of the work and provide an adequate background, avoiding a detailed literature survey or a summary of the results.

#### G.23.3 Material and methods

Provide sufficient details to allow the work to be reproduced by an independent researcher. Methods that are already published should be summarized, and indicated by a reference. If quoting directly from a previously published method, use quotation marks and also cite the source. Any modifications to existing methods should also be described.

### G.23.4 Results

Results should be clear and concise.

### G.23.5 Discussion

This should explore the significance of the results of the work, not repeat them. A combined Results and Discussion section is often appropriate. Avoid extensive citations and discussion of published literature.

### G.23.6 Conclusions

The main conclusions of the study may be presented in a short Conclusions section, which may stand alone or form a subsection of a Discussion or Results and Discussion section.

### G.23.7 Appendices

If there is more than one appendix, they should be identified as A, B, etc. Formulae and equations in appendices should be given separate numbering: Eq. (A.1), Eq. (A.2), etc.; in a subsequent appendix, Eq. (B.1) and so on. Similarly for tables and figures: Table A.1; Fig. A.1, etc.

### G.23.8 Essential title page information

- Title. Concise and informative. Titles are often used in information-retrieval systems. Avoid abbreviations and formulae where possible.
- Author names and affiliations. Please clearly indicate the given name(s) and family name(s) of each author and check that all names are accurately spelled. You can add your name between parentheses in your own script behind the English transliteration. Present the authors' affiliation addresses (where the actual work was done) below the names. Indicate all affiliations with a lower-case superscript letter immediately after the author's name and in front of the appropriate address. Provide the full postal address of each affiliation, including the country name and, if available, the e-mail address of each author.
- Corresponding author. Clearly indicate who will handle correspondence at all stages of refereeing and publication, also post-publication. This responsibility includes answering any future queries about Methodology and Materials. Ensure that the e-mail address is given and that contact details are kept up to date by the corresponding author.

- Present/permanent address. If an author has moved since the work described in the article was done, or was visiting at the time, a 'Present address' (or 'Permanent address') may be indicated as a footnote to that author's name. The address at which the author actually did the work must be retained as the main, affiliation address. Superscript Arabic numerals are used for such footnotes.

### G.23.9 Abstract

A concise and factual abstract is required. The abstract should state briefly the purpose of the research, the principal results and major conclusions. An abstract is often presented separately from the article, so it must be able to stand alone. For this reason, References should be avoided, but if essential, then cite the author(s) and year(s). Also, non-standard or uncommon abbreviations should be avoided, but if essential they must be defined at their first mention in the abstract itself.

The abstract must not exceed 200 words.

### G.23.10 Graphical abstract

A Graphical abstract is mandatory for this journal. It should summarize the contents of the article in a concise, pictorial form designed to capture the attention of a wide readership online. Authors must provide images that clearly represent the work described in the article. Graphical abstracts should be submitted as a separate file in the online submission system. Image size: please provide an image with a minimum of 531 × 1328 pixels (h × w) or proportionally more, but should be readable on screen at a size of 200 × 500 pixels (at 96 dpi this corresponds to 5 × 13 cm). Bear in mind readability after reduction, especially if using one of the figures from the article itself. Preferred file types: TIFF, EPS, PDF or MS Office files. See http://www.elsevier.com/graphicalabstracts for examples.

### G.23.11 Keywords

Immediately after the abstract, provide a maximum of 6 keywords, using American spelling and avoiding general and plural terms and multiple concepts (avoid, for example, 'and', 'of'). Be sparing with abbreviations: only abbreviations firmly established in the field may be eligible. These keywords will be used for indexing purposes.

### G.23.12 Abbreviations

Define abbreviations that are not standard in this field in a footnote to be placed on the first page of the article. Such abbreviations that are unavoidable in the abstract must be defined at

their first mention there, as well as in the footnote. Ensure consistency of abbreviations throughout the article.

### G.23.13 Acknowledgements

Collate acknowledgements in a separate section at the end of the article before the references and do not, therefore, include them on the title page, as a footnote to the title or otherwise. List here those individuals who provided help during the research (e.g., providing language help, writing assistance or proof reading the article, etc.).

### G.23.14 Formatting of funding sources

List funding sources in this standard way to facilitate compliance to funder's requirements:

Funding: This work was supported by the National Institutes of Health [grant numbers xxxx, yyyy]; the Bill & Melinda Gates Foundation, Seattle, WA [grant number zzzz]; and the United States Institutes of Peace [grant number aaaa].

It is not necessary to include detailed descriptions on the program or type of grants and awards. When funding is from a block grant or other resources available to a university, college, or other research institution, submit the name of the institute or organization that provided the funding.

If no funding has been provided for the research, please include the following sentence:

This research did not receive any specific grant from funding agencies in the public, commercial, or not-for-profit sectors.

### G.23.15 Units

Follow internationally accepted rules and conventions: use the international system of units (SI). If other units are mentioned, please give their equivalent in SI.

### G.23.16 Math formulae

Please submit math equations as editable text and not as images. Present simple formulae in line with normal text where possible and use the solidus (/) instead of a horizontal line for small fractional terms, e.g., X/Y. In principle, variables are to be presented in italics. Powers of e are often more conveniently denoted by exp. Number consecutively any equations that have to be displayed separately from the text (if referred to explicitly in the text).

### G.23.17 Footnotes

Footnotes should be used sparingly. Number them consecutively throughout the article. Many word processors can build footnotes into the text, and this feature may be used. Otherwise, please indicate the position of footnotes in the text and list the footnotes themselves separately at the end of the article. Do not include footnotes in the Reference list.

### G.23.18 Image manipulation

Whilst it is accepted that authors sometimes need to manipulate images for clarity, manipulation for purposes of deception or fraud will be seen as scientific ethical abuse and will be dealt with accordingly. For graphical images, this journal is applying the following policy: no specific feature within an image may be enhanced, obscured, moved, removed, or introduced. Adjustments of brightness, contrast, or color balance are acceptable if and as long as they do not obscure or eliminate any information present in the original. Nonlinear adjustments (e.g. changes to gamma settings) must be disclosed in the figure legend.

## G.24 Electronic artwork

**General points**

- Make sure you use uniform lettering and sizing of your original artwork.
- Embed the used fonts if the application provides that option.
- Aim to use the following fonts in your illustrations: Arial, Courier, Times New Roman, Symbol, or use fonts that look similar.
- Number the illustrations according to their sequence in the text.
- Use a logical naming convention for your artwork files.
- Provide captions to illustrations separately.
- Size the illustrations close to the desired dimensions of the published version.
- Submit each illustration as a separate file.

A detailed guide on electronic artwork is available.

You are urged to visit this site; some excerpts from the detailed information are given here.

### G.25 Formats

If your electronic artwork is created in a Microsoft Office application (Word, PowerPoint, Excel) then please supply 'as is' in the native document format.

Regardless of the application used other than Microsoft Office, when your electronic artwork is finalized, please 'Save as' or convert the images to one of the following formats (note the resolution requirements for line drawings, halftones, and line/halftone combinations given below):

- EPS (or PDF): Vector drawings, embed all used fonts.
- TIFF (or JPEG): Color or grayscale photographs (halftones), keep to a minimum of 300 dpi.
- TIFF (or JPEG): Bitmapped (pure black & white pixels) line drawings, keep to a minimum of 1000 dpi.
- TIFF (or JPEG): Combinations bitmapped line/half-tone (color or grayscale), keep to a minimum of 500 dpi

Please do not:

- Supply files that are optimized for screen use (e.g., GIF, BMP, PICT, WPG); these typically have a low number of pixels and limited set of colors;
- Supply files that are too low in resolution;
- Submit graphics that are disproportionately large for the content.

#### G.25.1 Color artwork

Please make sure that artwork files are in an acceptable format (TIFF (or JPEG), EPS (or PDF), or MS Office files) and with the correct resolution. If, together with your accepted article, you submit usable color figures then Elsevier will ensure, at no additional charge, that these figures will appear in color online (e.g., ScienceDirect and other sites) regardless of whether or not these illustrations are reproduced in color in the printed version. For color reproduction in print, you will receive information regarding the costs from Elsevier after receipt of your accepted article. Please indicate your preference for color: in print or online only. Further information on the preparation of electronic artwork.

### G.25.2 Figure captions

Ensure that each illustration has a caption. Supply captions separately, not attached to the figure. A caption should comprise a brief title (not on the figure itself) and a description of the illustration. Keep text in the illustrations themselves to a minimum but explain all symbols and abbreviations used.

### G.25.3 Tables

Please submit tables as editable text and not as images. Tables can be placed either next to the relevant text in the article, or on separate page(s) at the end. Number tables consecutively in accordance with their appearance in the text and place any table notes below the table body. Be sparing in the use of tables and ensure that the data presented in them do not duplicate results described elsewhere in the article. Please avoid using vertical rules and shading in table cells.

## G.26 References

### G.26.1 Citation in text

Please ensure that every reference cited in the text is also present in the reference list (and vice versa). Any references cited in the abstract must be given in full. Unpublished results and personal communications are not recommended in the reference list, but may be mentioned in the text. If these references are included in the reference list they should follow the standard reference style of the journal and should include a substitution of the publication date with either 'Unpublished results' or 'Personal communication'. Citation of a reference as 'in press' implies that the item has been accepted for publication and a copy of the title page of the relevant article must be submitted.

### G.26.2 Reference links

Increased discoverability of research and high quality peer review are ensured by online links to the sources cited. In order to allow us to create links to abstracting and indexing services, such as Scopus, CrossRef and PubMed, please ensure that data provided in the references are correct. Please note that incorrect surnames, journal/book titles, publication year and pagination may prevent link creation. When copying references, please be careful as they may already contain errors. Use of the DOI is highly encouraged.

A DOI is guaranteed never to change, so you can use it as a permanent link to any electronic article. An example of a citation using DOI for an article not yet in an issue is: VanDecar J.C.,

Russo R.M., James D.E., Ambeh W.B., Franke M. (2003). Aseismic continuation of the Lesser Antilles slab beneath northeastern Venezuela. Journal of Geophysical Research, https://doi.org/10.1029/2001JB000884. Please note the format of such citations should be in the same style as all other references in the paper.

### G.26.3 Web references

As a minimum, the full URL should be given and the date when the reference was last accessed. Any further information, if known (DOI, author names, dates, reference to a source publication, etc.), should also be given. Web references can be listed separately (e.g., after the reference list) under a different heading if desired, or can be included in the reference list.

### G.26.4 Data references

This journal encourages you to cite underlying or relevant datasets in your manuscript by citing them in your text and including a data reference in your Reference List. Data references should include the following elements: author name(s), dataset title, data repository, version (where available), year, and global persistent identifier. Add [dataset] immediately before the reference so we can properly identify it as a data reference. The [dataset] identifier will not appear in your published article.

### G.26.5 References in a special issue

Please ensure that the words 'this issue' are added to any references in the list (and any citations in the text) to other articles in the same Special Issue.

### G.26.6 Reference management software

Most Elsevier journals have their reference template available in many of the most popular reference management software products. These include all products that support Citation Style Language styles, such as Mendeley and Zotero, as well as EndNote. Using the word processor plug-ins from these products, authors only need to select the appropriate journal template when preparing their article, after which citations and bibliographies will be automatically formatted in the journal's style. If no template is yet available for this journal, please follow the format of the sample references and citations as shown in this Guide. If you use reference management software, please ensure that you remove all field codes before submitting the electronic manuscript. More information on how to remove field codes.

Users of Mendeley Desktop can easily install the reference style for this journal by clicking the following link:

http://open.mendeley.com/use-citation-style/international-journal-of-pharmaceutics

When preparing your manuscript, you will then be able to select this style using the Mendeley plug-ins for Microsoft Word or LibreOffice.

### G.26.7 Reference formatting

There are no strict requirements on reference formatting at submission. References can be in any style or format as long as the style is consistent. Where applicable, author(s) name(s), journal title/book title, chapter title/article title, year of publication, volume number/book chapter and the article number or pagination must be present. Use of DOI is highly encouraged. The reference style used by the journal will be applied to the accepted article by Elsevier at the proof stage. Note that missing data will be highlighted at proof stage for the author to correct. If you do wish to format the references yourself they should be arranged according to the following examples:

### G.26.8 Reference style

**Text**: All citations in the text should refer to:

1. **Single author**: the author's name (without initials, unless there is ambiguity) and the year of publication;
2. **Two authors**: both authors' names and the year of publication;
3. **Three or more authors**: first author's name followed by 'et al.' and the year of publication.

Citations may be made directly (or parenthetically). Groups of references can be listed either first alphabetically, then chronologically, or vice versa.

Examples: 'as demonstrated (Allan, 2000a, 2000b, 1999; Allan and Jones, 1999)…. Or, as demonstrated (Jones, 1999; Allan, 2000)… Kramer et al. (2010) have recently shown …'

List: References should be arranged first alphabetically and then further sorted chronologically if necessary. More than one reference from the same author(s) in the same year must be identified by the letters 'a', 'b', 'c', etc., placed after the year of publication.

**Examples:**

**Reference to a journal publication:**

Van der Geer, J., Hanraads, J.A.J., Lupton, R.A., 2010. The art of writing a scientific article. J. Sci. Commun. 163, 51–59. https://doi.org/10.1016/j.Sc.2010.00372.

Reference to a journal publication with an article number:

Van der Geer, J., Hanraads, J.A.J., Lupton, R.A., 2018. The art of writing a scientific article. Heliyon. 19, e00205. https://doi.org/10.1016/j.heliyon.2018.e00205.

**Reference to a book:**

Strunk Jr., W., White, E.B., 2000. The Elements of Style, fourth ed. Longman, New York.

**Reference to a chapter in an edited book:**

Mettam, G.R., Adams, L.B., 2009. How to prepare an electronic version of your article, in: Jones, B.S., Smith , R.Z. (Eds.), Introduction to the Electronic Age. E-Publishing Inc., New York, pp. 281–304.

**Reference to a website:**

Cancer Research UK, 1975. Cancer statistics reports for the UK. http://www.cancerresearchuk.org/aboutcancer/statistics/cancerstatsreport/ (accessed 13 March 2003).

**Reference to a dataset:**

[dataset] Oguro, M., Imahiro, S., Saito, S., Nakashizuka, T., 2015. Mortality data for Japanese oak wilt disease and surrounding forest compositions. Mendeley Data, v1. https://doi.org/10.17632/xwj98nb39r.1.

**Journal abbreviations source**

Journal names should be abbreviated according to the List of Title Word Abbreviations.

### G.27 Video

Elsevier accepts video material and animation sequences to support and enhance your scientific research. Authors who have video or animation files that they wish to submit with their article are strongly encouraged to include links to these within the body of the article. This can be done in the same way as a figure or table by referring to the video or animation content and noting in the body text where it should be placed. All submitted files should be properly labeled so that they directly relate to the video file's content. . In order to ensure that your video or animation material is directly usable, please provide the file in one of our recommended file formats with a preferred maximum size of 150 MB per file, 1 GB in total. Video and animation files supplied will be published online in the electronic version of your article in Elsevier Web products, including ScienceDirect. Please supply 'stills' with your files: you can choose any frame from the video or animation or make a separate image. These will be used instead of standard icons and will personalize the link to your video data. For more detailed instructions please visit our video instruction pages. Note: since video and animation cannot be embedded in the print version of the journal, please provide text for both the electronic and the print version for the portions of the article that refer to this content.

### G.28 Data visualization

Include interactive data visualizations in your publication and let your readers interact and engage more closely with your research. Follow the instructions here to find out about available data visualization options and how to include them with your article.

### G.29 Supplementary material

Supplementary material such as applications, images and sound clips, can be published with your article to enhance it. Submitted supplementary items are published exactly as they are received (Excel or PowerPoint files will appear as such online). Please submit your material together with the article and supply a concise, descriptive caption for each supplementary file. If you wish to make changes to supplementary material during any stage of the process, please make sure to provide an updated file. Do not annotate any corrections on a previous version. Please switch off the 'Track Changes' option in Microsoft Office files as these will appear in the published version.

### G.30 Research data

This journal encourages and enables you to share data that supports your research publication where appropriate, and enables you to interlink the data with your published articles. Research

data refers to the results of observations or experimentation that validate research findings. To facilitate reproducibility and data reuse, this journal also encourages you to share your software, code, models, algorithms, protocols, methods and other useful materials related to the project.

Below are a number of ways in which you can associate data with your article or make a statement about the availability of your data when submitting your manuscript. If you are sharing data in one of these ways, you are encouraged to cite the data in your manuscript and reference list. Please refer to the "References" section for more information about data citation. For more information on depositing, sharing and using research data and other relevant research materials, visit the research data page.

### G.30.1 Data linking

If you have made your research data available in a data repository, you can link your article directly to the dataset. Elsevier collaborates with a number of repositories to link articles on ScienceDirect with relevant repositories, giving readers access to underlying data that gives them a better understanding of the research described.

There are different ways to link your datasets to your article. When available, you can directly link your dataset to your article by providing the relevant information in the submission system. For more information, visit the database linking page.

For supported data repositories a repository banner will automatically appear next to your published article on ScienceDirect.

In addition, you can link to relevant data or entities through identifiers within the text of your manuscript, using the following format: Database: xxxx (e.g., TAIR: AT1G01020; CCDC: 734053; PDB: 1XFN).

### G.30.2 Mendeley Data

This journal supports Mendeley Data, enabling you to deposit any research data (including raw and processed data, video, code, software, algorithms, protocols, and methods) associated with your manuscript in a free-to-use, open access repository. During the submission process, after uploading your manuscript, you will have the opportunity to upload your relevant datasets directly to Mendeley Data. The datasets will be listed and directly accessible to readers next to your published article online.

For more information, visit the Mendeley Data for journals page.

### G.30.3 Data in Brief

You have the option of converting any or all parts of your supplementary or additional raw data into one or multiple data articles, a new kind of article that houses and describes your data. Data articles ensure that your data is actively reviewed, curated, formatted, indexed, given a DOI and publicly available to all upon publication. You are encouraged to submit your article for Data in Brief as an additional item directly alongside the revised version of your manuscript. If your research article is accepted, your data article will automatically be transferred over to Data in Brief where it will be editorially reviewed and published in the open access data journal, Data in Brief. Please note an open access fee of 500 USD is payable for publication in Data in Brief. Full details can be found on the Data in Brief website. Please use this template to write your Data in Brief.

### G.30.4 Data statement

To foster transparency, we encourage you to state the availability of your data in your submission. This may be a requirement of your funding body or institution. If your data is unavailable to access or unsuitable to post, you will have the opportunity to indicate why during the submission process, for example by stating that the research data is confidential. The statement will appear with your published article on ScienceDirect. For more information, visit the Data Statement page.

## G.31 Submission checklist

It is hoped that this list will be useful during the final checking of an article prior to sending it to the journal's Editor for review. Please consult this Guide for Authors for further details of any item.

**Ensure that the following items are present:**

One Author designated as corresponding Author:

- E-mail address
- Full postal address
- Telephone and fax numbers

All necessary files have been uploaded

- Keywords
- All figure captions
- All tables (including title, description, footnotes)

Further considerations:

- Use continuous line numbering (every 5 lines) to facilitate reviewing of the manuscript.
- Manuscript has been "spellchecked" and "grammar-checked"
- References are in the correct format for this journal
- All references mentioned in the Reference list are cited in the text, and vice versa
- Permission has been obtained for use of copyrighted material from other sources (including the Web)
- Color figures are clearly marked as being intended for color reproduction on the Web (free of charge) and in print or to be reproduced in color on the Web (free of charge) and in black-and-white in print
- If only color on the Web is required, black and white versions of the figures are also supplied for printing purposes

For any further information please visit our customer support site at service.elsevier.com.

### G.32 Online proof correction

Corresponding authors will receive an e-mail with a link to our online proofing system, allowing annotation and correction of proofs online. The environment is similar to MS Word: in addition to editing text, you can also comment on figures/tables and answer questions from the Copy Editor. Web-based proofing provides a faster and less error-prone process by allowing you to directly type your corrections, eliminating the potential introduction of errors.

If preferred, you can still choose to annotate and upload your edits on the PDF version. All instructions for proofing will be given in the e-mail we send to authors, including alternative methods to the online version and PDF.

We will do everything possible to get your article published quickly and accurately. Please use this proof only for checking the typesetting, editing, completeness and correctness of the text, tables and figures. Significant changes to the article as accepted for publication will only be considered at this stage with permission from the Editor. It is important to ensure that all corrections are sent back to us in one communication. Please check carefully before replying, as inclusion of any subsequent corrections cannot be guaranteed. Proofreading is solely your responsibility.

### G.33 Offprints

The corresponding author will, at no cost, receive a customized Share Link providing 50 days free access to the final published version of the article on ScienceDirect. The Share Link can be used for sharing the article via any communication channel, including email and social media. For an extra charge, paper offprints can be ordered via the offprint order form which is sent once the article is accepted for publication. Both corresponding and co-authors may order offprints at any time via Elsevier's Webshop. Corresponding authors who have published their article gold open access do not receive a Share Link as their final published version of the article is available open access on ScienceDirect and can be shared through the article DOI link.

### G.34 Author inquiries

Visit the Elsevier Support Center to find the answers you need. Here you will find everything from Frequently Asked Questions to ways to get in touch.

You can also check the status of your submitted article or find out when your accepted article will be published.

# Gill Smithies

Proofreading & Language Editing Services

59, Lewis Drive, Amanzimtoti, 4126, Kwazulu Natal

Cell: 071 352 5410 E-mail: moramist@vodamail.co.za


## Work Certificate

| | |
|---|---|
| To | Susanna M. Maree |
| Address | Centre of Excellence for Pharmaceutical Studies, Division of Pharmaceutics, Potchefstroom Campus, North West University |
| Date | 23/11/2018 |
| Subject | Transdermal delivery of selected statins formulated in Apricot Kernel Oil emulsions. |
| Ref | GS/SMM/01 |

I, Gill Smithies, certify that I have proofread the following dissertation, Transdermal delivery of selected statins formulated in Apricot Kernel Oil emulsions,
to the standard as required by NWU, Potchefstroom Campus.

Gill Smithies

21/11/2018